The role of stromal cells in the regulation of T cell responses

Thesis

for the degree of

doctor rerum naturalium
(Dr. rer. nat.)

approved by the Faculty of Natural Sciences of
Otto von Guericke University Magdeburg

by: M.Sc. Laura Knop
born on: 20.12.1988 in Hannover, Germany

Examiner: Prof. Dr. Thomas Schüler
Prof. Dr. Georg Gasteiger

submitted on: 21.11.2022
defended on: 04.04.2023

Table of contents

Summary

The adaptive immune system consists of T and B lymphocytes, which have the unique capability to differentiate into long-lived memory cells. The formation of **memory T cells (T_M)** is initiated in secondary lymphoid organs such as the lymph nodes (LNs). Upon infection, pro-inflammatory cytokines (e.g., **type I interferons (IFN-I)**) are produced, dendritic cells (DCs) take up pathogens in the periphery and migrate to the draining LNs. The contact of antigen-presenting mature DCs and naive T cells (T_N), equipped with appropriate T cell receptors, leads to T cell expansion and induces their differentiation into **interferon-γ (IFN-γ)**-producing effector T cells (T_{EFF})[1]. Most T_{EFF} undergo apoptosis after pathogen clearance, while a small population differentiates into T_M[1], which confer immediate protection upon secondary antigen contact[2]. **Interleukin-7 (IL-7)** is a critical survival factor for T_N and T_M, which is only produced in limited amounts in the body[3]. Lymphopenic hosts lack the IL-7-consuming T cell pool and IL-7 availability is increased[4]. Therefore, adoptively transferred T_N expand in lymphopenic mice and subsequently convert into **virtual memory T cells (T_{VM})**[5]. This so-called **lymphopenia-induced proliferation (LIP)** represents an alternative, foreign antigen-independent pathway of T_M generation[5].

For many years, research on T_M differentiation and maintenance focused mainly on T cell-intrinsic signaling processes and interactions with other immune cells, such as DCs[6,7]. However, it is becoming increasingly clear that environmental factors, including surrounding non-immune cells, can influence T_M fate decision[8,9]. For example, in the LNs, T cells are in close contact with **lymphoid stromal cells (LSCs)**, producing IL-7[10]. LSCs provide important survival and homing signals, e.g., by secreting chemokines that recruit T cells into IL-7-producing niches[10,11]. Importantly, LSCs express cytokine receptors, such as the IFN-I receptor (IFNAR) and the IFN-γ receptor (IFN-γR)[12], enabling them to adjust their gene expression profile to the degree of inflammation. Interestingly, IFNAR and IFN-γR signaling promote IL-7 expression[13,14]. This suggested a feedback loop enabling LSCs to promote IL-7-dependent $T_{(V)M}$ formation and generation in response to the pro-inflammatory cytokines IFN-I and IFN-γ. Various cell type-specific knockout mouse models were used to address whether these cytokine-dependent, T cell-extrinsic mechanisms contribute to $T_{(V)M}$ differentiation. The corresponding data were published in three research articles, which are summarized in this thesis.

I. Interferon-γ receptor signaling in dendritic cells restrains spontaneous proliferation of $CD4^+$ T cells in chronic lymphopenic mice (Knop et al., 2019[15])

II. IL-7 derived from lymph node fibroblastic reticular cells is dispensable for naive T cell homeostasis but crucial for central memory T cell survival (Knop et al., 2020[16])

III. IFNAR signaling in fibroblastic reticular cells can modulate $CD8^+$ memory fate decision (Knop et al., 2022[17])

Zusammenfassung

Das adaptive Immunsystem besteht aus T- und B-Lymphozyten, die zu langlebigen Gedächtniszellen differenzieren können. Die Bildung von **T-Gedächtniszellen (T_M)** wird in den sekundären lymphatischen Organen, wie z.B. den Lymphknoten (LN) initiiert. Bei einer Infektion werden pro-inflammatorische Zytokine (z.B. **Typ I Interferone (IFN-I)**) produziert und dendritische Zellen (DCs) transportieren aufgenommene Pathogene in die drainierenden LN. Dort präsentieren DCs Pathogen-spezifische Peptide über MHC-I und MHC-II Moleküle. Naive T-Zellen (T_N) mit hierfür spezifischen T-Zellrezeptoren expandieren und differenzieren zu **Interferon-γ (IFN-γ)**-produzierenden T-Effektorzellen (T_{EFF})[1]. Nach der Eliminierung des Pathogens werden die meisten T_{EFF} mittels Apoptose eliminiert, während ein kleiner Teil zu T_M differenziert[1], die bei erneutem Antigenkontakt eine verbesserte Protektion vermitteln[2]. **Interleukin-7 (IL-7)** ist ein wichtiger Überlebensfaktor für T_N und T_M, welcher nur in begrenzter Menge im Körper produziert wird[3]. In lymphopenischen Wirten steigt die Verfügbarkeit von IL-7, da IL-7-konsumierende T-Zellen fehlen[4]. Aus diesem Grund expandieren transferierte T_N in lymphopenischen Mäusen und differenzieren zu **virtuellen T-Gedächtniszellen (T_{VM})**[5]. Diese sog. **Lymphopenie-induzierte Proliferation (LIP)** stellt einen alternativen, Fremdantigen-unabhängigen Prozess zur Generierung von T_M dar[5].

Die Großzahl der Studien zu den Mechanismen der T_M Differenzierung analysierte vor allem T-Zell-intrinsische Signalprozesse, z.B. als Konsequenz von Interaktionen mit anderen Immunzellen, wie DCs[6,7]. Es wird jedoch zunehmend klar, dass auch Nicht-Immunzellen immunmodulatorisches Potential besitzen und so den Differenzierungsprozess von T_M beeinflussen könnten[8,9]. In den LN stehen T-Zellen z.B. in engem Kontakt mit nicht-hämatopoetischen, **lymphoiden Stromazellen (LSCs),** die den für T_N/T_M wichtigen Überlebensfaktor IL-7 produzieren[10]. LSCs sekretieren außerdem Homing-Faktoren wie Chemokine, die T-Zellen in IL-7-reiche Nischen locken[10,11]. Zusätzlich exprimieren LSCs Zytokinrezeptoren, wie den IFN-I Rezeptor (IFNAR) oder den IFN-γ Rezeptor (IFN-γR)[12] und können somit ihr Genexpressionsprofil der inflammatorischen Umgebung anpassen. Interessanterweise fördern IFNAR und IFN-γR Signalgebung die Expression von IL-7[13,14]. Aus den genannten Beobachtungen resultierte die Hypothese, dass ein IFN-I- und/oder IFN-γ-getriebener Rückkopplungsmechanismus die IL-7-Produktion durch LSCs und so das Überleben von $T_{(V)M}$ fördert. Ziel der vorliegenden Arbeit war es deshalb, die Zytokin-abhängigen Prozesse zu untersuchen, mit deren Hilfe LSCs die $T_{(V)M}$ Differenzierung beeinflussen. Zu diesem Zweck wurden verschiedene zelltypspezifische Knockout-Mausmodelle verwendet. Die entsprechenden Daten wurden in drei Artikeln publiziert, die in dieser Arbeit beschrieben werden.

I. Interferon-γ receptor signaling in dendritic cells restrains spontaneous proliferation of $CD4^+$ T cells in chronic lymphopenic mice (Knop et al., 2019[15])

II. IL-7 derived from lymph node fibroblastic reticular cells is dispensable for naive T cell homeostasis but crucial for central memory T cell survival (Knop et al., 2020[16])

III. IFNAR signaling in fibroblastic reticular cells can modulate $CD8^+$ memory fate decision (Knop et al., 2022[17])

1 Introduction

This thesis elucidates three interrelated studies that seek to improve our understanding of how T cell-extrinsic mechanisms regulate T cell homeostasis and memory differentiation. In the introduction, I will summarize the knowledge regarding T cell and lymphoid stromal cell (LSC) biology, which was available at the beginning of my thesis. As a central aspect, the roles of interleukin 7 (IL-7), interferon γ (IFN-γ) and type-I interferon (IFN-I) in the regulation of steady state T cell homeostasis as well as T cell immunity will be addressed and connected to LSC biology.

1.1 The immune system

The immune system has evolved as a complex environmental sensor safeguarding host survival. It contains many different cell types and can be considered a mobile organ that recognizes, interprets and responds to environmental changes. When pathogens invade the host, the two parts of the immune system are activated: the innate and the adaptive immunity (see Figure 1-1)[18,19]. Innate immune cells exert their effector functions rapidly. In contrast, immune cells from the adaptive immune system must be first activated in secondary lymphoid organs (SLOs), such as the spleen or the lymph nodes (LNs)[18,19].

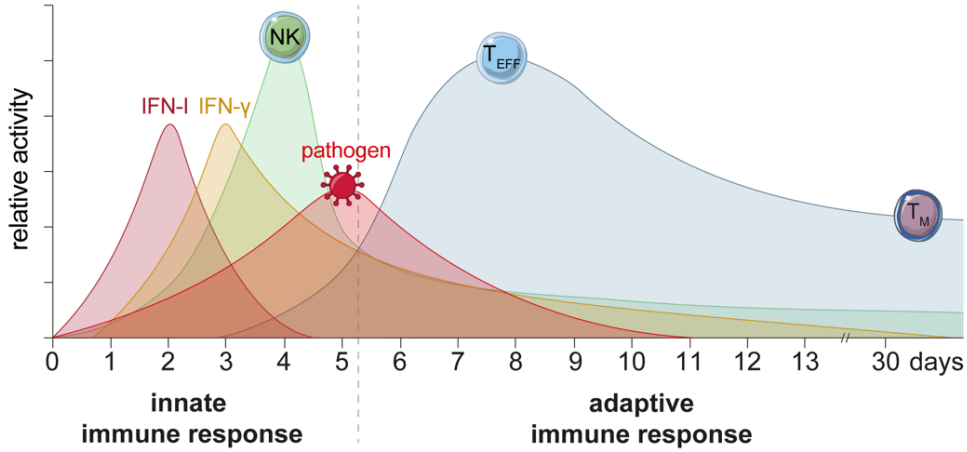

Figure 1-1. Kinetics of immune responses to primary infections (adapted from [20]). Upon infection, IFN-I is rapidly released, followed by the production of IFN-γ. Infected cells are killed by natural killer (NK) cells that contribute to IFN-γ release. The innate immune response continues while the adaptive immunity is initiated. Naive T cells are activated in the SLOs and undergo clonal expansion and differentiation into effector T cells (T_{EFF}). After pathogen clearance, most T_{EFF} undergo apoptosis and only a small fraction differentiates into long-lived memory T cells (T_M). This figure was created using illustrations from www.bioicons.com[21].

1.1.1 The innate immune system

Self-nonself discrimination is a hallmark of the immune system. For example, pathogen-associated molecular patterns (PAMPs) are specific for pathogens and are not expressed by healthy eukaryotes[22]. Upon infection with pathogens, innate immune cells expressing pattern recognition receptors (PRRs) recognize PAMPs, such as lipids, proteins, glycans and nucleic acids[18,19]. The combined recognition of PAMPs encoded by a particular pathogen results in specific activation patterns of immune-stimulating genes[23]. This allows the immune system to adjust its response to the infectious agent and optimize subsequent pathogen control and elimination.

Among the PRR-induced factors are interferons (IFNs), which represent the foundation of host responses to viral infections[24,25]. Based on their receptor specificity and sequence homology, IFNs are divided into three groups: IFN-I, -II and -III. Upon viral infection, **IFN-I** is rapidly released (see Figure 1-1), supporting the induction of an anti-viral state by inhibiting (1) viral entry, (2) viral replication and (3) virus release[26]. The group of IFN-I includes the structurally related members IFN-α, -β, -δ, -ε, -κ, -τ and -ο that are produced by a broad spectrum of cells[24,25]. IFN-I is bound by the IFN-I receptor (IFNAR) consisting of the two subunits IFNAR1 and IFNAR2 (see Figure 1-2), which are expressed on all nucleated cells[27,28]. IFNAR signaling leads to the transcription of IFN-stimulated genes (ISGs), which support cell metabolism and proliferation or induce apoptosis. As a positive feedback mechanism, IFN-I is induced upon IFNAR signaling and promotes cell activation in an autocrine, paracrine and systemic manner[29,30]. In contrast, IFNAR signaling is negatively regulated by the induction of suppressor of cytokine signaling protein 1 (SOCS-1) that interferes with Janus kinase (JAK) activation[31]. The importance of IFN-I for anti-viral immunity is demonstrated by the high viral susceptibility of IFNAR$^{-/-}$ mice[32]. In humans, *IFNAR1* homozygous nonsense mutations lead to life-threatening propagation of live viral vaccines[33].

Plasmacytoid dendritic cells are efficient producers of IFN-I[25]. **Dendritic cells (DCs)** belong to the heterogeneous group of phagocytes that also includes neutrophils and macrophages[18,19]. Upon activation, phagocytes take up pathogens and dead cells, hence contributing to infection control[34]. Neutrophils have the highest phagocytic activity among the granulocytes and are attracted from the blood to the inflamed tissues[35]. Besides directly killing pathogens, phagocytes play an essential role in initiating the adaptive immunity. Macrophages and DCs are professional antigen (Ag)-presenting cells (APCs) that process ingested Ags and present peptides on major histocompatibility complex (MHC) molecules[18,19]. While MHC class I (MHC-I) molecules are expressed on every nucleated cell, expression of MHC class II (MHC-II) molecules is more restricted, e.g., to APCs[36]. After activation via PRRs, DCs migrate to SLOs[37], present pathogen-related peptide-MHC-complexes and activate

T cells equipped with appropriate T cell receptors (TCRs)[38]. The activation of DCs also induces the up-regulation of MHC-I and MHC-II expression[39], resulting in increased Ag presentation and an enhanced likelihood of Ag recognition by T cells. Furthermore, cluster of differentiation 80 (CD80)/CD86 are up-regulated on DCs upon activation, providing essential co-stimulation for T cells[40,41]. Hence, DCs are an important cell population bridging the innate and adaptive immunity.

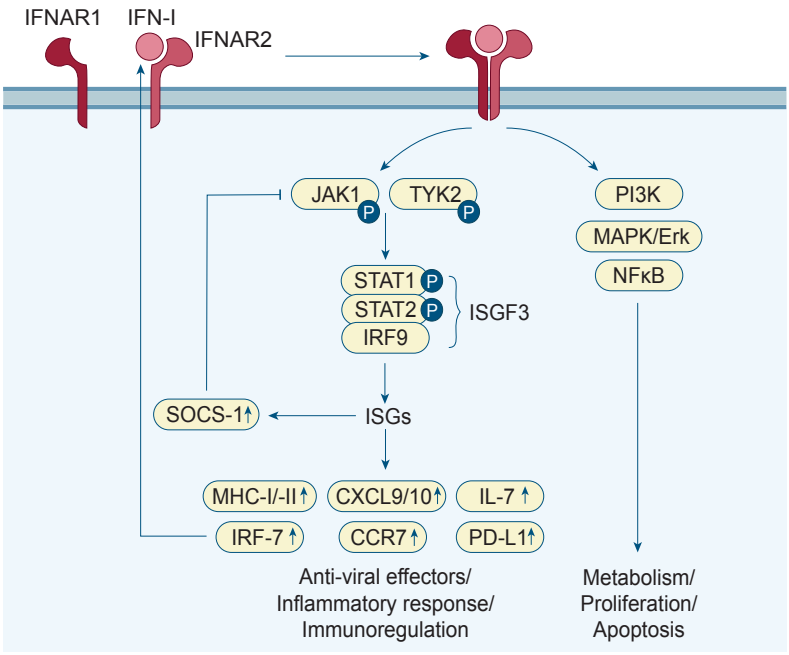

Figure 1-2. IFNAR signaling (adapted from [29]). The binding of IFN-I to IFNAR2 facilitates the recruitment of IFNAR1 and the assembly of the functional IFNAR-complex. IFNAR signaling activates JAK1 and tyrosine kinase 2 (TYK2), leading to the formation of the complex Interferon-stimulated gene factor 3 (ISGF3) consisting of phosphorylated signal transducer and activator of transcription 1/2 (STAT1/2) and interferon regulatory factor 9 (IRF9). The ISGF3 complex initiates the transcription of ISGs, among them SOCS-1, which inhibits JAK1. IRF7 further amplifies the IFN-I response by initiating IFN-I transcription. IFNAR signaling also activates the phosphoinositide 3−kinase (PI3K), mitogen-activated protein kinase/ extracellular signal-regulated kinase (MAPK/Erk) and nuclear factor kappa-light-chain-enhancer of activated B cells (NFκB) pathways that support metabolism, proliferation and apoptosis[29,30].

Besides phagocytes, tissue-resident innate immune cells contribute to the first line of cellular defense. For example, innate lymphoid cells (ILCs) are an early source of pro-inflammatory cytokines, thereby limiting excessive pathogen propagation[42]. ILCs share functional characteristics with T cell subsets but lack rearranged Ag receptors (for T cells, see chapter 1.1.2)[42,43]. Similar to their T cell counterparts, ILCs are classified into several subsets (ILC1/2/3) and mediate lymphoid tissue formation, tissue repair and homeostasis and contribute to immunity against pathogens[42,43]. Natural killer (NK) cells are a subset of ILCs that, upon activation, secrete cytotoxic granules triggering apoptosis in infected or cancerous cells[42,43]. Additionally, NK cells contribute to the production of the pro-inflammatory cytokine

interferon-γ (IFN-γ) as a result of PRR activation[44] (see Figure 1-1). IFN-γ exerts critical functions during immune responses against pathogens, such as enhancing the phagocytic activity of macrophages[45,46]. IFN-γ is the sole member of the IFN-II group and is bound by the IFN-γ receptor (IFN-γR)[28]. The IFN-γR consists of two ligand-binding (IFN-γR1) and two signal-transducing (IFN-γR2) domains[28,47] (see Figure 1-3). IFN-γ stimulation leads to phosphorylation of signal transducer and activator of transcription 1 (STAT1), increases cell metabolism and proliferation and induces apoptosis[48]. To prevent lethal tissue damage, IFN-γR signaling is counter-regulated by SOCS-1. In particular, IFN-γR signaling induces SOCS-1 up-regulation, thus establishing a negative feedback loop protecting the host from IFN-γ-mediated immunopathology[46,47]. IFN-γR1$^{-/-}$ mice are more susceptible to infections with bacteria (e.g., *Listeria monocytogenes*[49]) and viruses (e.g., vaccinia virus[49]), which underlines the vital role of IFN-γ during anti-bacterial and anti-viral immune responses. Likewise, in humans, IFN-γR loss-of-function mutations are associated with increased bacterial and viral infections[45]. Furthermore, IFN-γ is essential for the survival of parasitic infections, e.g., with *Toxoplasma gondii* [50].

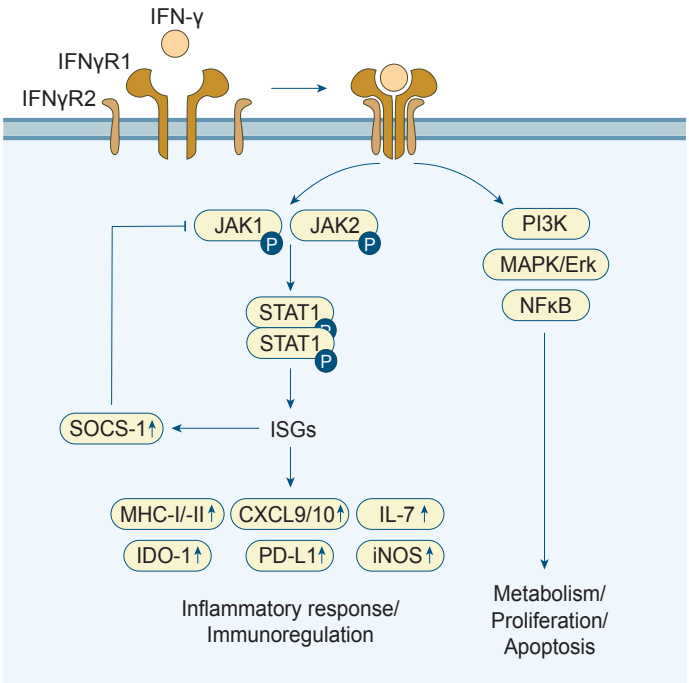

Figure 1-3. IFN-γR signaling (adapted from [45]). The binding of IFN-γ initiates the assembly of the IFN-γR, which consists of two IFNγR1 and two IFNγR2 subunits. IFNγR signaling induces activation of the JAK/STAT pathway. STAT1 is phosphorylated by JAK1/JAK2, dimerizes and translocates into the nucleus, where it initiates the transcription of ISGs. Furthermore, IFN-γ-stimulation activates the PI3K, MAPK/ERK and NFκB pathways. The negative regulator SOCS-1 is induced by IFN-γR signaling and blocks JAK2 activity[48,51].

1.1.2 The adaptive immune system

B and T lymphocytes form the adaptive immune system. The latter are, besides NK cells, a significant source of IFN-γ[52,53]. Upon infection, T/B cells can, as opposed to innate immune

cells, differentiate into long-lived memory cells that quickly and efficiently provide Ag-specific protection upon secondary infection with the same pathogen[18,19]. Contrary to innate immune cells, T and B lymphocytes are equipped with Ag-specific TCRs and B cell receptors (BCRs), respectively. The high degree of TCR and BCR diversity relies on somatic recombination of TCR/BCR-encoding gene segments, which occurs during T and B cell development in the thymus and bone marrow (BM), respectively[18,19].

This thesis focuses on T cells, which are described in the following sections.

T cell progenitors leave the BM and migrate into the thymus (see Figure 1-4), where T cell maturation proceeds[18,19]. The resulting naive T cells (T_N) are classified into two subsets: $CD4^+$ helper T cells and $CD8^+$ cytotoxic T cells.

$CD4^+$ helper T cells (T_H) promote B and $CD8^+$ T cell responses against many pathogens. Their functional maturation mainly relies on the pathogen-specific cytokine milieu present during primary antigen contact[18,19,54]. Depending on the pathogen type, different PRRs are activated in DCs[22]. Consequently, a set of pathogen-specific cytokines is produced, which in turn promotes the differentiation of recently primed $CD4^+$ T_N into specific effector cell subsets[18,19]. Based on their cytokine secretion, different effector T_H subsets can be distinguished[54]. For example, T_H1 cells are essential for controlling intracellular pathogens and release pro-inflammatory cytokines, such as IFN-γ. IL-4-producing T_H2 cells support the activation and differentiation of anti-parasitic immunoglobulin (Ig) 1/ IgE-secreting B cells. T_H17 cells are induced early during immune responses to extracellular pathogens and secrete the pro-inflammatory cytokine IL-17. The immunological function of regulatory $CD4^+$ T cells (T_{regs}) is to limit T cell responses, immunopathology and autoimmunity, e.g., by releasing anti-inflammatory IL-10[54].

Effector $CD8^+$ T cells produce pro-inflammatory cytokines such as IFN-γ and tumor necrosis factor α (TNF-α) and release cytotoxic perforin/granzyme B-containing granules to directly kill infected or malignant cells[55]. These so-called cytotoxic T lymphocytes (CTLs) derive from $CD8^+$ T_N, which are primed by DCs presenting MHC-I molecules loaded with e.g., pathogen-derived peptides[55].

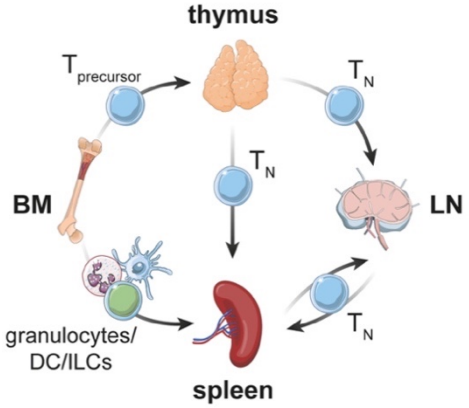

Figure 1-4. Immune cell migration. Granulocytes, DCs and ILCs develop in the BM and migrate into SLOs, such as the spleen. T cell precursors, generated in the BM, migrate into the thymus, where they complete maturation. The resulting T_N home into the SLOs (spleen and LNs), which they leave and re-enter in search of their cognate Ag. This figure was created using illustrations from www.bioicons.com[21]; organ icons were kindly provided by Vladyslava Dovhan.

1.1.2.1 T cell response to primary infections

After leaving the thymus, $CD4^+$ and $CD8^+$ T_N continuously recirculate between SLOs[56] (see Figure 1-4) and the majority cannot yet enter non-lymphoid tissues[57]. Hence, the initiation of adaptive immune responses requires Ag-shuttling from the site of infection to the draining LN, a task accomplished by migratory DCs (see Figure 1-5)[37]. To further increase the likelihood of productive T_N-DC interactions, LNs are sub-compartmentalized, providing specialized T cell areas where T_N priming occurs (see chapter 1.2)[58–60]. T_N homing to and positioning in LNs are guided by chemokines. For example, LN stromal cells produce the chemokines C-C motif ligand 19 (CCL19) and CCL21[12], which attract T_N expressing the corresponding C-C chemokine receptor type 7 (CCR7). Additionally, T_N are equipped with L-selectin (CD62L), enabling them to cross blood vessels to reach the LN T cell zone[61]. Once $CD4^+$ and $CD8^+$ T_N have reached the T cell areas, they scan APCs continuously searching for foreign Ag-derived cognate peptides presented on MHC-II or MHC-I complexes, respectively[18,19]. If T_N are not activated, they continue to recirculate and home to the next SLO[56]. Productive T_N-DC interactions result in clonal expansion of Ag-specific T cells, which differentiate into effector T cells (T_{EFF})[62,63]. TCR signaling provides one signal necessary for full T cell activation[64]. Co-stimulation presents a second signal, such as the recognition of DC-expressed CD80/CD86 through CD28 expressed on T cells[40,41]. Furthermore, pro-inflammatory cytokines, such as IFN-I, are the third signal required for full T cell activation resulting from the inflammatory environment[65]. The expansion of T_{EFF} reaches its maximum at about 7-8 days after primary Ag contact (see Figure 1-1 and Figure 1-6)[66,67] and the LN structure adapts to the enhanced space requirements of proliferating T_{EFF}[68,69]. $CD4^+$ T_H1 and $CD8^+$ T_{EFF} contribute to the production of IFN-γ that e.g., promotes Ag-presentation to $CD4^+$ and $CD8^+$ T cells by the up-regulation of MHC-I and MHC-II complexes[70–72]. Furthermore, IFN-γ and IL-12 support the differentiation of $CD4^+$ T cells into IFN-γ-secreting T_H1 cells[18,19]. To gain access to infected non-lymphoid tissues, T_{EFF} up-regulate the adhesion molecule CD44 and down-regulate CD62L[67]. The population of T_{EFF} is heterogeneous and can be divided into at least two subsets, terminal/short-lived effector T cells (T_{SLEC}), comprising the largest subtype, and memory precursor T cells (T_{MP})[73]. In the T_{SLEC} population individual cells compete for resources, such as Ag-peptide-MHC complexes, and for the occupation of ecological niches supporting their survival and function[74]. T_{SLEC} that fail to receive survival signals undergo Fas/FasL-mediated fratricide[75] after the pathogen is cleared[73] (contraction phase; see Figure 1-6). The contraction of the T_{SLEC} population represents a mechanism to re-establish a state of homeostasis, maintaining a diverse polyclonal T cell pool capable of reacting to new infections. In contrast to T_{SLEC}, the small population of T_{MP} survives and differentiates into long-lasting T_M[73]. T_{SLEC} and T_{MP} differ in the expression of the interleukin-7 receptor α chain (IL-7Rα; CD127) and the co-inhibitory receptor killer-cell lectin-like receptor G1 (KLRG-1), with T_{SLEC} being $CD127^{lo}KLRG\text{-}1^{hi}$ and T_{MP} being $CD127^{hi}KLRG\text{-}1^{lo}$ [73,76].

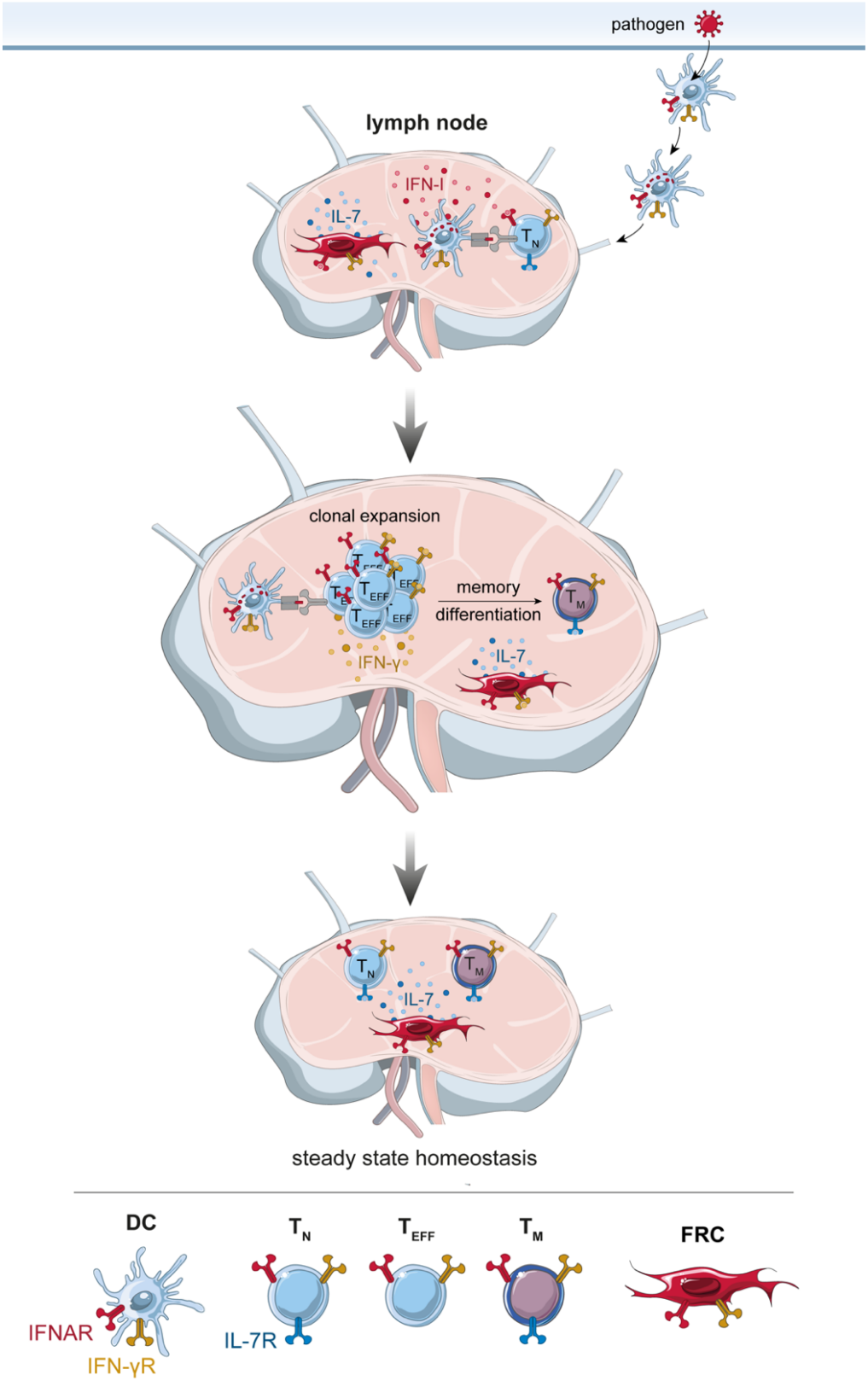

Figure 1-5. Primary adaptive immune responses are initiated in the LNs. (Top) DCs take up invading pathogens and migrate to the LNs [37], where fibroblastic reticular cells (FRCs) secrete the T cell survival factor IL-7 [10]. Activated DCs produce IFN-I [25] that binds to IFNAR-expressing DCs, T_N and FRCs. Additionally, DCs present Ag-derived peptides on MHC molecules to TCR-expressing T_N [18,19]. (Middle) Upon activation, T cells start proliferating and $CD4^+$ T_H1 and $CD8^+$ T_{EFF} produce IFN-γ [52,53] that is recognized by IFN-γR$^+$ DCs, T_{EFF} and FRCs. The LN expands to adapt to the increased space requirement [68,69]. Some activated T cells survive the contraction phase and differentiate into T_M [73]. (Bottom) After pathogen clearance, the LN size decreases again, reaching steady state homeostasis to enable new immune responses [68,69]. This figure was created using illustrations from www.bioicons.com [21]; LN icon was kindly provided by Vladyslava Dovhan.

1.1.2.2 Memory T cell subsets and differentiation

Based on their function and location, **T_M** can be divided into at least four subsets: stem cell memory (T_{SCM}), central memory (T_{CM}), effector memory (T_{EM}) and tissue-resident memory (T_{RM}) T cells[1,77]. T_{SCM} are $CD44^{lo}$ $CD62L^{hi}$ and have the highest self-renewing capacity. They exhibit stem-cell potential and can differentiate into T_{CM} and T_{EM}[78]. The role of T_{SCM} remains poorly defined, mainly because T_{SCM} and T_{CM} share characteristics such as self-renewal and differentiation capacity[1]. Upon re-infection, T_{CM} produce substantial amounts of the T cell growth factor IL-2 and differentiate into T_{EFF}[79]. $CD44^{hi}$ T_{CM} are preferentially located in SLOs and express the homing receptors CD62L and CCR7[77]. In contrast, $CD44^{hi}$ T_{EM} lack CD62L and CCR7 expression and mainly reside in non-lymphoid tissues[80]. $CD8^+$ T_{EM} display reduced self-renewal capacity but rapidly release effector molecules, such as IFN-γ and TNF-α, upon antigen re-encounter[79]. $CD44^{hi}$ T_{RM} support protection at barrier organs, such as the skin, intestine and lung and express integrin alpha E (CD103) binding to the cell adhesion molecule E-cadherin on epithelial cells[1,67,77,80–82].

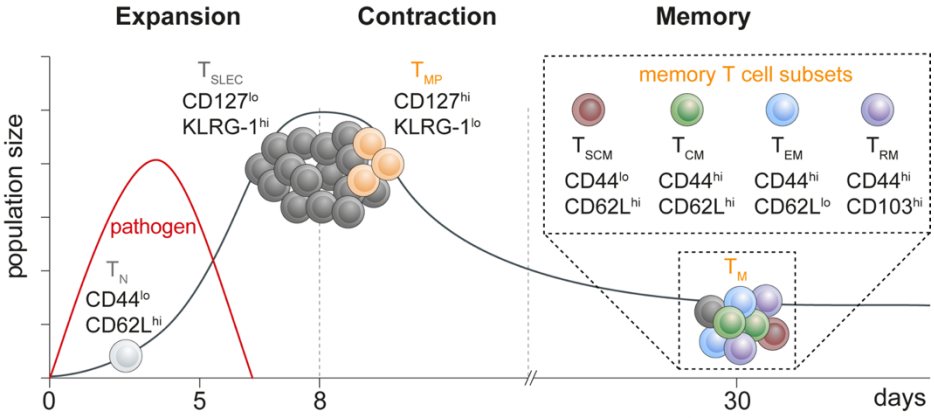

Figure 1-6. Kinetics of T cell responses (adapted from [1,66,67]). Upon infection, T_N proliferate and give rise to T_{SLEC} and T_{MP}. After the pathogen is eliminated, T_{SLEC} undergo apoptosis. T_{MP} further differentiate into T_M subsets, such as T_{SCM}, T_{CM} T_{EM} and T_{RM}. T_{SCM} show a high self-renewal and differentiation capacity. T_{CM} are preferentially located in the SLOs, whereas T_{EM} circulate between non-lymphoid tissues. T_{RM} are non-circulating and are found in organs that are in close contact with the environment, such as the skin, intestine and lung[1,67,77,80–82].

T_M formation is programmed within the first 24-72 h following T_N activation[83,84]. Factors affecting T_M differentiation include TCR signal strength, which is influenced by TCR affinity, the amount of Ag-MHC-complexes and TCR:Ag-MHC dwell time[67]. The prolonged interaction of T cells and Ag-presenting cells seems to favor asymmetric cell division. The TCR and other receptors are concentrated at the immunological synapse, hence daughter cells receive signals for T_{EFF} or T_M conversion differentially[85]. Additionally, the T_N precursor frequency affects the initial T_{CM}/T_{EM} fate decision and T_M proliferative capacity upon secondary Ag encounter[86,87].

In particular, the transfer of low T_N precursor frequencies leads to an accumulation of T_{EM}, likely due to less competition for Ag-presenting APCs and stronger TCR signaling[87].

Upon infection, cytokines, including IFN-I, are released, acting as a third signal during T cell activation[65] and shaping T_M formation[88]. For example, IFNAR signaling in $CD8^+$ T cells amplifies TCR signals, promotes their expansion and differentiation into T_M and protects them from NK-mediated cytolysis[30,89–91]. However, the relative importance of IFNAR signaling for $CD8^+$ T cell responses appears to vary with the type of pathogen[26]. Additionally, T cell activation is modulated by IFN-I-responsive DCs. In particular, IFNAR signaling in DCs supports T cell priming via (1) enhancing DC homing into LNs through up-regulation of CCR7, (2) inducing DC maturation and expression of T cell co-stimulatory molecules (CD80/86) and (3) enhancing Ag-presentation on DCs via up-regulation of MHC-I/-II[92–94].

Besides IFN-I, IFN-γ is present during T cell activation and coordinates immune responses for the long-time control of infections[24] (see Figure 1-1). The IFN-γ-dependent regulation of T cell responses is regulated by T cell-intrinsic and -extrinsic IFN-γR signaling. On the one hand, IFN-γR signaling in lymphocytic choriomeningitis virus (LCMV)-specific $CD4^+$ and $CD8^+$ T cells promotes T_{EFF} expansion and memory differentiation[95–97]. Hence, IFN-γ was suggested to be a third signal required for T cell activation[98]. Additionally, IFN-γ regulates the differentiation of $CD8^+$ T cell clones specific for different epitopes derived from the same pathogen. In particular, cell-autonomous IFN-γR signaling supports T_M differentiation of those clones responding to strong TCR agonists[99]. This mechanism helps to ensure the generation of T_M with high-affinity TCRs[99]. In other settings however, T cell responses are indirectly regulated by IFN-γ. For example, IFN-γR signaling in $CD8^+$ OT-I T cells seems dispensable for their expansion, contraction and memory differentiation during adoptive T cell transfers and peptide vaccination[100]. Instead, IFN-γ-responsive host cells seem essential in regulating these processes[100]. This suggests that the inflammatory context determines whether IFN-γ acts as a third signal in T cell activation.

As described above, the pro-inflammatory cytokines IFN-I and IFN-γ are translated into T cell-intrinsic signals and direct T cell differentiation and T_M formation according to the kind of invading pathogen. Additionally, chemokine expression patterns change in the course of immune responses. As a result, the spatial distribution of T cells in SLOs is altered to facilitate T_N priming and T_M recall responses. For example, $CD8^+$ T_{CM} are positioned in the outer LN regions, while priming of $CD8^+$ T_N occurs in the T cell areas in the center of the organ[101]. The recruitment of additional $CD8^+$ T_{CM} to pathogen-rich areas seems to be regulated by IFN-γ-secreting T_{CM} pre-positioned near the subcapsular sinus[101,102]. In particular, the IFN-γ-induced up-regulation of the chemokines C-X-C motif ligand 9/10 (CXCL9/10) in macrophages, stromal cells and DCs in the LN periphery attracts more C-X-C chemokine receptor type 3 (CXCR3)-expressing T_{CM}, thereby supporting host defence[101,102].

Furthermore, the acquisition and maintenance of different T cell phenotypes are regulated by the T cell's metabolic state, which in turn is affected by the microenvironment[67,103,104]. For example, T_N utilize mitochondrial oxidative phosphorylation to synthesize adenosine 5′-triphosphate (ATP)[67,103,104]. T_{EFF} additionally up-regulate glycolysis and glutaminolysis to fulfill their effector functions and provide biomass intermediates needed for clonal expansion[105]. As opposed to T_N, T_M have higher mitochondrial mass and show enhanced spare respiratory capacity, reflecting their higher capacity to generate maximum ATP levels under stress conditions[106]. Furthermore, T_M utilize triacylglycerides to produce energy by so-called fatty acid oxidation[67,103,104]. The glycerol uptake for fatty acid synthesis in T_M is mediated by the membrane channel protein aquaporin 9, which is expressed in an IL-7-dependent fashion[107]. Importantly, IL-7 is secreted by stromal cells[14,108–110] that are in direct contact with T cells, suggesting a contribution of stromal cell-derived IL-7 to the maintenance of T_M.

In summary, T cell differentiation and function rely on the combined action of signaling events induced in a cell-autonomous fashion together with those resulting from microenvironmental changes. This helps to ensure acute pathogen clearance and long-lived protection. Our understanding of how the surrounding microenvironment supports T_M fate decision is essential to improve T_M-dependent therapeutic treatments. So far, studies have focused on other immune cells shaping T_M formation[6,7]. However, stromal cells are integral parts of the T cell's microenvironment contributing to T cell homing into SLOs and the initiation of immune responses[58–60].

1.2 Compartmentalization of LNs by LSCs

As mentioned above, most naive T and B cells cannot enter non-lymphatic tissues, where infections most frequently occur. Therefore, the initiation of adaptive immune responses relies on the transport of peripheral Ags, either soluble or after engulfment by migratory DCs, to LNs draining the site of infection[37]. There, naive T and B cells are located in specialized anatomical compartments optimized to promote their activation, clonal expansion and functional maturation upon cognate Ag recognition[58–60]. The LN is divided into the cortex (B cell zone), paracortex (T cell zone) and medulla (see Figure 1-7). The B cell follicles are located directly underneath the subcapsular sinus (SCS), followed by the T cell zone. Lymph egress is regulated by the medulla comprised of medullary sinuses[58–60].

The complex architecture of LNs is organized by non-hematopoietic ($CD45^-$) lymphoid stromal cells (LSCs). At least nine LSC subpopulations were identified, including mesenchymal and endothelial cells[111,112]. Four main LSC subtypes are defined by the expression of the surface markers podoplanin (gp38) and the endothelial cell marker platelet endothelial cell adhesion molecule (PECAM-1)/CD31: double negative cells (DN; $gp38^-CD31^-$), blood endothelial cells (BECs; $gp38^-CD31^+$), lymphatic endothelial cells (LECs; $gp38^+CD31^+$) and

fibroblastic reticular cells (FRCs; gp38^{+}CD31^{-})[58–60]. The LSC subsets of follicular dendritic cells and marginal reticular cells are also crucial for the LN function, but are not a focus of this thesis.

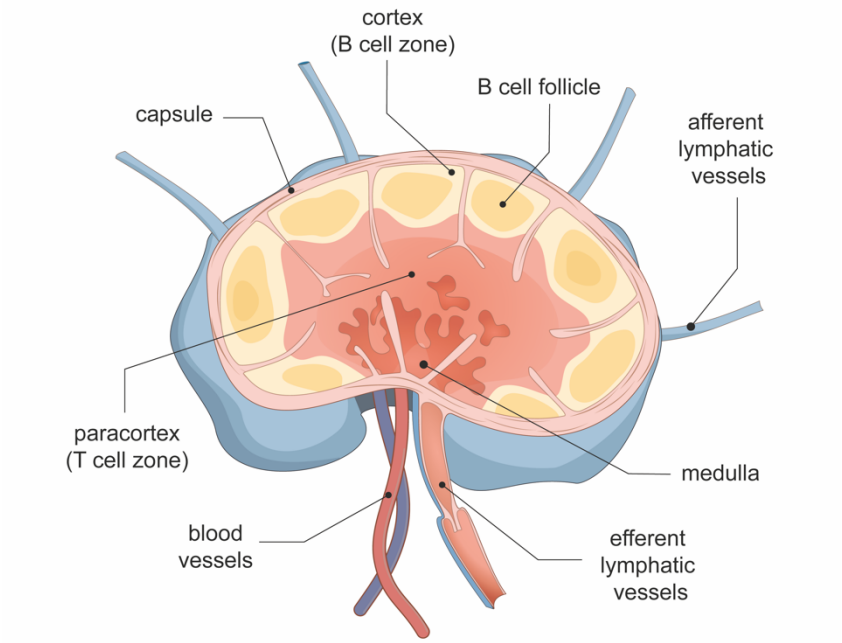

Figure 1-7. Lymph node structure. The LN is connected to the lymphatic system via afferent lymphatic vessels. All lymphatic vessels are comprised of LECs. The cortex (B cell zone) containing the B cell follicles is located directly underneath the capsule. The paracortex (T cell zone) is constructed by FRCs and is located in the center of the LN. T cells enter the paracortex through high endothelial venules that are assembled by BECs. Cells leaving the LN are first concentrated in the LEC-constructed medulla before exiting through the efferent lymphatic vessels[60]. LN illustration was kindly provided by Vladyslava Dovhan.

The subset of **DN** cells is mainly undefined but contains pericytes surrounding high endothelial venules (HEVs) in the LNs. Pericytes are located close to vessels and express a plethora of integrins, which suggests their contribution to regulating cell migration[12,60].

LNs are connected to the blood circulation by vessels that are composed of **BECs**. A unique subtype of BECs builds the HEVs that are the entry sites for T cells into the LNs. BECs support the recruitment of CCR7^{+} T_N cells into the lymph node by producing the chemokine CCL21[113,114].

LECs form the afferent lymphatic vessels in the SCS of the LN capsule, through which lymph drains into the LNs. LECs constitutively produce CCL21, which is secreted upon activation and attracting DCs[115]. The interaction between C-type lectin-like receptor 2 (CLEC-2) on DCs and gp38 on LECs facilitates DCs to pass the lymphatic vessel. In particular, gp38 modulates actomyosin contractility in LECs and enables DCs to reach the LN parenchyma[116], where T_N scan DCs for cognate peptide-MHC complexes. Non-activated T_N leave the LNs through cortical and medullary sinuses and efferent lymphatic vessels that also consist of LECs[58].

FRCs derive from mesenchymal lymphoid tissue organizer cells that are critical for LN-organogenesis[117,118]. CCR7-expressing T_N cells and DCs are attracted to the LN through FRC-released CCL19 and CCL21[119,120]. In the paracortex, FRCs form a dense network guiding T cell and DC migration[121]. This network connects the SCS and the B cell follicles with the T cell zone. In addition, FRCs secrete extracellular matrix fiber proteins (e.g., fibronectin and laminin), forming the conduit system in the paracortex that is used to transport small molecules, such as chemokines and Ags (see Figure 1-8). These conduits filter and guide liquid transportation from the afferent lymphatic vessels deep into the T cell zone[122,123]. DCs use small gaps between the FRCs to take up Ags from the conduit system and present it to T cells[123,124].

1.2.1 LSC-dependent regulation of T cell responses

LSCs represent less than 1% of all LN cells[125]. For a long time, they were supposed to be immunologically inert, solely forming the three-dimensional structure of SLOs. However, recent advances revealed that FRCs have immunomodulatory potential, thereby affecting different aspects of T cell homeostasis[58,126].

Regulation of T cell homeostasis

LN-FRCs and -LECs release the cytokine IL-7[10], which is an essential survival factor for T_N and T_M[127]. *In vitro* experiments suggested that FRC-derived IL-7 is vital for T_N survival[10]. However, T cells continuously circulate through the body and several organs contribute to IL-7 production[14,108–110,128,129]. Therefore, it remained unclear whether locally released IL-7 in the LN supports the survival of peripheral T cells. In Knop et al., 2020[16], we investigated the role of FRC/LEC-derived IL-7 in regulating peripheral T cell homeostasis *in vivo* (see chapter 4).

Regulation of T cell responses

FRC-released CCL19 and CCL21 attract CCR7-expressing DCs and T cells to the LNs, which increases the likelihood of DC-T cell interactions[119,120,130,131]. Additionally, CCL21 controls the motility and migration of $CCR7^+$ T cells and DCs inside the LN[130,131]. Upon viral infection, macrophages in the LN-SCS release IFN-I that is recognized by hematopoietic cells as well as LSCs and prevents lethal virus spread[132]. Furthermore, IFNAR-dependent up-regulation of programmed death ligand 1 (PD-L1) on LECs promotes their survival during immune responses[133]. Whether IFNAR signaling in LSCs impacts the differentiation of T_M remained an open question. In Knop et al., 2022[17], we investigated whether IFNAR signaling in FRCs affects the memory fate decision of $CD8^+$ T cells (see chapter 5).

Successful T-DC interactions lead to T_N activation and T_{EFF} proliferation. Hence, the LN size is adjusted to meet the increased space requirement of expanding lymphocytes

(see Figure 1-5)[134–136]. For example, CLEC-2 expressed on mature DCs mediates relaxation and stretching of FRCs by binding to gp38[68,69]. Additionally, proliferation of BECs, LECs and FRCs further supports swelling of the LN[137].

Upon activation, $CD8^+$ T_{EFF} release IFN-γ[138], which acts in an autocrine manner on T cells. As mentioned earlier, IFN-γR signaling in $CD8^+$ T cells promotes T_{EFF} expansion and memory differentiation[95–97]. However, stromal cells are also part of the T cell microenvironment and IFN-γ-responsive non-hematopoietic cells regulate multiple aspects of T cell responses. On the one hand, IFN-γ induces the expression of T cell stimulatory molecules by FRCs *in vitro*, such as MHC-I/-II and CD80[139]. The recruitment of activated $CD8^+$ T cells into the inflamed tissue is supported by the IFN-γ-induced up-regulation of vascular cell adhesion molecule 1 (VCAM-1) on endothelial cells[140]. Additionally, T_H1-secreted IFN-γ up-regulates CXCL9 and CXCL10 in epithelial cells, which recruits $CXCR3^+$ $CD8^+$ T_{EFF} cells to the inflammation site[141]. In contrast, T cell responses are also suppressed by IFN-γ-responsive non-hematopoietic cells. In the LN, IFN-γ counter-regulates CCL21 expression and the subsequent recruitment of T_N to the activated LN[142]. This feedback loop prevents further T cell priming and thus contributes to the termination of IFN-γ-associated immune responses[142]. This mechanism is supposed to be crucial for host survival since uncontrolled IFN-γ action can cause tissue damage and even the death of the host[143,144]. Likewise, T cell-derived IFN-γ reduces the density of lymphatic vessels in the LNs, potentially via down-regulating lymphangiogenic molecules in LECs[145]. This process is thought to counter-regulate immune responses as well[145]. In response to IFN-γ, FRCs and LECs express inducible nitric oxide synthase 2 (iNOS) and produce highly reactive nitric oxide (NO), thereby blocking T cell proliferation[146,147]. Furthermore, FRCs up-regulate indoleamine 2,3 dioxygenase 1 (IDO-1) that metabolizes L-tryptophan to kynurenines and depletes L-tryptophan from the local environment[146–148]. IDO-1 expression by mesenchymal stem cells was shown to have anti-proliferative effects on activated T cells[149].

In summary, LSCs support T cells in the steady state and under inflammatory conditions. LSCs are part of the T cell microenvironment and can respond to inflammatory stimuli, such as IFN-I and IFN-γ. However, whether IFNAR/IFN-γR signaling in LSCs regulates T_M differentiation *in vivo* remains poorly defined.

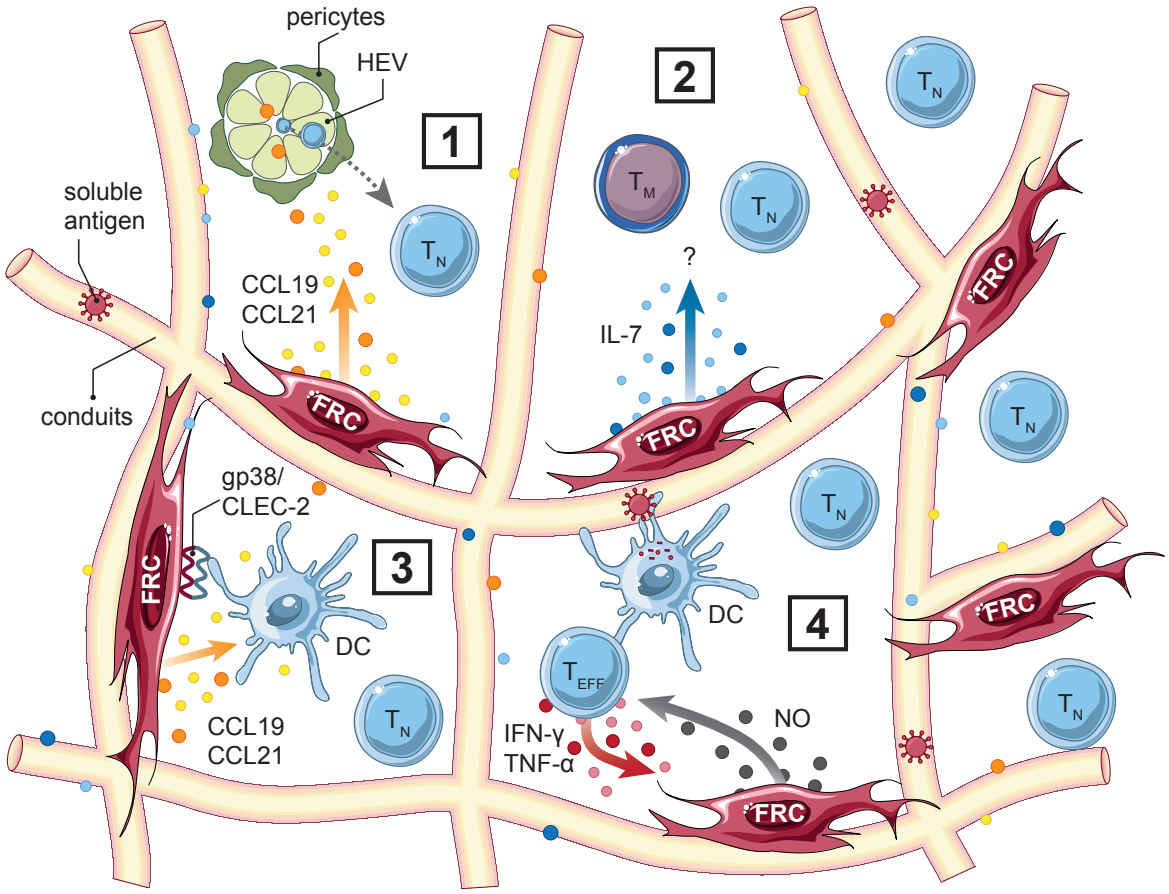

Figure 1-8. FRC-T cell interactions in the steady state and after infection (adapted from[150]). FRCs are located in the T cell zone of the lymph node and produce and form the conduit system, which transports Ags and soluble molecules deep into the paracortex. **(1)** The FRC-derived chemokines CCL19 and CCL21 attract CCR7$^+$ T cells and DCs into the LN. T cells enter the paracortex through HEVs, which are enclosed by pericytes. **(2)** We studied in Knop et al., 2020[16], whether LN-FRC-released IL-7 is essential for the survival of T_N/T_M *in vivo* (see chapter 4). **(3)** Gp38-CLEC-2 interactions with activated DCs cause stretching and relaxation of FRCs, thereby creating space for proliferating T cells. **(4)** IFN-γ and TNF-α are recognized by FRCs that start producing iNOS and release NO, which dampens T cell responses[150]. This figure was created using illustrations from www.bioicons.com[21].

1.3 Immune cell homeostasis

After pathogen clearance, T_{SLEC} undergo apoptosis, long-lived T_M occupy their anatomical niches and the immune system returns to a state of homeostasis (see Figure 1-5)[1]. Several homeostatic mechanisms are operative in order to (1) prevent uncontrolled immune activation, (2) limit the size of the peripheral T cell pool and (3) maintain a diverse T cell repertoire at the same time[74]. Similar to larger ecosystems harboring multiple species, the competition for survival factors is an important regulatory principle that also applies to the immune system. For example, T_N and T_M maintenance relies on IL-7[127], which is released by stromal cells[58] and also serves as a survival factor for other immune cells[151]. IL-7-dependent immune cells may occupy different ecological niches to limit competition and maximize survival. This hypothesis

was investigated in the second publication presented in this thesis (Knop et al., 2020[16]; see chapter 4).

1.3.1 Role of IL-7 in T cell homeostasis

IL-7 was initially described in 1988 as a growth-promoting factor for murine B cell precursors[152]. Over the last decades, knowledge regarding the biological activities of IL-7 has accumulated. Today IL-7 is known to be essential for the development of B cells, T cells and most ILC subsets[3,153,154]. The non-redundant role of IL-7 for the survival of T/B lymphocyte precursors was demonstrated in IL-7 and IL-7R knockout mice that exhibit profound defects in T and B cell development and lack mature T and B cells[155,156]. Likewise, defective IL-7R expression in humans causes severe combined immunodeficiency (SCID), represented by reduced T cell numbers[157].

IL-7 is bound by the IL-7R, which is a heterodimeric receptor consisting of the IL-7Rα chain (CD127) and the common γ-chain (CD132) (see Figure 1-9)[153]. IL-7R signaling involves phosphorylation of STAT5 and degradation of the transcription factor forkhead box O1 (Foxo1)[3,153]. IL-7 withdrawal leads to translocation of Foxo1 into the nucleus and expression of CD62L, CCR7 and IL-7Rα, thereby regulating T cell trafficking and survival[158]. The pro-survival signals initiated by IL-7R signaling mainly result from an increased metabolic activity and the induction of anti-apoptotic molecules, such as B-cell lymphoma 2 (Bcl-2) and myeloid cell leukemia-1 (Mcl-1)[153].

During T cell ontogeny, the expression of IL-7Rα is strongly regulated[3,153,159]. In the BM, common-lymphoid progenitors express IL-7Rα and give rise to the T and B cell lineages[160]. Emigrating from the BM, IL-7Rα$^-$ early thymic progenitors seed the thymus (see Figure 1-4) and give rise to all αβ$^+$ T cells[18,19]. During thymocyte development, the IL-7Rα is up-regulated and the resulting peripheral T_N are IL-7Rα$^+$ [160]. Interestingly, T cells intermittently down-regulate the IL-7Rα after ligand binding[161]. The oscillating nature of IL-7Rα-expression ensures the survival of T cells by preventing IL-7-induced cell death[161]. The intermittent down-regulation of IL-7Rα is observed in T cells but does not apply to retinoid orphan receptor γ t (RORγt$^+$) ILCs[162]. Hence, IL-7-dependent immune cell subsets differentially consume IL-7, which supports the maintenance of IL-7-dependent homeostasis.

Upon TCR stimulation, the activation of the PI3K pathway leads to degradation of Foxo1, thereby suppressing IL-7Rα expression[160,163]. Therefore, IL-7Rα expression rapidly declines in the majority of the T_{EFF} population after activation[73]. As opposed to IL-7Rα$^-$ T_{SLEC}, T_{MP} retain IL-7Rα expression in the effector phase[73]. The resulting T_M continue to express IL-7Rα since they require IL-7 signals for long-term survival[127,164]. For example, IL-7R signaling in CD8$^+$ T_M induces the up-regulation of the glycerol transporter aquaporin 9 (AQP9)[107], thereby promoting fatty acid oxidation and subsequent ATP synthesis[67,103,104].

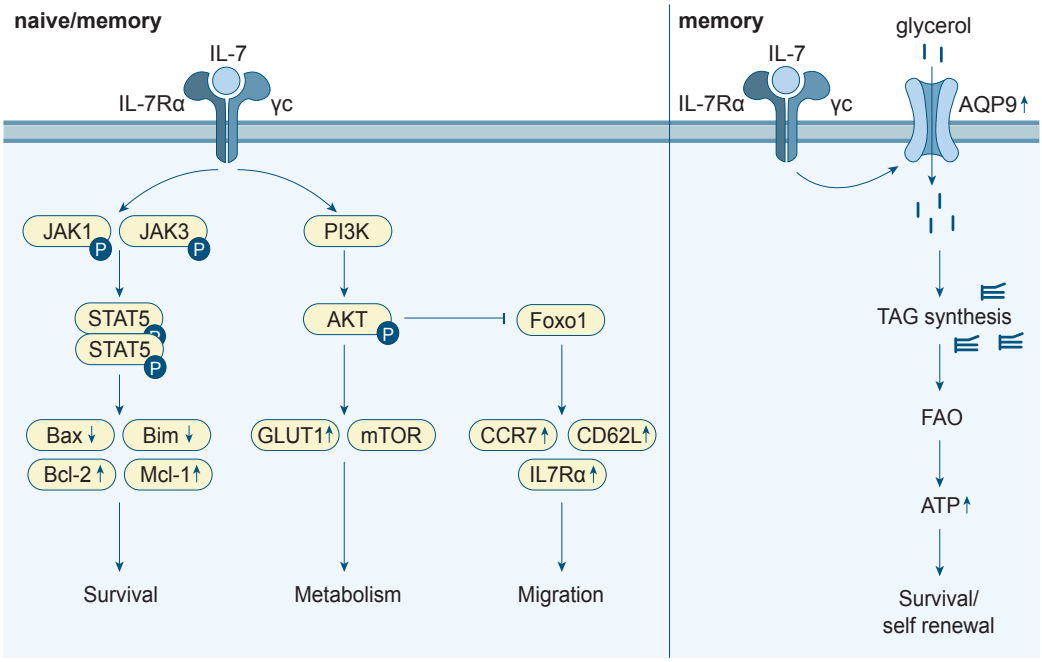

Figure 1-9. IL-7R signaling in T_N and T_M (adapted from [107,165]). In T_N and T_M, IL-7R signaling activates JAK1/3, which phosphorylate STAT5. Dimers of phosphorylated STAT5 translocate into the nucleus and up-regulate pro-survival factors, such as Bcl-2 and Mcl-1. Furthermore, pSTAT5 leads to the down-regulation of pro-apoptotic molecules, such as Bax and Bim. The IL-7R-induced activation of the PI3K pathway leads to the activation of mammalian target of rapamycin (mTOR) and the up-regulation of the glucose transporter 1 (GLUT1). Foxo1 is degraded upon PI3K activation. Without IL-7 stimulation, Foxo1 is activated and up-regulates CCR7, CD62L and IL-7Rα[3,160,166]. In T_M, the IL-7R-dependent expression of AQP9 facilitates the influx of glycerol, triacylglyceride (TAG) synthesis and consequently the generation of ATP through fatty acid oxidation[107].

1.3.2 Lymphopenia-induced proliferation of T cells and development of virtual memory T cells

In a healthy host, IL-7 is continuously consumed by IL-7-dependent cells and controls the size of the T cell pool[166]. Under lymphopenic conditions however, the T cell pool is reduced. Lymphopenia can be inherited and occurs under SCID conditions[5,167]. For example, recombination-activating gene 1 $(Rag1)^{-/-}$ mice lack mature T/B cells and are severely lymphopenic[168]. Human *RAG* gene mutations are associated with severe infections or autoimmunity as well[169]. Furthermore, lymphopenia can be acquired, e.g., as a result of infections with human immunodeficiency virus (HIV) or severe acute respiratory syndrome coronavirus type 2 (SARS-CoV2). Additionally, lymphopenia is caused by medical interventions, such as chemotherapy or radiation[5,167].

T_N survival requires accessibility to IL-7[170–172] and depends on continuous low-level TCR signaling by self-peptide-MHC complexes[173–175]. Due to the lack of lymphocytes in lymphopenic hosts, the amount of IL-7 increases and self-peptide-MHC-complexes become more available[4,5,176]. Since the overabundance of both factors promotes T cell activation, T_N transferred into a lymphopenic host undergo **lymphopenia-induced proliferation (LIP)** and

differentiate into so-called **virtual memory T cells (T_{VM})**[5]. Similar to Ag-experienced T_M, T_{VM} display high levels of CD44 and produce substantial amounts of IFN-γ upon short-term stimulation[177–179]. Notably, the LIP-induced accumulation of IFN-γ^+ T cells is associated with autoimmunity[5,167,180,181].

The degree of LIP varies strongly between T cell clones as it is determined by cell-intrinsic properties such as TCR affinity for self-peptide-MHC-complexes and the abundance of molecules counter-regulating TCR signaling, such as CD5[182,183]. For example, DO11.10 TCR-transgenic $CD4^+$ T cells, recognizing the I-A^d-restricted, chicken ovalbumin (ova)-derived peptide $ova_{323-339}$, undergo LIP in irradiated hosts[184]. In contrast, LIP of $CD4^+$ OT-II TCR-transgenic T cells specific for $ova_{323-339}$ presented by I-A^b is by far less pronounced[184]. LIP of T cells is also regulated by T cell-extrinsic factors. Interestingly, neonatal mice naturally display lymphopenia because the T cell pool is not yet established[185,186]. Therefore, freshly generated T_N undergo IL-7-dependent LIP in neonates and develop into long-lived T_{VM} that are sustained in adult mice[185,186]. However, only a small fraction of T_N undergoes LIP in neonates because IL-7R-dependent ILCs limit LIP of most T_N in the first weeks of life[187]. Furthermore, the capability of the host to respond to IFN-γ is crucial to limit LIP of TCR-transgenic $CD8^+$ OT-I T cells (recognizing $ova_{257-264}$-peptide presented on H-$2K^b$)[100]. Whether T cell-extrinsic mechanisms contribute to the blockade of OT-II LIP remained unclear. In Knop et al., 2019[15], we investigated whether IFN-γR signaling in host cells suppresses LIP of $CD4^+$ OT-II T cells (see chapter 3).

2 Objectives and experimental approaches

Publication I

Title: Interferon-γ receptor signaling in dendritic cells restrains spontaneous proliferation of $CD4^+$ T cells in chronic lymphopenic mice[15]

In Knop et al., 2019, we aimed to decipher whether IFN-γR signaling in non-T cells contributes to the suppression of OT-II LIP. To answer this question, we applied adoptive T cell transfers into lymphopenic mice. In particular, we analyzed the LIP of $CD4^+$ OT-II T cells after transfer into IFN-$\gamma R^{-/-}$ x $Rag1^{-/-}$ ($Rag^{\gamma Rko}$) mice using flow cytometry. Additionally, we examined the contribution of OT-II-derived or host-derived IFN-γ to OT-II LIP. The role of the commensal microflora in modulating OT-II LIP in IFN-$\gamma R^{-/-}$ x $Rag1^{-/-}$ mice was further studied using antibiotic treatments. We observed an accumulation of DCs and IL-6 in OT-II reconstituted IFN-$\gamma R^{-/-}$ x $Rag1^{-/-}$ mice. Hence, OT-II expansion was analyzed during antibody blockade of IL-6. To elucidate the contribution of IFN-γR signaling in DCs on OT-II LIP, we used a Cre-loxP-based approach to restore the IFN-γR specifically on DCs and analyzed OT-II LIP in these mice.

Publication II

Title: IL-7 derived from lymph node fibroblastic reticular cells is dispensable for naive T cell homeostasis but crucial for central memory T cell survival[16]

In Knop et al., 2020, we asked whether LN-LSC-derived IL-7 affects T_N/T_M homeostasis. To distinguish the contribution of LEC- and FRC-derived IL-7 to the survival of T_N/T_M, we first generated and characterized conditional IL-7 knockout (IL-$7^{fl/fl}$) mice. To delete IL-7 expression in LECs or FRCs, we crossed IL-$7^{fl/fl}$ mice to LEC-specific Lyve1-Cre ($LEC^{\Delta IL\text{-}7}$) or FRC-specific Prx1-Cre mice ($FRC^{\Delta IL\text{-}7}$), respectively. Additionally, mice with a simultaneous IL-7 deletion in LECs and FRCs were generated ($LEC/FRC^{\Delta IL\text{-}7}$). Using flow cytometry, we determined the relative impact of either IL-7 source on $CD4^+/CD8^+$ T_N as well as T_{EM}/T_{CM} homeostasis in LNs and spleens of healthy mice. Furthermore, the TCR repertoires were analyzed via a flow cytometry-based approach. The contribution of FRC-derived IL-7 in T_M formation was further studied by applying OT-I T cell transfers and peptide vaccination.

Publication III

Title: IFNAR signaling in fibroblastic reticular cells can modulate $CD8^+$ memory fate decision[17]

In Knop et al., 2022, we investigated whether IFNAR signaling in FRCs affects T_M fate decision. To delete IFNAR-expression in FRCs, conditional IFNAR knockout ($IFNAR^{fl/fl}$) mice were crossed to Prx1-Cre mice ($FRC^{\Delta IFNAR}$). T_M formation was studied in two different scenarios using flow cytometry. On the one hand, we applied OT-I T cell transfers and vaccinations and analyzed the T cell response in the expansion, contraction and memory phase. Furthermore, LN-LSCs were analyzed one day post OT-I transfer and subsequent vaccination. Additionally, the mRNA expression of chemokines and IL-7 was analyzed in LNs. On the other hand, we infected $FRC^{\Delta IFNAR}$ and controls with vesicular stomatitis virus and analyzed the polyclonal T cell response in the different phases.

3 Publication I

Title: Interferon-γ receptor signaling in dendritic cells restrains spontaneous proliferation of $CD4^+$ T cells in chronic lymphopenic mice[15]

Journal: Frontiers in Immunology

Publication year: 2019

DOI: 10.3389/fimmu.2019.00140

Authors:

LK	Laura Knop	TB	Thomas Blankenstein
CF	Charlotte Frommer	TK	Thomas Kammertoens
DS	Diana Stoycheva	ID	Ildiko Rita Dunay
KD	Katrin Deiser	TS	Thomas Schüler
UK	Ulrich Kalinke		

Table 3-1. Author contributions in publication I.

Author	Contribution in %
Study design and supervision	
LK, DS	10 each
TS	90
Performance of experiments	
LK	60
CF	30
DS, KD	5 each
Data collection and figure preparation	
LK	100
Data analysis and interpretation	
LK	30
CF, DS, KD, UK, TB, TK, ID	5 each
TS	35
Manuscript preparation	
LK	25
CF, DS, KD, UK, TB, TK, ID	10 together
TS	65

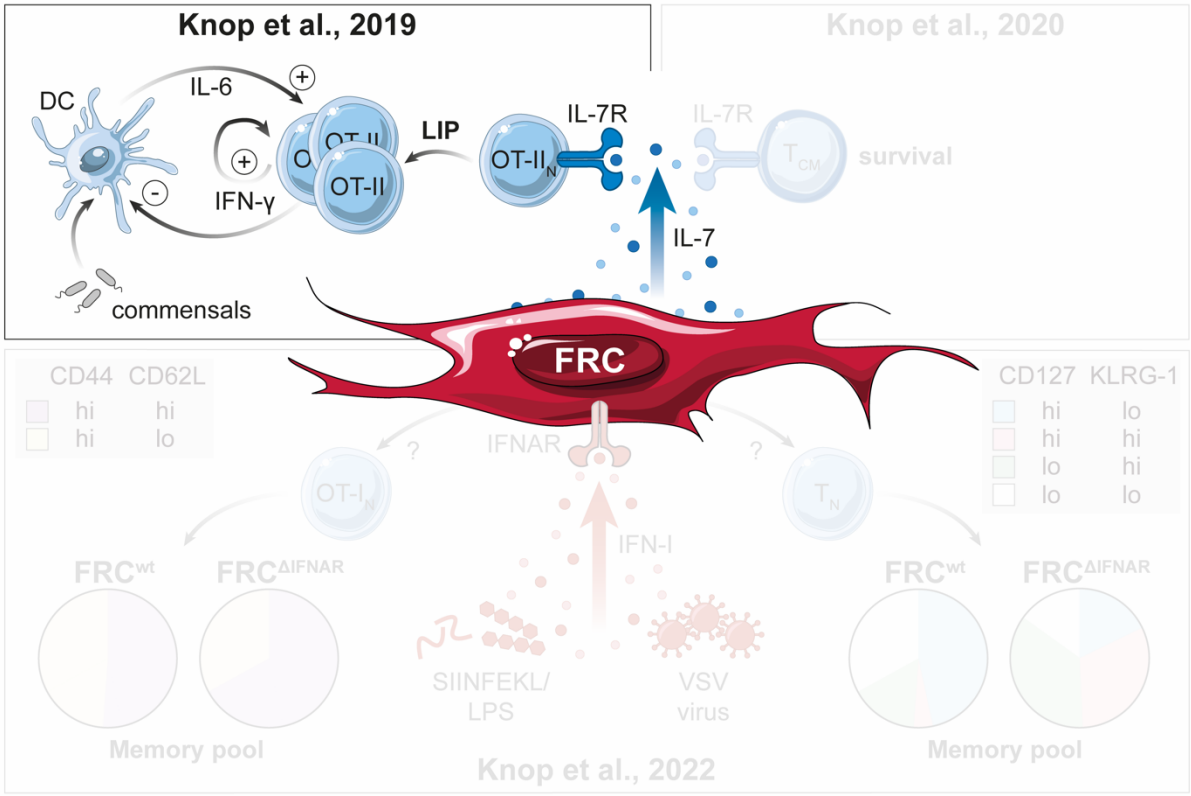

Figure 3-1. Graphical representation of Knop et al., 2019[15]**.** In lymphopenic hosts, stromal cell-released IL-7 and self-peptide-MHC-complexes are highly available because of a lack of consuming cells[4,5,176]. Upon transfer into T/B cell-deficient hosts, T_N undergo LIP and produce IFN-γ[5,167]. Their capability to undergo LIP depends on the T cell clone and OT-II $CD4^+$ T cells have a reduced LIP capacity[184]. Whether T cell-extrinsic factors contribute to suppression of OT-II LIP remained unclear. In Knop et al., 2019, we observed that OT-II T cells were undergoing LIP in IFN-γR deficient lymphopenic hosts[15]. This process depended on an intact microflora and we detected increased DC numbers and an accumulation of IL-6. IFN-γR-expression on DCs alone was sufficient to restrict LIP of OT-II T cells. This figure was created using illustrations from www.bioicons.com[21].

frontiers in Immunology

ORIGINAL RESEARCH
published: 07 February 2019
doi: 10.3389/fimmu.2019.00140

Interferon-γ Receptor Signaling in Dendritic Cells Restrains Spontaneous Proliferation of CD4$^+$ T Cells in Chronic Lymphopenic Mice

Laura Knop[1†], Charlotte Frommer[1†], Diana Stoycheva[1†], Katrin Deiser[1], Ulrich Kalinke[2], Thomas Blankenstein[3,4,5], Thomas Kammertoens[3], Ildiko Rita Dunay[6] and Thomas Schüler[1]*

[1] Institute of Molecular and Clinical Immunology, Medical Faculty, Otto-von-Guericke University, Magdeburg, Germany, [2] TWINCORE, Centre for Experimental and Clinical Infection Research, a joint venture between the Helmholtz Centre for Infection Research and the Medical School Hannover, Institute for Experimental Infection Research, Hannover, Germany, [3] Institute of Immunology, Charité-Universitätsmedizin Berlin, Berlin, Germany, [4] Max-Delbrück-Center for Molecular Medicine, Berlin, Germany, [5] Berlin Institute of Health, Berlin, Germany, [6] Institute of Inflammation and Neurodegeneration, Medical Faculty, Otto-von-Guericke University, Magdeburg, Germany

OPEN ACCESS

Edited by:
Loretta Tuosto,
Sapienza University of Rome, Italy

Reviewed by:
Niklas Beyersdorf,
Universität Würzburg, Germany
Hyun Park,
National Cancer Institute (NCI),
United States

***Correspondence:**
Thomas Schüler
thomas.schueler@med.ovgu.de

[†] These authors have contributed equally to this work

Specialty section:
This article was submitted to T Cell Biology, a section of the journal Frontiers in Immunology

Received: 31 August 2018
Accepted: 17 January 2019
Published: 07 February 2019

Citation:
Knop L, Frommer C, Stoycheva D, Deiser K, Kalinke U, Blankenstein T, Kammertoens T, Dunay IR and Schüler T (2019) Interferon-γ Receptor Signaling in Dendritic Cells Restrains Spontaneous Proliferation of CD4$^+$ T Cells in Chronic Lymphopenic Mice. Front. Immunol. 10:140. doi: 10.3389/fimmu.2019.00140

In lymphopenic mice, T cells become activated and undergo lymphopenia-induced proliferation (LIP). However, not all T cells are equally sensitive to lymphopenia. Several lymphopenia-insensitive T cell clones were described and their non-responsiveness was mainly attributed to clone-specific properties. Here, we provide evidence for an additional, host-dependent mechanism restraining LIP of lymphopenia-insensitive CD4$^+$ T cells. We show that such cells undergo LIP in lymphopenic mice lacking IFN-γ receptor (IFN-γR) expression, a process, which is promoted by the autocrine action of T cell-derived IFN-γ. Additionally, LIP of lymphopenia-insensitive CD4$^+$ T cells requires an intact microflora and is accompanied by the massive accumulation of IL-6 and dendritic cells (DCs). Consistent with these results, IL-6 neutralization and the DC-specific restoration of IFN-γR expression are both sufficient to restrict LIP. Hence, the insensitivity of CD4$^+$ T cells to lymphopenia relies on cell-intrinsic properties and a complex interplay between the commensal microflora, IL-6, IFN-γR$^+$ DCs, and T cell-derived IFN-γ.

Keywords: CD4$^+$ T cells, interferon-γ, lymphopenia, lymphopenia-induced proliferation (LIP), dendritic cells

INTRODUCTION

In lymphocyte-competent hosts, T cells continuously utilize homeostatic factors such as Interleukin-7 (IL-7) and self-peptide-MHC complexes and thereby limit their availability (1). Due to the lack of IL-7-consuming T cells, IL-7 accumulates in lymphopenic mice (2) and humans (3). IL-7 is a potent activation and survival signal for T cells and its overabundance promotes T cell responses (4). Consequently, the adoptive transfer of polyclonal naive CD4$^+$ T cells into lymphopenic mice leads to their activation and subsequent lymphopenia-induced proliferation (LIP) (5, 6). However, LIP represents a mixed reaction in response to different stimuli. While IL-7 overabundance induces a comparably slow homeostatic proliferation (HP) of T cells, the commensal microflora triggers a rapid response referred to as spontaneous proliferation (SP) (7–11). Nevertheless, naive T cells undergoing LIP differentiate into interferon-γ (IFN-γ)-producing effector/memory T cells, which is frequently associated with autoimmunity (12, 13).

The degree of LIP varies strongly between T cell clones (14–16). For example, ovalbumin (OVA)-specific CD4$^+$ TCR-transgenic (tg) OT-II T cells, contrary to polyclonal CD4$^+$ T cells, do not undergo LIP in irradiated hosts (14) and expand only moderately in fully lymphopenic Rag-deficient (Rag$^{-/-}$) mice (10). TCR signal strength is a major factor that regulates the sensitivity of a T cell to lymphopenia (15, 16). It is affected by a complex interplay between TCR avidity and molecules modulating TCR signal transduction (15, 17, 18). Hence, cell-intrinsic mechanisms appear to determine whether a T cell is sensitive to lymphopenia or not. However, it remained unclear whether extrinsic mechanisms prevent LIP of lymphopenia-insensitive CD4$^+$ T cells.

In the present study, we show that lymphopenia-insensitive OT-II cells expand massively in IFN-γ receptor (IFN-γR)-deficient Rag$^{-/-}$ (Rag$^{\gamma Rko}$) mice, a phenomenon that is not observed in IFN-γ-deficient Rag$^{-/-}$ (Rag$^{\gamma ko}$) mice. LIP of OT-II cells is associated with a strong increase in systemic IL-6 and subsequent T cell accumulation. The lack of IFN-γ and IFN-γR expression by OT-II cells impaired LIP to some degree arguing for a growth promoting, autocrine effect of OT-II-derived IFN-γ. Furthermore, we show that the commensal microflora is crucial for OT-II LIP in Rag$^{\gamma Rko}$ mice, which is accompanied by the massive expansion of dendritic cells (DCs). Finally, we show that IFN-γR expression exclusively in DCs is sufficient to restrict OT-II expansion, DC accumulation and IL-6 production in Rag$^{\gamma Rko}$ mice. In summary, we provide evidence that the suppression of CD4$^+$ T cell activation in response to lymphopenia is determined by a combination of both, clone-specific properties and environmental factors such as the commensal microflora, IL-6 and IFN-γR expression by DCs.

MATERIALS AND METHODS

Mice and Adoptive T Cell Transfer

Thy1.1$^+$ B6.PL-Thy1a/Cy and Thy1.2$^+$ B6.129S7-Rag1^{tm1Mom}/J (Rag$^{-/-}$), C57BL/6J (B6), B6.SJL-Ptprc^{a}Pepc^b/BoyJ (CD45.1$^+$), B6.129S7-Ifnγ^{tm1Ts} (IFN-γ$^{-/-}$), B6.129S7-Ifngr^{tm1Agt} (IFN-γR$^{-/-}$), B6.Cg-Tg(TcraTcrb)425Cbn/J (OT-II) (expressing a transgenic TCR specific for the chicken ovalbumin (OVA)-derived, I-A^b-restricted peptide OVA$_{323-339}$), B6.Cg-Tg(Itgax-EGFP-CRE-DTR-LUC)2Gjh/Crl (CD11c-GCDL) (19) and pCAG^{loxP}STOP^{loxP}-IFNγR-IRES-GFP (IFN-γR^{SO}) transgenic mice (20) were housed under specific pathogen-free conditions. Mice were crossed to generate Thy1.1/.2/CD45.1/.2-disparate Rag$^{-/-}$OT-II (OT-II^{WT}), Rag$^{-/-}$IFN-γR$^{-/-}$OT-II (OT-II$^{\gamma Rko}$), and Rag$^{-/-}$IFN-γ$^{-/-}$OT-II (OT-II$^{\gamma ko}$) T cell donors. Lymphopenic Rag$^{-/-}$ (Rag^{WT}), Rag$^{-/-}$IFN-γ$^{-/-}$ (Rag$^{\gamma ko}$), Rag$^{-/-}$IFN-γR$^{-/-}$ (Rag$^{\gamma Rko}$), and Rag$^{-/-}$IFN-γR$^{-/-}$ × CD11c-GCDL × IFN-γR^{SO} (Rag$^{\gamma Rko}$ × IFN-γR$^{CD11c-ON}$) mice served as T cell recipients. For the adoptive transfers shown in **Figures 2A,B**, B6 or CD45.1$^+$ mice served as non-lymphopenic controls. For T cell transfers, single cell suspensions were prepared from spleens and lymph nodes of donor mice by forcing the organs through metal sieves. To lyse erythrocytes, cell suspensions were incubated with Ammonium-Chloride-Potassium lysis buffer for 90 s and subsequent addition of RPMI with 10% FCS. After washing with PBS/2mM EDTA, cell suspensions were resuspended in PBS and filtered through 40 μm cell strainers (BD and Corning, Durham, NC). Single cell suspensions were counted, stained with fluorochrome-labeled antibodies for 30 min at 4°C and analyzed by flow cytometry to determine the frequency and activation state of OT-II cells (**Supplementary Figure 1**). Cell suspensions containing 1.6–10 × 10^5 naive CD4$^+$ OT-II T cells were injected i.v. into the tail vein of recipient mice. For CFSE labeling, donor single cell suspensions (2.2–3.2 × 10^7 cells/ml) were incubated with 7.5 μM CFSE (Biolegend) in PBS for 20 min at 37°C. Subsequently, cells were washed twice with ice cold PBS or RPMI/10% FCS and were resuspended in PBS prior to injection. Cell suspensions containing 7.5–8 × 10^5 CFSE$^+$ OT-II T cells were injected i.v. into the tail vein of recipient mice. Ten to thirteen days after transfer, spleens and lymph nodes were isolated and single cell suspensions were prepared as described. Erythrocyte lysis was performed with spleen cell samples. Cells were counted and directly stained with fluorochrome-labeled antibodies for 30 min at 4°C after blocking FcR with purified anti-CD32/CD16 monoclonal antibodies (2.4G2 ATCC® HB-197™). To neutralize IL-6 *in vivo*, mice were i.p. injected with 500 μg of anti-IL-6 (MP5-20F3; BioXCell) 2 days prior to OT-II transfer. Treatment was repeated every third day. Control mice received 500 μg control IgG1 (HRPN; BioXCell). To deplete the commensal microflora, mice were treated with 0.5 g/l vancomycin, 1.0 g/l metronidazole, 1.0 g/l ampicillin, and 1.0 g/l neomycinsulfate via the drinking water 4 weeks prior to and during the experiment (21). Mice treated with antibiotics did not show any obvious clinical symptoms. At the day of analysis, however, their cecum was enlarged indicating successful depletion of the commensal microflora.

Flow Cytometry

The following antibodies and reagents were used: anti-CD4 (RM4-5; Biolegend/eBioscience), -CD11c (N418; BD/Biolegend), -CD44 (IM7; Biolegend), -CD45.1 (A20; Biolegend), -CD62L (MEL-14; Biolegend), CD127 (A7R34; BD/Biolegend), -KLRG-1 (2F1; Biolegend/eBioscience), -Ki67 (SolA15; eBioscience), -I-A^b (AF6-120.1; Biolegend), -Thy1.1 (OX-7; Biolegend), -TCR Vα2 (B20.1; Biolegend), streptavidin-BV510 (Biolegend) and streptavidin-PE (Biolegend). For intranuclear staining of Ki67, cells were first stained with the indicated antibodies directed against cell surface molecules. Afterwards cells were fixed with the Foxp3/Transcription Factor Staining Buffer Set (eBioscience) according to the manufacturer's instructions and subsequently incubated with anti-Ki67 for 30 min at 4°C. Samples were measured on LSRFortessa flow cytometer (Becton Dickinson) and analyzed by FlowJo 9 and 10 software (FlowJo, LLC). To calculate the fold expansion of OT-II cells or DCs, the respective cell populations were quantified. For each experiment a mean value was calculated for the Rag^{WT} group. Finally, cell numbers of individual mice, including Rag^{WT} mice, were calculated in relation to the mean value of the Rag^{WT} group. Relative mean fluorescence intensities (MFIs) and relative frequencies of OT-II cells or DCs were calculated in analogy.

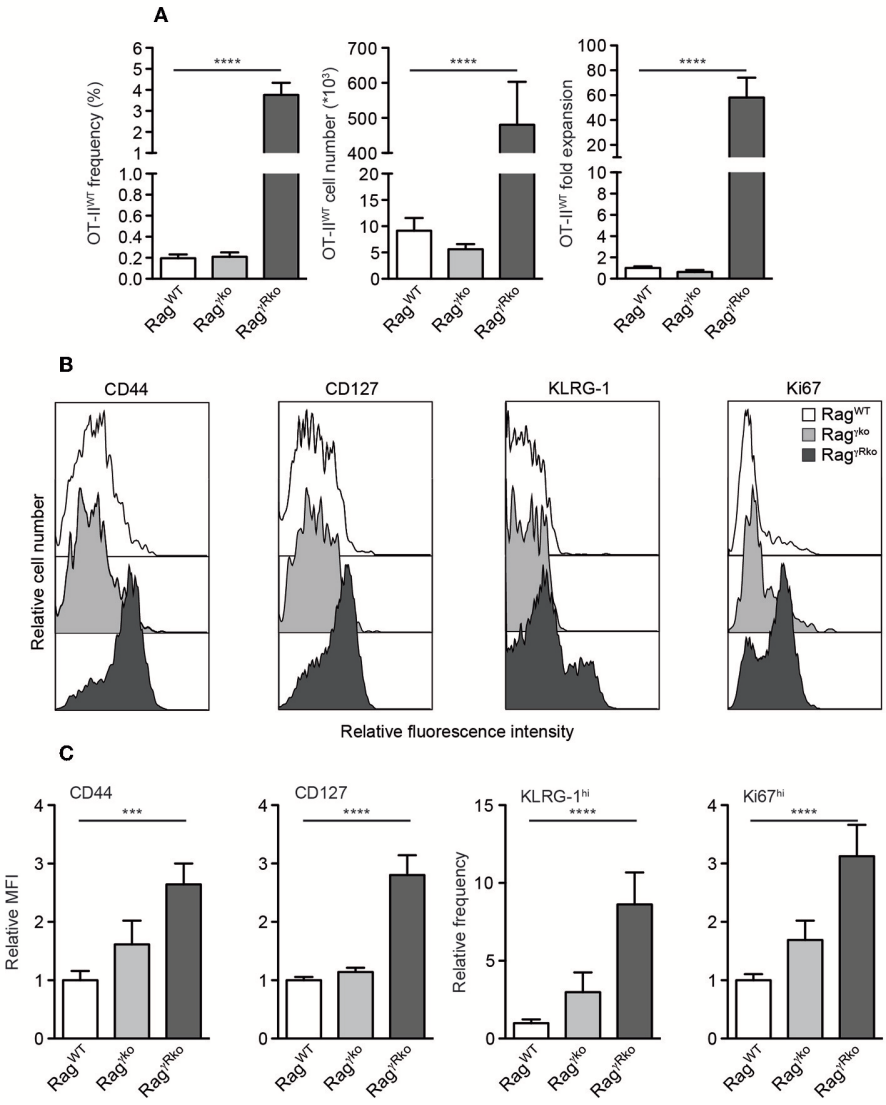

FIGURE 1 | CD4+ T cell LIP is amplified in IFN-γR-deficient mice. **(A–C)** CD4+Thy1.1+ OT-II^{WT} T cells were adoptively transferred into Rag^{WT}, Rag$^{\gamma ko}$ and Rag$^{\gamma Rko}$ mice (all Thy1.1−). After 10–12 days, recipient splenocytes were analyzed by flow cytometry. **(A)** Shown are frequencies, cell numbers and fold expansion of OT-II^{WT} cells. **(B)** Relative fluorescence intensities, **(C)** relative MFIs for CD44 and CD127 and relative frequencies of KLRG-1^{hi} and Ki67^{hi} cells were determined after gating on CD4+Thy1.1+ OT-II^{WT} cells. **(A,C)** Shown are pooled results from 3 to 4 independent experiments with a total of 11–17 mice per group and **(B)** representative histograms from corresponding samples. **(A,C)** Graphs show mean values + SEM and statistical significances (***$p \leq 0.001$; ****$p \leq 0.0001$) were calculated to values in Rag^{WT} mice.

IFN-γ and IL-6 Detection

Blood (supplemented with EDTA) was centrifuged 10 min at 500 × g and 4°C. The supernatant was centrifuged again 10 min at 900 × g and 4°C to obtain the plasma that was analyzed by an IFN-γ or IL-6 specific ELISA (eBioscience) according to manufacturer's instructions.

Statistical Analysis

Statistical analysis and graphical representations were done using Prism 5 software (GraphPad Software). Statistical significance was determined using a non-parametric two-tailed Mann-Whitney *U*-test. *$p \leq 0.05$; **$p \leq 0.01$; ***$p \leq 0.001$; ****$p \leq 0.0001$.

RESULTS

Host IFN-γR Expression Restrains Commensal-Driven OT-II LIP

We have shown that host IFN-γR signaling restricts LIP of CD8+ T cells (22). Whether this mechanism prevents LIP of CD4+ OT-II T cells was unclear. To address this issue, naive CD4+ T cells from Rag−/− OT-II TCR^{tg} mice (OT-II^{WT} cells) were

adoptively transferred into IFN-γR-deficient Rag$^{-/-}$ (Rag$^{\gamma Rko}$) and IFN-γR-competent Rag$^{-/-}$ (Rag^{WT}) mice. To elucidate a potential contribution of host-derived IFN-γ, IFN-γ-deficient Rag$^{-/-}$ mice (Rag$^{\gamma ko}$) were reconstituted with OT-II^{WT} cells in parallel. Within 10–12 days, OT-II^{WT} cells expanded massively in Rag$^{\gamma Rko}$ but not in Rag^{WT} or Rag$^{\gamma ko}$ spleens (**Figure 1A**). LIP was associated with the up-regulation of CD44, CD127, KLRG-1, and Ki67 indicating full activation and proliferation of OT-II^{WT} cells in Rag$^{\gamma Rko}$ mice (**Figures 1B,C**). LIP is induced in T cell areas of secondary lymphoid organs (SLOs) (23) and IFN-γ regulates T cell migration to and positioning in SLOs (24–26), which is guided by chemokine-producing stromal cells (27). However, stromal cell composition differs significantly between lymph nodes (LNs) and spleen (28). We therefore asked next whether OT-II expansion is equally well induced in either SLO. To address this question, CFSE-labeled OT-II^{WT} cells were transferred into Rag^{WT} and Rag$^{\gamma Rko}$ mice. C57BL/6 (B6) served as non-lymphopenic controls. After 12 days, recipient LNs and spleens were analyzed. As shown in **Figures 2A,B**, the frequencies of CFSE^{lo} OT-II^{WT} cells were lower in LNs than in spleen of both recipients. However, CFSE^{lo} OT-II^{WT} cells were clearly more abundant in Rag$^{\gamma Rko}$ spleens and LNs (**Figures 2A,B**) indicating higher frequencies of rapidly dividing OT-II^{WT} cells in either organ. Of note, in addition to the rapidly dividing CFSE^{lo} OT-II cells, a population of CFSE^{int} cells was detectable in the spleen, but not LNs, of Rag$^{\gamma Rko}$ mice (**Figures 2A,B**). This suggests different, organ-specific velocities of OT-II LIP. Nonetheless, OT-II^{WT} LIP was most pronounced in the spleens of Rag$^{\gamma Rko}$ mice. We therefore focused on this organ in the following experiments.

Under lymphopenic conditions, the rapid-type of T cell proliferation relies on the presence of an intact commensal microflora (7, 10). Whether this is also the case for OT-II expansion in Rag$^{\gamma Rko}$ mice was studied next. For this purpose, Rag^{WT} and Rag$^{\gamma Rko}$ mice were treated with a mixture of antibiotics prior to and during reconstitution with OT-II^{WT} cells. This treatment regimen efficiently depletes commensals (21, 29). As expected, OT-II^{WT} expansion was impaired in untreated Rag^{WT} mice but was very efficient in untreated Rag$^{\gamma Rko}$ mice (**Figure 2C**, white bars). On the contrary, antibiotic treatment blocked OT-II^{WT} LIP in Rag$^{\gamma Rko}$ mice (**Figure 2C**). Together, the data presented so far indicate that recipient IFN-γR expression restrains commensal-driven spontaneous proliferation (SP) (7–11) of OT-II cells under lymphopenic conditions.

IL-6 Accumulates in Rag$^{\gamma Rko}$ Mice and Promotes OT-II SP

IL-6 promotes commensal-dependent SP of CD4$^+$ and CD8$^+$ T cells in lymphopenic mice (9, 10). To elucidate whether IL-6 levels are altered in our experimental system, plasma samples from OT-II^{WT}-reconstituted Rag^{WT} and Rag$^{\gamma Rko}$ were analyzed 10–12 days after T cell transfer. As shown in **Figure 3A**, plasma levels of IL-6 were strongly elevated in OT-II^{WT}-reconstituted Rag$^{\gamma Rko}$ mice (**Figure 3A**; + OT-II^{WT}) but not in untreated controls (**Figure 3A**; –OT-II^{WT}). In order to test whether IL-6 promotes OT-II^{WT} SP in Rag$^{\gamma Rko}$ mice, Rag^{WT}, and Rag$^{\gamma Rko}$ mice were treated with neutralizing monoclonal anti-IL-6 antibodies (αIL-6 mAb) prior to and after reconstitution with OT-II^{WT} cells. Control mice received isotype-matched control mAbs. As shown in **Figure 3B**, αIL-6 treatment did not affect frequencies, cell numbers or relative expansion rates of OT-II^{WT} cells in Rag^{WT} mice. As expected, OT-II^{WT} cells were by far most abundant in isotype-treated Rag$^{\gamma Rko}$ mice, an effect that was fully reverted by IL-6 neutralization. Accordingly, expression levels of CD44 and Ki67 were strongly reduced in OT-II^{WT} cells recovered from αIL-6-treated Rag$^{\gamma Rko}$ mice as compared to isotype-treated controls (**Figures 3C,D**). Hence, IL-6 is up-regulated upon T cell transfer and is crucial for OT-II^{WT} activation, proliferation and subsequent accumulation in Rag$^{\gamma Rko}$ mice.

OT-II-Derived IFN-γ Promotes SP in an Autocrine Fashion

T cell-intrinsic IL-6R signaling promotes the expansion of IFN-γ-producing effector/memory CD4$^+$ T cells under lymphopenic and non-lymphopenic conditions (30, 31). Consequently, the blockade of OT-II^{WT} activation and subsequent SP in αIL-6-treated Rag$^{\gamma Rko}$ mice (**Figures 3B–D**) correlated with a strong reduction of plasma IFN-γ levels (**Figure 3E**).

Since IFN-γ directly promotes CD4$^+$ T cell responses (32–34), we hypothesized that OT-II-derived IFN-γ supports SP in Rag$^{\gamma Rko}$ mice in an autocrine fashion. To test this hypothesis, IFN-γ-deficient OT-II (OT-II$^{\gamma ko}$) cells were transferred into Rag$^{\gamma Rko}$ and Rag^{WT} mice. After 11–12 days, OT-II$^{\gamma ko}$ frequencies, cell numbers and relative expansion rates were determined. As shown in **Figure 4A**, some expansion of OT-II$^{\gamma ko}$ cells was detectable in Rag$^{\gamma Rko}$. This was associated with the up-regulation of CD44, KLRG-1 and Ki67 (**Figures 4B,C**). Importantly, however, OT-II$^{\gamma ko}$ cells expanded less well in Rag$^{\gamma Rko}$ mice (∼10-fold; **Figure 4A**) than OT-II^{WT} cells (∼50-fold; **Figure 1A**) suggesting a growth-promoting effect of autocrine IFN-γ.

To further test this possibility, equal numbers of OT-II^{WT} and OT-II$^{\gamma Rko}$ cells were co-transferred into Rag$^{\gamma Rko}$ and Rag^{WT} mice. OT-II^{WT} cells expanded ∼60-fold while OT-II$^{\gamma Rko}$ cells expanded only ∼20-fold (**Figure 4D**). Thus, SP of OT-II$^{\gamma ko}$ and OT-II$^{\gamma Rko}$ cells occurs in Rag$^{\gamma Rko}$ mice. Compared to OT-II^{WT} cells, OT-II$^{\gamma ko}$ and OT-II$^{\gamma Rko}$ expansion was less pronounced suggesting that OT-II-derived IFN-γ promotes SP in an autocrine fashion. However, we cannot exclude a contribution of host-derived IFN-γ, which accumulates in IFN-γR-deficient mice due to lack of its consumption (22).

IFN-γR$^+$ DCs Restrain CD4$^+$ T Cell SP in Rag$^{\gamma Rko}$ Mice

Dendritic cells (DCs) producing elevated levels of IL-6 promote aberrant T cell activation and subsequent IFN-γ synthesis (35). Furthermore, the induction of EAE relies on the accumulation of IL-6-producing DCs (36). Under lymphopenic conditions, MyD88-dependent recognition of the commensal microflora is sufficient to induce IL-6 production by DCs thereby promoting SP of CD4$^+$ T cells (10) similar to what we have observed in OT-II^{WT}-reconstituted Rag$^{\gamma Rko}$ mice. Furthermore, DCs express high levels of MHCII, which is crucial for CD4$^+$ T cell LIP (14, 37). Based on these data we speculated that DC responses were altered in Rag$^{\gamma Rko}$ mice. When splenic CD11c$^+$MHCII^{hi} DCs were quantified in OT-II^{WT}-reconstituted Rag^{WT} and

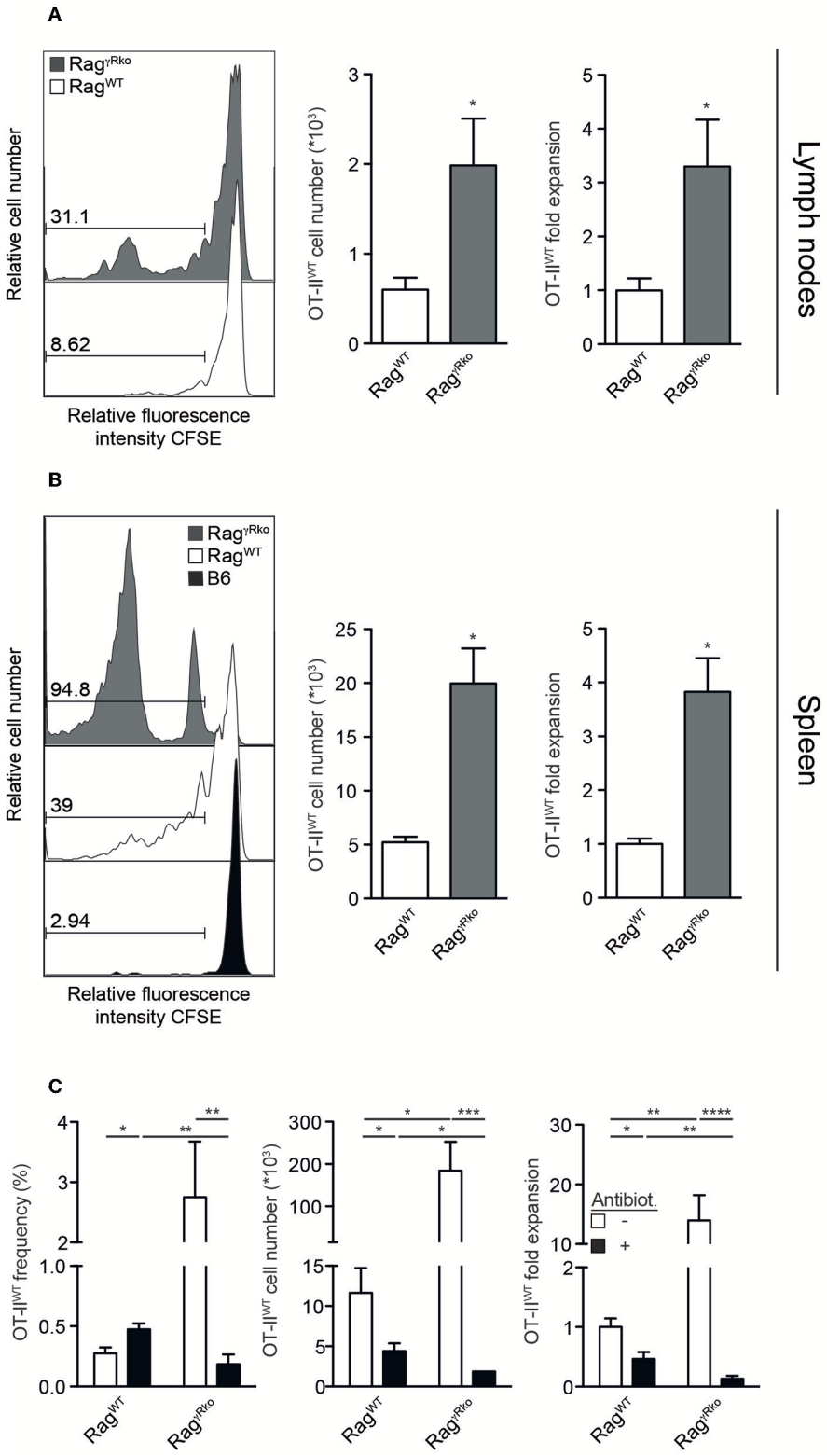

FIGURE 2 | OT-II LIP is more pronounced in spleen than in lymph nodes. **(A,B)** CFSE-labeled OT-II^{WT} cells were adoptively transferred into Rag^{WT}, Rag$^{\gamma Rko}$ mice and **(B)** B6 mice. After 12 days, recipient **(A)** lymph nodes and **(B)** spleen were analyzed by flow cytometry. **(A,B)** Histograms show relative fluorescence intensities for CFSE after gating on CD4$^+$CD45.1$^+$ OT-II^{WT} cells and numbers indicate percentages. Bar diagrams show cell numbers and fold expansion of OT-II^{WT} cells (mean

(Continued)

FIGURE 2 | values + SEM; *$p \leq 0.05$). Results in bar diagrams were pooled from 6 mice per group analyzed in one experiment. **(A)** Histograms are representative of one experiment with 6 Rag^{WT} and 6 $Rag^{\gamma Rko}$. **(B)** Histograms are representative of 2 independent experiments with a total of 10 Rag^{WT}, 10 $Rag^{\gamma Rko}$, and 4 B6 mice. **(C)** OT-II^{WT} cells were adoptively transferred into Rag^{WT} and $Rag^{\gamma Rko}$ mice. After 11–13 days, recipient splenocytes were analyzed by flow cytometry. Four weeks prior to and during T cell transfer, mice were treated with antibiotics (Antibiot.) or were left untreated. Shown are pooled results (mean values + SEM; *$p \leq 0.05$; **$p \leq 0.01$; ***$p \leq 0.001$; ****$p \leq 0.0001$) from 2 independent experiments with a total of 8–9 mice per group.

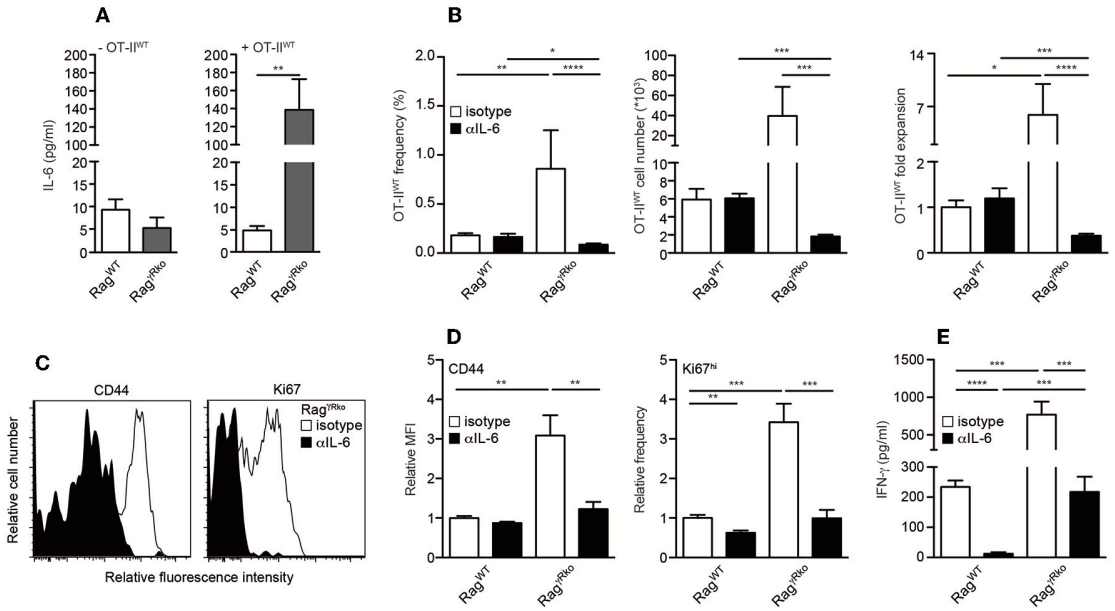

FIGURE 3 | IL-6 accumulates in $Rag^{\gamma Rko}$ mice and promotes OT-II SP. **(A–E)** Rag^{WT} and $Rag^{\gamma Rko}$ mice were reconstituted with OT-II^{WT} cells as described in **Figure 1**. **(A)** Untreated mice served as controls (-OT-II^{WT}). **(B–D)** Prior to and after T cell reconstitution, mice were treated with neutralizing anti-IL-6 (αIL-6) or isotype-machted control antibodies (isotype). Ten to twelve days after T cell transfer, **(A)** IL-6 and **(E)** IFN-γ plasma levels were determined by ELISA and **(B–D)** recipient splenocytes were analyzed by flow cytometry. **(B)** Shown are frequencies, cell numbers and fold expansion of OT-II^{WT} cells in isotype- and αIL-6-treated Rag^{WT} and $Rag^{\gamma Rko}$ mice. **(C)** Relative fluorescence intensities, **(D)** relative MFIs for CD44 and relative frequencies of $Ki67^{hi}$ cells were determined after gating on $CD4^+Thy1.1^+$ OT-II^{WT} cells in isotype- and αIL-6-treated $Rag^{\gamma Rko}$ mice. **(A,B,D,E)** Shown are pooled results from 2 to 3 independent experiments with a total of 5–11 mice per group and **(C)** representative histograms from corresponding samples. **(A,B,D,E)** Graphs show mean values + SEM; *$p \leq 0.05$; **$p \leq 0.01$; ***$p \leq 0.001$; ****$p \leq 0.0001$.

$Rag^{\gamma Rko}$ mice, their numbers were strongly increased in the latter (**Figure 5A**; + OT-II^{WT}). This was not the case in untreated $Rag^{\gamma Rko}$ mice (**Figure 5A**; –OT-II^{WT}) suggesting that OT-II^{WT} activation is a prerequisite for DC accumulation in $Rag^{\gamma Rko}$ recipients.

Whether the DC-specific restoration of IFN-γR expression is sufficient to block OT-II^{WT} SP and subsequent DC accumulation in $Rag^{\gamma Rko}$ mice was tested next. For this purpose, we made use of a novel transgenic mouse line, allowing IFN-γR expression after the Cre-mediated deletion of a loxP-flanked DNA-Stop cassette (20). To activate this "switch-on" (IFN-γR^{SO}) construct and express the transgenic IFN-γR specifically in DCs, IFN-γR^{SO} mice were crossed to CD11c-GCDL mice expressing Cre under the control of the CD11c promoter (19). Subsequently, CD11c-GCDL × IFN-γR^{SO} mice were crossed to $Rag^{\gamma Rko}$ mice in order to generate T and B cell-deficient, fully lymphopenic $Rag^{\gamma Rko}$ × CD11c-GCDL × IFN-γR^{SO} mice lacking IFN-γR expression on all cells except DCs. These mice are termed $Rag^{\gamma Rko}$ × IFN-$\gamma R^{CD11c-ON}$ hereafter. Finally, OT-II^{WT} cells were transferred into Rag^{WT} mice, $Rag^{\gamma Rko}$ × IFN-$\gamma R^{CD11c-ON}$, and $Rag^{\gamma Rko}$ controls. After 11–13 days, the numbers of splenic OT-II^{WT} cells were determined. As opposed to Rag^{WT} mice, OT-II^{WT} cells expanded strongly in $Rag^{\gamma Rko}$ mice (**Figure 5B**). The values obtained with $Rag^{\gamma Rko}$ × IFN-$\gamma R^{CD11c-ON}$ mice reached intermediate levels showing that IFN-γR expression by DCs is sufficient to restrain OT-II^{WT} SP. Similarly, DC expansion was most pronounced in OT-II^{WT}-reconstituted $Rag^{\gamma Rko}$ mice, reached intermediate levels in $Rag^{\gamma Rko}$ × IFN-$\gamma R^{CD11c-ON}$ mice and was least efficient in Rag^{WT} mice (**Figure 5C**; +OT-II^{WT}). On the contrary, DC numbers did not differ between untreated Rag^{WT}, $Rag^{\gamma Rko}$ × IFN-$\gamma R^{CD11c-ON}$ and $Rag^{\gamma Rko}$ mice (**Figure 5C**; –OT-II^{WT}) suggesting a causal link between OT-II^{WT} SP and DC expansion in $Rag^{\gamma Rko}$ mice (**Figures 5A,C**). Importantly, specific IFN-γR expression by DCs was sufficient to limit expansion of OT-II^{WT} cells and DCs as well as IL-6 up-regulation (**Figure 5D**) in $Rag^{\gamma Rko}$ × IFN-$\gamma R^{CD11c-ON}$ mice.

The efficacy of $CD4^+$ T cell responses correlates positively with the amount of IFN-γ available in the early phase of the response (32, 34). We have shown previously that IFN-γ accumulates in IFN-γR-deficient mice, most probably due to

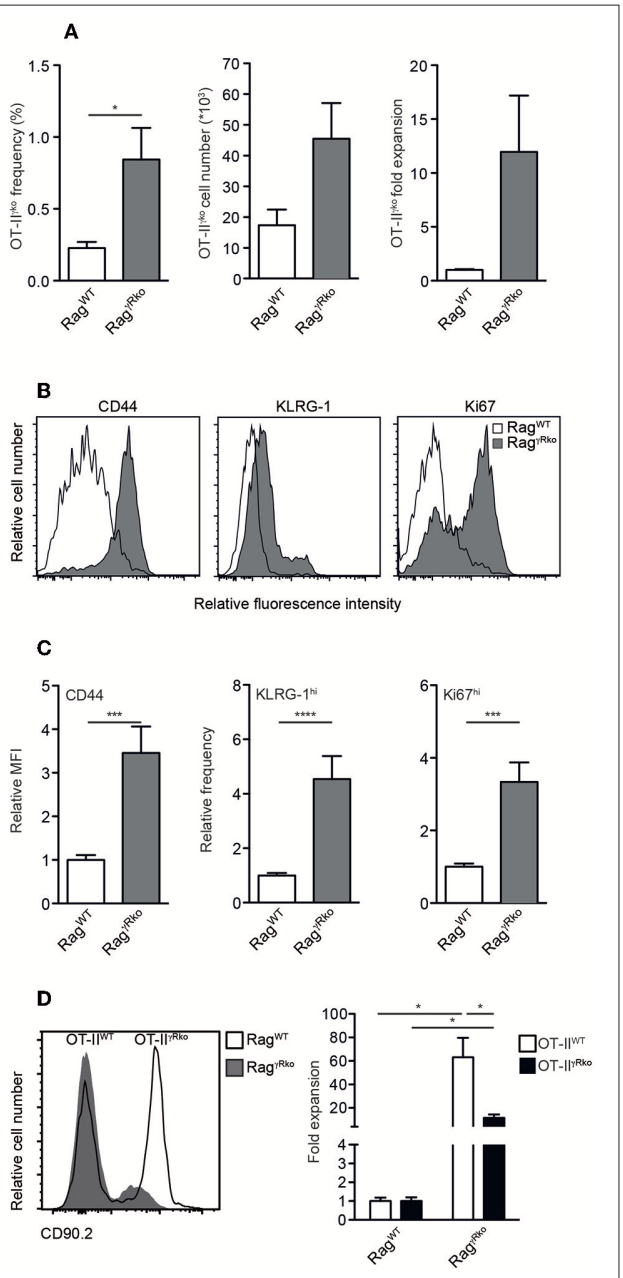

FIGURE 4 | CD4+ T cell-derived IFN-γ promotes SP in an autocrine manner. **(A–C)** OT-II$^{\gamma ko}$ (3–4 independent experiments with 12–17 mice per group) or **(D)** equal numbers of Thy1.1+ OT-II^{WT} and Thy1.1/1.2+ OT-II$^{\gamma Rko}$ T cells (4 mice per group) were transferred simultaneously into Thy1.2+ Rag^{WT} and Rag$^{\gamma Rko}$ mice. After 11–12 days, recipient splenocytes were analyzed by flow cytometry as described in **Figure 1**. Overlay shows the relative abundance of Thy1.1+ OT-II^{WT} and Thy1.1/1.2+ OT-II$^{\gamma Rko}$ T cells in Rag^{WT} and Rag$^{\gamma Rko}$ mice. **(A,C,D)** Graphs show mean values + SEM; *$p \leq 0.05$; ***$p \leq 0.001$; ****$p \leq 0.0001$.

the lack of its receptor-mediated clearance (22). Hence, elevated levels of steady-state IFN-γ may explain the rapid and strong induction of OT-II^{WT} responses in Rag$^{\gamma Rko}$ mice. To test whether decreased OT-II^{WT} responses in Rag$^{\gamma Rko}$ × IFN-γR$^{CD11c-ON}$ mice (**Figure 5B**) correlate with reduced steady-state IFN-γ levels, we compared plasma samples of untreated Rag$^{\gamma Rko}$ and Rag$^{\gamma Rko}$ × IFN-γR$^{CD11c-ON}$ mice. As shown in **Figure 5E**, IFN-γ levels were significantly lower in Rag$^{\gamma Rko}$ × IFN-γR$^{CD11c-ON}$ mice. This suggests that IFN-γR+ DCs consume IFN-γ thereby reducing its availability for OT-II^{WT} cells. This competition for IFN-γ would provide an explanation for the reduced levels of SP in Rag$^{\gamma Rko}$ × IFN-γR$^{CD11c-ON}$ mice (**Figure 5B**).

DISCUSSION

T cell clones are not equally sensitive to lymphopenia-related activation signals (14–16). For example, ovalbumin-specific CD4+ T cells from OT-II TCR^{tg} mice represent one of several T cells clones, which are resistant to lymphopenia-induced activation (14). It is well accepted that T cell clone-specific features such as CD5 levels correlate closely with the sensitivity to lymphopenia (15, 16, 38). Here, we provide evidence for an additional, recipient-dependent mechanism that restrains expansion of adoptively transferred CD4+ T cells. This mechanism relies on a complex interplay between the commensal microflora, IFN-γR+ DCs and CD4+ T cells.

The commensal microflora triggers IFN-γ production by various immune cells in the steady-state (39, 40). In IFN-γR-deficient mice, IFN-γ accumulates due to the lack of its consumption (22). Thus, elevated IFN-γ levels in Rag$^{\gamma Rko}$ mice may provide early activation signals to OT-II cells initiating the rapid expansion we have observed. This interpretation is in accordance with our finding that both, OT-II^{WT} expansion and steady-state levels of IFN-γ, were decreased in Rag$^{\gamma Rko}$ × IFN-γR$^{CD11c-ON}$ mice. This suggests that IFN-γR+ DCs efficiently reduce amounts of circulating IFN-γ thereby restricting its availability for OT-II cells.

However, increased rates of OT-II expansion in Rag$^{\gamma Rko}$ mice do not only rely on host-derived IFN-γ. As we have shown here, OT-II-derived IFN-γ acts in an autocrine manner. Hence, host- and OT-II-derived IFN-γ may synergize in promoting full-blown OT-II expansion in Rag$^{\gamma Rko}$ mice. OT-II expansion is accompanied by the up-regulation of CD127, which would facilitate their IL-7-dependent survival (41–43) and provides one explanation for the accumulation of OT-II cells in Rag$^{\gamma Rko}$ mice. Importantly, the accumulation of DCs and IL-6 correlates positively with the degree of OT-II expansion in Rag$^{\gamma Rko}$ mice and might be interrelated. DCs produce IL-6 in response to the commensal microflora (10) and express MHCII, which are both required for CD4+ T cell expansion under lymphopenic conditions (10, 14, 37). Since (i) T cell-intrinsic IL-6R signaling is critical for CD4+ T cell responses (30, 31), (ii) IL-6 prevents apoptosis of naive and effector CD4+ T cells (44, 45), and (iii) counter-regulates DC function (35, 46–50) we suggest a direct, growth-promoting and/or anti-apoptotic effect of IL-6 on OT-II cells expanding in Rag$^{\gamma Rko}$ mice. Although the T cell-stimulatory potential of DC-derived IL-6 is well established (10, 35, 36) recent findings identified multiple hematopoietic and non-hematopoietic cell types as potential IL-6 producers (36). Importantly, different IL-6 producers appear to regulate

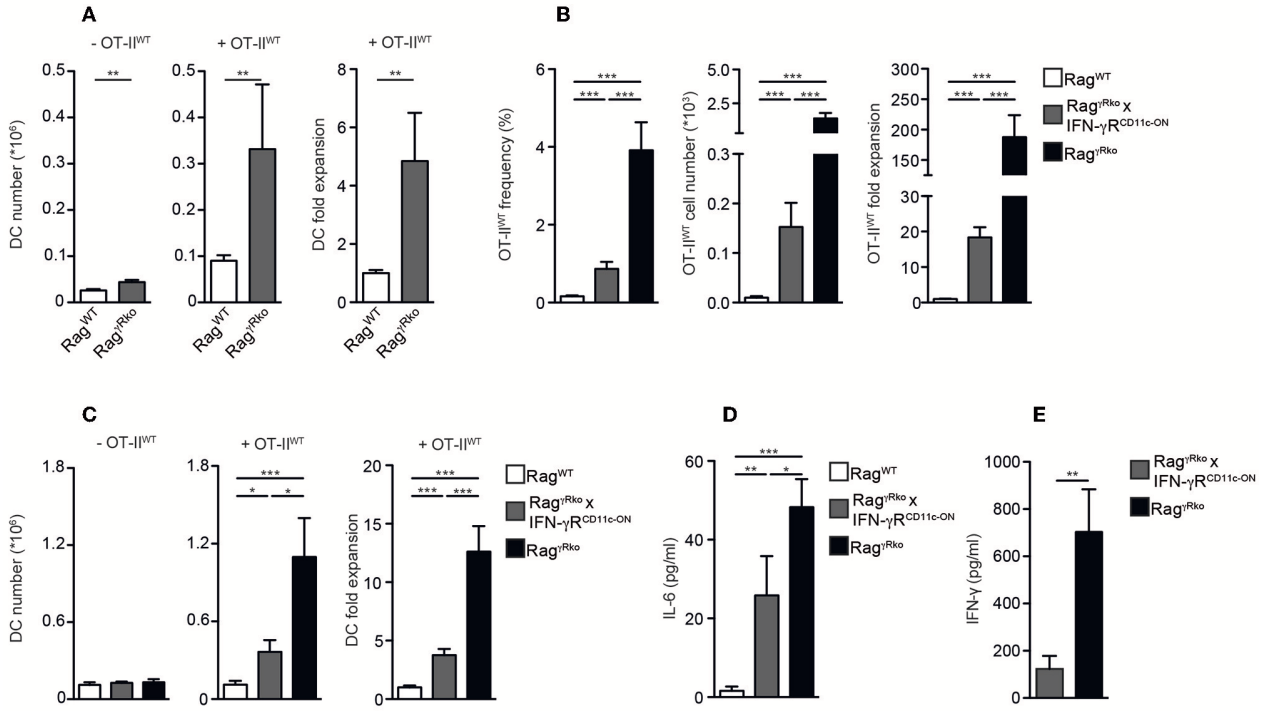

FIGURE 5 | IFN-γR$^+$ DCs restrain CD4$^+$ T cell SP in Rag$^{\gamma Rko}$ mice. **(A–D)** OT-II^{WT} cells were adoptively transferred into Rag^{WT} and Rag$^{\gamma Rko}$ mice. After 11–13 days, recipient splenocytes were analyzed by flow cytometry. **(A)** Results of 2–6 independent experiments with a total of 10–25 mice were pooled to calculate the numbers and fold expansion of CD11c$^+$MHCII^{hi} DCs after reconstitution with OT-II^{WT} cells (+OT-II^{WT}). DC numbers from untreated Rag^{WT} and Rag$^{\gamma Rko}$ mice were determined as well (-OT-II^{WT}). **(B–D)** Frequencies, cell numbers and fold expansion of OT-II^{WT} cells/DCs as well as plasma IL-6 levels were analyzed in Rag^{WT}, Rag$^{\gamma Rko}$ × CD11c-GCDL × IFN-γR^{SO} (Rag$^{\gamma Rko}$ × IFN-γR$^{CD11c-ON}$) and Rag$^{\gamma Rko}$ mice. Pooled results of 2 independent experiments with a total of 8 mice per group are shown. **(E)** Steady-state levels of IFN-γ were determined in plasma samples of 8–9 untreated Rag$^{\gamma Rko}$ × IFN-γR$^{CD11c-ON}$ and Rag$^{\gamma Rko}$ mice. **(A–E)** Graphs show mean values + SEM; *$p \leq 0.05$; **$p \leq 0.01$; ***$p \leq 0.001$.

different aspects of the same CD4$^+$ T cell response (36). Hence, it remains to be shown for our experimental system whether (i) DCs and/or other cell types up-regulate IL-6 expression in OT-II-reconstituted Rag$^{\gamma Rko}$ mice, whether (ii) the elevation of IL-6 levels in these mice results from the accumulation of DCs producing constant amounts of IL-6, and whether (iii) there is a causal relationship between the cellular origin of IL-6 and its growth-promoting effect. As reported only recently, definite answers to such questions would require the combined use of cell type-specific IL-6 reporter as well as conditional IL-6 knockout mice (36) and their integration into our experimental systems. However, this would be beyond the scope of this study and therefore remains an important task for the future.

From previous experiments we know that only effector, but not naive, OT-II^{WT} cells activate immature DCs (51). This suggests that IFN-γ-associated OT-II activation is an integral part of a self-amplifying loop in Rag$^{\gamma Rko}$ mice, which involves the T cell-dependent accumulation of DCs, which in turn promote OT-II expansion. The lack of IFN-γR signaling in DCs increases their lifespan (52) and T cell-stimulatory potential (53) providing an additional explanation for the accumulation of DCs in Rag$^{\gamma Rko}$ mice. In accordance with this interpretation, IFN-γR re-expression in DCs is sufficient to disrupt this self-amplifying loop and to down-modulate DC accumulation, IL-6 levels and OT-II cell expansion.

In summary, we demonstrate that the sensitivity of CD4$^+$ T cells to lymphopenia is not only determined by cell-intrinsic properties but also by a complex interplay between CD4$^+$ T cells, the commensal microflora and IFN-γR$^+$ DCs. We postulate that T cell- and host cell-specific mechanisms have to co-operate to restrain spontaneous proliferation, the commensal-driven form of LIP. The molecular nature and the relative importance of either mechanism may vary for different T cell clones.

ETHICS STATEMENT

Animal experiments were performed according to institutional guidelines and were approved by the Landesverwaltungsamt Sachsen-Anhalt (Permit Number: 2-1155/2-1288 Uni MD).

AUTHOR CONTRIBUTIONS

LK, CF, DS, and KD performed and analyzed the experiments. LK substantially contributed to manuscript preparation. UK and ID analyzed and discussed the data. TB and TK provided

essential material, analyzed and discussed the data. TS designed and supervised the study, analyzed and discussed the data and wrote the manuscript with the help of the other co-authors.

FUNDING

This work was supported by the Deutsche Forschungsgemeinschaft [Sonderforschungsbereich TR36 (B2, B7), SFB854 (B15), and DU 1112/5-1].

ACKNOWLEDGMENTS

We thank E. Denks and J. Giese for excellent technical assistance and Natalio Garbi for CD11c-GCDL mice.

SUPPLEMENTARY MATERIAL

The Supplementary Material for this article can be found online at: https://www.frontiersin.org/articles/10.3389/fimmu.2019.00140/full#supplementary-material

REFERENCES

1. Takada K, Jameson SC. Naive T cell homeostasis: from awareness of space to a sense of place. *Nat Rev Immunol.* (2009) 9:823–32. doi: 10.1038/nri2657
2. Guimond M, Veenstra RG, Grindler DJ, Zhang H, Cui Y, Murphy RD, et al. Interleukin 7 signaling in dendritic cells regulates the homeostatic proliferation and niche size of CD4(+) T cells. *Nat Immunol.* (2009) 10:149–57. doi: 10.1038/ni.1695
3. Napolitano LA, Grant RM, Deeks SG, Schmidt D, De Rosa SC, Herzenberg LA, et al. Increased production of IL-7 accompanies HIV-1-mediated T-cell depletion: implications for T-cell homeostasis. *Nat Med.* (2001) 7:73–9. doi: 10.1038/83381
4. Mackall CL, Fry TJ, Gress RE. Harnessing the biology of IL-7 for therapeutic application. *Nat Rev Immunol.* (2011) 11:330–42. doi: 10.1038/nri2970
5. Tan JT, Dudl E, LeRoy E, Murray R, Sprent J, Weinberg KI, et al. IL-7 is critical for homeostatic proliferation and survival of naive T cells. *Proc Natl Acad Sci USA.* (2001) 98:8732–7. doi: 10.1073/pnas.161126098
6. Tan JT, Ernst B, Kieper WC, LeRoy E, Sprent J, Surh CD. Interleukin (IL)-15 and IL-7 jointly regulate homeostatic proliferation of memory phenotype CD8+ cells but are not required for memory phenotype CD4+ cells. *J Exp Med.* (2002) 195:1523–32. doi: 10.1084/jem.20020066
7. Kieper WC, Troy A, Burghardt JT, Ramsey C, Lee JY, Jiang H-Q, et al. Recent immune status determines the source of antigens that drive homeostatic T cell expansion. *J Immunol.* (2005) 174:3158–63. doi: 10.4049/jimmunol.174.6.3158
8. Min B, Foucras G, Meier-Schellersheim M, Paul WE. Spontaneous proliferation, a response of naive CD4 T cells determined by the diversity of the memory cell repertoire. *Proc Natl Acad Sci USA.* (2004) 101:3874–9. doi: 10.1073/pnas.0400606101
9. Tajima M, Wakita D, Noguchi D, Chamoto K, Yue Z, Fugo K, et al. IL-6-dependent spontaneous proliferation is required for the induction of colitogenic IL-17-producing CD8+ T cells. *J Exp Med.* (2008) 205:1019–27. doi: 10.1084/jem.20071133
10. Feng T, Wang L, Schoeb TR, Elson CO, Cong Y. Microbiota innate stimulation is a prerequisite for T cell spontaneous proliferation and induction of experimental colitis. *J Exp Med.* (2010) 207:1321–32. doi: 10.1084/jem.20092253
11. Do J-S, Foucras G, Kamada N, Schenk AF, Shaw M, Nuñez G, et al. Both exogenous commensal and endogenous self antigens stimulate T cell proliferation under lymphopenic conditions. *Cell Immunol.* (2012) 272:117–23. doi: 10.1016/j.cellimm.2011.11.002
12. Totsuka T, Kanai T, Nemoto Y, Makita S, Okamoto R, Tsuchiya K, et al. IL-7 Is essential for the development and the persistence of chronic colitis. *J Immunol.* (2007) 178:4737–48. doi: 10.4049/jimmunol.178.8.4737
13. Calzascia T, Pellegrini M, Lin A, Garza KM, Elford AR, Shahinian A, et al. CD4 T cells, lymphopenia, and IL-7 in a multistep pathway to autoimmunity. *Proc Natl Acad Sci USA.* (2008) 105:2999–3004. doi: 10.1073/pnas.0712135105
14. Ernst B, Lee DS, Chang JM, Sprent J, Surh CD. The peptide ligands mediating positive selection in the thymus control T cell survival and homeostatic proliferation in the periphery. *Immunity* (1999) 11:173–81. doi: 10.1016/S1074-7613(00)80092-8
15. Kassiotis G, Zamoyska R, Stockinger B. Involvement of avidity for major histocompatibility complex in homeostasis of naive and memory T cells. *J Exp Med.* (2003) 197:1007–16. doi: 10.1084/jem.20021812
16. Kieper WC, Burghardt JT, Surh CD. A role for TCR affinity in regulating naive T cell homeostasis. *J Immunol.* (2004) 172:40–4. doi: 10.4049/jimmunol.172.1.40
17. Smith K, Seddon B, Purbhoo MA, Zamoyska R, Fisher AG, Merkenschlager M. Sensory adaptation in naive peripheral CD4 T cells. *J Exp Med.* (2001) 194:1253–61. doi: 10.1084/jem.194.9.1253
18. Salmond RJ, Brownlie RJ, Morrison VL, Zamoyska R. The tyrosine phosphatase PTPN22 discriminates weak self peptides from strong agonist TCR signals. *Nat Immunol.* (2014) 15:875–83. doi: 10.1038/ni.2958
19. Tittel AP, Heuser C, Ohliger C, Llanto C, Yona S, Hämmerling GJ, et al. Functionally relevant neutrophilia in CD11c diphtheria toxin receptor transgenic mice. *Nat Methods* (2012) 9:385–90. doi: 10.1038/nmeth.1905
20. Kammertoens T, Friese C, Arina A, Idel C, Briesemeister D, Rothe M, et al. Tumour ischaemia by interferon-γ resembles physiological blood vessel regression. *Nature* (2017) 545:98–102. doi: 10.1038/nature22311
21. Rakoff-Nahoum S, Paglino J, Eslami-Varzaneh F, Edberg S, Medzhitov R. Recognition of commensal microflora by toll-like receptors is required for intestinal homeostasis. *Cell* (2004) 118:229–41. doi: 10.1016/j.cell.2004.07.002
22. Sercan O, Stoycheva D, Hämmerling GJ, Arnold B, Schüler T. IFN-gamma receptor signaling regulates memory CD8+ T cell differentiation. *J Immunol.* (2010) 184:2855–62. doi: 10.4049/jimmunol.0902708
23. Dummer W, Ernst B, LeRoy E, Lee D, Surh C. Autologous regulation of naive T cell homeostasis within the T cell compartment. *J Immunol.* (2001) 166:2460–8. doi: 10.4049/jimmunol.166.4.2460
24. Mueller SN, Hosiawa-Meagher KA, Konieczny BT, Sullivan BM, Bachmann MF, Locksley RM, et al. Regulation of homeostatic chemokine expression and cell trafficking during immune responses. *Science* (2007) 317:670–4. doi: 10.1126/science.1144830
25. Sung JH, Zhang H, Moseman EA, Alvarez D, Iannacone M, Henrickson SE, et al. Chemokine guidance of central memory T cells is critical for antiviral recall responses in lymph nodes. *Cell* (2012) 150:1249–63. doi: 10.1016/j.cell.2012.08.015
26. Kastenmüller W, Torabi-Parizi P, Subramanian N, Lämmermann T, Germain RN. A spatially-organized multicellular innate immune response in lymph nodes limits systemic pathogen spread. *Cell* (2012) 150:1235–48. doi: 10.1016/j.cell.2012.07.021
27. Bajénoff M, Egen JG, Koo LY, Laugier JP, Brau F, Glaichenhaus N, et al. Stromal cell networks regulate lymphocyte entry, migration, and territoriality in lymph nodes. *Immunity* (2006) 25:989–1001. doi: 10.1016/j.immuni.2006.10.011
28. Onder L. A novel bacterial artificial chromosome-transgenic Podoplanin–Cre mouse targets lymphoid organ stromal cells *in vivo*. *Front Immunol.* (2011) 2:50. doi: 10.3389/fimmu.2011.00050
29. Shalapour S, Deiser K, Sercan O, Tuckermann J, Minnich K, Willimsky G, et al. Commensal microflora and interferon-gamma promote steady-state interleukin-7 production *in vivo*. *Eur J Immunol.* (2010) 40:2391–400. doi: 10.1002/eji.201040441
30. Nish SA, Schenten D, Wunderlich FT, Pope SD, Gao Y, Hoshi N, et al. T cell-intrinsic role of IL-6 signaling in primary and memory responses. *Elife* (2014) 3:e01949. doi: 10.7554/eLife.01949

31. Li B, Jones LL, Geiger TL. IL-6 promotes T cell proliferation and expansion under inflammatory conditions in association with low-level RORγt expression. *J Immunol.* (2018) 201:2934–46. doi: 10.4049/jimmunol.1800016
32. Whitmire JK, Benning N, Whitton JL. Cutting edge: early IFN-gamma signaling directly enhances primary antiviral CD4+ T cell responses. *J Immunol.* (2005) 175:5624–8. doi: 10.4049/jimmunol.175.9.5624
33. Whitmire JK, Eam B, Benning N, Whitton JL. Direct interferon-gamma signaling dramatically enhances CD4+ and CD8+ T cell memory. *J Immunol.* (2007) 179:1190–7. doi: 10.4049/jimmunol.179.2.1190
34. Whitmire JK, Benning N, Eam B, Whitton JL. Increasing the CD4+ T cell precursor frequency leads to competition for IFN-gamma thereby degrading memory cell quantity and quality. *J Immunol.* (2008) 180:6777–85. doi: 10.4049/jimmunol.180.10.6777
35. Liu J, Han C, Xie B, Wu Y, Liu S, Chen K, et al. Rhbdd3 controls autoimmunity by suppressing the production of IL-6 by dendritic cells via K27-linked ubiquitination of the regulator NEMO. *Nat Immunol.* (2014) 15:612–22. doi: 10.1038/ni.2898
36. Heink S, Yogev N, Garbers C, Herwerth M, Aly L, Gasperi C, et al. Trans-presentation of IL-6 by dendritic cells is required for the priming of pathogenic TH17 cells. *Nat Immunol.* (2017) 18:74–85. doi: 10.1038/ni.3632
37. Do J-S, Min B. Differential requirements of MHC and of DCs for endogenous proliferation of different T-cell subsets *in vivo*. *Proc Natl Acad Sci USA.* (2009) 106:20394–8. doi: 10.1073/pnas.0909954106
38. Cho J-H, Kim H-O, Surh CD, Sprent J. T cell receptor-dependent regulation of lipid rafts controls naive CD8+ T cell homeostasis. *Immunity* (2010) 32:214–26. doi: 10.1016/j.immuni.2009.11.014
39. Keilbaugh SA, Shin ME, Banchereau RF, McVay LD, Boyko N, Artis D, et al. Activation of RegIIIbeta/gamma and interferon gamma expression in the intestinal tract of SCID mice: an innate response to bacterial colonisation of the gut. *Gut* (2005) 54:623–9. doi: 10.1136/gut.2004.056028
40. Niess JH, Leithäuser F, Adler G, Reimann J. Commensal gut flora drives the expansion of proinflammatory CD4 T cells in the colonic lamina propria under normal and inflammatory conditions. *J Immunol.* (2008) 180:559–68. doi: 10.4049/jimmunol.180.1.559
41. Schluns KS, Kieper WC, Jameson SC, Lefrançois L. Interleukin-7 mediates the homeostasis of naïve and memory CD8 T cells *in vivo*. *Nat Immunol.* (2000) 1:426–32. doi: 10.1038/80868
42. Rathmell JC, Farkash EA, Gao W, Thompson CB. IL-7 enhances the survival and maintains the size of naive T cells. *J Immunol.* (2001) 167:6869–76. doi: 10.4049/jimmunol.167.12.6869
43. Shklovskaya E, Fazekas de St Groth B. Severely impaired clonal deletion of CD4+ T cells in low-dose irradiated mice: role of T cell antigen receptor and IL-7 receptor signals. *J Immunol.* (2006) 177:8320–30. doi: 10.4049/jimmunol.177.12.8320
44. Teague TK, Marrack P, Kappler JW, Vella AT. IL-6 rescues resting mouse T cells from apoptosis. *J Immunol.* (1997) 158:5791–6.
45. Rochman I, Paul WE, Ben-Sasson SZ. IL-6 increases primed cell expansion and survival. *J Immunol.* (2005) 174:4761–7. doi: 10.4049/jimmunol.174.8.4761
46. Chomarat P, Banchereau J, Davoust J, Palucka AK. IL-6 switches the differentiation of monocytes from dendritic cells to macrophages. *Nat Immunol.* (2000) 1:510–4. doi: 10.1038/82763
47. Ratta M, Fagnoni F, Curti A, Vescovini R, Sansoni P, Oliviero B, et al. Dendritic cells are functionally defective in multiple myeloma: the role of interleukin-6. *Blood* (2002) 100:230–7. doi: 10.1182/blood.V100.1.230
48. Park S-J, Nakagawa T, Kitamura H, Atsumi T, Kamon H, Sawa S, et al. IL-6 regulates *in vivo* dendritic cell differentiation through STAT3 activation. *J Immunol.* (2004) 173:3844–54. doi: 10.4049/jimmunol.173.6.3844
49. Bleier JI, Pillarisetty VG, Shah AB, DeMatteo RP. Increased and long-term generation of dendritic cells with reduced function from IL-6-deficient bone marrow. *J Immunol.* (2004) 172:7408–16. doi: 10.4049/jimmunol.172.12.7408
50. Kitamura H, Kamon H, Sawa S, Park SJ, Katunuma N, Ishihara K, et al. IL-6-STAT3 controls intracellular MHC class II alphabeta dimer level through cathepsin S activity in dendritic cells. *Immunity* (2005) 23:491–502. doi: 10.1016/j.immuni.2005.09.010
51. Schüler T, Blankenstein T. Naive CD8(+) but not CD4(+) T cells induce maturation of dendritic cells. *J Mol Med.* (2002) 80:533–41. doi: 10.1007/s00109-002-0360-4
52. Do J-S, Asosingh K, Baldwin WM, Min B. Cutting edge: IFN-γR signaling in non-T cell targets regulates T cell-mediated intestinal inflammation through multiple mechanisms. *J Immunol.* (2014) 192:2537–41. doi: 10.4049/jimmunol.1303101
53. Nirschl CJ, Suárez-Fariñas M, Izar B, Prakadan S, Dannenfelser R, Tirosh I, et al. IFNγ-dependent tissue-immune homeostasis is co-opted in the tumor microenvironment. *Cell* (2017) 170:127–41.e15. doi: 10.1016/j.cell.2017.06.016

Conflict of Interest Statement: The authors declare that the research was conducted in the absence of any commercial or financial relationships that could be construed as a potential conflict of interest.

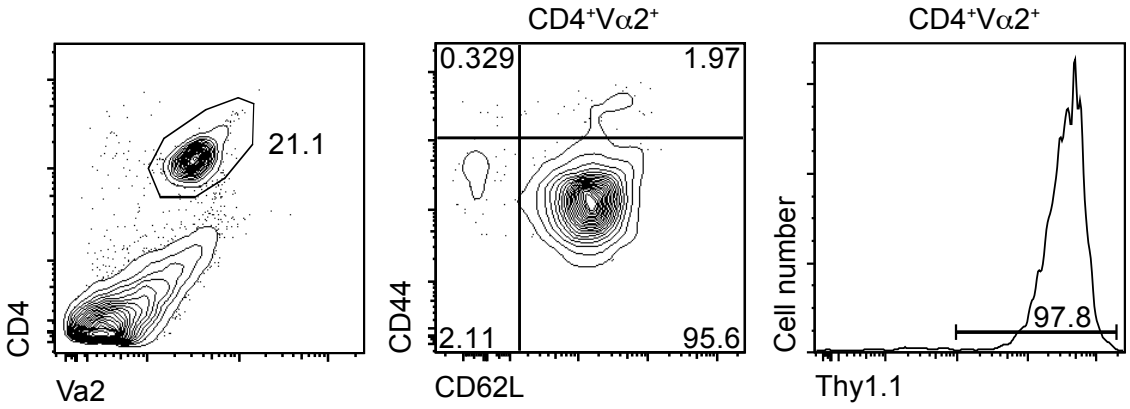

Supplementary Figure 1

Purity and phenotype of transferred OT-II^{WT} T cells. Single cell suspensions prepared from spleens and lymph nodes of Rag$^{-/-}$OT-II (OT-II^{WT}) mice were analyzed by flow cytometry to determine OT-II cell frequency and activation state prior to adoptive transfer. Shown are representative results. Numbers indicate percentages.

4 Publication II

Title: IL-7 derived from lymph node fibroblastic reticular cells is dispensable for naive T cell homeostasis but crucial for central memory T cell survival[16]

Journal: European Journal of Immunology

Publication year: 2020

DOI: 10.1002/eji.201948368

Authors:

LK	Laura Knop	LP	Lars Philipsen
KD	Katrin Deiser	HF	Hans J. Fehling
UB	Ute Bank	AM	Andreas J. Müller
AW	Amelie Witte	UK	Ulrich Kalinke
JM	Juliane Mohr	TS	Thomas Schüler

Table 4-1. Author contributions in publication II.

Author	Contribution in %
Study design and supervision	
LK, KD	10 each
TS	80
Performance of experiments	
LK	60
KD	25
UB, AW	5 each
JM, LP	2,5 each
Data collection and figure preparation	
LK	100
Data analysis and interpretation	
LK	35
KD, HF, AM, UK	5 each
UB, AW, JM, LP	2,5 each
TS	35
Manuscript preparation	
LK	25
KD, UB, AW, JM, LP, HF, AM, UK	10 together
TS	65

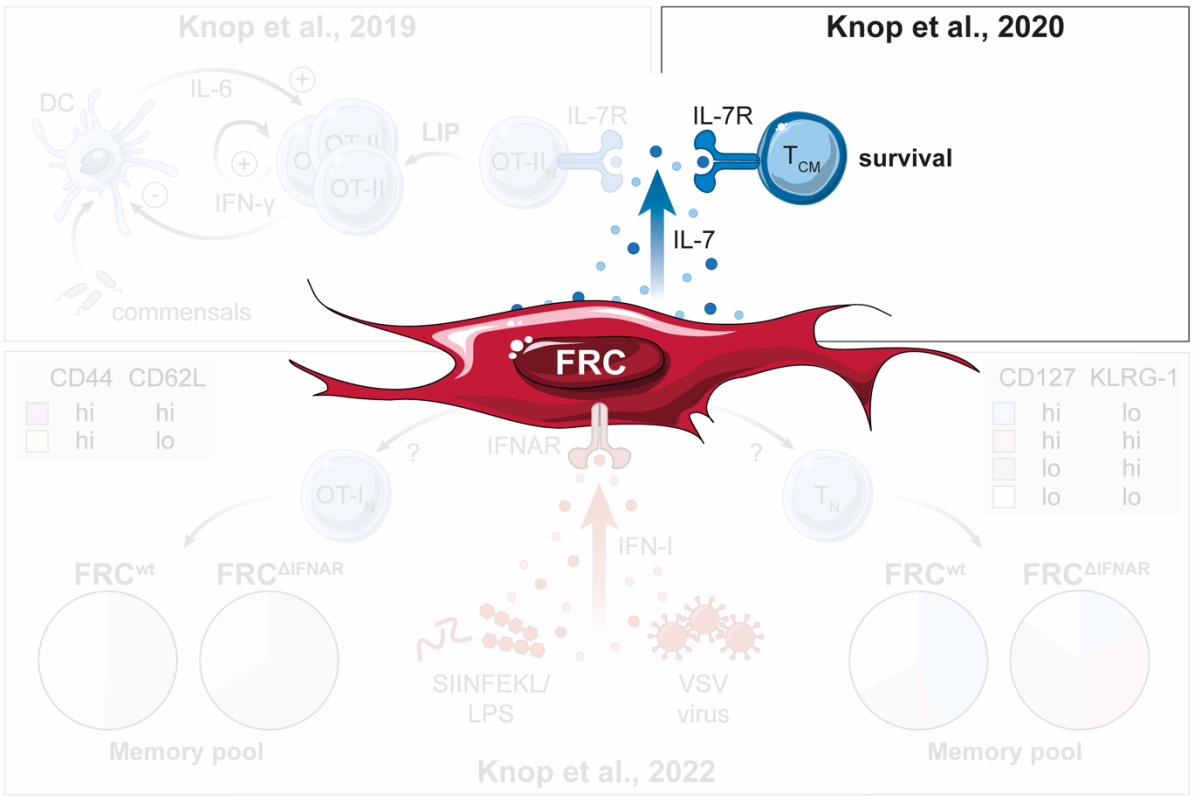

Figure 4-1. Graphical representation of Knop et al., 2020[16]**.** T cells rely on access to SLOs[189,190] and the cytokine IL-7 for survival[127,191]. In the LNs, non-hematopoietic stromal cells, such as FRCs and LECs, are producers of IL-7[10]. It remained unclear whether FRC/LEC-derived IL-7 contributes to T_N or T_M survival *in vivo*. In Knop et al., 2020, we suggest that FRC-derived IL-7 contributes to T_{CM} homeostasis in the LNs[16]. In contrast, LEC- and FRC-derived IL-7 seems dispensable for T_N survival. This figure was created using illustrations from www.bioicons.com[21].

Eur. J. Immunol. 2020. 00: 1–12 DOI: 10.1002/eji.201948368

European Journal of Immunology

Tissue immunology and leukocyte trafficking

Basic

Research Article

IL-7 derived from lymph node fibroblastic reticular cells is dispensable for naive T cell homeostasis but crucial for central memory T cell survival

Laura Knop[*1], Katrin Deiser*[*1], Ute Bank[1], Amelie Witte[1], Juliane Mohr[1], Lars Philipsen[1], Hans J. Fehling[2], Andreas J. Müller[1,3], Ulrich Kalinke[4] and Thomas Schüler[1]*

[1] Institute of Molecular and Clinical Immunology, Medical Faculty, Otto-von-Guericke University, Magdeburg, Germany
[2] Institute of Immunology, University Clinics Ulm, Ulm, Germany
[3] Intravital Microscopy in Infection and Immunity, Helmholtz Centre for Infection Research, Braunschweig, Germany
[4] TWINCORE, Centre for Experimental and Clinical Infection Research, a joint venture between the Helmholtz Centre for Infection Research and the Medical School Hannover, Institute for Experimental Infection Research, Hannover, Germany

The survival of peripheral T cells is dependent on their access to peripheral LNs (pLNs) and stimulation by IL-7. In pLNs fibroblastic reticular cells (FRCs) and lymphatic endothelial cells (LECs) produce IL-7 suggesting their contribution to the IL-7-dependent survival of T cells. However, IL-7 production is detectable in multiple organs and is not restricted to pLNs. This raises the question whether pLN-derived IL-7 is required for the maintenance of peripheral T cell homeostasis. Here, we show that numbers of naive T cells (T_N) remain unaffected in pLNs and spleen of mice lacking *Il7* gene activity in pLN FRCs, LECs, or both. In contrast, frequencies of central memory T cells (T_{CM}) are reduced in FRC-specific IL-7 KO mice. Thus, steady state IL-7 production by pLN FRCs is critical for the maintenance of T_{CM}, but not T_N, indicating that both T cell subsets colonize different ecological niches in vivo.

Keywords: central memory T cells · fibroblastic reticular cells · IL-7 · naive T cells · T cell homeostasis

Additional supporting information may be found online in the Supporting Information section at the end of the article.

Introduction

IL-7 is indispensable for naive (T_N) and memory T cell (T_M) survival [1,2]. Correspondingly, IL-7-deficient (IL-$7^{-/-}$) mice suffer from severe lymphopenia [3] and adoptively transferred T_N fail to survive in such recipients [4]. Conversely, the administration of recombinant IL-7 supports T cell survival, e.g., via the upregulation of anti-apoptotic B-cell lymphoma-2 (Bcl-2) [1], myeloid cell leukemia-1 (Mcl-1) [5], and the promotion of metabolic functions [6–8].

Correspondence: Dr. Thomas Schüler
e-mail: thomas.schueler@med.ovgu.de

*These authors contributed equally to this work.

The maintenance of the T_N pool relies on the accessibility of secondary lymphoid organs (SLOs) where IL-7 is produced by lymphoid stromal cells (LSCs) [9]. In peripheral lymph nodes, for example, fibroblastic reticular cells (FRCs) and lymphatic endothelial cells (LECs) are the main sources of IL-7 [9]. Co-culture experiments demonstrated that FRC-derived IL-7 promotes T cell survival [9]. IL-7 binds to the ECM [10,11] suggesting that it might exert its function in close vicinity to the site of production. Due to the facts that T cell survival is impaired in vivo if either IL-7 action or peripheral LN (pLN) access is blocked [1,4,9,12,13], it has been proposed that circulating T_N receive IL-7-dependent survival signals in pLNs [14–17]. Since T_{CM} and T_N have similar migration patterns in vivo [18] and both rely on IL-7 [1,4], pLN FRCs are supposed to be critical for the IL-7-dependent persistence of both T cell subsets in vivo [15,17]. A potential contribution of LEC-derived IL-7 has been suggested as well [19].

However, various non-hematopoietic stromal cells express IL-7 [20–23] and its steady state levels vary strongly between different organs [24,25]. For example, intestine and skin produce high levels of IL-7 in the steady state while only low levels of *Il7* gene activity are detectable in the adult liver [24,25]. Since T_N and T_{CM} continuously recirculate between SLOs, blood, and lymph [26], they might utilize IL-7 derived from various organs. Hence, it remained unclear whether the maintenance of peripheral T cell homeostasis relies on the local action of IL-7 in pLNs and/or systemic effects of IL-7 produced by alternative sources.

In order to answer this question, we generated conditional IL-7 KO (IL-$7^{fl/fl}$) mice and inactivated *Il7* gene activity in a cell type-specific manner in pLNs. Here, we show that T_N numbers remained unaltered in pLNs and spleens of LEC- and FRC-specific IL-7 KO ($LEC^{\Delta IL\text{-}7}$ and $FRC^{\Delta IL\text{-}7}$) mice. In apparent contrast, T_{CM} abundance was significantly reduced in $FRC^{\Delta IL\text{-}7}$ mice, an effect that was most pronounced for $CD8^+$ T_{CM} in pLNs. In summary, we provide evidence that FRC-derived IL-7 is dispensable for the systemic survival of T_N cells. On the contrary, however, IL-7 produced by pLN FRCs is crucial for the maintenance of T_{CM} homeostasis indicating that T_N and T_{CM} occupy different ecological niches in vivo.

Results

Ubiquitous *Il7* gene inactivation impairs peripheral T cell homeostasis

In order to elucidate whether pLN-derived IL-7 is crucial for the maintenance of peripheral T cell homeostasis, we generated conditional IL-7 KO (IL-$7^{fl/fl}$) mice (Supporting Information Fig. 1A). IL-$7^{fl/fl}$ mice were crossed to conventional IL-7 KO (IL-$7^{-/-}$) mice [3] and mice ubiquitously expressing the loxP-specific recombinase Cre (PGK-Cre^+) [27] to obtain PGK-Cre^+IL-$7^{-/fl}$ mice. PGK-Cre-mediated inactivation of the $Il7^{fl}$ allele was very efficient as shown by the fact that *Il7* mRNA was undetectable in PGK-Cre^+IL-$7^{-/fl}$ mice (Supporting Information Fig. 1B).

Next, we compared the impact of conditional and conventional *Il7* gene inactivation on IL-7-dependent lymphocyte homeostasis. While mice harboring one intact $Il7^{wt}$ allele (PGK-Cre^-IL-$7^{-/wt}$, PGK-Cre^+IL-$7^{-/wt}$, and PGK-Cre^-IL-$7^{-/fl}$ mice) had comparable numbers of T and B cells in the spleen, ubiquitous *Il7* gene inactivation in PGK-Cre^+IL-$7^{-/fl}$ mice was associated with a strong decrease of T and B cell numbers similar to IL-$7^{-/-}$ mice (Fig. 1A). Importantly, the lack of IL-7 production in PGK-Cre^+IL-$7^{-/fl}$ and IL-$7^{-/-}$ mice was accompanied by the selective reduction of $CD44^{lo}CD62L^{hi}$ $CD4^+$ and $CD8^+$ T_N as well as the enrichment of $CD44^{hi}$ $CD4^+$ and $CD8^+$ memory T cells (T_M; Fig. 1B and C).

In summary, IL-7-dependent T cell homeostasis is similarly impaired in IL-$7^{-/-}$ and PGK-Cre^+IL-$7^{-/fl}$ mice thus confirming (i) the efficient Cre-mediated inactivation of the $Il7^{fl}$ allele and (ii) the crucial importance of IL-7 for T_N generation and maintenance. Hence, our IL-$7^{fl/fl}$ mouse is a suitable tool to study the impact of pLN-specific *Il7* gene inactivation on peripheral T cell homeostasis.

LEC-derived IL-7 is dispensable for peripheral T cell homeostasis

In pLNs, $CD45^-$ stromal cells comprise $gp38^+CD31^-$ FRCs, $gp38^+CD31^+$ LECs, $gp38^-CD31^+$ blood endothelial cells (BECs) and $gp38^-CD31^-$ double negative cells (DNs) [28] (Fig. 2A). Lyve-1-expressing LECs produce IL-7 in pLNs and throughout the body [29] and are supposed to be important regulators of IL-7-dependent peripheral T cell homeostasis [19]. In order to test this hypothesis, we generated $LEC^{\Delta IL\text{-}7}$ mice lacking *Il7* gene expression specifically in LECs. For this purpose, Lyve1-Cre-transgenic (Lyve1-Cre^+) mice [30] were crossed to IL-$7^{fl/fl}$ mice. Lyve1-Cre^+ mice harboring at least one intact *Il7* allele (LEC^{wt} mice) served as controls. $CD45^-$ stromal cells were purified from LNs of $LEC^{\Delta IL\text{-}7}$ and LEC^{wt} mice and relative *Il7* mRNA levels were quantified by RT-qPCR. In agreement with a previous report [9], LECs produced considerable amounts of *Il7* mRNA in control mice, even though tenfold less than FRCs (Fig. 2A). Of note, *Il7* mRNA levels were strongly reduced in LECs from $LEC^{\Delta IL\text{-}7}$ mice indicating successful *Il7* gene inactivation. On the contrary, *Il7* mRNA levels in FRCs, BECs, and DNs were comparable in $LEC^{\Delta IL\text{-}7}$ and LEC^{wt} mice.

In order to study whether LEC-derived IL-7 affects peripheral T cell homeostasis, $CD4^+$ and $CD8^+$ T cells were quantified in pLNs and spleens of $LEC^{\Delta IL\text{-}7}$ and LEC^{wt} mice. As shown in Fig. 2B, T cell numbers were indistinguishable between both mouse lines. Furthermore, relative frequencies and numbers of $CD44^{lo}CD62L^{hi}$ T_N, $CD44^{hi}CD62L^{lo}$ T_{EM}, and $CD44^{hi}CD62L^{hi}$ T_{CM} were comparable in pLNs and spleens (Fig. 2C–H), although $CD4^+$ T_{CM} frequencies were reduced in pLNs of $LEC^{\Delta IL\text{-}7}$ mice (Fig. 2C and D). In conclusion, *Il7* gene inactivation in LECs does not have major effects on quantitative and qualitative aspects of peripheral T cell homeostasis.

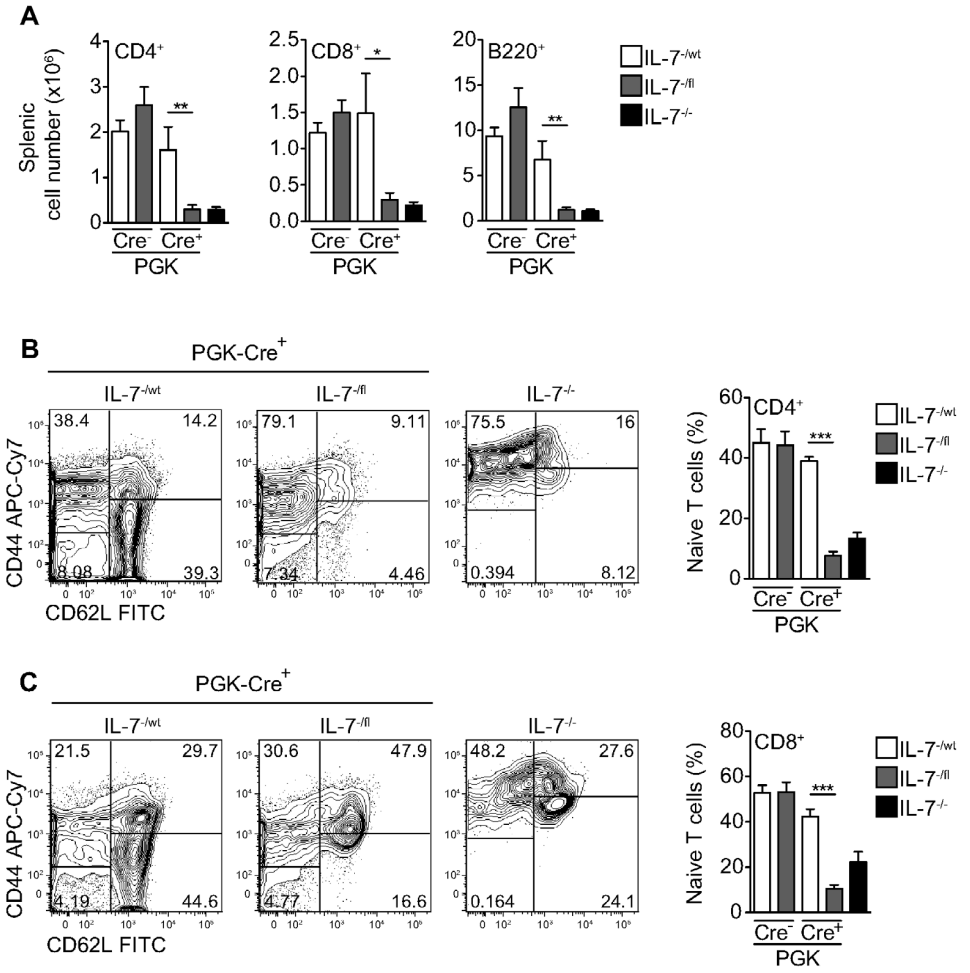

Figure 1. Ubiquitous *Il7* gene inactivation impairs T cell homeostasis. (A) Absolute cell numbers of $CD3^+CD4^+$ or $CD3^+CD8^+$ T cells and $B220^+$ B cells were determined in the spleen of the indicated mouse lines. (B and C) Shown are representative contour plots for the CD44/CD62L expression profiles of (B) $CD3^+CD4^+$ or (C) $CD3^+CD8^+$ T cells in spleen. Numbers in contour plots indicate percentages. Frequencies of naive (B) $CD3^+CD4^+CD44^{lo}CD62L^{hi}$ and (C) $CD3^+CD8^+CD44^{lo}CD62L^{hi}$ T cells are summarized in bar diagrams. (A–C) The data displayed in bar diagrams represent mean ± SEM of seven to nine mice per group analyzed in two independent experiments by flow cytometry. Statistical significances were tested using a non-parametric two-tailed Mann–Whitney *U*-test ($^*p \le 0.05$; $^{**}p \le 0.01$; $^{***}p \le 0.001$).

FRC-derived IL-7 does not affect size and TCR diversity of the peripheral T cell pool

Prx1-Cre-transgenic (Prx1-Cre^+) mice express Cre in BM stromal cells [31], which are crucial for IL-7-dependent B cell development [32]. Whether this mouse model is suitable for targeting FRCs in pLNs was analyzed next. For this purpose, Prx1-Cre^+ mice were crossed to ROSA26 reporter mice expressing red fluorescent protein (RFP) upon Cre-mediated activation of the reporter construct [33]. Peripheral LNs of Prx1-$Cre^+$$ROSA26^{RFP}$ mice were analyzed by flow cytometry to determine the degree of cell type-specific recombination. Among $CD45^-$ stromal cells, around 80% of FRCs expressed RFP while LECs, BECs, and DNs showed only negligible levels of recombination (Fig. 3A and B). Of note, Cre activity was barely detectable in $CD45^+$ immune cells (Fig. 3A) as well as splenic LSCs (data not shown). Hence, Prx1-Cre^+ mice allow gene targeting in pLN FRCs.

In order to inactivate *Il7* gene activity in pLN FRCs, Prx1-Cre^+ mice were crossed to $IL\text{-}7^{fl/fl}$ mice. As compared to FRC^{wt} littermate controls, *Il7* mRNA levels were reduced by approximately 83% in pLNs of $FRC^{\Delta IL\text{-}7}$ mice (Fig. 3C) confirming that FRCs are the major source of IL-7 in pLNs. In contrast, *Il7* mRNA levels in the spleen of $FRC^{\Delta IL\text{-}7}$ mice remained unaltered (Fig. 3C), probably due to the different developmental origins of splenic and LN FRCs [34,35]. Importantly, FRC-specific *Il7* inactivation did not affect frequencies of LSC subsets (Fig. 3D), overall morphology, and chemokine secretion in pLNs (Supporting Information Fig. 2A–D).

When $CD4^+$ and $CD8^+$ T cells were quantified in pLNs and spleens of $FRC^{\Delta IL\text{-}7}$ and FRC^{wt} mice, no significant differences

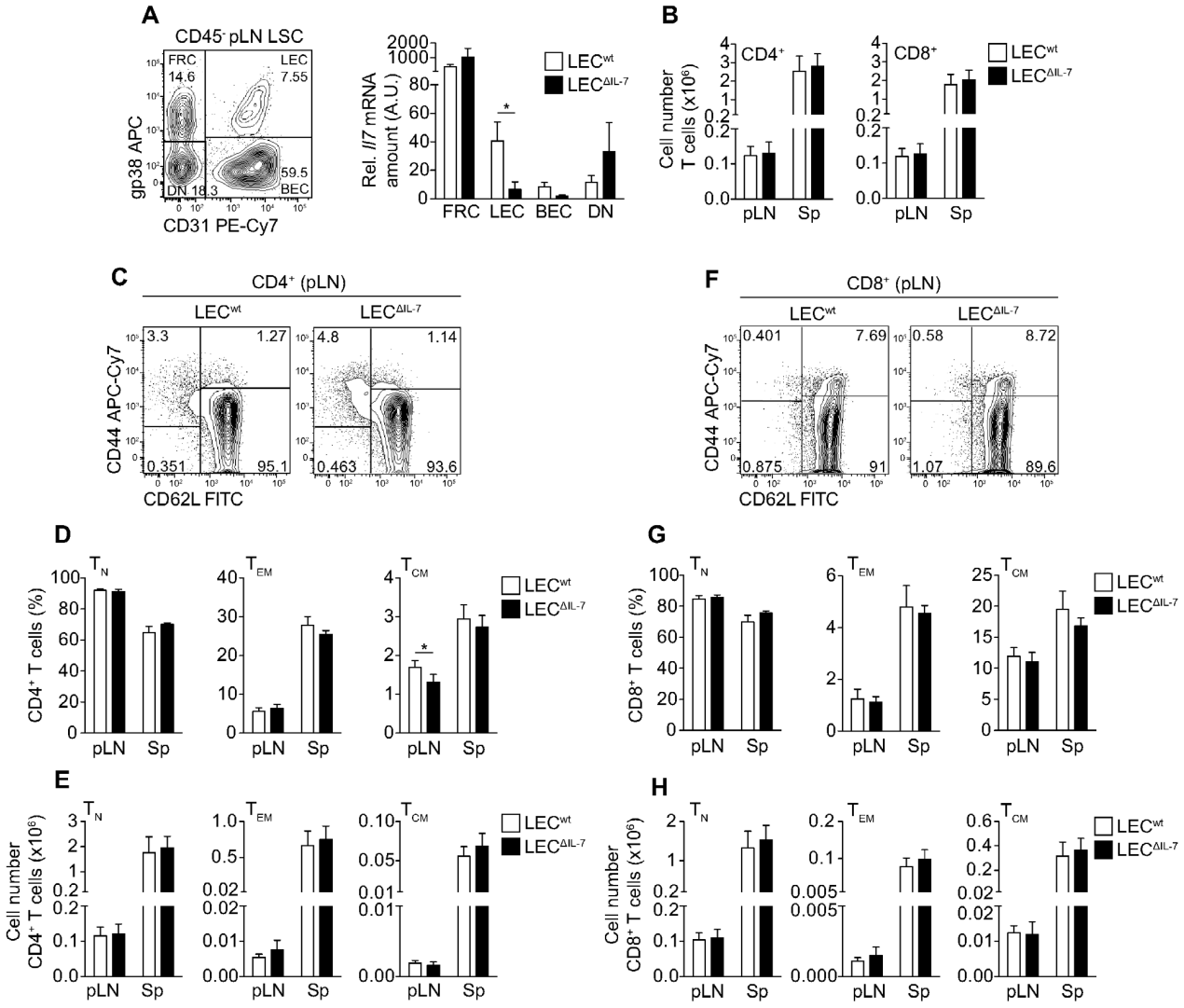

Figure 2. LEC-derived IL-7 is dispensable for peripheral T cell homeostasis. (A) Based on their differential expression of gp38 and CD31, live TER-119$^-$CD45$^-$ pLN LSCs can be subdivided into gp38$^+$CD31$^-$ FRCs, gp38$^+$CD31$^+$ LECs, gp38$^-$CD31$^+$ BECs, and gp38$^-$CD31$^-$ DNs. Shown is a representative contour plot from LEC$^{\Delta IL\text{-}7}$ mice; numbers indicate percentages. The indicated LSC subsets were purified by flow cytometry from LNs of LEC^{wt} (Lyve1-Cre$^+$IL-7$^{-/wt}$ and Lyve1-Cre$^-$IL-7$^{wt/wt}$) and LEC$^{\Delta IL\text{-}7}$ (Lyve1-Cre$^+$IL-7$^{-/fl}$) mice. Three independent sorts with pooled pLNs from three to four mice per group (in total nine to ten mice per group) were performed. Once, cells from two sorts were pooled. Relative *Il7* mRNA amounts were determined by RT-qPCR in relation to *Hprt*. Data displayed in the bar diagram are representative of two data points per group analyzed in two independent RT-qPCR experiments and show mean ± SEM of triplicates. Statistical significances were tested using a nonparametric two-tailed Mann–Whitney *U*-test (*$p \leq 0.05$). (B) Absolute numbers of CD3$^+$CD4$^+$ and CD3$^+$CD8$^+$ T cells were determined in pLNs and spleen (Sp). (C, D, F, and G) Frequencies and (E and H) absolute numbers of naive (T_N; CD44^{lo}CD62L^{hi}), effector memory (T_{EM}; CD44^{hi}CD62L^{lo}) and central memory (T_{CM}; CD44^{hi}CD62L^{hi}) T cells were determined after gating on (C–E) CD3$^+$CD4$^+$ and (F–H) CD3$^+$CD8$^+$ cells isolated from pLNs or spleen. (C and F) Shown are representative contour plots and numbers indicate percentages. (B–H) Data was collected using flow cytometry. (B–H) The data shown in bar diagrams represent mean ± SEM combined from 11–12 LEC^{wt} (Lyve1-Cre$^+$IL-7$^{-/wt}$) and LEC$^{\Delta IL\text{-}7}$ (Lyve1-Cre$^+$IL-7$^{-/fl}$) mice per group analyzed in six independent experiments. Statistical significances were tested using a non-parametric two-tailed Mann–Whitney *U*-test (*$p \leq 0.05$).

were detected in either case (Fig. 3E and G). Furthermore, TCR Vβ repertoires of CD4$^+$ and CD8$^+$ T cells were indistinguishable between FRC$^{\Delta IL\text{-}7}$ and FRC^{wt} mice (Fig. 3F and H). Hence, the size and diversity of the peripheral T cell pool is independent of pLN FRC-derived IL-7.

Next, we assessed whether LEC-derived IL-7 compensates for the lack of FRC-derived IL-7. For this purpose, FRC$^{\Delta IL\text{-}7}$ mice were crossed to LEC$^{\Delta IL\text{-}7}$ mice to generate double Cre-transgenic FRC/LEC$^{\Delta IL\text{-}7}$ mice lacking *Il7* gene expression in both, FRCs and LECs. Similar to LEC$^{\Delta IL\text{-}7}$ (Fig. 2B) or FRC$^{\Delta IL\text{-}7}$ mice (Fig. 3E and G), CD4$^+$ and CD8$^+$ T cells were equally abundant in FRC/LEC$^{\Delta IL\text{-}7}$ and FRC/LEC^{wt} controls (Fig. 3I and J) arguing against a compensatory effect of LEC-derived IL-7 in FRC$^{\Delta IL\text{-}7}$ mice.

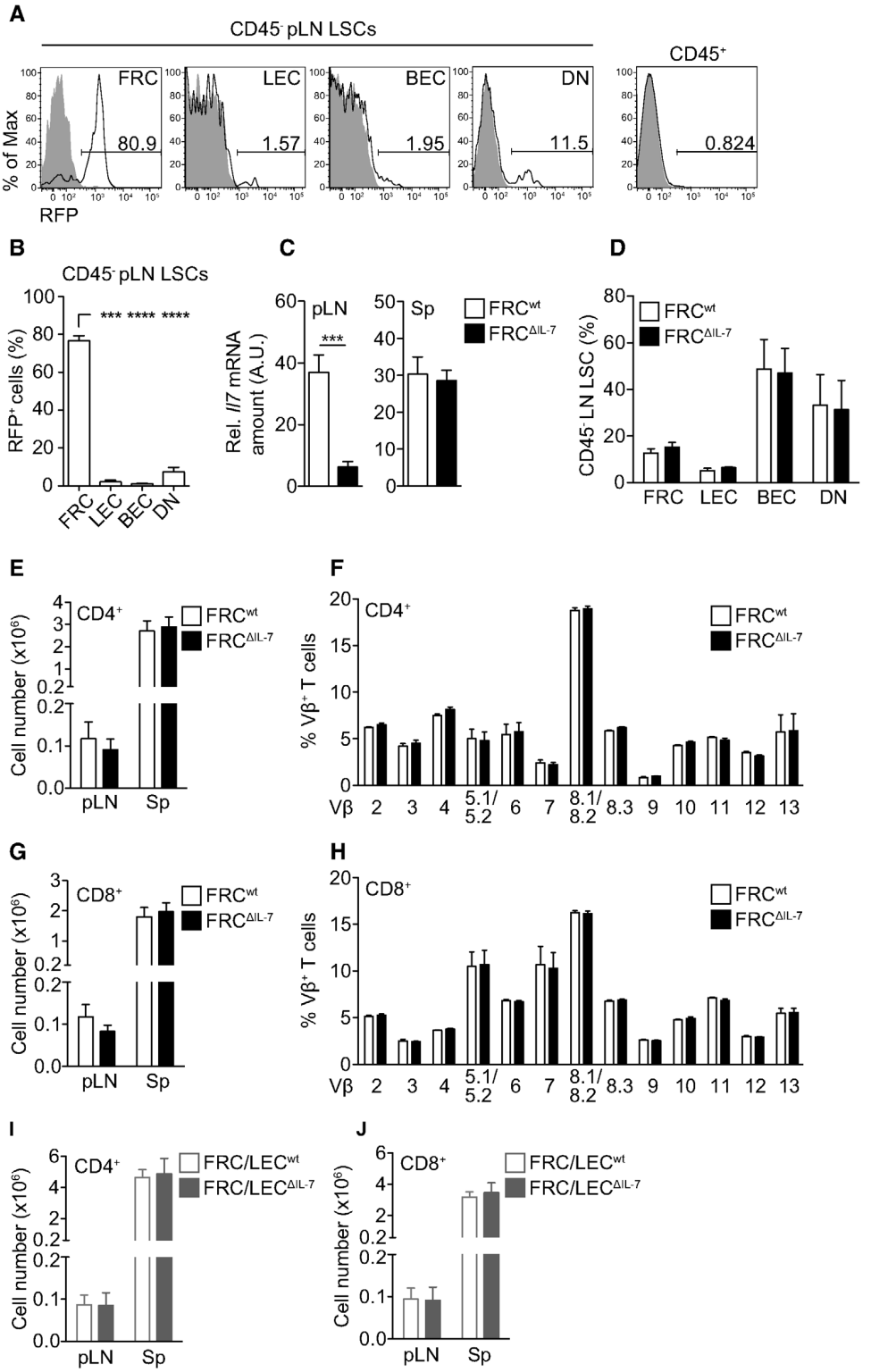

Figure 3. FRC-derived IL-7 does not affect size and diversity of the peripheral T cell pool. (A and B) Peripheral LNs were isolated from Prx1-Cre^{+}ROSA26^{RFP} (white curves) and Prx1-Cre^{-}ROSA26^{RFP} (grey curves) mice to determine recombination efficiency in live TER-119^{-}CD45^{-} LSCs and TER-119^{-}CD45^{+} leukocytes. (A) Numbers indicate percentages of RFP^{+} cells in Prx1-Cre^{+}ROSA26^{RFP} mice. (B) Data show percentages of RFP^{+} cells for the indicated LSC subsets (mean ± SEM). Data were pooled from four to five independent experiments with one to three mice per group. For FRCs, LECs, BECs, and DNs 13, 8, 13, and 13 individual data points were acquired, respectively. (C) Relative *Il7* mRNA amounts were determined

FRC-derived IL-7 determines T_{CM} abundance

Bcl-2 is a direct target of IL-7 [1] and is expressed at particularly high levels by $CD8^+$ T_M [36]. In order to test whether Bcl-2 expression is altered in the absence of FRC-derived IL-7, $CD8^+$ T_N and T_M derived from pLNs and spleens were analyzed. As shown in Fig. 4A, frequencies and numbers of $CD44^{hi}Bcl\text{-}2^{hi}$ $CD8^+$ T_M were significantly reduced in pLNs, but not spleens, of $FRC^{\Delta IL\text{-}7}$ mice. IL-7 conditions $CD8^+$ T cells for the IL-15-induced upregulation of Eomesodermin (Eomes) [37], a transcription factor promoting $CD8^+$ T_M differentiation [38]. As shown in Fig. 4B, $CD44^{hi}Eomes^{hi}$ $CD8^+$ T_M were strongly reduced in pLNs of $FRC^{\Delta IL\text{-}7}$ mice. Again, these differences between FRC^{wt} and $FRC^{\Delta IL\text{-}7}$ mice were most evident in pLNs. However, there was a tendency of reduced $CD8^+$ T_M frequencies and cell numbers in spleens of $FRC^{\Delta IL\text{-}7}$ mice (Fig. 4A and B).

To analyze this IL-7-dependent T_M defect in more detail, CD44 and CD62L expression was analyzed on $CD8^+$ T cells from pLNs and spleens of FRC^{wt} and $FRC^{\Delta IL\text{-}7}$ mice. Frequencies and numbers of $CD8^+$ $CD44^{lo}CD62L^{hi}$ T_N and $CD44^{hi}CD62L^{lo}$ T_{EM} were indistinguishable in pLNs and spleens of FRC^{wt} and $FRC^{\Delta IL\text{-}7}$ mice (Fig. 4C–E). In apparent contrast, frequencies of $CD8^+$ $CD44^{hi}CD62L^{hi}$ T_{CM} were significantly reduced in pLNs and spleens of $FRC^{\Delta IL\text{-}7}$ mice (Fig. 4D). With regard to absolute $CD8^+$ T_{CM} numbers, this difference between both mouse strains was limited to pLNs (Fig. 4E). $CD4^+$ T_N and $CD4^+$ T_{EM} frequencies and numbers were unaltered in pLNs and spleens of FRC^{wt} and $FRC^{\Delta IL\text{-}7}$ mice (Fig. 4F–H). Similar to $CD8^+$ T_{CM} (Fig. 4D), frequencies of $CD4^+$ T_{CM} were reduced in $FRC^{\Delta IL\text{-}7}$ pLNs but were only slightly affected in spleens (Fig. 4G). Absolute cell numbers were not significantly different in pLNs and spleens of both mouse strains (Fig. 4H). Hence, *Il7* gene inactivation in FRCs is associated with a reduction of $CD8^+$ T_{CM}, an effect that was by far less pronounced for $CD4^+$ T_{CM}.

The survival of both, T_N and T_{CM}, critically relies on IL-7 [1,4] suggesting that either incomplete *Il7* gene inactivation or the presence of non-pLN-derived IL-7 created IL-7 levels in $FRC^{\Delta IL\text{-}7}$ pLNs that were sufficient for T_N survival but too low for T_{CM} maintenance. However, this assumption would predict different efficacies of IL-7 utilization by T_N and T_{CM}. Consistent with this idea and recent data [39], IL-7 treatment induced a more efficient IL-7 receptor α (IL-7Rα; CD127) down-regulation by $CD8^+$ T_N compared to T_{CM} (Supporting Information Fig. 3A). IL-7R signaling leads to the phosphorylation of STAT5 that in turn regulates genes controlling T cell survival [40,41]. Interestingly, more pronounced IL-7Rα down-modulation by $CD8^+$ T_N (Supporting Information Fig. 3A) correlated with more efficient STAT5 phosphorylation (Supporting Information Fig. 3B). This argues for a more effective utilization of IL-7 by $CD8^+$ T_N and provides an explanation for their survival in $FRC^{\Delta IL\text{-}7}$ mice. Conversely, $CD8^+$ T_{CM} appear to require higher levels of FRC-derived IL-7 for survival.

Unimmunized adult mice contain virtual memory $CD8^+$ T cells ($CD8^+$ vT_M), which are generated independently of foreign antigen contact as a result of lymphopenia-induced proliferation (LIP) in the neonatal phase [42–47]. As we have shown previously, IL-7 promotes $CD8^+$ vT_M formation [45]. Whether and how FRC-derived IL-7 also affects the formation/maintenance of foreign antigen-specific $CD8^+$ T_{CM} was tested next. For this purpose, FRC^{wt} and $FRC^{\Delta IL\text{-}7}$ mice were reconstituted with TCR-transgenic $CD8^+$ OT-I T cells specific for the OVA-derived peptide SIINFEKL. In order to mimic a viral infection, recipient mice were immunized with a mixture of PolyI:C and SIINFEKL 24 h later. PolyI:C induces pro-inflammatory cytokines such as IFN-α/β and IFN-γ, which promote IL-7 upregulation [24,48] and the subsequent formation and maintenance of T_M [8,49]. Thirty days after vaccination the numbers of splenic $CD8^+$ OT-I T_M were comparable between FRC^{wt} and $FRC^{\Delta IL\text{-}7}$ mice (Fig. 4I). However, similar to the experiments shown above, T_{CM} frequencies were clearly reduced in $FRC^{\Delta IL\text{-}7}$ mice whereas T_{EM} appeared to be less dependent on FRC-derived IL-7 (Fig. 4J and K). This finding indicates that FRC-derived IL-7 helps to maintain both, virtual as well as foreign antigen-specific $CD8^+$ T_{CM}.

Discussion

In steady state, IL-7 is supposed to be produced at constant levels [50], mainly by radio-resistant stromal cells [1,51]. T_N and T_M express high levels of the IL-7R enabling them to remove IL-7 from the system continuously [50]. As soon as the peripheral T cell pool reaches a critical size, IL-7 production and consumption reach the equilibrium and the survival of additional T cells is prevented. Hence, the maintenance of T cell homeostasis relies on the competition for limiting amounts of IL-7 [14,50,52].

The seminal work by Link et al. identified LECs and FRCs as main sources of IL-7 in pLNs. Additionally, co-culture experiments

in pLNs (left) and spleens (Sp; right) of FRC^{wt} ($Prx1\text{-}Cre^+IL\text{-}7^{-/wt}$ and $Prx1\text{-}Cre^+IL\text{-}7^{wt/wt}$) and $FRC^{\Delta IL\text{-}7}$ ($Prx1\text{-}Cre^+IL\text{-}7^{-/fl}$ and $Prx1\text{-}Cre^+IL\text{-}7^{fl/fl}$) mice by RT-qPCR in relation to *Hprt*. Data are representative of five to nine mice per group analyzed in two to five independent RT-qPCR experiments and show mean ± SEM of triplicates. (D) Frequencies of viable $TER\text{-}119^-CD45^-$ LSC subsets were determined in CD45-depleted LNs of FRC^{wt} ($Prx1\text{-}Cre^+IL\text{-}7^{-/wt}$) and $FRC^{\Delta IL\text{-}7}$ ($Prx1\text{-}Cre^+IL\text{-}7^{-/fl}$) mice. In three independent experiments, peripheral LNs of three mice were pooled and three individual data points were acquired for FRCs, LECs, BECs, and DNs. Shown are pooled results (mean ± SEM). (E and G) Absolute numbers and the (F and H) composition of the Vβ TCR repertoire were determined for (E and F) $CD3^+CD4^+$ and (G and H) $CD3^+CD8^+$ T cells in (E and G) pLN/Sp and (F and H) Sp of FRC^{wt} ($Prx1\text{-}Cre^+IL\text{-}7^{wt/wt}$) and $FRC^{\Delta IL\text{-}7}$ ($Prx1\text{-}Cre^+IL\text{-}7^{fl/fl}$) mice by flow cytometry. Data (mean ± SEM) were pooled from (E and G) three independent experiments with a total of 11 mice per group and (F and H) two independent experiments with a total of six mice per group. (I and J) Absolute numbers of (I) $CD3^+CD4^+$ and (J) $CD3^+CD8^+$ T cells were determined in pLNs and Sp of FRC/LEC^{wt} ($Prx1\text{-}Cre^+Lyve1\text{-}Cre^-IL\text{-}7^{-/wt}$) and $FRC/LEC^{\Delta IL\text{-}7}$ ($Prx1\text{-}Cre^+Lyve1\text{-}Cre^+IL\text{-}7^{-/fl}$) mice. Data (mean ± SEM) were pooled from four to six independent experiments with a total of 10–11 mice per group. (A, B, D–J) Data were analyzed using flow cytometry. (C–J) Statistical significances were tested using a non-parametric two-tailed Mann–Whitney *U*-test (***$p \le 0.001$; ****$p \le 0.0001$).

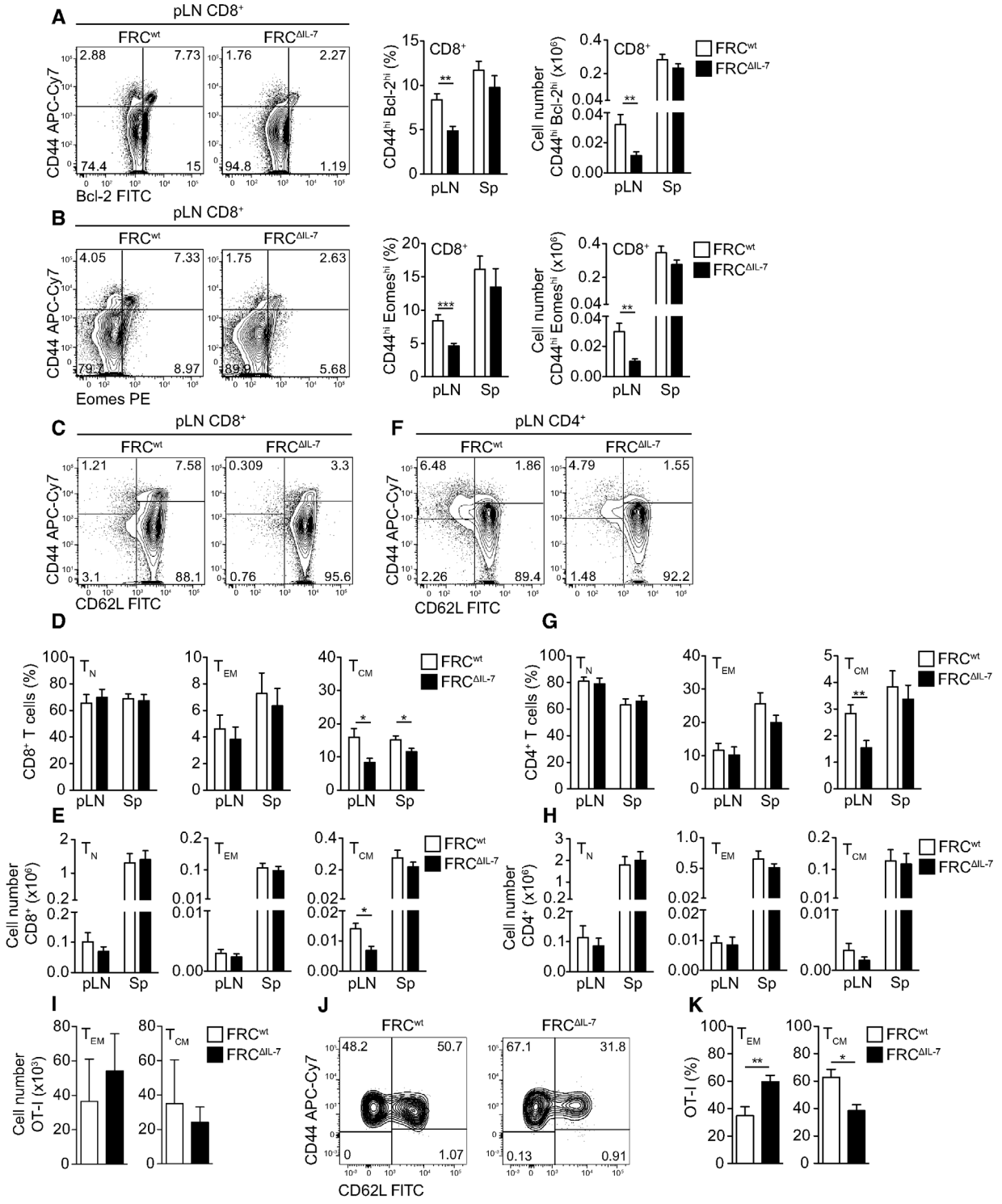

Figure 4. FRC-derived IL-7 determines T_{CM} abundance in pLNs. (A–E) $CD3^+CD8^+$ and (F–H) $CD3^+CD4^+$ T cells from pLNs and spleens (Sp) of FRC^{wt} ($Prx1\text{-}Cre^+IL\text{-}7^{wt/wt}$) and $FRC^{\Delta IL\text{-}7}$ ($Prx1\text{-}Cre^+IL\text{-}7^{fl/fl}$) mice were analyzed for their expression of the indicated molecules. (A, B, C, and F) Shown are representative contour plots and numbers indicate percentages. Bar diagrams represent percentages or numbers of (A) $CD44^{hi}Bcl\text{-}2^{hi}$, (B) $CD44^{hi}Eomes^{hi}$ cells or (D, E, G, H) T_N ($CD44^{lo}CD62L^{hi}$), T_{EM} ($CD44^{hi}CD62L^{lo}$), and T_{CM} ($CD44^{hi}CD62L^{hi}$). (A–H) Data in bar diagrams represent pooled results (mean ± SEM) from 10–11 mice combined and analyzed in three independent experiments. (I–K) $FRC^{\Delta IL\text{-}7}$ ($Prx1\text{-}Cre^+IL\text{-}7^{fl/fl}$) and FRC^{wt} ($Prx1\text{-}Cre^+IL\text{-}7^{wt/wt}$) mice (all $Thy1.2^+$) received 7×10^5 naive $CD8^+Thy1.1^+$ OT-I T cells. Twenty-four hours later, recipient mice were vaccinated

revealed that FRC-derived IL-7 promotes T_N survival [9] suggesting that circulating T_N receive IL-7-dependent survival signals in pLNs [14–17]. Besides its impact on T_N homeostasis, IL-7 also promotes the formation and maintenance of other pLN-homing immune cells including $CD8^+$ T_{CM} [1,8,40] and $ROR\gamma t^+$ type 3 innate lymphoid cells (ILC3) [53,54]. Therefore, a common pool of FRC-derived IL-7 is supposed to regulate homeostasis of multiple immune cells in pLNs [17].

There is accumulating evidence that $CD8^+$ T_N and T_M pools are regulated independently [55–57] indicating that they colonize different ecological niches [55–57]. In the immune system, ecological niches are defined by the combination of resources affecting the survival and function of a particular immune cell population [57]. In order to limit competition and enable the simultaneous survival of multiple immune cell types, ecological niches must be segregated. However, niche segregation of $CD8^+$ T_N and T_{CM} appears to be incomplete as suggested by their common IL-7 dependence [40,56]. Nevertheless, we do not know yet if niche segregation involves the IL-7-dependent spatial separation of both cell types. The uneven distribution of IL-7-producing FRCs [29,58] suggests that, similar to chemokines [59,60], areas of high and low IL-7 density exist in pLNs. Based on their differential IL-7 demands, this assumption would predict the accumulation of $CD8^+$ T_N and T_{CM} in separate pLN regions. Of note, the degree of local $CD8^+$ T_N and T_{CM} segregation in pLNs varies strongly between experimental systems [61,62]. Whether this context-dependent effect correlates with the presence or absence of IL-7-producing FRCs in particular regions is still unclear since, at least to our knowledge, reliable reagents for IL-7 protein detection in pLNs are still missing.

Although we cannot fully exclude that different anatomical locations modulate distinct aspects of IL-7-dependent $CD8^+$ T_N and T_{CM} homeostasis, our results indicate that variable IL-7 sensitivities of $CD8^+$ T_N and T_{CM} contribute to the segregation of their ecological niches. In agreement with a recent study [39], we confirmed that IL-7R signaling is less efficient in $CD8^+$ T_{CM}. In a situation of limited IL-7 availability, this property would provide an explanation for the reduction of virtual as well as foreign antigen-specific $CD8^+$ T_{CM} in $FRC^{\Delta IL\text{-}7}$ mice. Furthermore, our results are in line with the current paradigm of IL-7-dependent T cell homeostasis proposing that the optimized utilization of limiting IL-7 amounts is prerequisite for the survival of the greatest possible number of IL-7-dependent immune cells [63]. Based on this model, the degree of competition between different IL-7-consuming cells would be restricted and the limited space within pLNs would be used most optimally [14,50].

The insensitivity of T_N to FRC-specific *Il7* inactivation may be due to the fact that T_N are anyway capable of surviving short phases of IL-7 deficiency [63]. Indeed, IL-7 binding induces the down-modulation of IL-7R expression by T_N more rapidly than by T_{CM} rendering them insensitive to further IL-7 signals [63]. This effect is transient and appears to fulfill at least two functions. First, the amount of IL-7 consumed by a single T_N is restricted thereby optimizing IL-7 availability for other immune cells [63]. Second, permanent IL-7R signaling would cause chronic T cell activation and subsequent activation-induced cell death [64]. Keeping in mind that (i) multiple organs produce IL-7 [24,25] and (ii) T_N continuously circulate through the body, they may tolerate the partial IL-7-deficiency in $FRC^{\Delta IL\text{-}7}$ pLNs because they received critical IL-7 signals elsewhere. Alternatively, incomplete *Il7* gene inactivation in $FRC^{\Delta IL\text{-}7}$ pLNs may allow the production of residual IL-7, which is just sufficient to promote local T_N survival. In any case, our data demonstrate that T_{CM} and T_N do not tolerate the reduction of IL-7 in $FRC^{\Delta IL\text{-}7}$ pLNs equally well. As shown for polyclonal $CD8^+$ T cells in the steady state and for $CD8^+$ OT-I T cells after vaccination, T_{CM} prove to be particularly sensitive to IL-7 ablation in FRCs. However, $CD8^+$ T_{CM} are only partially reduced in $FRC^{\Delta IL\text{-}7}$ mice. Whether this is due to the survival of $CD8^+$ T_{CM} subsets with reduced IL-7 demands remains to be shown in the future.

When we compared $FRC^{\Delta IL\text{-}7}$ and FRC^{wt} pLNs, we did not observe any obvious differences (Supporting Information Fig. 2A–C). T and B lymphocyte distribution, stromal cell localization, and relative distances between FRCs and lymphocytes appeared normal in $FRC^{\Delta IL\text{-}7}$ mice (Supporting Information Fig. 2A–C). Furthermore, chemokine expression was comparable between $FRC^{\Delta IL\text{-}7}$ and FRC^{wt} pLNs (Supporting Information Fig. 2D) and ILC3 contributing to the IL-7-dependent regulation of T cell homeostasis [51,54,65] were similarly abundant (Supporting Information Fig. 2E). Hence, our findings argue for normal LN development and function in the absence of FRC-derived IL-7. This strongly suggests that the reduction of T_{CM} in $FRC^{\Delta IL\text{-}7}$ results from a lack of IL-7-dependent homing/survival signals rather than structural and/or functional alterations of $FRC^{\Delta IL\text{-}7}$ pLNs.

In summary, we provide evidence that IL-7 produced by pLN FRCs regulates T cell homeostasis. As opposed to the current model, our data demonstrate that pLN FRC-derived IL-7 is of limited importance for the local and systemic survival of T_N. On the contrary, the maintenance of T_{CM} critically relies on steady state levels of FRC-derived IL-7 suggesting that T_N and T_{CM} colonize different ecological niches in vivo.

Material and Methods

Mice

Prx1-Cre [66] (stock no. 005584) and Lyve1-Cre [30] (stock no. 012601) mice were purchased from The Jackson Laboratory.

i.v. with a mixture of 50 μg SIINFEKL and 50 μg PolyI:C. Thirty days post vaccination, recipient splenocytes were analyzed by flow cytometry. (I) Cell numbers and (K) frequencies of T_{EM} ($CD44^{hi}CD62L^{lo}$) and T_{CM} ($CD44^{hi}CD62L^{hi}$) were determined after gating on $CD8^+Thy1.1^+$ OT-I T cells. (J) Shown are representative contour plots and numbers indicate percentages. (I and K) Shown are pooled results (mean ± SEM) from eight to nine mice analyzed in three independent experiments. (A–K) Data were analyzed using flow cytometry. Statistical significances were tested using a non-parametric two-tailed Mann–Whitney *U*-test ($*p \le 0.05$; $**p \le 0.01$; $***p \le 0.001$).

Together with IL-7$^{-/-}$ [3], PGK-Cre [27], Flpo [67], Rag1$^{-/-}$ Thy1.1^{+} OT-I [68], and ROSA26^{RFP} [33] mice, they were maintained under specific pathogen-free conditions at the central animal facility of the Medical Faculty of the Otto-von-Guericke-University Magdeburg. Whenever possible, control littermates were used. Experimental procedures were approved by the relevant animal experimentation committee and performed in compliance with international and local animal welfare legislations (Landesverwaltungsamt Sachsen-Anhalt Permit Number: 42502-2-1288 UniMD).

Generation of IL-7$^{fl/fl}$ mice and genotyping

The C57BL6/N (B6) embryonic stem cell (ES) line JM8A3.N1 harboring the "knockout-first" allele *Il7*$^{tm1a(EUCOMM)Wtsi}$ was provided by The European Conditional Mouse Mutagenesis Program (EUCOMM). Mice harboring the *Il7*$^{tm1a(EUCOMM)Wtsi}$ allele were generated by standard blastocyst injection and crossed to Flpo-transgenic mice [67] in order to remove the FRT-flanked part of the targeting construct (Supporting Information Fig. 1A). Resulting mice harboring floxed *Il7* alleles (*Il7*^{fl}) were crossed to the indicated Cre-transgenic mice in order to delete exons 3 and 4. Mice were genotyped by PCR using the forward primer 5'-AGAGGATGCAGGGACACATCTGCC-3 (upstream FRT site 1), the reverse primers 5'-ATTTTCCTGATTCTACTTACTGGC-3' (upstream exon 3) and 5'-CAACGGGTTCTTCTGTTAGTCC-3' (downstream FRT site 1) exhibiting a 445 bp band for the *Il7*$^{tm1a(EUCOMM)Wtsi}$ allele, a 680 bp band for the floxed *Il7* allele, and a 523 bp band for the WT allele.

Cell isolation

To obtain single cell suspensions from pLNs and spleens, organs were forced through metal strainers in PBS/2 mM EDTA (Carl Roth) and erythrocytes were lysed. For erythrocyte lysis, spleen cells were re-suspended in ammonium-chloride-potassium lysis buffer for 90 s followed by the addition of RPMI 1640 (Biochrom) containing 10% (v/v) FCS (PAN Biotech) and 1% (v/v) penicillin/streptomycin (P/S; Gibco). After centrifugation, spleen cells were re-suspended in PBS/2 mM EDTA and filtered through 40 μm cell strainers (Corning, Durham, NC).

For LSC and ILC isolation, fat-free pLNs were cut into small (1 × 1 mm) pieces in RPMI 1640/10% FCS/1% P/S. Peripheral LN fragments were vortexed and the supernatant was removed after the organ pieces had settled. This process was repeated three times. Cells in the supernatant were collected and ILCs were analyzed by flow cytometry. pLN fragments were transferred into 12-well plates containing 1 mL digestion medium I (0.2 mg/mL Collagenase P [Roche], 0.2 mg/mL Dispase II [Roche], 10 μg/mL DNase I [Sigma], and 5 μg/mL Latrunculin B [Calbiochem] in RPMI 1640 supplemented with 10% FCS/1% P/S). After incubation for 30 min at 37°C and 5% (v/v) CO_2, 1 mL digestion medium II (0.4 mg/mL Collagenase P, 0.2 mg/mL Dispase II, 10 μg/mL DNase I, and 5 μg/mL Latrunculin B in RPMI 1640/10% FCS/1 % P/S) was added and the samples were re-suspended. After incubation for 30 min at 37°C and 5% CO_2, 0.5 mL RPMI 1640/10% FCS/1% P/S/ 10 mM EDTA was added to stop digestion. Cell suspensions were filtered through 70 μm cell strainers and cells were washed with PBS/2 mM EDTA. Cells were resuspended in PBS/2 mM EDTA and filtered through 40 μm cell strainers.

Adoptive T cell transfer

Naive (CD44^{lo}CD62L^{hi}) CD8^{+} T cells (Supporting Information Fig. 6C) expressing a transgenic TCR (Vα2Vβ5) specific for the chicken OVA-derived, H2-K^{b}–restricted peptide OVA$_{257–264}$ (SIINFEKL), were isolated from LNs and spleen of Rag1$^{-/-}$ Thy1.1^{+} OT-I mice using CD8a-specific MicroBeads and AutoMACS (Miltenyi Biotec) according to the manufacturer's recommendations. Thy1.2^{+} recipients received 4–7 × 10^{5} OT-I T cells (purity > 81.7%) via i.v. injection into the tail vein. Twenty-four hours after T cell transfer recipient mice were immunized with a mixture of 50 μg SIINFEKL (Biosyntan) and 50 μg PolyI:C (Invivogen).

In vitro IL-7 stimulation

Single cell suspensions of peripheral and mesenteric lymph nodes were adjusted to 5 × 10^{6} cells/mL and incubated for 30 min at 37°C and 5% CO_2 in RPMI 1640 supplemented with 10% FCS/1% P/S/2 mM L-glutamine (Gibco)/1 mM sodium pyruvate (Gibco)/0.1 mM HEPES (Gibco)/50 μM 2-mercaptothanol (Sigma) and 1 ng/mL recombinant mouse (protein carrier free) IL-7 (EBioscience, Thermo Fisher Scientific).

Flow cytometry cell sorting of LSCs

LSCs were isolated from peripheral and mesenteric lymph nodes as described above. LN cells were incubated with purified anti-CD16/32 (2.4G2 ATCC® HB-197™) in staining buffer (PBS/0.5% [w/v] BSA (AppliChem)/2 mM EDTA) for 10 min at 4°C. Subsequently, cells were stained with biotinylated CD45- and TER-119-specific antibodies in staining buffer containing anti-CD16/32 for 30 min at 4°C. CD45^{+} and TER-119^{+} cells were depleted using Dynabeads Biotin Binder (Invitrogen). In brief, cells were re-suspended in staining buffer to 1 × 10^{7} cells/mL and 50 μL pre-washed magnetic beads were added. Cells were incubated for 30 min at 4°C under gentle rotation and CD45^{+} and TER-119^{+} cells were removed subsequently using a DynaMag-15 (Thermo Fisher Scientific). Remaining cells were stained with fluorochrome-labeled gp38- and CD31-specific antibodies as well as streptavidin-FITC for 30 min at 4°C. Finally, after washing with PBS/2 mM EDTA, the cells were re-suspended in RPMI 1640/10% FCS/1% P/S. For dead cell exclusion, 7-aminoactinomycin D (7-AAD; BioLegend) was added 5 min prior to cell sorting using a FACSARIA III (Becton Dickinson). Live (7-AAD^{-}),

TER-119$^-$CD45$^-$ LSC subsets were sorted based on their differential gp38/CD31 expression. Purities of the indicated LSC subsets were >73.3 % (data not shown).

Flow cytometry

The following reagents were purchased from BioLegend: anti-mouse Bcl-2 (10C4), CD3 (145-2C11), CD3 (17A2), CD4 (RM4-5), CD5 (53-7.3), CD8a (53-6.7), CD11c (N418), CD19 (6D5), CD44 (IM7), CD45 (30-F11), CD62L (MEL-14), CD127 (A7R34), gp38 (8.1.1), Gr1 (RB6-8C5), NK1.1. (PK136), TER-119 (TER-119), Thy1.1 (OX-7), Vα2 (B20.1), 7-AAD viability staining solution, and streptavidin-FITC. Anti-mouse CD31 (390), Eomes (Dan11mag), and RORγ(t) (B2D) were purchased from eBioscience. Anti-mouse CD45R (B220; RA3-6B2) and the anti-mouse TCR Vβ screening panel were purchased from BD Biosciences. Prior to staining with fluorochrome-labeled antibodies, single cell suspensions were incubated with 50 μL of anti-mouse CD16/32 in staining buffer for 10 min at 4°C. Afterward, cells were incubated with 50 μL of fluorochrome-labeled antibodies diluted in anti-CD16/32 containing staining buffer. After incubation for 30 min at 4°C, cells were washed with 200 μL PBS/ 2 mM EDTA. For intranuclear stainings (except pSTAT5), samples were processed using the FoxP3/Transcription Factor Staining Buffer Set (eBioscience, Thermo Fisher Scientific) according to the manufacturer's recommendations. For staining of pSTAT5, cell samples were fixed for 30 min at 4°C with Fixation Buffer (BioLegend) and washed with 200 μL Intracellular Staining Permeabilization Wash Buffer (BioLegend). Subsequently, cells were incubated with anti-mouse pSTAT5 Y694 (47; BD Biosciences) in wash buffer for 30 min at 4°C, washed with 200 μL Wash Buffer and finally resuspended in PBS/2 mM EDTA prior to analysis. For LSC analyses, 7-AAD was added 5 min prior to data acquisition. Samples were measured on a LSRFortessa (Becton Dickinson) and analyzed with FlowJo 9/10 software (FlowJo, LLC) according to the "Guidelines for the use of flow cytometry and cell sorting in immunological studies" [69]. Individual gating strategies are depicted in Supporting Information Figs. 1, 2, and 4–6.

Reverse transcriptase PCR (RT-PCR) and real-time quantitative PCR (RT-qPCR)

Colon samples were transferred into CK14 2 mL tubes (Peqlab/VWR) containing 700 μL TRIzol reagent (Invitrogen) and homogenized in a Precellys 24 homogenizer (Peqlab/VWR). Peripheral LNs were transferred into CK14 0.5 mL tubes (Peqlab/VWR) containing 200 μL TRIzol reagent and homogenized. Sorted LSCs were re-suspended in 500 μL TRIzol reagent. For RNA extraction, chloroform (Sigma–Aldrich) was added and total RNA was isolated according to the manufacturer's instructions.

Isolated RNA was quantified by photometric Nanodrop (Thermo Fisher Scientific) measurement. RNA was reverse-transcribed using random hexamer primers and the advantage RT-for-PCR kit (Takara Clontech) according to the manufacturer's instructions.

For RT-PCR analyses of colon samples, the Taqman® Gene Expression Master Mix (Thermo Fisher Scientific) and the following TaqMan® Gene Expression Assays (Thermo Fisher Scientific) were used according to the manufacturer's instructions: *Il7* (FAM-MGB probe Mm01295804_m1) and *Hprt* (FAM-MGB probe Mm00446968_m1). PCR products were analyzed by agarose gel electrophoresis.

For RT-qPCR analyses of sorted LSCs and whole pLNs, the Taqman® Gene Expression Master Mix (Thermo Fisher Scientific) and the following TaqMan® Gene Expression Assays (Thermo Fisher Scientific) were used according to the manufacturer's instructions: *Ccl19* (FAM-MGB probe Mm00839967_g1), *Ccl21* (FAM-MGB probe Mm03646971_gH), *Cxcl9* (FAM-MGB probe Mm000434946_m1), *Cxcl10* (FAM-MGB probe Mm00445235_m1), *Cxcl13* (FAM-MGB probe Mm00444534_m1), *Il7* (FAM-MGB probe Mm01295805_m1), and *Hprt* (FAM-MGB probe Mm00446968_m1). Samples were analyzed in triplicates and C_T values were exported from the ABI PRISM 7000 (Applied Biosystems) sequence detection system. The relative quantifications were calculated according to the ΔC_T method.

Automated multidimensional fluorescence microscopy by multi-epitope-ligand cartography

Multi-epitope-ligand cartography (MELC) was performed as described previously [70]. Briefly, pLNs were embedded into Tissue-Tek® O.C.T.™ compound (Sakura Finetek), frozen on dry ice, and stored at –80°C. Ten micrometer cryo-sections adhered to silane-coated cover slides (Thermo Fisher Scientific) were fixed with PBS/2% (w/v) paraformaldehyde (Sigma–Aldrich), permeabilized with PBS/0.2% (v/v) Triton-X-100 (Carl Roth) and blocked with PBS/1 % (w/v) BSA (Sigma–Aldrich) + 30% (v/v) normal goat serum (Invitrogen). Tissue samples were transferred to an inverted wide-field fluorescence microscope (Leica DMi8, 20× air lens NA 0.80; Leica Microsystems). The automated cyclic robotic process started with the incubation of the first fluorochrome-labeled antibody (tag). After a series of washing steps, the fluorescence signals and a corresponding phase contrast image were acquired by a cooled charge-coupled device camera (Apogee KX4; Apogee Instruments). The specific signal of the given tag was removed by bleaching the fluorescent dye followed by recording of post-bleaching fluorescence signals and repetition of incubation-imaging-bleaching-cycle. The appropriate working dilutions, incubation times, and positions within the MELC experiment of the used tags (anti-mouse CD3 (17A2), CD31 (390), CD8a (53-6.7), gp38 (8.1.1), CD45 (30-F11), CD54 (YN1/1.7.4), CD44 (IM7), and CD45R/B220 (RA3-6B2) were purchased from BioLegend, anti-mouse CD4 (RM4-5) from BD Biosciences, PI from Sigma–Aldrich) were validated systematically using conditions suitable to MELC [70]. The series of fluorescence images produced by each tag were aligned pixel-wise using the corresponding phase

contrast images. The automated algorithm reaches an alignment accuracy of 0.1 pixels. Illumination faults of the images were corrected using flat-field correction. Post-bleaching images were subtracted from the following fluorescence tag images. Section artifacts were excluded as invalid by a manual mask-setting process. We developed pipelines for the Cell Profiler software package [71] in order to detect (i) all cells within the tissue section using the staining of PI, CD45, CD44, and CD54, and (ii) to create masks for gp38 and CD31 positive signals. Using these masks of gp38 and CD31 the FRC region was defined as $gp38^+$ and $CD31^-$. For each cell, the mean fluorescent intensity and the smallest distance to the reference region FRC was calculated. The resulting matrix of intensities and distances were exported into an FCS file and uploaded to the online cytometry analysis platform "cytobank.org" for multiparametric analysis.

Statistical analyses

Statistical analyses and graphical representations were performed using Prism 5.0d/f (GraphPad Software Inc.). Statistical significances were determined using non-parametric two-tailed Mann–Whitney U tests; $^{*}p \leq 0.05$; $^{**}p \leq 0.01$; $^{***}p \leq 0.001$; $^{****}p \leq 0.0001$.

Acknowledgements: T.S. designed and supervised the study with the help of L.K. and K.D.; L.K., K.D., U.B., A.W., J.M., and L.P. performed experiments and analyzed data; H.J.F. provided essential reagents; A.J.M. and U.K. analyzed and discussed the data; T.S. analyzed the data and wrote the manuscript with the help of the other co-authors. We thank R. Naumann, J. Giese, E. Denks, C. Kozowsky, G. Höbbel, J. Nichelmann, and M. Berger for support and K. Anastassiadis for PGK-Cre- and Flpo-transgenic mice. This work was supported by the Deutsche Forschungsgemeinschaft (Sonderforschungsbereiche TR36 (project B7; to T.S.), SFB854 (project B15; to U.K. and T.S.), and DFG priority program 1937 (project SCHU 2326/2-1; to T.S.).

Conflict of interest: The authors declare no competing financial or commercial interests.

References

1 **Schluns, K. S., Kieper, W. C., Jameson, S. C. and Lefrançois, L.**, *Nat. Immunol.* 2000. **1**: 426–432

2 **Boyman, O., Purton, J. F., Surh, C. D. and Sprent, J.**, *Curr. Opin. Immunol.* 2007. **19**: 320–326

3 **von Freeden-Jeffry, U., Vieira, P., Lucian, L. A., McNeil, T., Burdach, S. E. and Murray, R.**, *J. Exp. Med.* 1995. **181**: 1519–1526

4 **Tan, J. T., Dudl, E., LeRoy, E., Murray, R., Sprent, J., Weinberg, K. I. and Surh, C. D.**, *Proc. Natl. Acad. Sci. U. S. A.* 2001. **98**: 8732–8737

5 **Opferman, J. T., Letai, A., Beard, C., Sorcinelli, M. D., Ong, C. C. and Korsmeyer, S. J.**, *Nature* 2003. **426**: 671–676

6 **Wofford, J. A., Wieman, H. L., Jacobs, S. R., Zhao, Y. and Rathmell, J. C.**, *Blood* 2008. **111**: 2101–2111

7 **Jacobs, S. R., Michalek, R. D. and Rathmell, J. C.**, *J. Immunol.* 2010. **184**: 3461–3469

8 **Cui, G., Staron, M. M., Gray, S. M., Ho, P.-C., Amezquita, R. A., Wu, J. and Kaech, S. M.**, *Cell* 2015. **161**: 750–761

9 **Link, A., Vogt, T. K., Favre, S., Britschgi, M. R., Acha-Orbea, H., Hinz, B., Cyster, J. G. et al.**, *Nat. Immunol.* 2007. **8**: 1255–1265

10 **Ariel, A., Hershkoviz, R., Cahalon, L., Williams, D. E., Akiyama, S. K., Yamada, K. M., Chen, C. et al.**, *Eur. J. Immunol.* 1997. **27**: 2562–2570

11 **Banwell, C. M., Partington, K. M., Jenkinson, E. J. and Anderson, G.**, *Eur. J. Immunol.* 2000. **30**: 2125–2129

12 **Dai, Z. and Lakkis, F. G.**, *J. Immunol.* 2001. **167**: 6711–6715

13 **Dummer, W., Ernst, B., LeRoy, E., Lee, D. and Surh, C.**, *J. Immunol.* 2001. **166**: 2460–2468

14 **Takada, K. and Jameson, S. C.**, *Nat. Rev. Immunol.* 2009. **9**: 823–832

15 **Huang, H.-Y. and Luther, S. A.**, *Semin. Immunol.* 2012. **24**: 175–189

16 **Chang, J. E. and Turley, S. J.**, *Trends. Immunol.* 2015. **36**: 30–39

17 **Alexandre, Y. O. and Mueller, S. N.**, *Immunol. Rev.* 2018. **283**: 77–85

18 **Weninger, W., Crowley, M. A., Manjunath, N. and von Andrian, U. H.**, *J. Exp. Med.* 2001. **194**: 953–966

19 **Miller, C. N., Hartigan-O'Connor, D. J., Sup Lee, M., Laidlaw, G., Cornelissen, I. P., Matloubian, M., Coughlin, S. R. et al.**, *Int. Immunol.* 2013.

20 **Heufler, C., Topar, G., Grasseger, A., Stanzl, U., Koch, F., Romani, N., Namen, A. E. et al.**, *J. Exp. Med.* 1993. **178**: 1109–1114

21 **Watanabe, M., Ueno, Y., Yajima, T., Iwao, Y., Tsuchiya, M., Ishikawa, H., Aiso, S. et al.**, *J. Clin. Invest.* 1995. **95**: 2945–2953

22 **Tokoyoda, K., Egawa, T., Sugiyama, T., Choi, B.-I. and Nagasawa, T.**, *Immunity* 2004. **20**: 707–718

23 **Alp, Ö.S., Durlanik, S., Schulz, D., McGrath, M., Grün, J. R., Bardua, M., Ikuta, K. et al.**, *Eur. J. Immunol.* 2015.

24 **Shalapour, S., Deiser, K., Sercan, O., Tuckermann, J., Minnich, K., Willimsky, G., Blankenstein, T. et al.**, *Eur. J. Immunol.* 2010. **40**: 2391–2400

25 **Shalapour, S., Deiser, K., Kühl, A. A., Glauben, R., Krug, S. M., Fischer, A., Sercan, O. et al.**, *PLoS One* 2012. **7**: e31939

26 **Masopust, D. and Schenkel, J. M.**, *Nat. Rev. Immunol.* 2013. **13**: 309–320

27 **Lallemand, Y., Luria, V., Haffner-Krausz, R. and Lonai, P.**, *Transgenic. Res.* 1998. **7**: 105–112

28 **Turley, S. J., Fletcher, A. L. and Elpek, K. G.**, *Nat Rev. Immunol.* 2010. **10**: 813–825

29 **Hara, T., Shitara, S., Imai, K., Miyachi, H., Kitano, S., Yao, H., Tani-ichi, S. et al.**, *J. Immunol.* 2012. **189**: 1577–1584

30 **Pham, T. H. M., Baluk, P., Xu, Y., Grigorova, I., Bankovich, A. J., Pappu, R., Coughlin, S. R. et al.**, *J. Exp.Med.* 2010. **207**: 17–27

31 **Greenbaum, A., Hsu, Y.-M. S., Day, R. B., Schuettpelz, L. G., Christopher, M. J., Borgerding, J. N., Nagasawa, T. et al.**, *Nature* 2013. **495**: 227–230

32 **Cordeiro Gomes, A., Hara, T., Lim, V. Y., Herndler-Brandstetter, D., Nevius, E., Sugiyama, T., Tani-Ichi, S. et al.**, *Immunity* 2016. **45**: 1219–1231

33 **Luche, H., Weber, O., Nageswara Rao, T., Blum, C. and Fehling, H. J.**, *Eur. J. Immunol.* 2007. **37**: 43–53

34 **Castagnaro, L., Lenti, E., Maruzzelli, S., Spinardi, L., Migliori, E., Farinello, D., Sitia, G. et al.**, *Immunity* 2013. **38**: 782–791

35 **Golub, R., Tan, J., Watanabe, T. and Brendolan, A.**, *Trends. Immunol.* 2018. **39**: 503–514

36 **Grayson, J. M., Zajac, A. J., Altman, J. D. and Ahmed, R.**, *J. Immunol.* 2000. **164**: 3950–3954

37 **Li, Q., Rao, R. R., Araki, K., Pollizzi, K., Odunsi, K., Powell, J. D. and Shrikant, P. A.**, *Immunity* 2011. **34**: 541–553

38 **Banerjee, A., Gordon, S. M., Intlekofer, A. M., Paley, M. A., Mooney, E. C., Lindsten, T., Wherry, E. J. et al.**, *J. Immunol.* 2010. **185**: 4988–4992

39 **Kim, H. K., Chung, H., Kwon, J., Castro, E., Johns, C., Hawk, N. V., Hwang, S. et al.**, *Front. Immunol.* 2019.**10**

40 **Surh, C. D. and Sprent, J.**, *Immunity* 2008. **29**: 848–862

41 **Rochman, Y., Spolski, R. and Leonard, W. J.**, *Nat. Rev. Immunol.* 2009. **9**: 480–490

42 **Ichii, H., Sakamoto, A., Hatano, M., Okada, S., Toyama, H., Taki, S., Arima, M. et al.**, *Nat. Immunol.* 2002. **3**: 558–563

43 **Le Campion, A., Bourgeois, C., Lambolez, F., Martin, B., Leaument, S., Dautigny, N., Tanchot, C. et al.**, *Proc. Natl. Acad. Sci. U. S. A.* 2002. **99**: 4538–4543

44 **Min, B., McHugh, R., Sempowski, G. D., Mackall, C., Foucras, G. and Paul, W. E.**, *Immunity* 2003. **18**: 131–140

45 **Schüler, T., Hämmerling, G. J. and Arnold, B.**, *J. Immunol.* 2004. **172**: 15–19

46 **Haluszczak, C., Akue, A. D., Hamilton, S. E., Johnson, L. D., Pujanauski, L., Teodorovic, L., Jameson, S. C. et al.**, *J. Exp. Med.* 2009. **206**: 435–448

47 **Smith, N. L., Patel, R. K., Reynaldi, A., Grenier, J. K., Wang, J., Watson, N. B., Nzingha, K. et al.**, *Cell* 2018. **174**: 117–130.e14

48 **Sawa, Y., Arima, Y., Ogura, H., Kitabayashi, C., Jiang, J.-J., Fukushima, T., Kamimura, D. et al.**, *Immunity* 2009. **30**: 447–457

49 **Kaech, S. M., Tan, J. T., Wherry, E. J., Konieczny, B. T., Surh, C. D. and Ahmed, R.**, *Nat. Immunol.* 2003. **4**: 1191–1198

50 **Mazzucchelli, R. and Durum, S. K.**, *Nat. Rev. Immunol.* 2007. **7**: 144–154

51 **Martin, C. E., Spasova, D. S., Frimpong-Boateng, K., Kim, H.-O., Lee, M., Kim, K. S. and Surh, C. D.**, *Immunity* 2017. **47**: 171–182.e4

52 **Jameson, S. C.**, *Nat. Rev. Immunol.* 2002. **2**: 547–556

53 **Satoh-Takayama, N., Lesjean-Pottier, S., Vieira, P., Sawa, S., Eberl, G., Vosshenrich, C. A. J. and Di Santo, J. P.**, *J. Exp. Med.* 2010. **207**: 273–280

54 **Yang, J., Cornelissen, F., Papazian, N., Reijmers, R. M., Llorian, M., Cupedo, T., Coles, M. et al.**, *J. Exp. Med.* 2018.

55 **Freitas, A. A. and Rocha, B.**, *Annu. Rev. Immunol.* 2000. **18**: 83–111

56 **Almeida, A. R., Amado, I. F., Reynolds, J., Berges, J., Lythe, G., Molina-París, C. and Freitas, A. A.**, *Front. Immunol.* 2012. **3**: 125

57 **Veiga-Fernandes, H. and Freitas, A. A.**, *Trends. Immunol.* 2017. **38**: 777–788

58 **Repass, J. F., Laurent, M. N., Carter, C., Reizis, B., Bedford, M. T., Cardenas, K., Narang, P. et al.**, *Genesis* 2009. **47**: 281–287

59 **Ulvmar, M. H., Werth, K., Braun, A., Kelay, P., Hub, E., Eller, K., Chan, L. et al.**, *Nat. Immunol.* 2014. **15**: 623–630

60 **Jafarnejad, M., Zawieja, D. C., Brook, B. S., Nibbs, R. J. B. and Moore, J. E.**, *J. Immunol.* 2017. **199**: 2291–2304

61 **Kastenmüller, W., Brandes, M., Wang, Z., Herz, J., Egen, J. G. and Germain, R. N.**, *Immunity* 2013. **38**: 502–513

62 **Sung, J. H., Zhang, H., Moseman, E. A., Alvarez, D., Iannacone, M., Henrickson, S. E., de la Torre, J. C. et al.**, *Cell* 2012. **150**: 1249–1263

63 **Park, J. H., Yu, Q., Erman, B., Appelbaum, J. S., Montoya-Durango, D., Grimes, H. L. and Singer, A.**, *Immunity* 2004. **21**: 289–302

64 **Kimura, M. Y., Pobezinsky, L. A., Guinter, T. I., Thomas, J., Adams, A., Park, J.-H., Tai, X. et al.**, *Nat. Immunol.* 2013. **14**: 143–151

65 **Bank, U., Deiser, K., Finke, D., Hämmerling, G. J., Arnold, B. and Schüler, T.**, *J. Immunol.* 2016.

66 **Logan, M., Martin, J. F., Nagy, A., Lobe, C., Olson, E. N. and Tabin, C. J.**, *Genesis* 2002. **33**: 77–80

67 **Kranz, A., Fu, J., Duerschke, K., Weidlich, S., Naumann, R., Stewart, A. F. and Anastassiadis, K.**, *Genesis* 2010. **48**: 512–520

68 **Stoycheva, D., Deiser, K., Stärck, L., Nishanth, G., Schlüter, D., Uckert, W. and Schüler, T.**, *J. Immunol.* 2015. **194**: 553–559

69 **Cossarizza, A., Chang, H. D., Radbruch, A., Acs, A., Adam, D., Adam-Klages, S., Agace, W. W. et al.**, *Eur. J. Immunol.* 2019. **49**: 1457–1973

70 **Schubert, W., Bonnekoh, B., Pommer, A. J., Philipsen, L., Böckelmann, R., Malykh, Y., Gollnick, H. et al.**, *Nat. Biotechnol.* 2006. **24**: 1270–1278

71 **Carpenter, A. E., Jones, T. R., Lamprecht, M. R., Clarke, C., Kang, I. H., Friman, O., Guertin, D. A. et al.**, *Genome. Biol.* 2006. **7**: R100

Abbreviations: **Bcl-2**: B-cell lymphoma 2 · **BEC**: blood endothelial cell · **DN**: gp38$^-$ CD31$^-$ double negative cell · **Eomes**: eomesodermin · **FRC**: fibroblastic reticular cell · **ILC**: innate lymphoid cell · **LEC**: lymphatic endothelial cell · **LIP**: lymphopenia-induced proliferation · **LSC**: lymphoid stromal cell · **Pln**: peripheral LN · **T_{CM}**: central memory T cell · **T_M**: memory T cells · **T_N**: naive T cell · **vT_M**: virtual memory T cell

Full correspondence: Dr. Thomas Schüler, Institute of Molecular and Clinical Immunology, Medical Faculty, Otto-von-Guericke University, Leipziger Strasse 44, 39120 Magdeburg, Germany
e-mail: thomas.schueler@med.ovgu.de

The peer review history for this article is available at https://publons.com/publon/10.1002/eji.201948368

Received: 23/8/2019
Revised: 23/1/2020
Accepted: 7/2/2020
Accepted article online: 11/2/2020

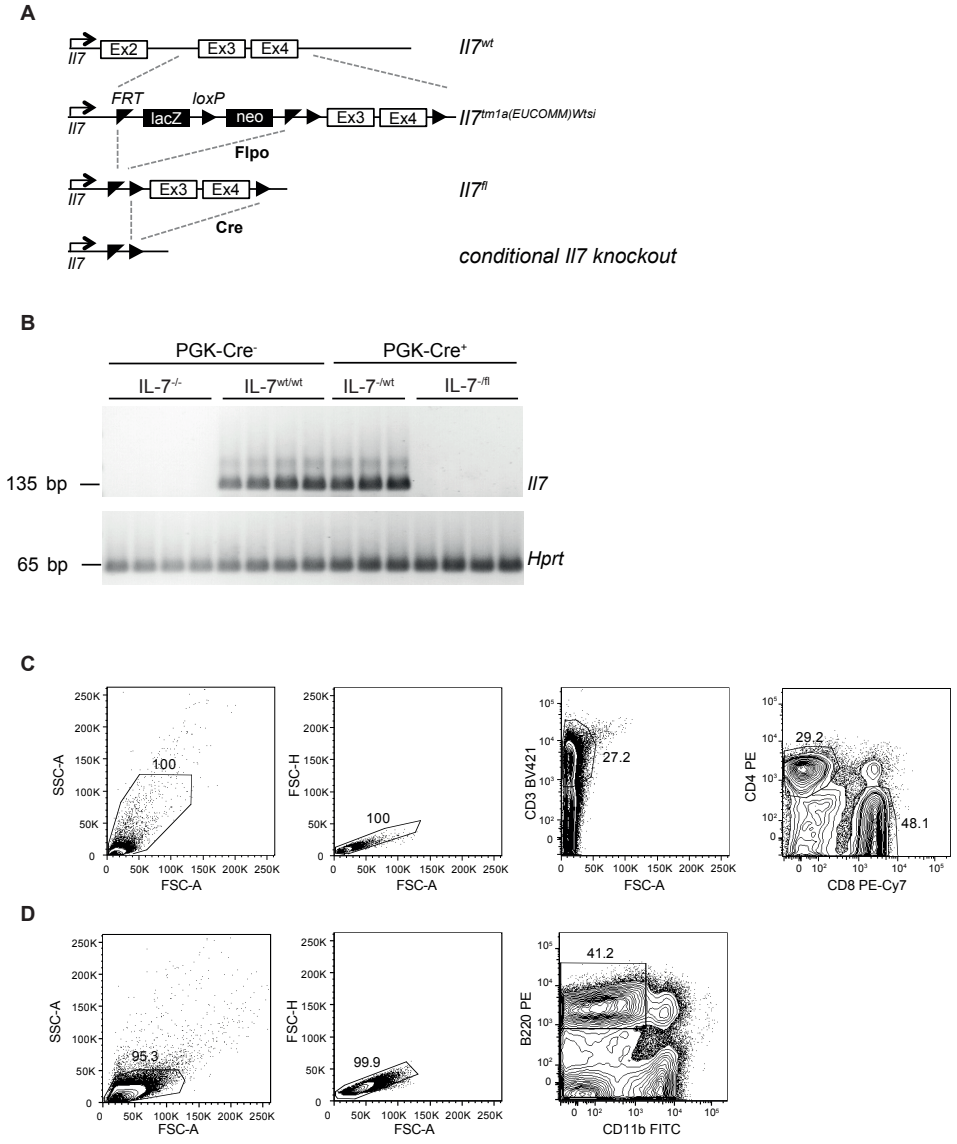

Figure S1. Generation of conditional IL-7 knockout (IL-7$^{fl/fl}$) mice. (A) Schematic representations of the wild type *Il7* (*Il7^{wt}*), the targeted "knockout-first" allele *Il7$^{tm1a(EUCOMM)Wtsi}$*, the "floxed" *Il7* (*Il7^{fl}*) and the *conditional Il7 knockout* allele. The C57BL6/N (B6) embryonic stem (ES) cell line JM8A3.N1 harboring the "knockout-first" allele *Il7$^{tm1a(EUCOMM)Wtsi}$* was provided by EUCOMM. Mice harboring the *Il7$^{tm1a(EUCOMM)Wtsi}$* allele were crossed to transgenic mice ubiquitously expressing the recombinase Flpo [67] in order to remove the FRT-flanked sequences. The resulting "floxed" *Il7* allele (*Il7^{fl}*) carries loxP sites flanking exons 3 and 4 and can be inactivated by Cre-mediated recombination generating a *conditional Il7 knockout* allele. **(B)** RNA was isolated from the colon of the indicated mouse lines and analyzed for the relative abundance of *Il7* and *Hprt* mRNA by RT-PCR. Each lane represents an individual mouse. In total 6-8 mice per group were analyzed in 2 independent experiments. **(C, D)** Representative gating strategies for flow cytometric analyses of splenic **(C)** CD3$^+$CD4$^+$ or CD3$^+$CD8$^+$ T cells and **(D)** B220$^+$ B cells (Figure 1). Numbers indicate percentages.

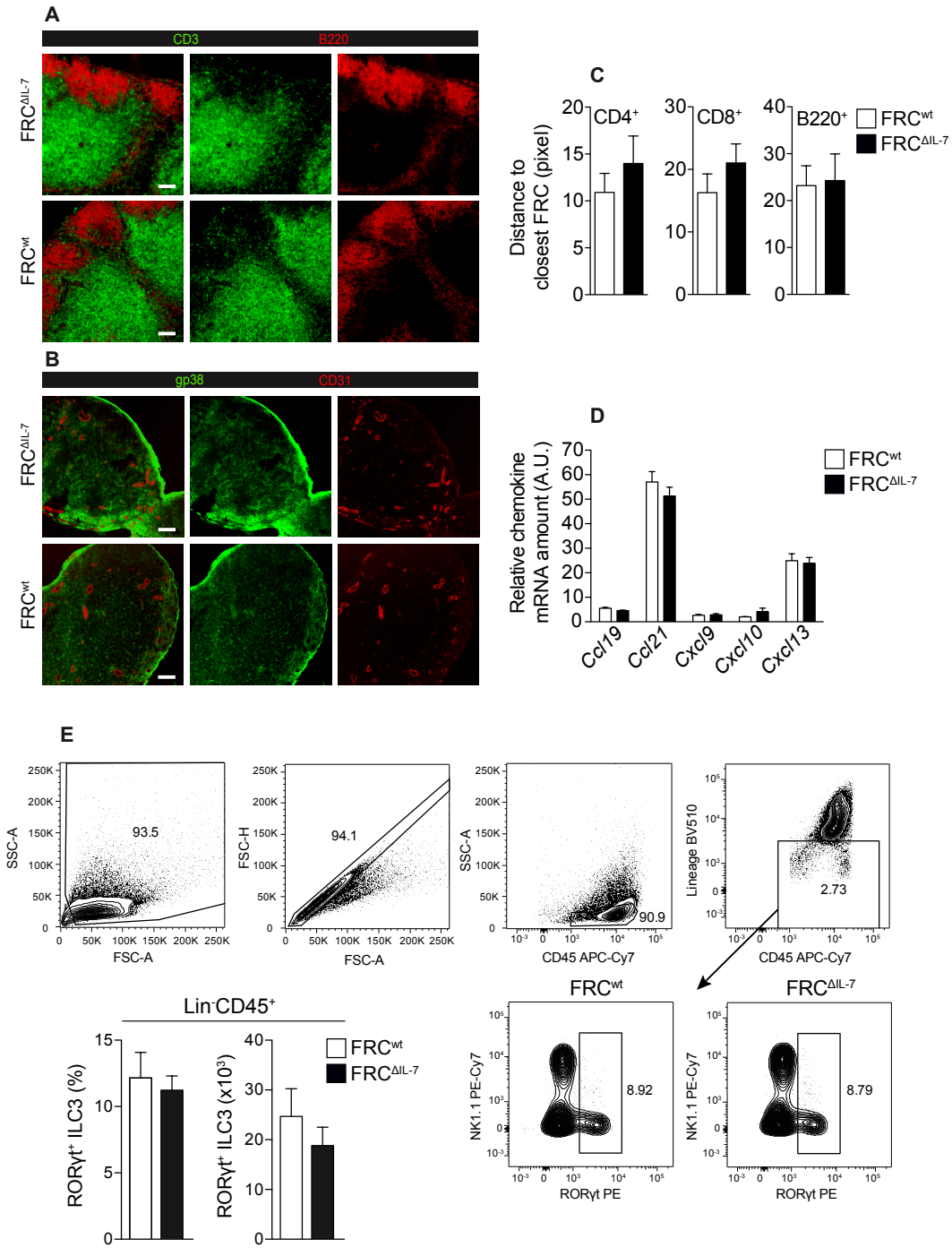

Figure S2. FRC-derived IL-7 does not alter the spatial distribution of T and B cells or stromal cells in the pLNs. (A-C) Multi-epitope ligand cartography (MELC) was performed for pLNs from FRC^{wt} (Prx1-Cre^{+}IL-7$^{wt/wt}$) and FRC$^{\Delta IL\text{-}7}$ (Prx1-Cre^{+}IL-7$^{fl/fl}$) mice (resolution: 0.45 µm per pixel; scale bars = 100 µm). **(A, B)** Shown are single and combined fluorescence signals for **(A)** CD3 (green) and B220 (red) and **(B)** for gp38 (green) and CD31 (red). **(C)** Distances between CD3^{+}CD4^{+}, CD3^{+}CD8^{+} or B220^{+} cells and next neighboring FRCs were calculated as described in Materials and Methods. Data represent pooled results (mean + SEM) from 6 mice per group analyzed in 3 independent experiments. **(D)** Relative *Ccl19*, *Ccl21*, *Cxcl9*, *Cxcl10* or *Cxcl13* mRNA amounts were determined in pLNs of FRC^{wt} (Prx1-Cre^{+}IL-7$^{-/wt}$ and Prx1-Cre^{+}IL-7$^{wt/wt}$) and FRC$^{\Delta IL\text{-}7}$ (Prx1-Cre^{+}IL-7$^{-/fl}$ and Prx1-Cre^{+}IL-7$^{fl/fl}$) mice by RT-qPCR in relation to *Hprt*. Data are representative of 7-8 mice per group analyzed

in four independent RT-qPCR experiments and show mean + SEM of triplicate averages. **(E)** Peripheral LNs of FRC^{wt} ($Prx1\text{-}Cre^{+}IL\text{-}7^{wt/wt}$) and $FRC^{\Delta IL\text{-}7}$ ($Prx1\text{-}Cre^{+}IL\text{-}7^{fl/fl}$) mice were analyzed by flow cytometry for frequencies and absolute cell numbers of $ROR\gamma t^{+}$ ILC3s after gating on $lineage^{-}$ (negative for CD3, CD5, CD8, CD11c, CD19 and Gr1) $CD45^{+}$ cells. Shown is the gating strategy, representative contour plots (numbers indicate percentages) and pooled results (mean + SEM) from 3 independent experiments with a total of 7-9 mice per group.

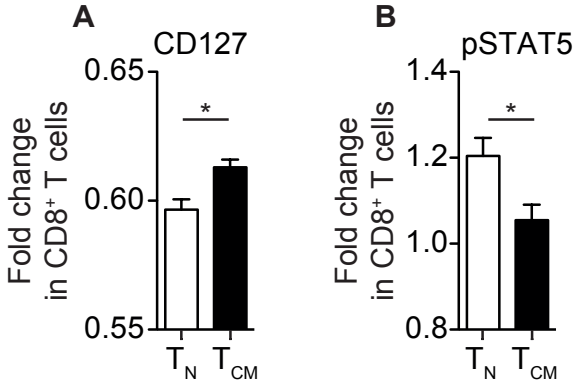

Figure S3. CD8$^+$ T_N utilize IL-7 more efficiently than CD8$^+$ T_M. (A, B) LN cells from IL-7-competent mice (Prx1-Cre$^-$IL-7$^{wt/wt}$ and Prx1-Cre$^-$IL-7$^{fl/fl}$) were incubated for 30 min with recombinant mouse IL-7 (1 ng/mL). Mean fluorescence intensities (MFIs) of **(A)** CD127 (IL-7Rα) and **(B)** phospho-STAT5 (pSTAT5) were calculated in relation to MFIs measured before stimulation in CD3$^+$CD8$^+$ T_N (CD44^{lo}CD122^{lo}) and T_M (CD44^{hi}CD122^{hi}). Data in bar diagrams represent pooled results (mean + SEM) from five data points measured in one experiment. For each data point the LNs of two mice were pooled.

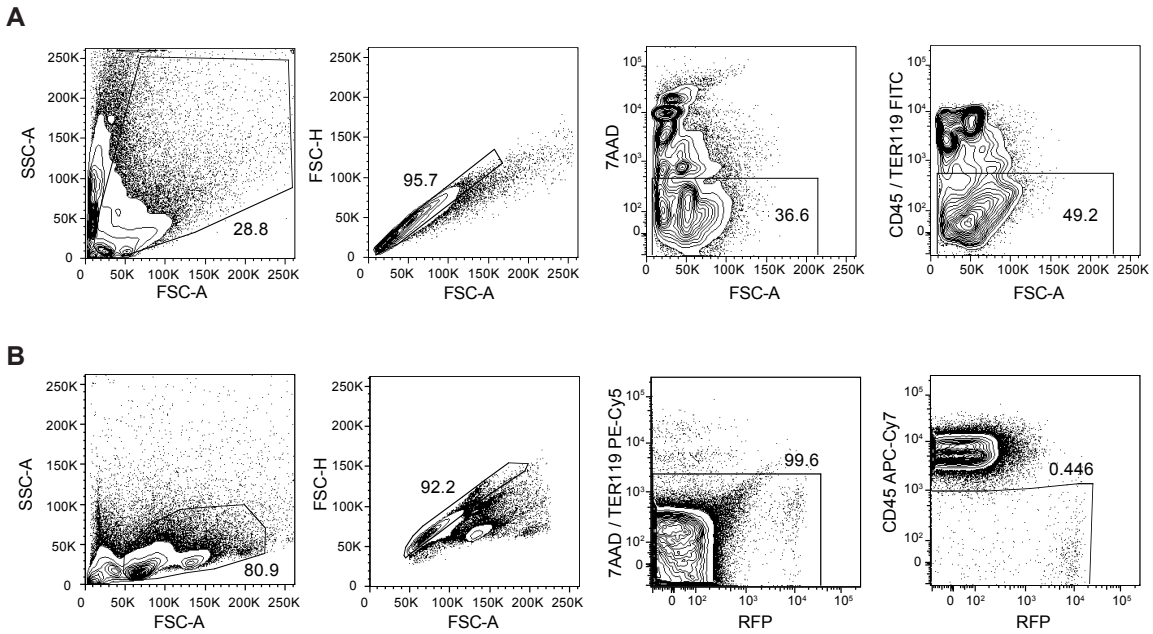

Figure S4. Representative gating strategies for flow cytometry cell sorting and flow cytometric analyses of LSCs. (A, B) Shown are representative gating strategies for **(A)** Figure 2A and 3D and **(B)** for Figures 3A and B. **(A, B)** Numbers indicate percentages.

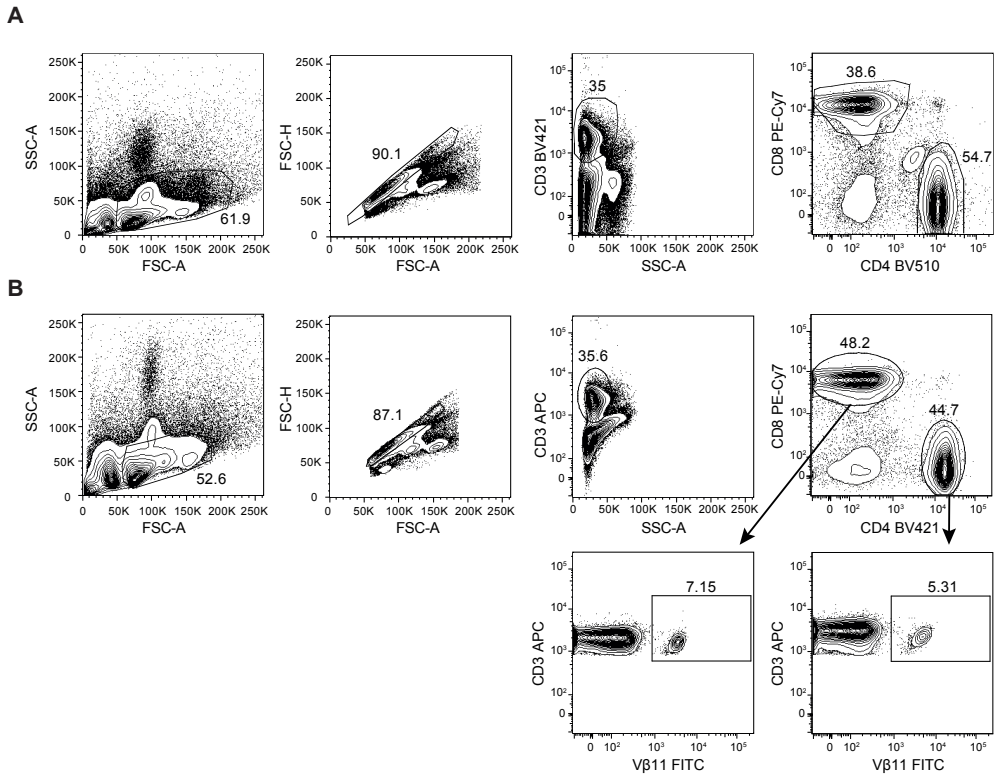

Figure S5. Representative gating strategies for flow cytometric analyses of T cells. (A, B) Shown are representative gating strategies for **(A)** Figures 2B-H; 3E, G, I, J and 4C-H and **(B)** for Figures 3F and H. **(A, B)** Numbers indicate percentages.

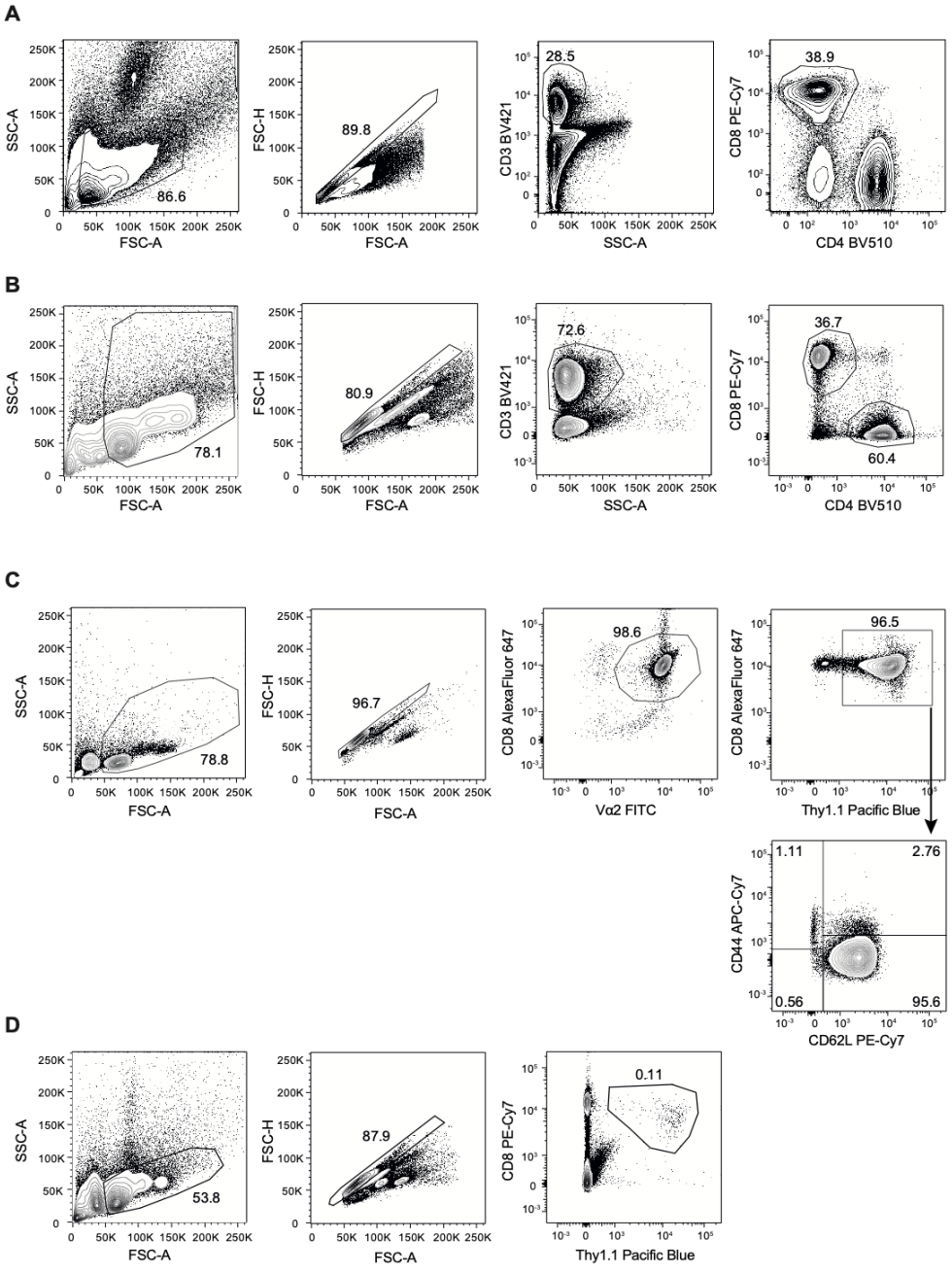

Figure S6. Representative gating strategies for flow cytometric analyses of Bcl-2, Eomes, CD127 and pSTAT5 expression in T cells and gating strategy of OT-I T cells. (A-D) Shown are representative gating strategies for Figures 4A and B, **(B)** Figures S3A and S3B, **(C)** the purification procedure of $CD8^{+}Thy1.1^{+}$ OT-I T cells and **(D)** for Figures I-K. **(A-D)** Numbers indicate percentages.

5 Publication III

Title: IFNAR signaling in fibroblastic reticular cells can modulate $CD8^+$ memory fate decision[17]

Journal: European Journal of Immunology

Publication year: 2022

DOI: 10.1002/eji.202149760

Authors:

LK	Laura Knop	UB	Ute Bank
JS	Julia Spanier	ID	Ildiko Rita Dunay
PL	Pia-K. Larsen	UK	Ulrich Kalinke
AW	Amelie Witte	TS	Thomas Schüler

Table 5-1. Author contributions in publication III.

Author	Contribution in %
Study design and supervision	
LK, UK	20 each
JS	10
TS	50
Performance of experiments	
LK	50
JS	30
PL	10
AW, UB	5 each
Data collection and figure preparation	
LK	90
JS	10
Data analysis and interpretation	
LK	30
JS, ID	5 each
PL, AW, UB	2,5 each
UK	20
TS	32,5
Manuscript preparation	
LK	25
JS, PL, AW, UB, ID	5 together
UK	5
TS	65

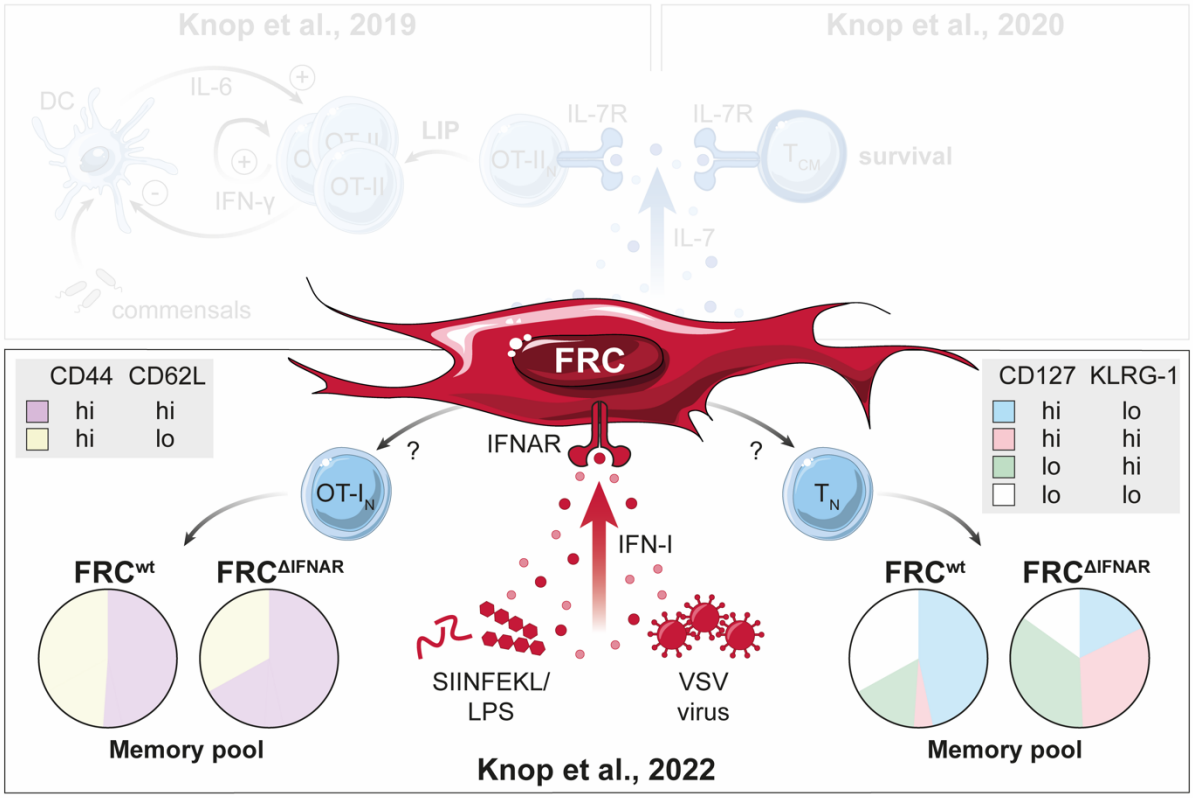

Figure 5-1. Graphical representation of Knop et al., 2022[17]**.** The pro-inflammatory cytokine IFN-I is released upon inflammation[26] and acts on several immune cell types that modulate CD8$^+$ T cell responses[92–94]. It was shown that LSCs, such as FRCs, express the IFNAR at high levels[12,112,137]. Whether, IFNAR signaling in FRCs regulates the differentiation of CD8$^+$ T_M remained an open question. We show in Knop et al., 2022, that memory fate decision of CD8$^+$ T cells is regulated by IFNAR signaling in FRCs[17]. Interestingly, FRC-specific IFNAR signaling modulates T_M differentiation in a context-dependent manner: during transfer of OT-I CD8$^+$ T cells and vaccination with SIINFEKL-peptide and lipopolysaccharide (LPS) and during vesicular stomatitis virus (VSV) infection. This figure was created using illustrations from www.bioicons.com[21].

Eur. J. Immunol. 2022. 0: 1–11 DOI: 10.1002/eji.202149760

European Journal of Immunology

Adaptive immunity

Basic

Research Article

IFNAR signaling in fibroblastic reticular cells can modulate CD8$^+$ memory fate decision

Laura Knop[*1], *Julia Spanier*[*2], *Pia-Katharina Larsen*[2], *Amelie Witte*[1], *Ute Bank*[1], *Ildiko R. Dunay*[3], *Ulrich Kalinke*[**2] and *Thomas Schüler*[**1]

[1] Institute of Molecular and Clinical Immunology, Medical Faculty, Otto-von-Guericke University, Magdeburg, Germany
[2] Institute for Experimental Infection Research, TWINCORE, Centre for Experimental and Clinical Infection Research, Helmholtz Centre for Infection Research and the Hannover Medical School, Hannover, Germany
[3] Institute of Inflammation and Neurodegeneration, Medical Faculty, Otto-von-Guericke University, Magdeburg, Germany

CD8$^+$ memory T cells (T_M) are crucial for long-term protection from infections and cancer. Multiple cell types and cytokines are involved in the regulation of CD8$^+$ T cell responses and subsequent T_M formation. Besides their direct antiviral effects, type I interferons (IFN-I) modulate CD8$^+$ T cell immunity via their action on several immune cell subsets. However, it is largely unclear how nonimmune cells are involved in this multicellular network modulating CD8$^+$ T_M formation. Fibroblastic reticular cells (FRCs) form the 3D scaffold of secondary lymphoid organs, express the IFN-I receptor (IFNAR), and modulate adaptive immune responses. However, it is unclear whether and how early IFNAR signals in lymph node (LN) FRCs affect CD8$^+$ T_M differentiation. Using peptide vaccination and viral infection, we studied CD8$^+$ T_M differentiation in mice with an FRC-specific IFNAR deletion ($FRC^{\Delta IFNAR}$). We show here that the differentiation of CD8$^+$ TCR-transgenic T cells into central memory cells (T_{CM}) is enhanced in peptide-vaccinated $FRC^{\Delta IFNAR}$ mice. Conversely, vesicular stomatitis virus infection of $FRC^{\Delta IFNAR}$ mice is associated with impaired T_{CM} formation and the accumulation of vesicular stomatitis virus specific double-positive CD127^{hi}KLRG-1^{hi} effector memory T cells. In summary, we provide evidence for a context-dependent contribution of FRC-specific IFNAR signaling to CD8$^+$ T_M differentiation.

Keywords: FRCs · IFNAR · T cell memory

Additional supporting information may be found online in the Supporting Information section at the end of the article.

Introduction

Besides diverse subsets of immune cells, secondary lymphoid organs (SLOs) harbor nonhematopoietic stromal cells that constitute the 3D scaffold of the respective organ [1]. The induction of CD8$^+$ T cell responses in SLOs relies on an intact fibroblastic reticular cell (FRC) network [2]. For the initiation of CD8$^+$ T cell responses, FRC-derived chemokines, such as CCL19 and CCL21,

Correspondence: Thomas Schüler
e-mail: thomas.schueler@med.ovgu.de

[*] Laura Knop and Julia Spanier contributed equally to this work.
[**] Ulrich Kalinke and Thomas Schüler jointly supervised this work.

are required to attract sufficient naïve $CD8^+$ T cells to SLOs where priming occurs [3]. Furthermore, CCL19 and CCL21 guide $CD8^+$ T cells to areas, where survival factors, such as interleukin-7 (IL-7), are available [4–6]. We have shown recently that FRCs are the major source of IL-7 in lymph nodes (LNs). The FRC-specific deletion of IL-7 caused the selective reduction of $CD8^+$ central memory T cells (T_{CM}), whereas naïve T cells were unaffected [7]. This implies an important contribution of FRCs to $CD8^+$ T_{CM} differentiation and/or survival [8]. However, the up-stream signaling events involved in the FRC-mediated modulation of IL-7-dependent $CD8^+$ memory T cell (T_M) homeostasis are still unclear.

FRCs are equipped with various cytokine receptors including those for type I interferons (IFN-I) [9–11]. IFN-I receptor (IFNAR) signaling promotes *Il7* gene activity [12] and modulates effector $CD8^+$ T cell (T_{EFF}) responses at multiple levels [13]. For example, it promotes the T cell priming capability of dendritic cells [14], modulates $CD8^+$ T cell homing to SLOs [15], amplifies TCR signals [16], and protects $CD8^+$ T cells from natural killer cell-mediated killing [17]. A recent report demonstrated that FRCs contribute to the IFNAR-dependent regulation of antiviral $CD8^+$ T_{EFF} responses [18]. However, it remained unclear whether IFNAR signaling in FRCs affects $CD8^+$ T_M formation and/or maintenance.

Here, we analyzed $CD8^+$ T cell responses in mice lacking IFNAR signaling selectively in FRCs ($FRC^{\Delta IFNAR}$). We show that the development of T_{CM} is enhanced in $FRC^{\Delta IFNAR}$ mice reconstituted with TCR-transgenic (TCR^{tg}) $CD8^+$ T cells and subsequent peptide vaccination. In response to vesicular stomatitis virus (VSV) infection, however, $CD127^{hi}KLRG\text{-}1^{hi}$ $CD8^+$ effector memory (T_{EM})-like cells accumulate in $FRC^{\Delta IFNAR}$ mice indicating that the type of immunogen determines the impact of FRC-specific IFNAR signals on $CD8^+$ T_M differentiation. In summary, our data provide evidence for a context-dependent contribution of IFNARsignaling in FRCs to $CD8^+$ T_M fate decision.

Results

IFNAR signaling in FRCs determines OT-I T_M differentiation

Prx1-Cre mice [19] allow selective gene targeting of LN FRCs [7]. To assess whether IFNAR signaling in FRCs affects T_M differentiation, Prx1-Cre mice were intercrossed with conditional IFNAR knockout ($IFNAR^{fl/fl}$) mice [15] to obtain $FRC^{\Delta IFNAR}$ mice. Prx1-Cre^+ mice harboring intact *Ifnar1* alleles served as controls (FRC^{wt}).

In a first approach, $CD8^+$ TCR^{tg} OT-I T cells, which are specific for the ovalbumin-derived peptide SIINFEKL, were adoptively transferred to $FRC^{\Delta IFNAR}$ and FRC^{wt} mice. The following day, recipient mice were vaccinated intravenously with a mixture of SIINFEKL and LPS, which activates IFNAR signaling within 12 h [9]. The analysis of the spleen, peripheral LNs and bone marrow (BM) on days 7, 14, and 30 post vaccination (dpv) revealed that numbers of OT-I T cells were very similar in $FRC^{\Delta IFNAR}$ and control mice at any given time point (Fig. 1A).

Notably, on day 30 the frequencies of $CD44^{hi}CD62L^{hi}$ OT-I T_{CM} were increased in the spleen of $FRC^{\Delta IFNAR}$ mice (Fig. 1B and C). Correspondingly, the abundance of $CD44^{hi}CD62L^{lo}$ OT-I T_{EM} was reduced at this time point (Fig. 1B and C). In contrast, in LNs and BM T_{CM}/T_{EM} ratios were overall similar in both mouse lines at all time points analyzed, although LN T_{CM} frequencies were reduced at 14 dpv in $FRC^{\Delta IFNAR}$ mice. On days 7 and 14, frequencies of $CD44^{hi}CD62L^{hi}$ and $CD44^{hi}CD62L^{lo}$ OT-I cells were indistinguishable in spleens of $FRC^{\Delta IFNAR}$ mice and controls, similar to PD-1 and Ki-67 levels at 30 dpv (Fig. 1E and F). Interestingly, at this timepoint, elevated frequencies of splenic $CD127^{hi}KLRG\text{-}1^{lo}$ and IFN-γ^+TNF-α^+ OT-I T_M correlated with increased Bcl-2 expression in $FRC^{\Delta IFNAR}$ mice (Fig. 1D, G, and H). Thus, the lack of IFNAR signaling in FRCs favors the generation of long-lived, polyfunctional OT-I T_{CM}.

Early IFNAR signals in FRCs modulate chemokine levels in activated LNs

Within the first few hours after primary antigen contact, $CD8^+$ T_M development is programmed [20, 21]. Importantly, transient IFNAR blockade in the early phase of antiviral immune responses improves $CD8^+$ T_M formation [22]. To address whether FRC-intrinsic IFNAR signals in the priming phase affect $CD8^+$ T_M formation [9], we first analyzed the frequencies and phenotypes of FRCs from OT-I-reconstituted $FRC^{\Delta IFNAR}$ and FRC^{wt} mice 24 h after peptide vaccination (+OT-I). Untreated mice served as controls (-OT-I). As shown in Fig. 2A, LN stroma composition and FRC frequencies were comparable in vaccinated $FRC^{\Delta IFNAR}$ and FRC^{wt} mice. Similar results were obtained with untreated mice. Hence, altered T_{CM}/T_{EM} ratios in $FRC^{\Delta IFNAR}$ mice at 30 dpv do not result from early alterations in FRC frequencies.

Besides the production of CCL19 and CCL21 in the steady-state [4, 23], LN stromal cells upregulate CXCL9 and CXCL10 in response to infection-induced IFNAR signaling [9, 24, 25]. Localization of $CD8^+$ T_{EFF} within LNs and subsequent memory fate decision is regulated by the CXCL9/CXCL10-binding receptor CXCR3 [26]. However, it was not clear to which extent IFNAR signaling in FRCs contributes to the overall production of CCL19, CCL21, CXCL9, and CXCL10 in LNs. To address this, chemokine mRNA levels were determined in LNs of treated (+OT-I; 24 h post vaccination) and untreated (-OT-I; - vaccination) $FRC^{\Delta IFNAR}$ and FRC^{wt} mice (Fig. 2B). *Ccl21* mRNA was most abundant in untreated mice and declined in treated recipient mice, irrespective of their genotype (Fig. 2B). In contrast, *Cxcl9* and *Cxcl10* expression increased after vaccination in OT-I-reconstituted $FRC^{\Delta IFNAR}$ and FRC^{wt} mice, but to a lesser extent in $FRC^{\Delta IFNAR}$ mice than in controls. Hence, vaccination-induced *Ccl21* downregulation is independent of IFNAR signaling in FRCs, whereas the upregulation of *Cxcl9* and *Cxcl10* is affected by IFNAR triggering. Correspondingly, *Il7* expression was slightly lower in LNs of vaccinated $FRC^{\Delta IFNAR}$ mice (Fig. 2C).

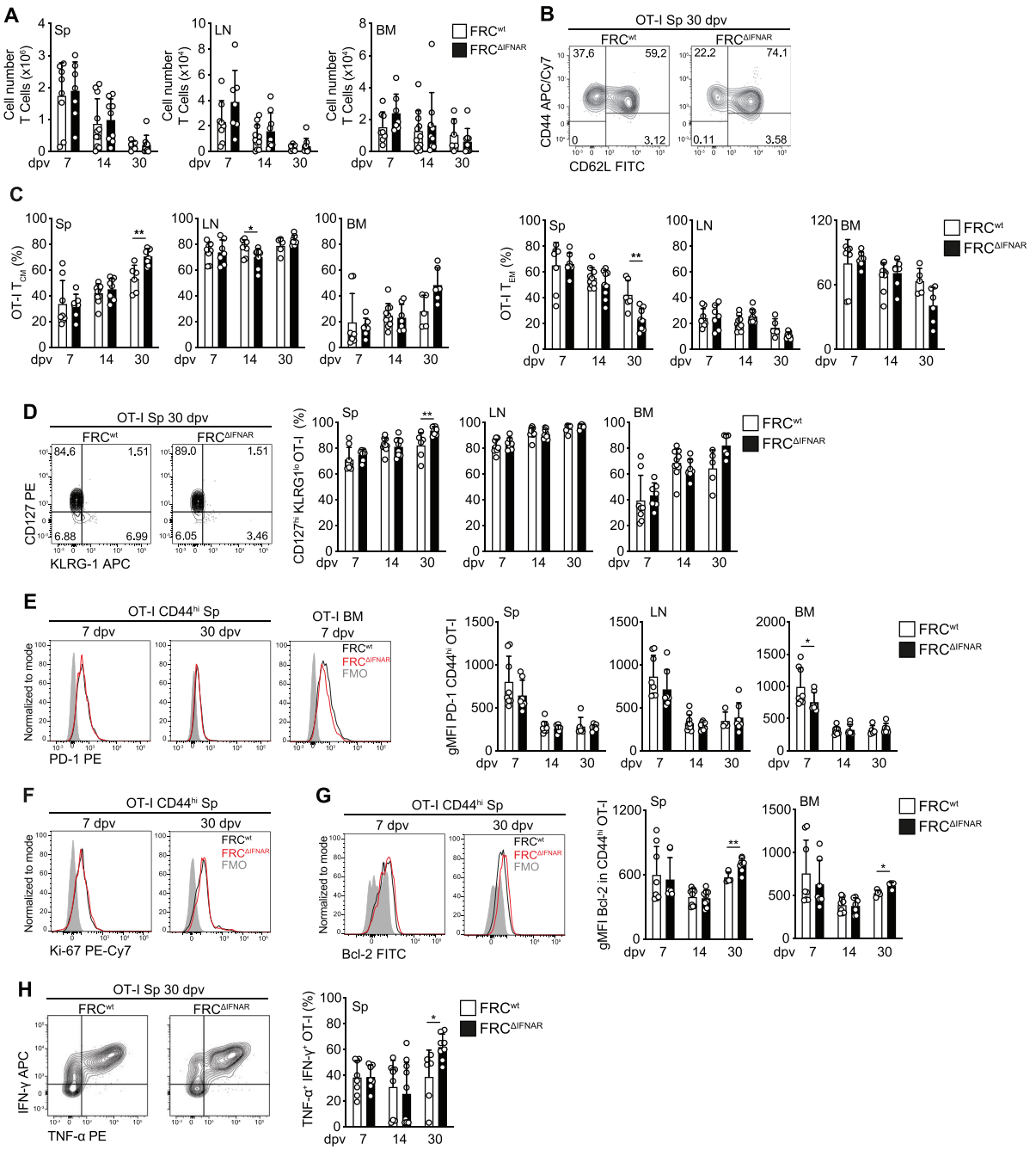

Figure 1. IFNAR signaling in FRCs determines OT-I T_M differentiation. (A–H) Twenty-four hours after reconstitution with CD8$^+$ Thy1.1$^+$ OT-I T cells, Thy1.1$^-$ FRC^{wt} and FRC$^{\Delta IFNAR}$ mice (all Thy1.1$^-$) were immunized with a mixture of SIINFEKL and LPS. 7, 14, and/or 30/31 days post vaccination (dpv) OT-I T cells were isolated from lymph nodes (LN), spleen (Sp), or bone marrow (BM) and analyzed by flow cytometry. (A) Numbers of CD8$^+$ Thy1.1$^+$ OT-I T cells in FRC$^{\Delta IFNAR}$ and FRC^{wt} mice are shown at 7, 14, and 30/31 dpv. (B, D) Representative contour plots are shown for the (B) CD44/CD62L or (D) CD127/KLRG-1 expression profiles after gating on CD8$^+$ Thy1.1$^+$ OT-I T cells at 30/31 dpv in the spleen. Numbers indicate percentages of the respective population. (C) Frequencies of central memory (T_{CM}; CD44^{hi}CD62L^{hi}) and effector memory (T_{EM}; CD44^{hi}CD62L^{lo}) after gating on CD8$^+$ Thy1.1$^+$ OT-I T cells are summarized in bar diagrams. (D) Frequencies of CD127^{hi}KLRG-1^{lo} after gating on CD8$^+$ Thy1.1$^+$ OT-I T cells are summarized in bar diagrams. (E–G) The expression of (E) PD-1, (F) Ki-67, and (G) Bcl-2 was analyzed after gating on CD8$^+$ Thy1.1$^+$ CD44^{hi} OT-I T cells at 30/31 dpv. Shown are representative histograms (fluorescence minus one control in gray) and data for gMFIs are summarized in bar diagrams. (H) Splenocytes were restimulated in vitro for 4 h with 1 μM SIINFEKL. Shown are representative contour plots for the IFN-γ/TNF-α expression profile after gating on CD8$^+$ Thy1.1$^+$ OT-I T cells at 30/31 dpv. Numbers indicate percentages. Frequencies of IFN-γ$^+$TNF-α$^+$ cells after gating on CD8$^+$ Thy1.1$^+$ OT-I T cells at 30/31 dpv are summarized in bar diagrams. (A–H) Data are representative of 4–10 mice analyzed in two independent experiments. Bar diagrams represent mean ± SD. Statistical comparisons were made via Mann–Whitney *U* test and statistically significant values are indicated (*$p \leq 0.05$; **$p \leq 0.01$). FRCs, fibroblastic reticular cells; IFNAR, IFN-I receptor.

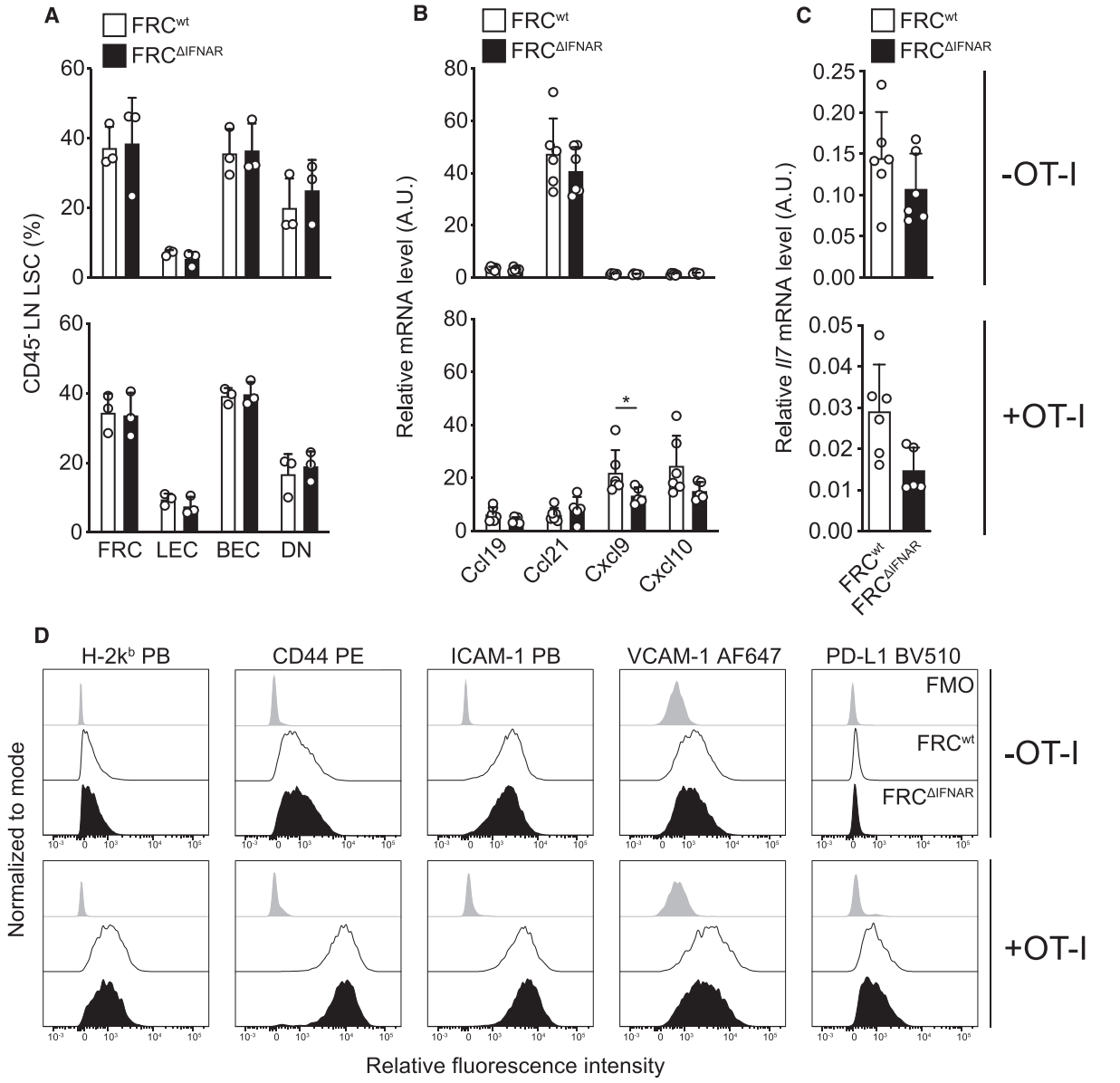

Figure 2. FRC functions are largely unaltered in FRC$^{\Delta IFNAR}$ mice before and during adoptive T cell transfer. (A–D) Untreated (-OT-I, -vaccination) FRC$^{\Delta IFNAR}$ and FRC^{wt} mice or FRC$^{\Delta IFNAR}$ and FRC^{wt} mice receiving OT-I and SIINFEKL/LPS were analyzed 1 dpv (+OT-I, + vaccination; as described in Fig. 1). (A) Frequencies of TER-119$^-$CD45$^-$ LSC subsets were determined in LNs by flow cytometry. Based on their differential expression of gp38 and CD31, live TER-119$^-$CD45$^-$ LN LSCs can be subdivided into gp38$^+$CD31$^-$ FRCs, gp38$^+$CD31$^+$ lymphatic endothelial cells (LECs), gp38$^-$CD31$^+$ blood endothelial cells (BECs), and gp38$^-$CD31$^-$ DNs. LNs of three mice were pooled in each of three independent experiments. Bar diagrams show mean ± SD from three data points. (B, C) Relative (B) *Ccl19*, *Ccl21*, *Cxcl9*, and *Cxcl10* or (C) *Il7* mRNA amounts were determined in LNs by RT-qPCR in relation to *Hprt*. Data (mean ± SD) are representative of six mice per group analyzed in (B) three or (C) one RT-qPCR experiment(s). (D) Relative fluorescence intensities for H-2k^b, CD44, ICAM-1, VCAM-1, and PD-L1, analyzed by flow cytometry on viable TER-119$^-$CD45$^-$gp38$^+$CD31$^-$ FRCs isolated from LNs. Gray curves indicate fluorescence minus one (FMO) control lacking the H-2k^b, CD44, ICAM-1, VCAM-1, or PD-L1 antibody, respectively. Histograms are representative of two independent experiments each with pooled LNs from two to three mice per group. (A–C) Statistical comparisons were made via Mann–Whitney *U* test and statistically significant values are indicated ($^*p \leq 0.05$). FRCs, fibroblastic reticular cells; LN, lymph node; LSCs, lymphoid stromal cells.

On the contrary, FRCs derived from untreated FRC$^{\Delta IFNAR}$ and FRC^{wt} mice expressed similar levels of the cell surface molecules H-2K^b, CD44, ICAM-1, VCAM-1, and PD-L1. Upon vaccination, FRCs similarly upregulated these molecules in FRC$^{\Delta IFNAR}$ and FRC^{wt} mice (Fig. 2D). Comparable results were obtained for lymphatic endothelial cells (LECs), blood endothelial cells (BECs), and double-negative cells (DNs) (Supporting information Fig. S1).

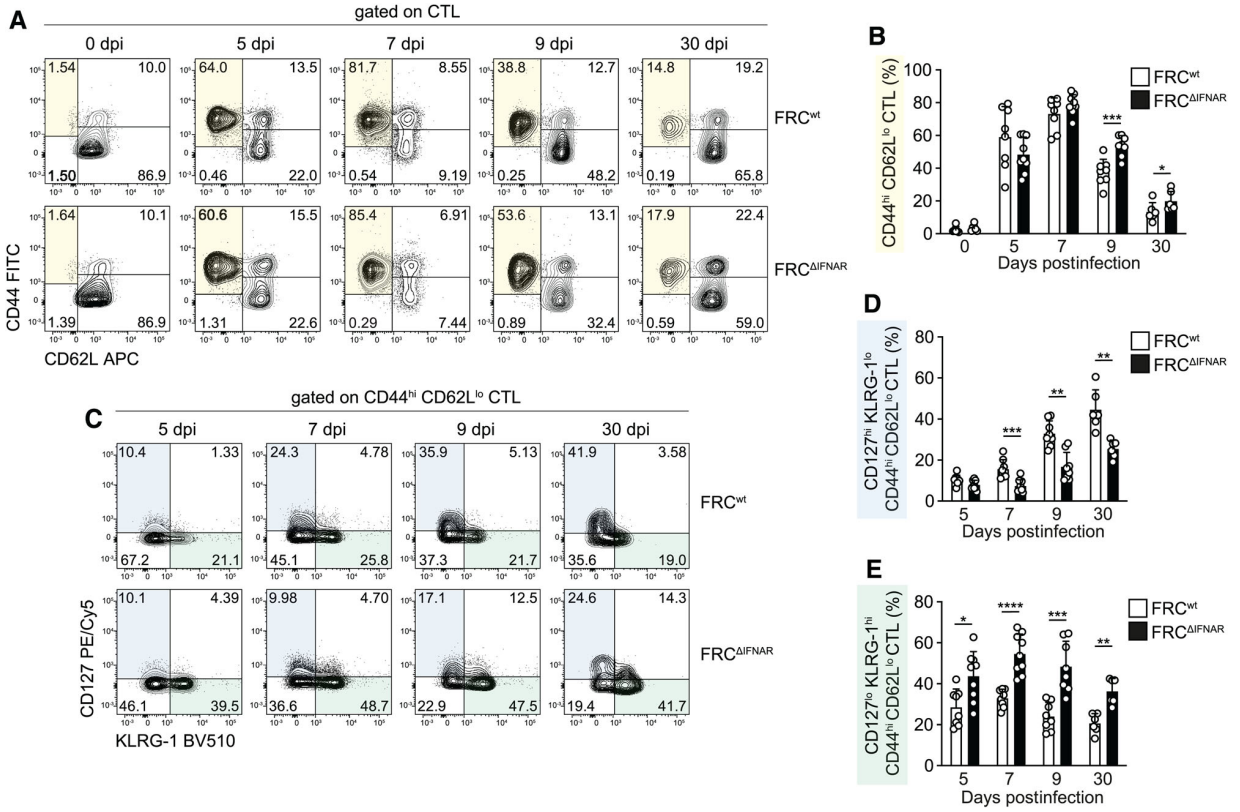

Figure 3. IFNAR signaling in FRCs regulates CD8$^+$ T cell memory differentiation during vesicular stomatitis virus (VSV) infection. (A–E) FRC$^{\Delta IFNAR}$ and FRC^{wt} mice were infected i.v. with 2×10^6 plaque forming units of VSV. Mice were bled before and on days 5, 7, 9, and 30 post infection (dpi), and blood was analyzed for CD3$^+$CD8$^+$ T cells (CTLs) by flow cytometry. (A, C) Representative contour plots are shown for (A) CD44/CD62L expression after gating on CD3$^+$CD8$^+$ CTLs or (C) CD127/KLRG-1 expression after gating on CD3$^+$CD8$^+$CD44^{hi}CD62L^{lo} CTLs. Numbers indicate percentages. (B) Bar diagram (mean ± SD) represents frequency of CD44^{hi}CD62L^{lo} after gating on CD3$^+$CD8$^+$ CTLs measured before infection (0) or 5, 7, 9, and 30 dpi. (D, E) Frequencies (mean ± SD) of (D) CD127^{hi}KLRG-1^{lo} and (E) CD127^{lo}KLRG-1^{hi} were determined after gating on CD3$^+$CD8$^+$CD44^{hi}CD62L^{lo} CTLs at 5, 7, 9, and 30 dpi. (A–E) Data are from one to two independent experiments with six to nine mice per group. Statistical comparisons were made via Mann–Whitney *U* test and statistically significant values are indicated (*$p \le 0.05$; **$p \le 0.01$; ***$p \le 0.001$; ****$p \le 0.0001$). FRCs, fibroblastic reticular cell; IFNAR, IFN-I receptor.

In summary, the frequencies of lymphoid stromal cells (LSCs), the expression of H-2K^b, CD44, ICAM-1, VCAM-1, and PD-L1 on FRCs, and the abundance of *Ccl19* and *Ccl21* in LNs were very similar in untreated FRC$^{\Delta IFNAR}$ and FRC^{wt} mice (Fig. 2A–D) arguing for a rather selective contribution of IFNAR signaling to FRC development and function during steady state. However, after vaccination, *Cxcl9*, and to a lesser extent *Cxcl10* and *Il7*, expression were reduced in FRC$^{\Delta IFNAR}$ mice indicating early IFNAR signaling in FRCs in our experimental system [9].

IFNAR signaling in FRCs affects the composition of the antiviral CD8$^+$ memory T cell pool

As mentioned above, early IFNAR blockade improves the formation of antiviral CD8$^+$ T$_M$ [22]. Whether the lack of IFNAR signaling in FRCs modulates the differentiation of polyclonal CD8$^+$ T cells in response to VSV infection was tested next. For this purpose, we first verified that the T cell pools of naïve FRC$^{\Delta IFNAR}$ and FRC^{wt} mice were overall similar (Supporting information Fig. S2). FRC$^{\Delta IFNAR}$ and FRC^{wt} mice survived VSV infection equally well (Supporting information Fig. S3) arguing against major differences in B-cell development (data not shown) and anti-VSV antibody responses, which are vital for host survival [27]. However, CD8$^+$ T$_M$ development was altered in FRC$^{\Delta IFNAR}$ mice. As depicted in Fig. 3A and B, frequencies of CD8$^+$CD44^{hi}CD62L^{lo} T cells in peripheral blood were comparable at days 5 and 7 post infection (dpi). In contrast, their relative abundance was elevated in FRC$^{\Delta IFNAR}$ mice at 9 and 30 dpi (Fig. 3A and B).

To investigate the kinetics of T$_M$ differentiation in more detail, we analyzed CD127 and KLRG-1 expression in CD8$^+$CD44^{hi}CD62L^{lo} T cells. In accordance with previous reports [28, 29], frequencies of CD127^{hi}KLRG-1^{lo} cells increased progressively in FRC^{wt} mice from 5 to 30 dpi. In FRC$^{\Delta IFNAR}$ mice, however, elevated frequencies of CD127^{hi}KLRG-1^{lo} cells were first observed at 9 dpi. Of note, in FRC$^{\Delta IFNAR}$ mice the abundance of CD127^{hi}KLRG-1^{lo} cells remained below that observed in FRC^{wt} mice at 7–30 dpi (Fig. 3C and D). The delayed formation of

CD127^{hi}KLRG-1^{lo} cells in infected FRC$^{\Delta IFNAR}$ mice was paralleled by increased frequencies of CD127^{lo}KLRG-1^{hi} cells throughout the entire observation period (Fig. 3C and E). Importantly, the CD127^{lo}KLRG-1^{hi} T cell population declined from 7 to 30 dpi in both mouse lines (Fig. 3E), suggesting a similar half-life of these T cells. Hence, elevated frequencies of CD127^{lo}KLRG-1^{hi} T cells in FRC$^{\Delta IFNAR}$ mice at day 30 appear to result from their more efficient generation during the early phase of the response.

To analyze the VSV-specific CD8$^+$ T cell response in more detail, we monitored VSV nucleoprotein (NP)-specific CD8$^+$ T cells in peripheral blood of infected FRC$^{\Delta IFNAR}$ and FRC^{wt} mice (Fig. 4). Frequencies of VSV NP-specific CD8$^+$ T cells were comparable in FRC$^{\Delta IFNAR}$ and FRC^{wt} mice throughout the observation period, arguing for similar numbers of VSV NP-specific clones in the naïve CD8$^+$ T cell compartment in mice of both genotypes (Fig. 4A). At 5 dpi, most VSV NP-specific CD8$^+$ T cells displayed a CD44^{hi}CD62L^{lo} phenotype, which was maintained until the memory phase, irrespective of the genotype of the mice analyzed (Fig. 4B and C).

Despite the aforementioned similarities, we observed differences with respect to KLRG-1 expression. Already at 7 dpi, the frequency of VSV NP-specific CD44^{hi}CD62L^{lo} CD8$^+$ T cells expressing high levels of KLRG-1 was strongly elevated in FRC$^{\Delta IFNAR}$ mice (Fig. 4D and G). This effect was maintained at 9 dpi and was most pronounced in the memory phase at 30 dpi (Fig. 4D and G). Among the KLRG-1^{hi} cells, a population of double-positive CD127^{hi}KLRG-1^{hi} CD44^{hi}CD62L^{lo} CD8$^+$ T$_M$ accumulated in FRC$^{\Delta IFNAR}$ mice, which was barely detectable in FRC^{wt} mice (Fig. 4D and F). Correspondingly, most NP-specific CD44^{hi}CD62L^{lo} CD8$^+$ T$_M$ in FRC^{wt} mice were CD127^{hi}KLRG-1^{lo}, while this population was significantly reduced in FRC$^{\Delta IFNAR}$ mice (Fig. 4D and E).

Thus, our data demonstrate that the absence of IFNAR signals in FRCs is associated with the accumulation of KLRG-1^{hi} anti-VSV CD8$^+$ T$_M$. This process appears to be programmed in the early phase of the response, as shown by the fact that the frequency of VSV-specific CD8$^+$ KLRG-1^{hi} T cells was already elevated at 7 dpi and further increased until 30 dpi.

Discussion

Based on their homing patterns, CD8$^+$ T$_M$ can be divided into different subsets. For example, CD8$^+$ T$_{CM}$ and CD8$^+$ T$_{EM}$ recirculate between SLOs and nonlymphoid tissues, respectively. This functional diversity enables long-lived CD8$^+$ T$_M$ to provide systemic protection against recurrent infections, irrespective of the pathogen entry site [30].

So far, most studies focused on the cell-intrinsic pathways controlling CD8$^+$ T$_M$ diversification and maintenance [30–32]. However, CD8$^+$ T$_M$ are part of multicellular networks sensing pathogen-associated tissue perturbations [33]. Various immune and nonimmune cells contribute to these signaling hubs, which can be found in most if not all tissues in the body [33]. In LNs, chemokines and cytokines produced by FRCs regulate various aspects of T cell responses including CD8$^+$ T$_M$ differentiation and survival [8]. For example, in the steady state, CCL19 and CCL21 attract naïve T cells into LNs to increase the likelihood of productive T-APC interactions in case of infection [34]. Furthermore, the IL-7-dependent survival of CD8$^+$ T$_{CM}$ in LNs relies on FRCs, which contribute to CCL19/21 gradients guiding CD8$^+$ T$_{CM}$ into niches rich in IL-7 [4, 6, 7]. In case of viral infections, protective CD8$^+$ T cell responses rely on IFNAR signaling in multiple cell types [13], which must be well balanced to provide optimal protection [35]. Suboptimal IFNAR signaling in particular cell types may affect the entire network of IFNAR-dependent cellular interactions controlling CD8$^+$ T$_M$ differentiation and/or maintenance.

Of note, IFN-I-dependent immunomodulation already occurs before pathogen contact [36]. In the steady state, the commensal microflora promotes low-level IFN-I production, which results in tonic IFNAR signaling. This elevates the activation thresholds of innate immune cells thereby increasing their responsiveness to subsequent infections [14, 37]. As shown in Fig. 2B and C, neither chemokine nor IL-7 production differed significantly between untreated FRC^{wt} and FRC$^{\Delta IFNAR}$ mice. Similarly, (1) the frequencies of FRCs (Fig. 2A), (2) the composition of the T cell repertoire, and (3) the abundance of T$_{CM}$/T$_{EM}$ were indistinguishable between untreated FRC^{wt} and FRC$^{\Delta IFNAR}$ mice (Supporting information Fig. S2). The same was true for FRC surface markers (Fig. 2D) indicating that the steady state regulation of the aforementioned parameters is independent of tonic IFNAR signaling in FRCs.

As a result of infection, CCL21 expression is downregulated in SLOs thereby restricting recruitment and further priming of naïve T cells [38]. This mechanism is IFN-γ dependent and remained unaffected in vaccinated FRC$^{\Delta IFNAR}$ mice (Fig. 2B). In accordance with previous reports [24, 25], we observed the early upregulation of CXCL9 and CXCL10 in activated LNs, which was less pronounced in FRC$^{\Delta IFNAR}$ mice (Fig. 2B). Although we cannot exclude a contribution of other immune and/or nonimmune cells, IFNAR$^+$ FRCs appear critical for chemokine induction in the early phase of an immune response [26]. In activated LNs, CXCL9/CXCL10 gradients guide primed CD8$^+$ T cells to specialized niches where differentiation proceeds [26]. Consequently, CD8$^+$ T$_{EFF}$ migration and the subsequent generation of KLRG-1^{hi} cells are impaired in CXCL10- and IFNAR-deficient mice [26]. Similar findings were obtained in lymphocytic choriomeningitis virus-infected FRC$^{\Delta IFNAR}$ mice [18] as well as in our OT-I system, though at later time points (at 30 dpv; Fig. 1D).

Besides tissue localization, the type of pathogen determines the differentiation program of CD8$^+$ T$_{EFF}$ [31]. For example, the generation and subsequent accumulation of KLRG-1^{lo} CD8$^+$ T cells in response to *Listeria monocytogenes* infection are strongly delayed [39]. On the contrary, high frequencies of KLRG-1^{lo} CD8$^+$ T cells are generated early after VSV infection and are maintained in long term [39]. CD8$^+$ T$_{EFF}$ expressing low levels of KLRG-1 and high levels of the IL-7 receptor α (IL-7Rα; CD127) typically give rise to long-lived T$_M$ expressing high levels of the anti-apoptotic molecule B-cell lymphoma 2 (Bcl-2) [28, 40]. However, cell-fate-mapping experiments revealed that CD8$^+$ T$_{EFF}$ expressing high

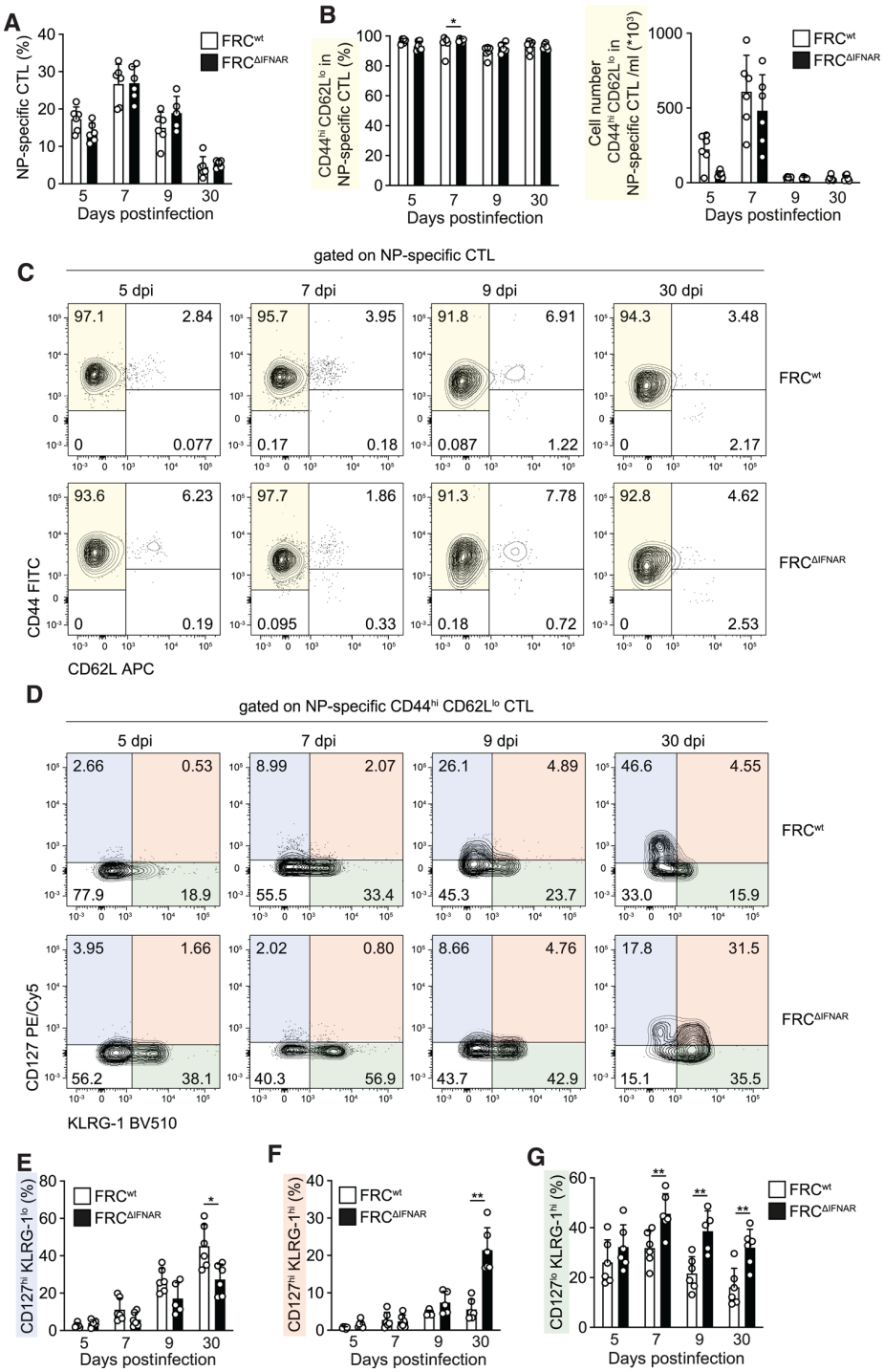

Figure 4. IFNAR signaling in FRCs regulates the differentiation of nucleoprotein (NP)-specific CD8$^+$ memory T cells. (A–G) FRC$^{\Delta IFNAR}$ and FRC^{wt} mice were infected as described in Fig. 3 and blood was analyzed by flow cytometry. (A, B) Bar diagrams show (A) frequencies of total VSV NP-specific (CD3$^+$CD8$^+$) CTLs as well as (B) frequencies and total numbers of CD44^{hi}CD62L^{lo} NP-specific CTLs. (C, D) Representative contour plots are shown for (C) CD44/CD62L expression on NP-specific CTLs or (D) CD127/KLRG-1 expression after gating on CD3$^+$CD8$^+$CD44^{hi}CD62L^{lo} NP-specific CTLs at 5, 7, 9, and 30 dpi. Numbers indicate percentages. (E–G) Frequencies of (E) CD127^{hi}KLRG-1^{lo}, (F) CD127^{hi}KLRG-1^{hi}, and (G) CD127^{lo}KLRG-1^{hi} after gating on CD44^{hi}CD62L^{lo} NP-specific CTLs are summarized in bar diagrams. (A, B, E–G) Bar diagrams show mean ± SD from five to six mice analyzed per group in one experiment. Statistical comparisons were made via Mann–Whitney *U* test and statistically significant values are indicated (*$p \leq 0.05$; **$p \leq 0.01$). FRCs, fibroblastic reticular cells; IFNAR, IFN-I receptor.

levels of both KLRG-1 and CD127 are also a potent source of T_M [41]. As shown here, the formation of VSV NP-specific KLRG-1^{lo} $CD8^+$ T_M was strongly impaired in $FRC^{\Delta IFNAR}$ mice. Instead, and as opposed to FRC^{wt} mice, $CD127^{hi/lo}$KLRG-1^{hi} $CD8^+$ T_M accumulated in $FRC^{\Delta IFNAR}$ mice. Despite these phenotypic differences, the VSV NP-specific $CD8^+$ T_M pool was similar in size in both hosts. This suggests that IFNAR signaling in FRCs does not affect the frequency but rather the phenotype of VSV NP-specific $CD8^+$ T_M precursors and their progeny, at least with respect to KLRG-1 and CD127. However, different patterns of $CD8^+$ T_M differentiation were observed after peptide vaccination of OT-I-reconstituted mice. This may be due to FRC-independent differences between both experimental systems. For instance, $CD8^+$ T_M differentiation correlates with the number of naïve $CD8^+$ T cells activated upon primary antigen contact [42, 43]. The precursor frequencies generated by adoptive transfer of naïve $CD8^+$ OT-I T cells are much higher compared with those of VSV-specific cells in the naïve polyclonal $CD8^+$ T cell repertoire. Furthermore, the amount of antigen affects T_{CM}/T_{EM} fate decision [44]. Given that IFNAR signaling limits viral replication in FRCs [18] and mouse embryonic fibroblasts [45], we cannot fully exclude elevated levels of viral replication and subsequent antigen accumulation in VSV-infected $FRC^{\Delta IFNAR}$ mice. Although this potential effect did not impair the clearance of primary VSV infections (Supporting information Fig. S3), we cannot exclude that altered dynamics of viral replication and subsequent antigen availability affected $CD8^+$ T_M differentiation in $FRC^{\Delta IFNAR}$ mice. As opposed to viruses, peptide vaccines do not replicate and are rapidly removed from the system. Hence, a direct comparison of the data obtained with peptide vaccination and VSV infection is of limited value. Nevertheless, our results imply that the relative contribution of $IFNAR^+$ FRCs to $CD8^+$ T_M differentiation is context-dependent and thus varies between experimental systems.

Our data strongly suggest that FRC-specific IFNAR signaling modulates early FRC-$CD8^+$ T cell interactions in LNs and helps to adapt subsequent $CD8^+$ T_M differentiation to the inflammatory context. This is in agreement with a recent report showing that transient blockade of IFNAR signaling strongly increases $CD8^+$ T_M formation [22]. This could be determined by a combination of pathogen-related parameters including the amount of IFN-I induced in the priming phase of the response [46]. Using bone marrow chimeras and FRC-specific IFN-β luciferase reporter mice [47], we observed the induction of IFN-I responses in radio-resistant stromal cells already 24 h after VSV infection (Supporting information Fig. S5A). Among these stromal cells, FRCs contributed to the IFN-I response in LNs (Supporting information Fig. S5B and C), which are mandatory for the priming of VSV-specific $CD8^+$ T cells [3]. Whether the autocrine action of FRC-derived IFN-I affects the immunomodulatory function of FRCs remains to be elucidated. In $FRC^{\Delta IFNAR}$ mice, the Cre expression is not restricted to the LN but also active in BM stromal cells [48]. Since naïve $CD8^+$ T cells can be primed in the BM [49], which also serves a survival niche for $CD8^+$ T_M [50, 51], we cannot formally exclude a contribution of IFNAR signaling in BM FRCs to our results. Nevertheless, our data suggest an important contribution of early IFNAR signaling in FRCs programming subsequent VSV-specific $CD8^+$ T_M differentiation, a process that is mainly initiated in LNs [3].

In summary, we provide evidence for an early, context-dependent contribution of FRC-specific IFNAR signals to $CD8^+$ memory fate decision. Hence, efforts aiming at the optimization of vaccination strategies should not only focus on $CD8^+$ T cell intrinsic pathways but also consider the multicellular interactions involved in the early events of an immune response.

Materials and methods

Mice and viruses

B6.Cg-Tg(Prrx1-cre)1Cjt/J (Prx1-Cre) [19] (stock no. 005584) mice were purchased from The Jackson Laboratory. C57BL/6J mice were purchased from Envigo. Together with $IFNAR^{fl/fl}$ [15], Thy1.1^+ Rag$1^{-/-}$ OT-I [52], B6.Bruce4-ifnb1tm2.2Lien (short: IFN-$\beta^{+/\Delta\beta\text{-luc}}$; reporter expressed ubiquitously) [47], and B6.Bruce4-ifnb1tm2.1Lien (short: IFN-$\beta^{flox\beta\text{-luc}/flox\beta\text{-luc}}$; conditional reporter mice) [47] were maintained under specific pathogen-free conditions at the central animal facility of the Medical Faculty of the Otto-von-Guericke-University Magdeburg and the TWINCORE, Centre for Experimental and Clinical Infection Research, Hannover. Whenever possible, control littermates were used. VSV-Indiana (Mudd-Summers isolate), originally obtained from D. Kolakofsky (University of Geneva, Geneva, Switzerland), was grown on BHK-21 cells. Virus was harvested from conditioned culture medium and titers were determined by plaque formation on Vero cells as previously described [53]. Virus was injected intravenously.

Cell isolation

Single-cell suspensions from peripheral LNs and spleen were obtained as previously described [7]. Organs were forced through metal strainers in PBS/2 mM EDTA (Carl Roth) and erythrocytes were lysed in the spleen. BM was flushed out using PBS/2 mM EDTA (Carl Roth), 27G needles (B. Braun), and syringes (BD Biosciences). For erythrocyte lysis, spleen and BM cells were re-suspended in ammonium-chloride-potassium lysis buffer for 90 s followed by the addition of RPMI 1640 (Biochrom) containing 10% (v/v) FCS (PAN Biotech) and 1% (v/v) penicillin/streptomycin (P/S; Gibco). After centrifugation, all organs were re-suspended in PBS/2 mM EDTA and filtered through 40 μm cell strainers (Corning, Durham, NC).

For LSC isolation, peripheral LNs were digested as previously described [7]. In brief, fat-free LNs were cut into small (1 × 1 mm) pieces in RPMI 1640/10% FCS/1% P/S. LN fragments were vortexed and the supernatant was removed after the organ pieces had settled. This process was repeated three times. LN fragments were transferred into 12-well plates containing 1 mL digestion

medium I (0.2 mg/mL Collagenase P [Roche], 0.2 mg/mL Dispase II [Roche], 10 μg/mL DNase I [Sigma] and 5 μg/mL Latrunculin B [Calbiochem] in RPMI 1640 supplemented with 10% FCS/1% P/S). After incubation for 30 min at 37°C and 5% (v/v) CO_2, 1 mL digestion medium II (0.4 mg/mL Collagenase P, 0.2 mg/mL Dispase II, 10 μg/mL μDNase I, and 5 μg/mL Latrunculin B in RPMI 1640/10% FCS/1 % P/S) was added and the samples were re-suspended. After incubation for 30 min at 37°C and 5% CO_2, 0.5 mL RPMI 1640/10% FCS/1% P/S/ 10 mM EDTA was added to stop digestion. Cell suspensions were filtered through 70 μm cell strainers and cells were washed with PBS/2 mM EDTA. Cells were re-suspended in PBS/2 mM EDTA and filtered through 40 μm cell strainers.

Adoptive T cell transfer

OT-I T cells were prepared as previously described [7]. In brief, naïve ($CD44^{lo}CD62L^{hi}$) $CD8^+$ T cells expressing a transgenic TCR (Vα2Vβ5) specific for the chicken OVA-derived, H-$2K^b$–restricted peptide $OVA_{257–264}$ (SIINFEKL), were isolated from LNs and spleen of $Rag1^{-/-}$ $Thy1.1^+$ OT-I mice using CD8a-specific MicroBeads and AutoMACS (Miltenyi Biotec) according to the manufacturer's recommendations. Between 6.8 and 7.5×10^5 OT-I T cells (purity > 90.7%) were injected i.v. into the tail vein of $Thy1.1^-$ recipients. For peptide vaccination, a mixture of 50 μg SIINFEKL (Biosyntan) and 50 μg lipopolysaccharide (*Escherichia coli* O111:B4; Sigma-Aldrich) was injected i.v. into the tail vein of OT-I-reconstituted recipients.

Flow cytometry

The following reagents were purchased from BioLegend: Bcl-2-FITC (BCL/10C4), CD3-AF700 (17A2), CD3ε-BV421 (145-2C11), CD4-BV510 (RM4-5), CD4-APC/Cy7 (GK1.5), CD8a-PE/Cy5 (53-6.7), CD8a-PE/Cy7 (53-6.7), CD44-APC/Cy7 (IM7), CD44-FITC (IM7), CD44-PE (IM7), CD45-APC/Cy7 (30-F11), CD54/ICAM-1-PB (YN1/1.7.4), CD62L-FITC (MEL-14), CD90.1-PB (OX-7), CD106/VCAM-1-AF647 (429 MVCAM.A), CD127/IL-7Rα-PE (A7R34), CD274/PD-L1-biotin (10F.9G2), CD279/PD-1-BV605 (29F.1A12), gp38/Podoplanin-AF488 (8.1.1), H-$2k^b$/MHC-I-PB (AF6-88.5), IFN-γ-APC (XMG1.2), Ki-67-PB (16A8), KLRG-1-APC (2F1/KLRG-1), KLRG-1-BV510 (2F1/KLRG-1), KLRG-1-BV605 (2F1/KLRG-1), TER-119-PE/Cy5 (TER-119), TNF-α-PE (MP6-XT22), 7-AAD viability staining solution, and streptavidin-BV510. CD127/IL-7Rα-PE/Cy5 (A7R34), CD31-PE/Cy7 (390), Ki-67-PE/Cy7 (SolA15), and CD279/PD-1-PE (J43) were purchased from eBioscience. CD8a-BUV395 (53-6.7), CD62L-APC (MEL-14), and the anti-mouse TCR Vβ screening panel were purchased from BD Biosciences. CD44-FITC (IM7) and CD127/IL-7Rα-PE-Cy5 were purchased from Invitrogen. The extent of expanding VSV-specific nucleoprotein 52-59 (H-2Kb – RGYVYQGL)-positive T lymphocytes was assessed by pentamer immunolabeling (ProImmune). For analyses of blood lymphocytes, 25 μL blood (obtained through retro-bulbar bleeding with microhematocrit capillaries (Hirschmann)) was stained with VSV-pentamer for 10 min at 4°C. Afterward, fluorochrome-labeled antibodies were added and the samples were incubated for 15 min at 4°C. Blood cell lysis and fixation were performed using 1 mL FACS lysing solution (BD Biosciences) for 20 min at room temperature in the dark. Cells were washed with staining buffer (2% BSA in DPBS, 20 mM EDTA, 0.2% natriumazid, 1×PBS in ddH_2O).

Before staining with fluorochrome-labeled antibodies, single-cell suspensions of LNs, spleens, and BM were incubated with 50 μL of anti-mouse CD16/32 (purified from 2.4G2 ATCC HB-197) in staining buffer for 10 min at 4°C. Afterward, cells were incubated with 50 μL of fluorochrome-labeled antibodies diluted in anti-CD16/32 containing staining buffer. After incubation for 30 min at 4°C, cells were washed with 200 μL PBS/2 mM EDTA. For LSC analyses, 7-AAD was added 5 min before data acquisition. For intranuclear staining of Bcl-2, samples were processed using the FoxP3/transcription factor staining buffer set (eBioscience, Thermo Fisher Scientific) according to the manufacturer's recommendations. For intracellular cytokine staining, cells were re-stimulated for 4 h with 1 μM SIINFEKL (Biosyntan) in the presence of brefeldin A (BioLegend) and monensin A (BioLegend), stained with surface antibodies as described above, fixed with the intracellular staining kit (BioLegend) according to the manufacturer's instructions, and stained with anti–IFN-γ or anti-TNF-α. Samples were measured on an LSRFortessa and LSRII flow cytometer (Becton Dickinson) and analyzed with FlowJo 10 software (FlowJo, LLC) according to the "Guidelines for the use of flow cytometry and cell sorting in immunological studies (third edition)" [54]. Individual gating strategies are depicted in Supporting information Figs. S6–S8.

Reverse transcriptase PCR and real-time quantitative PCR

Peripheral LNs were homogenized in CK14 0.5-mL tubes (Peqlab/VWR) containing 200 μL TRIzol reagent (Invitrogen) in a Precellys 24 homogenizer (Peqlab/VWR). Total RNA was extracted using chloroform (Sigma-Aldrich) according to the manufacturer's instructions (Invitrogen). Isolated RNA was quantified by photometric Nanodrop (Thermo Fisher Scientific) measurement and reverse-transcribed using random hexamer primers and the advantage RT-for-PCR kit (Takara Clontech) according to the manufacturer's instructions. For real-time quantitative PCR (RT-qPCR) analyses, the Taqman gene expression master mix (Thermo Fisher Scientific) and the following TaqMan gene expression assays (Thermo Fisher Scientific) were used according to the manufacturer's instructions: *Ccl19* (FAM-MGB probe Mm00839967_g1), *Ccl21* (FAM-MGB probe Mm03646971_gH), *Cxcl9* (FAM-MGB probe Mm000434946_m1), *Cxcl10* (FAM-MGB probe Mm00445235_m1), *Il7* (FAM-MGB probe Mm01295805_m1), and *Hprt* (FAM-MGB probe Mm00446968_m1). Samples were analyzed in triplicates and C_T values were exported from the ABI PRISM 7000 (Applied

Biosystems) sequence detection system. The relative quantifications were calculated according to the ΔC_T method and data points represent triplicate averages.

Generation of bone marrow chimeric mice

Mice were lethally irradiated with 9 Gy and the following day, they were i.v. reconstituted with 1×10^7 BM cells in PBS of the indicated genotype. BM cells were isolated by flushing femur and tibia with RPMI 1640 medium supplemented with 10% FCS, 10 mM HEPES, 1 mM sodium pyruvate, 2 mM Glutamax, 100 U/mL penicillin, 100 μg/mL streptomycin (all from Life Technologies), and 0.1 mM β-mercaptoethanol. Cells were then treated with RBC lysis buffer (Sigma-Aldrich) and washed with PBS. BM chimeric mice were used for experiments after at least 8 weeks of recovery.

Detection of bioluminescence in vitro and by in vivo imaging

One day before in vivo imaging, mice were shaved for better signal detection. Immediately after i.v. injection of 100 μL luciferin (30 mg/mL in PBS/20 g mouse weight), mice were anesthetized using isoflurane and analyzed in an IVIS live imaging instrument (IVIS Spectrum CT) under transient isoflurane anesthesia. The acquired images were analyzed using Living Image 4.3.1 software.

For the detection of luciferase activity in different organs in vitro, the respective organs were prepared and weighed at the indicated time points after infection and stored at −80°C until analysis. The samples were thawed on ice and calculated amounts of Glo Lysis buffer (Promega) in relation to the organ weight was added to the samples. Tissues were homogenized in Lysing Matrix A tubes for 60 s (4 m/s) in an organ homogenizer (MP Biomedicals). Each homogenate (20 μL/well) was pipetted to a 96-well plate. For luciferase measurements, 20 μL/well of Bright Glo Luciferin (Perkin Elmer) was added to determine bioluminescence activity using a plate reader (BioTek). Data were normalized to background values obtained before adding luciferin. All steps were prepared on ice. The luciferase activity was measured with an integration time of 10 s.

Statistical analyses

Statistical analyses and graphical representations were performed using Prism 8 (GraphPad Software Inc.). Statistical significances were determined using nonparametric one-tailed (Supporting information Fig. S5) or two-tailed Mann–Whitney *U* tests (Figs. 1–4, Supporting information Figs. S2 and S4; $*p \leq 0.05$; $**p \leq 0.01$; $***p \leq 0.001$; $****p \leq 0.0001$).

Acknowledgements: We thank J. Giese for excellent technical assistance and the animal care staff for support. This work was supported by the Deutsche Forschungsgemeinschaft (Sonderforschungsbereich SFB854 (project B15) and L. Knop was a fellow of the LOM-stipend from the Medical Faculty of the Otto-von-Guericke University Magdeburg.
Open Access funding enabled and organized by Projekt DEAL.

Conflict of interest: The authors declare no commercial or financial conflict of interest.

Author contributions: TS and UK designed and supervised the study with the help of LK and JS; LK, JS, PKL, AW, and UB performed experiments and analyzed data together with IRD, UK, and TS; TS wrote the manuscript with the help of the other coauthors.

Ethics statement: Experimental procedures were approved by the relevant animal experimentation committee and performed in compliance with international and local animal welfare legislations (Niedersächsisches Landesamt für Verbraucherschutz und Lebensmittelsicherheit, permit AZ. 33.12-42502-04-12/1025 and 13/1072 and Landesverwaltungsamt Sachsen-Anhalt, permit no. 42502-2-1288 UniMD).

Data availability statement: The data that support the findings of this study are available from the corresponding author upon reasonable request.

Peer review: The peer review history for this article is available at https://publons.com/publon/10.1002/eji.202149760

References

1 **Krishnamurty, A. T.** and **Turley, S. J.**, Lymph node stromal cells: cartographers of the immune system. *Nat. Immunol.* 2020. **21**: 369–380.

2 **Scandella, E.**, **Bolinger, B.**, **Lattmann, E.**, **Miller, S.**, **Favre, S.**, **Littman, D. R.**, **Finke, D.** et al., Restoration of lymphoid organ integrity through the interaction of lymphoid tissue-inducer cells with stroma of the T cell zone. *Nat. Immunol.* 2008. **9**: 667–675.

3 **Karrer, U.**, **Althage, A.**, **Odermatt, B.**, **Roberts, C. W. M.**, **Korsmeyer, S. J.**, **Miyawaki, S.**, **Hengartner, H.** et al., On the key role of secondary lymphoid organs in antiviral immune responses studied in alymphoplastic (aly/aly) and spleenless (Hox11−/−) mutant mice. *J. Exp. Med.* 1997. **185**: 2157–2170.

4 **Link, A.**, **Vogt, T. K.**, **Favre, S.**, **Britschgi, M. R.**, **Acha-Orbea, H.**, **Hinz, B.**, **Cyster, J. G.** et al., Fibroblastic reticular cells in lymph nodes regulate the homeostasis of naive T cells. *Nat. Immunol.* 2007. **8**: 1255–1265.

5 **Cui, G.**, **Staron, M. M.**, **Gray, S. M.**, **Ho, P.-C.**, **Amezquita, R. A.**, **Wu, J.** and **Kaech, S. M.**, IL-7-Induced Glycerol Transport and TAG Synthesis Promotes Memory CD8(+) T Cell Longevity. *Cell* 2015. **161**: 750–761.

6 **Jung, Y. W.**, **Kim, H. G.**, **Perry, C. J.** and **Kaech, S. M.**, CCR7 expression alters memory CD8 T-cell homeostasis by regulating occupancy in IL-7- and IL-15-dependent niches. *Proc. Natl. Acad. Sci. USA* 2016. **113**: 8278–8283.

7 **Knop, L.**, **Deiser, K.**, **Bank, U.**, **Witte, A.**, **Mohr, J.**, **Philipsen, L.**, **Fehling, H. J.** et al., IL-7 derived from lymph node fibroblastic reticular cells is

dispensable for naive T cell homeostasis but crucial for central memory T cell survival. *Eur. J. Immunol.* 2020. **50**: 846–857.

8 **Alexandre, Y. O.** and **Mueller, S. N.**, Stromal cell networks coordinate immune response generation and maintenance. *Immunol. Rev.* 2018. **283**: 77–85.

9 **Malhotra, D., Fletcher, A. L., Astarita, J., Lukacs-Kornek, V., Tayalia, P., Gonzalez, S. F., Elpek, K. G.** et al., Transcriptional profiling of stroma from inflamed and resting lymph nodes defines immunological hallmarks. *Nat. Immunol.* 2012. **13**: 499–510.

10 **Gregory, J. L., Walter, A., Alexandre, Y. O., Hor, J. L., Liu, R., Ma, J. Z., Devi, S.** et al., nfection Programs Sustained Lymphoid Stromal Cell Responses and Shapes Lymph Node Remodeling upon Secondary Challenge. *Cell Rep.* 2017. **18**: 406–418.

11 **Rodda, L. B., Lu, E., Bennett, M. L., Sokol, C. L., Wang, X., Luther, S. A., Barres, B. A.** et al., Single-Cell RNA Sequencing of Lymph Node Stromal Cells Reveals Niche-Associated Heterogeneity. *Immunity* 2018. **48**: 1014–1028.

12 **Sawa, Y., Arima, Y., Ogura, H., Kitabayashi, C., Jiang, J.-J., Fukushima, T., Kamimura, D.** et al., Hepatic interleukin-7 expression regulates T cell responses. *Immunity* 2009. **30**: 447–457.

13 **Crouse, J., Kalinke, U.** and **Oxenius, A.**, Regulation of antiviral T cell responses by type I interferons. *Nat. Rev. Immunol.* 2015. **15**: 231–242.

14 **Schaupp, L., Muth, S., Rogell, L., Kofoed-Branzk, M., Melchior, F., Lienenklaus, S., Ganal-Vonarburg, S. C.** et al., Microbiota-Induced Type I Interferons Instruct a Poised Basal State of Dendritic Cells. *Cell* 2020. **181**: 1080–1096.e19.

15 **Kamphuis, E., Junt, T., Waibler, Z., Forster, R.** and **Kalinke, U.**, Type I interferons directly regulate lymphocyte recirculation and cause transient blood lymphopenia. *Blood* 2006. **108**: 3253–3261.

16 **Richer, M. J., Nolz, J. C.** and **Harty, J. T.**, Pathogen-specific inflammatory milieux tune the antigen sensitivity of CD8(+) T cells by enhancing T cell receptor signaling. *Immunity* 2013. **38**: 140–152.

17 **Crouse, J., Bedenikovic, G., Wiesel, M., Ibberson, M., Xenarios, I., Von Laer, D., Kalinke, U.** et al., Type I interferons protect T cells against NK cell attack mediated by the activating receptor NCR1. *Immunity* 2014. **40**: 961–973.

18 **Perez-Shibayama, C., Islander, U., Lütge, M., Cheng, H. W., Onder, L., Ring, S. S., De Martin, A.** et al., Type I interferon signaling in fibroblastic reticular cells prevents exhaustive activation of antiviral CD8+ T cells. *Sci. Immunol.* 2020. **5**.

19 **Logan, M., Martin, J. F., Nagy, A., Lobe, C., Olson, E. N.** and **Tabin, C. J.**, Expression of Cre Recombinase in the developing mouse limb bud driven by a Prxl enhancer. *Genesis* 2002. **33**: 77–80.

20 **Kaech, S. M.** and **Ahmed, R.**, Memory CD8+ T cell differentiation: initial antigen encounter triggers a developmental program in naïve cells. *Nat. Immunol.* 2001. **2**: 415–422.

21 **van Stipdonk, M. J., Lemmens, E. E.** and **Schoenberger, S. P.**, Naïve CTLs require a single brief period of antigenic stimulation for clonal expansion and differentiation. *Nat. Immunol.* 2001. **2**: 423–429.

22 **Palacio, N., Dangi, T., Chung, Y. R., Wang, Y., Loredo-Varela, J. L., Zhang, Z.** and **Penaloza-MacMaster, P.**, Early type I IFN blockade improves the efficacy of viral vaccines. *J. Exp. Med.* 2020. **217**: e20191220.

23 **Woolf, E., Grigorova, I., Sagiv, A., Grabovsky, V., Feigelson, S. W., Shulman, Z., Hartmann, T.** et al., Lymph node chemokines promote sustained T lymphocyte motility without triggering stable integrin adhesiveness in the absence of shear forces. *Nat. Immunol.* 2007. **8**: 1076–1085.

24 **Kastenmüller, W., Brandes, M., Wang, Z., Herz, J., Egen, J. G.** and **Germain, R. N.**, Peripheral prepositioning and local CXCL9 chemokine-mediated guidance orchestrate rapid memory CD8+ T cell responses in the lymph node. *Immunity* 2013. **38**: 502–513.

25 **Sung, J. H., Zhang, H., Moseman, E. A., Alvarez, D., Iannacone, M., Henrickson, S. E., de la Torre, J. C.** et al., Chemokine guidance of central memory T cells is critical for antiviral recall responses in lymph nodes. *Cell* 2012. **150**: 1249–1263.

26 **Duckworth, B. C., Lafouresse, F., Wimmer, V. C., Broomfield, B. J., Dalit, L., Alexandre, Y. O., Sheikh, A. A.** et al., Effector and stem-like memory cell fates are imprinted in distinct lymph node niches directed by CXCR3 ligands. *Nat. Immunol.* 2021. **22**: 434–448.

27 **Bründler, M., Aichele, P., Bachmann, M., Kitamura, D., Rajewsky, K.** and **Zinkernagel, R. M.**, Immunity to viruses in B cell-deficient mice: influence of antibodies on virus persistence and on T cell memory. *Eur. J. Immunol.* 1996. **26**: 2257–2262.

28 **Kaech, S. M., Tan, J. T., Wherry, E. J., Konieczny, B. T., Surh, C. D.** and **Ahmed, R.**, Selective expression of the interleukin 7 receptor identifies effector CD8 T cells that give rise to long-lived memory cells. *Nat. Immunol.* 2003. **4**: 1191–1198.

29 **Joshi, N. S., Cui, W., Chandele, A., Lee, H. K., Urso, D. R., Hagman, J., Gapin, L.** et al., Inflammation directs memory precursor and short-lived effector CD8(+) T cell fates via the graded expression of T-bet transcription factor. *Immunity* 2007. **27**: 281–295.

30 **Jameson, S. C.** and **Masopust, D.**, Understanding Subset Diversity in T Cell Memory. *Immunity* 2018. **48**: 214–226.

31 **Chang, J. T., Wherry, E. J.** and **Goldrath, A. W.**, Molecular regulation of effector and memory T cell differentiation. *Nat. Immunol.* 2014. **15**: 1104–1115.

32 **Henning, A. N., Roychoudhuri, R.** and **Restifo, N. P.**, Epigenetic control of CD8+ T cell differentiation. *Nat. Rev. Immunol.* 2018. **18**: 340–356.

33 **Masopust, D.** and **Soerens, A. G.**, Tissue-Resident T Cells and Other Resident Leukocytes. *Annu. Rev. Immunol.* 2019. **37**: 521–546.

34 **Qi, H., Kastenmüller, W.** and **Germain, R. N.**, Spatiotemporal Basis of Innate and Adaptive Immunity in Secondary Lymphoid Tissue. *Annu. Rev. Cell Dev. Biol.* 2014. **30**: 141–167.

35 **Yao, C., Bora, S. A., Parimon, T., Zaman, T., Friedman, O. A., Palatinus, J. A., Surapaneni, N. S.** et al., Cell-Type-Specific Immune Dysregulation in Severely Ill COVID-19 Patients. *Cell Rep.* 2021. **34**: 108590.

36 **Gough, D. J., Messina, N. L., Clarke, C. J., Johnstone, R. W.** and **Levy, D. E.**, Constitutive type I interferon modulates homeostatic balance through tonic signaling. *Immunity* 2012. **36**: 166–174.

37 **Abt, M. C., Osborne, L. C., Monticelli, L. A., Doering, T. A., Alenghat, T., Sonnenberg, G. F., Paley, M. A.** et al., Commensal bacteria calibrate the activation threshold of innate antiviral immunity. *Immunity* 2012. **37**: 158–170.

38 **Mueller, S. N., Hosiawa-Meagher, K. A., Konieczny, B. T., Sullivan, B. M., Bachmann, M. F., Locksley, R. M., Ahmed, R.** et al., Regulation of homeostatic chemokine expression and cell trafficking during immune responses. *Science* 2007. **317**: 670–674.

39 **Obar, J. J., Jellison, E. R., Sheridan, B. S., Blair, D. A., Pham, Q. M., Zickovich, J. M.** and **Lefrançois, L.**, Pathogen-induced inflammatory environment controls effector and memory CD8+ T cell differentiation. *J. Immunol.* 2011. **187**: 4967–4978.

40 **Grayson, J. M., Zajac, A. J., Altman, J. D.** and **Ahmed, R.**, Cutting edge: increased expression of Bcl-2 in antigen-specific memory CD8+ T cells. *J. Immunol.* 2000. **164**: 3950–3954.

41 **Herndler-Brandstetter, D., Ishigame, H., Shinnakasu, R., Plajer, V., Stecher, C., Zhao, J., Lietzenmayer, M.** et al., KLRG1+ Effector CD8+ T Cells Lose KLRG1, Differentiate into All Memory T Cell Lineages, and Convey Enhanced Protective Immunity. *Immunity* 2018. **48**: 716–729.e8.

42 **Marzo, A. L.**, **Klonowski, K. D.**, **Le Bon, A.**, **Borrow, P.**, **Tough, D. F.** and **Lefrançois, L.**, Initial T cell frequency dictates memory CD8+ T cell lineage commitment. *Nat. Immunol.* 2005. **6**: 793–799.

43 **Badovinac, V. P.**, **Haring, J. S.** and **Harty, J. T.**, Initial T cell receptor transgenic cell precursor frequency dictates critical aspects of the CD8(+) T cell response to infection. *Immunity* 2007. **26**: 827–841.

44 **Jameson, S. C.** and **Masopust, D.**, Diversity in T cell memory: an embarrassment of riches. *Immunity* 2009. **31**: 859–871.

45 **Stirnweiss, A.**, **Ksienzyk, A.**, **Klages, K.**, **Rand, U.**, **Grashoff, M.**, **Hauser, H.** and **Kröger, A.**, IFN regulatory factor-1 bypasses IFN-mediated antiviral effects through viperin gene induction. *J. Immunol.* 2010. **184**: 5179–5185.

46 **Thompson, L. J.**, **Kolumam, G. A.**, **Thomas, S.** and **Murali-Krishna, K.**, Innate inflammatory signals induced by various pathogens differentially dictate the IFN-I dependence of CD8 T cells for clonal expansion and memory formation. *J. Immunol.* 2006. **177**: 1746–1754.

47 **Lienenklaus, S.**, **Cornitescu, M.**, **Zietara, N.**, **Łyszkiewicz, M.**, **Gekara, N.**, **Jabłónska, J.**, **Edenhofer, F.** et al., Novel reporter mouse reveals constitutive and inflammatory expression of IFN-beta in vivo. *J. Immunol.* 2009. **183**: 3229–3236.

48 **Greenbaum, A.**, **Hsu, Y.-M. S.**, **Day, R. B.**, **Schuettpelz, L. G.**, **Christopher, M. J.**, **Borgerding, J. N.**, **Nagasawa, T.** et al., CXCL12 in early mesenchymal progenitors is required for haematopoietic stem-cell maintenance. *Nature* 2013. **495**: 227–230.

49 **Feuerer, M.**, **Beckhove, P.**, **Garbi, N.**, **Mahnke, Y.**, **Limmer, A.**, **Hommel, M.**, **Hämmerling, G. J.** et al., Bone marrow as a priming site for T-cell responses to blood-borne antigen. *Nat. Med.* 2003. **9**: 1151–1157.

50 **Alp, Ö. S.**, **Durlanik, S.**, **Schulz, D.**, **McGrath, M.**, **Grün, J. R.**, **Bardua, M.**, **Ikuta, K.** et al., Memory CD8(+) T cells colocalize with IL-7(+) stromal cells in bone marrow and rest in terms of proliferation and transcription. *Eur. J. Immunol.* 2015. **45**: 975–987.

51 **Chang, H. D.**, **Tokoyoda, K.** and **Radbruch, A.**, Immunological memories of the bone marrow. *Immunol. Rev.* 2018. **283**: 86–98.

52 **Stoycheva, D.**, **Deiser, K.**, **Stärck, L.**, **Nishanth, G.**, **Schlüter, D.**, **Uckert, W.** and **Schüler, T.**, IFN-γ regulates CD8+ memory T cell differentiation and survival in response to weak, but not strong, TCR signals. *J. Immunol.* 2015. **194**: 553–559.

53 **Spanier, J.**, **Lienenklaus, S.**, **Paijo, J.**, **Kessler, A.**, **Borst, K.**, **Heindorf, S.**, **Baker, D. P.** et al., Concomitant TLR/RLH signaling of radioresistant and radiosensitive cells is essential for protection against vesicular stomatitis virus infection. *J. Immunol.* 2014. **193**: 3045–3054.

54 **Cossarizza, A.**, **Chang, H. D.**, **Radbruch, A.**, **Abrignani, S.**, **Addo, R.**, **Akdis, M.**, **Andrä, I.** et al., Guidelines for the use of flow cytometry and cell sorting in immunological studies (third edition). *Eur. J. Immunol.* 2021. **51**: 2708–3145.

Abbreviations: **dpi**: day post infection · **dpv**: day post vaccination · **FRC**: fibroblastic reticular cell · **IFNAR**: IFN-I receptor · **LSC**: lymphoid stromal cell · **NP**: nucleoprotein · **SLO**: secondary lymphoid organ · $\mathbf{T_{CM}}$: central memory T cell · $\mathbf{T_{EFF}}$: effector T cell · $\mathbf{T_{EM}}$: effector memory T cell · $\mathbf{T_M}$: memory T cell · **VSV**: vesicular stomatitis virus

Full correspondence:: Thomas Schüler, Institute of Molecular and Clinical Immunology, Medical Faculty, Otto-von-Guericke University, Leipziger Strasse 44, 39120 Magdeburg, Germany
e-mail: thomas.schueler@med.ovgu.de

Received: 8/12/2021
Revised: 27/2/2022
Accepted: 31/3/2022
Accepted article online: 1/4/2022

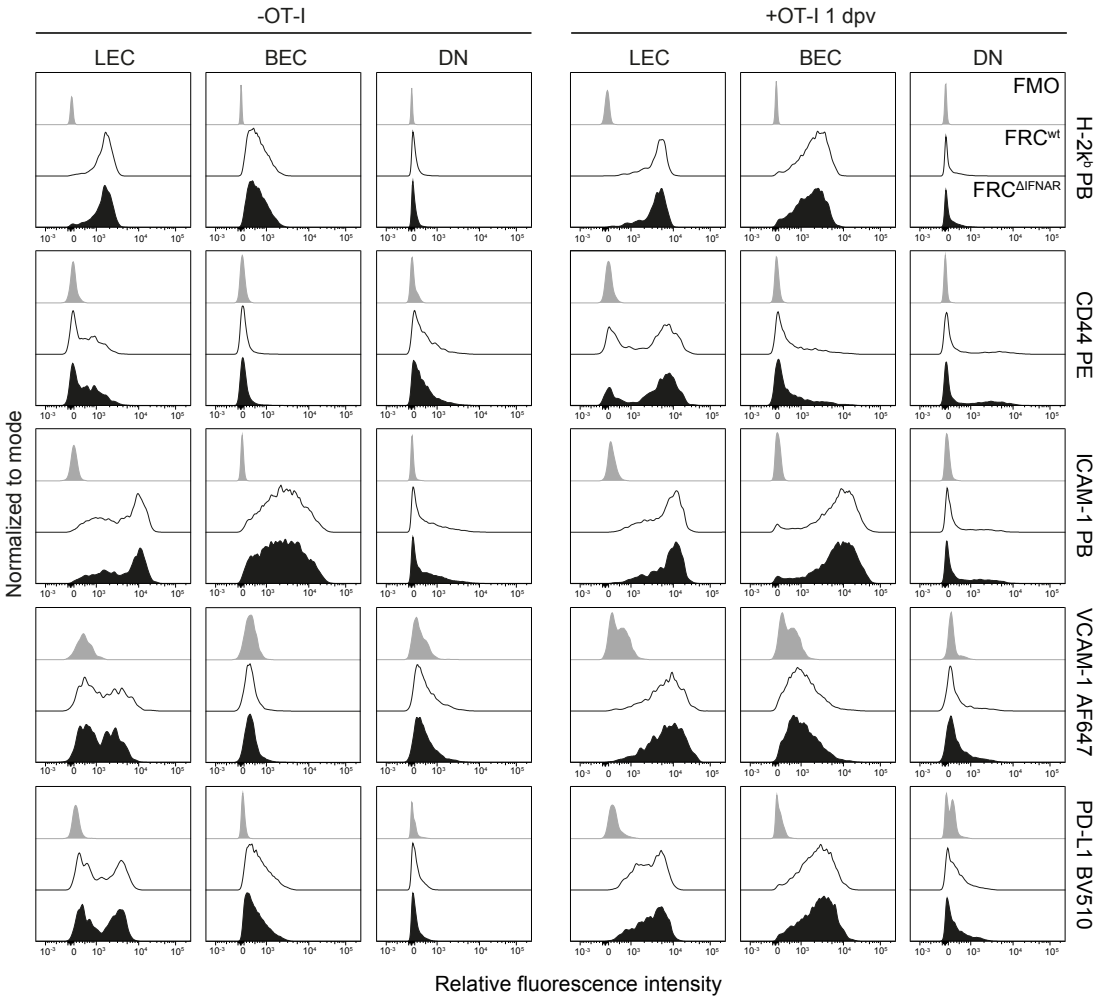

Supplementary Figure 1. MHC-I, CD44, ICAM-1, VCAM-1 and PD-L1 expression remain unaltered in non-FRC LN stromal subsets in FRC$^{\Delta IFNAR}$ mice. (A) Relative fluorescence intensities for H-2k^b, CD44, ICAM-1, VCAM-1 and PD-L1 were analyzed by flow cytometry on viable TER-119$^-$CD45$^-$ gp38$^+$CD31$^+$ LECs, gp38$^-$CD31$^+$ BECs and gp38$^-$CD31$^-$ DNs isolated from LNs of FRC$^{\Delta IFNAR}$ and FRC^{wt} mice under steady state conditions or after 1 day post vaccination and OT-I transfer (as described in Fig. 1). Grey curves indicate fluorescence minus one (FMO) controls lacking the H-2k^b, CD44, ICAM-1, VCAM-1 or PD-L1 antibody, respectively. Histograms are representative for two independent experiments each with pooled LNs from 3 mice per group.

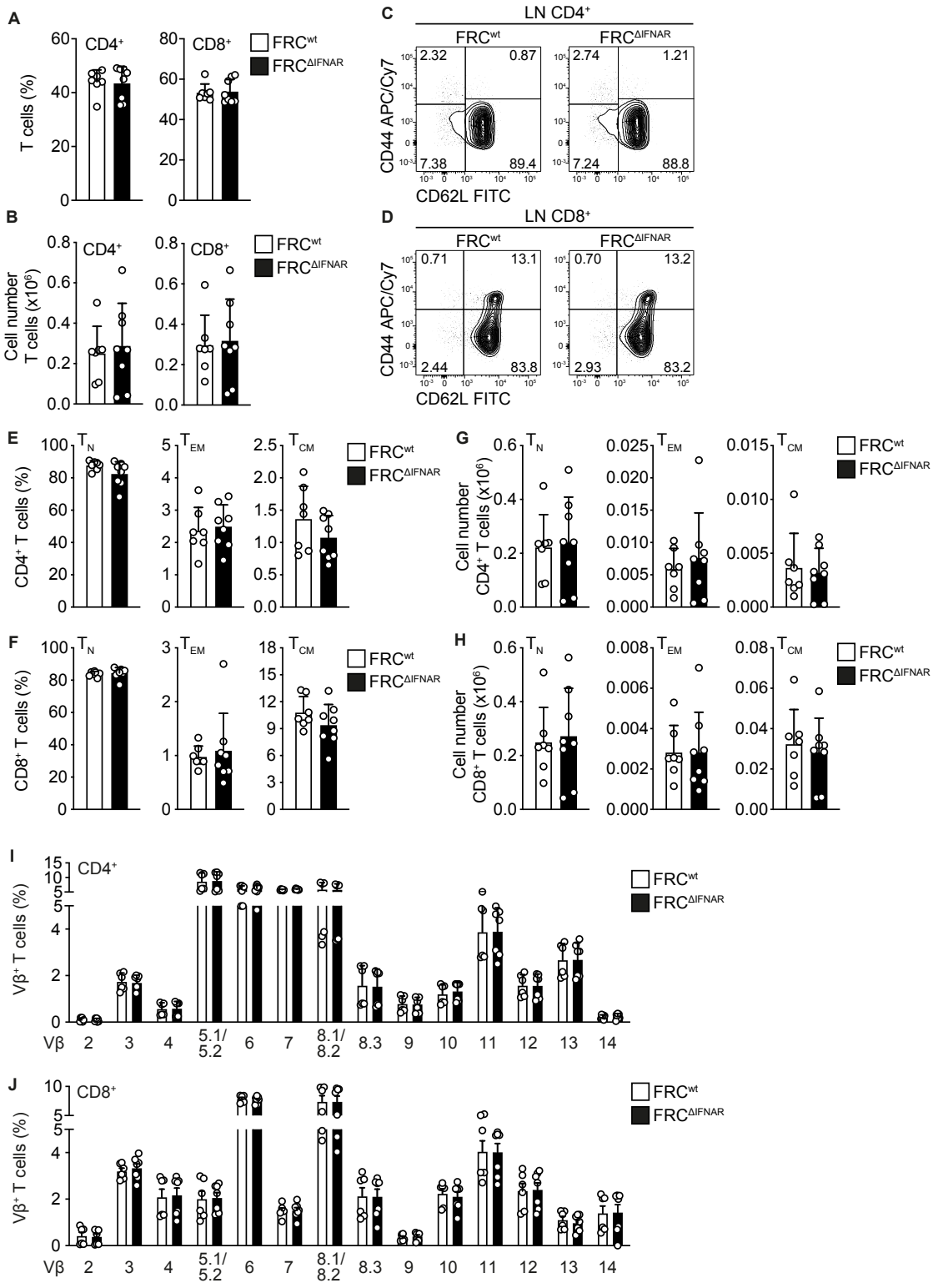

Supplementary Figure 2. Steady state T cell homeostasis is largely unaffected by IFNAR signaling in FRCs. (A) Frequencies and **(B)** absolute numbers of $CD3^+CD4^+$ and $CD3^+CD8^+$ T cells were determined in LNs of untreated $FRC^{\Delta IFNAR}$ and FRC^{wt} mice by flow cytometry. **(E, F)** Frequencies or **(G, H)** cell numbers of naïve (T_N; $CD44^{lo}CD62L^{hi}$), effector memory (T_{EM}; $CD44^{hi}CD62L^{lo}$) and central memory (T_{CM}; $CD44^{hi}CD62L^{hi}$) T cells were determined after gating on **(C, E, G)** $CD3^+CD4^+$ and **(D, F, H)** $CD3^+CD8^+$ cells. **(C, D)** Shown are representative contour plots for CD44/CD62L expression after gating on **(C)** $CD3^+CD4^+$ and **(D)** $CD3^+CD8^+$ isolated from LNs and numbers indicate percentages. **(I, J)** Composition of the Vβ TCR repertoire was determined by flow cytometry after gating on **(I)** $CD3^+CD4^+$ and **(J)** $CD3^+CD8^+$ T cells in LNs. **(A, B, E-J)** Bar diagrams show mean + SD from 6-8 mice analyzed in two independent experiments. Statistical analyses were performed using a Mann-Whitney U test.

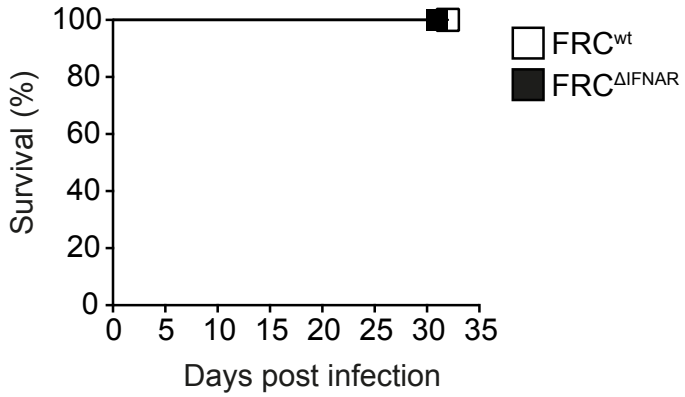

Supplementary Figure 3. Survival of FRC$^{\Delta IFNAR}$ and FRC^{wt} mice during VSV-infection. FRC$^{\Delta IFNAR}$ and FRC^{wt} mice were infected as described in Fig. 3. Survival was monitored on a daily basis. Data are representative for 6-9 mice per group analyzed in 1-2 independent experiments.

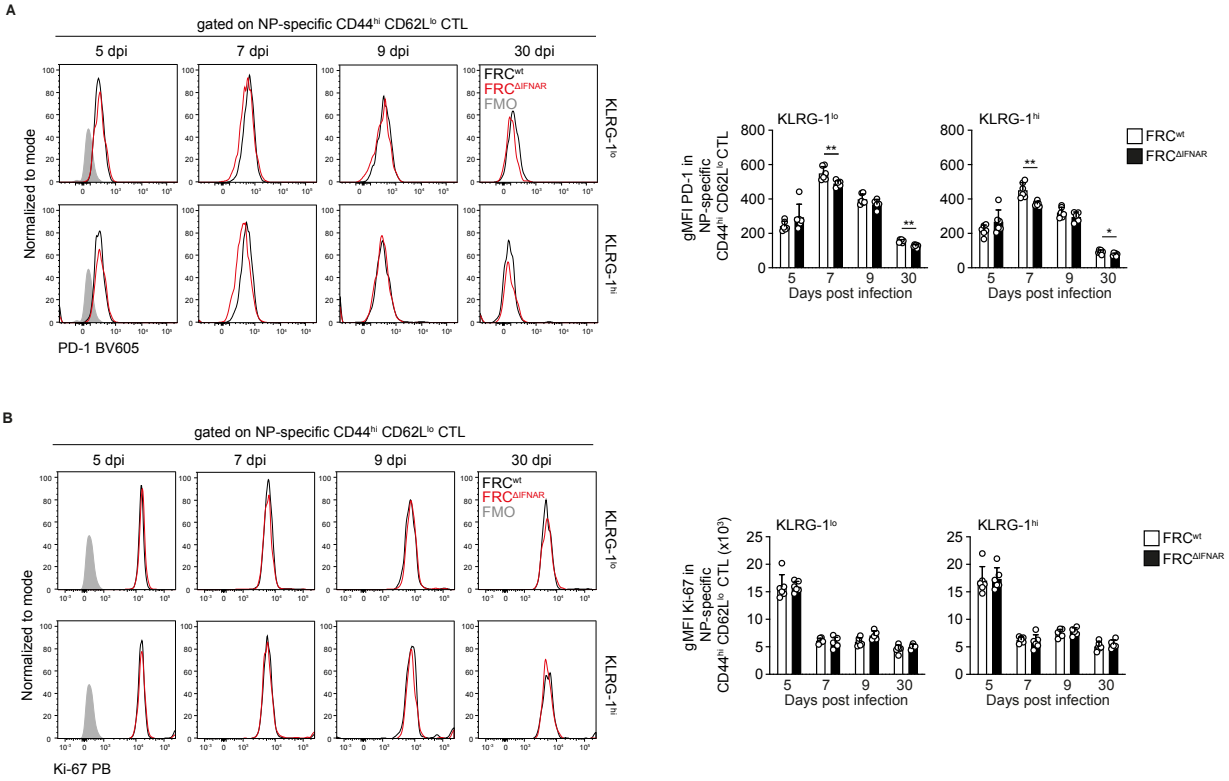

Supplementary Figure 4. IFNAR signaling in FRCs regulates PD-1 expression in NP-specific CTLs. (A, B) $FRC^{\Delta IFNAR}$ and FRC^{wt} mice were infected as described in Fig. 3. The expression of **(A)** PD-1 and **(B)** Ki-67 was analyzed by flow cytometry after gating on KLRG-1^{hi} or KLRG-1^{lo} $CD44^{hi}CD62L^{lo}$ NP-specific CTLs in the blood. Shown are representative histograms (fluorescence minus one controls in gray) and data for gMFIs are summarized in bar diagrams (mean + SD). Data are representative for 5-6 mice per group analyzed in one experiment. Statistical comparisons were made via Mann-Whitney U test and statistically significant values are indicated (*$p \leq 0.05$; **$p \leq 0.01$).

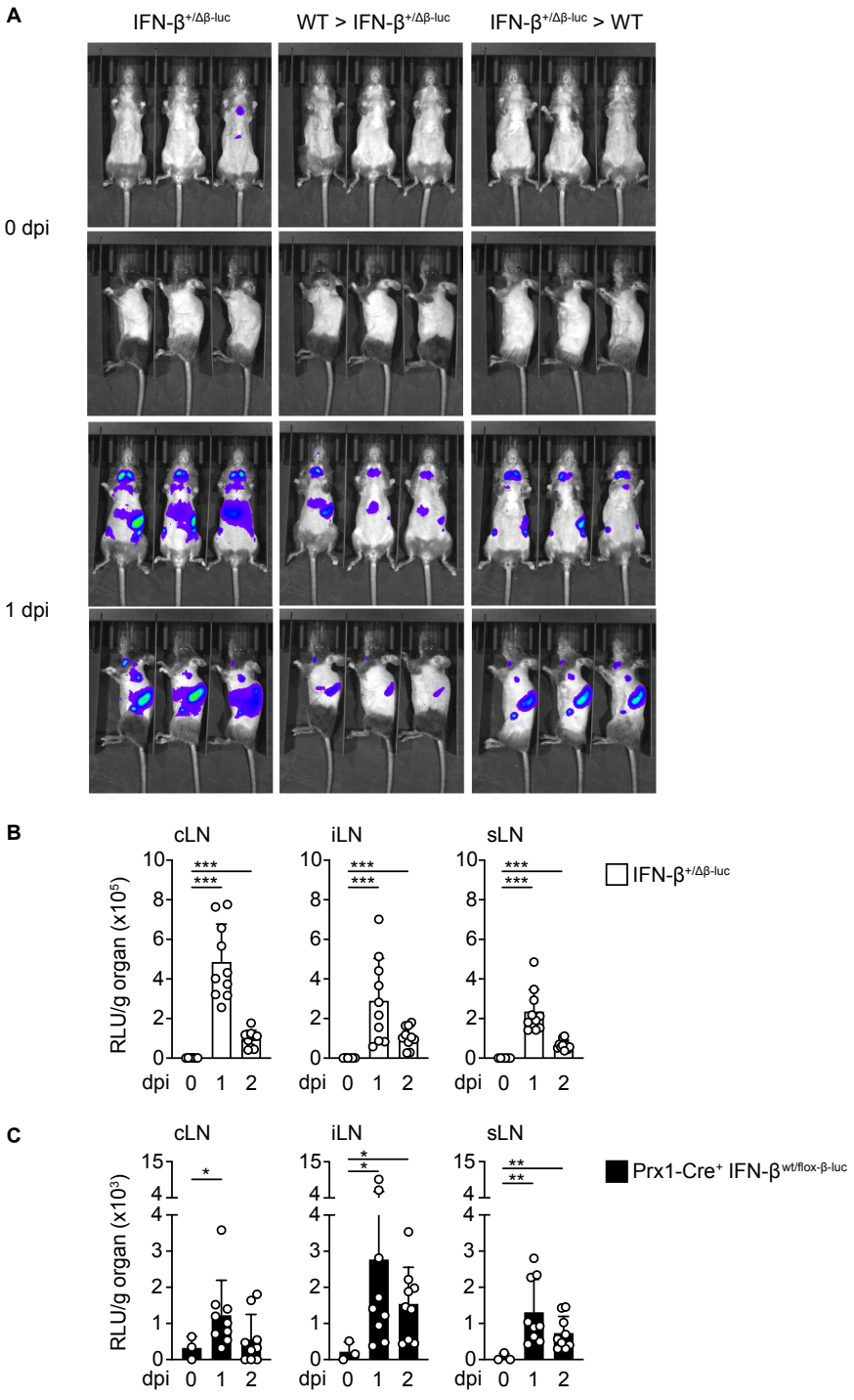

Supplementary Figure 5. FRCs mount IFN-β responses after VSV infection. (A) WT and IFN-β$^{+/\Delta\beta\text{-luc}}$ mice were lethally irradiated with 9 Gray and 24 h later the mice were reconstituted by i.v. injection with IFN-β$^{+/\Delta\beta\text{-luc}}$ or WT bone marrow. Eight weeks after reconstitution mice were infected i.v. with 2×10⁶ pfu VSV. One day prior to and 1 day post infection (dpi), luciferin was injected i.v. and luciferase activity was monitored by *in vivo* imaging. Shown are 3 mice/group from one representative experiment out of three (in total 12 mice). **(B)** IFN-β$^{+/\Delta\beta\text{-luc}}$ and **(C)** Prx1-Cre^{+}IFN-β$^{wt/flox\text{-}\beta\text{-luc}}$ reporter mice were infected i.v. with 2×10⁶ pfu VSV. At the indicated time points after infection cervical LNs (cLN), submandibular LNs (sLN) and inguinal LNs (iLN) were removed, organ homogenates were prepared, luciferin was added and the luminescence was quantified (RLU = relative light unit). Data are from three independently performed experiments and indicate mean + SD from 3-9 analyzed mice. **(B, C)** Statistical comparisons were made via one-tailed Mann-Whitney U test (*p ≤ 0.05; **p ≤ 0.01; ***p ≤ 0.001).

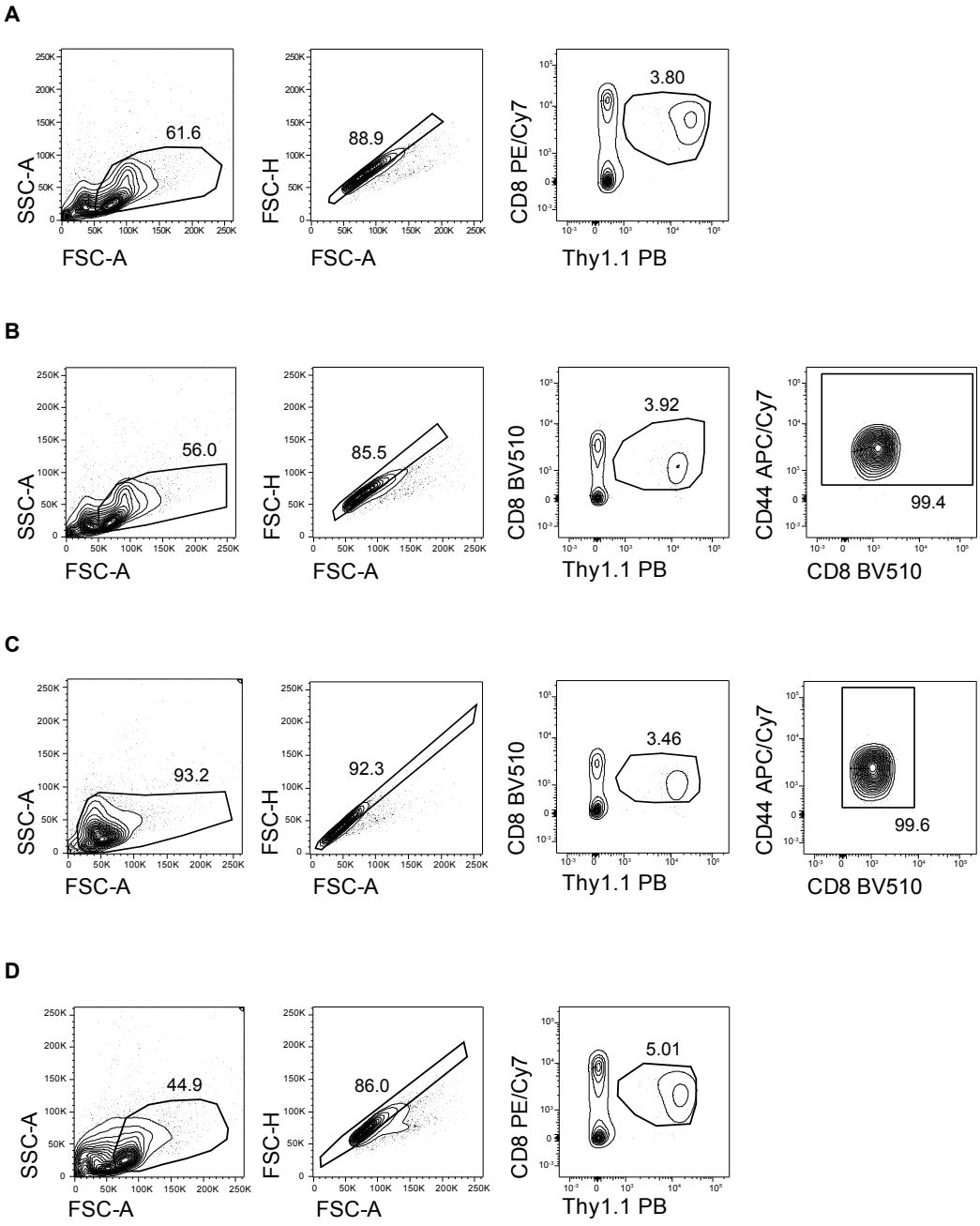

Supplementary Figure 6. Representative gating strategies for flow cytometric analyses of OT-I T cells. (A-D) Shown are representative gating strategies for **(A)** Figure 1A-D, **(B)** Figure 1E, **(C)** Figure 1F, G and **(D)** Figure 1H. Numbers indicate percentages.

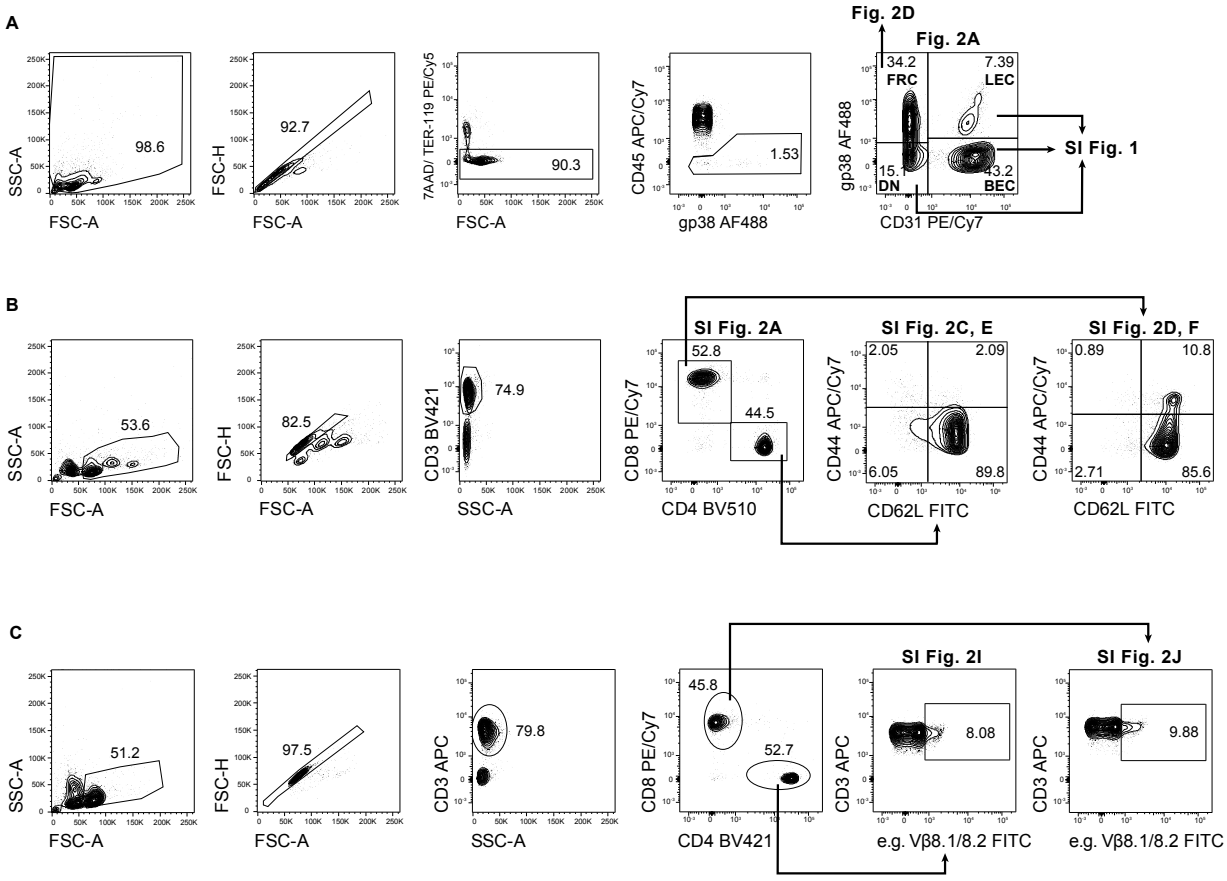

Supplementary Figure 7. Representative gating strategies for flow cytometric analyses of LSCs and T cells in untreated FRC$^{\Delta IFNAR}$ and FRC^{wt} mice. (A-D) Shown are representative gating strategies for **(A)** Figure 2A, D and SI Figure 1, **(B)** SI Figure 2A-H and **(C)** SI Figure 2I, J. Numbers indicate percentages.

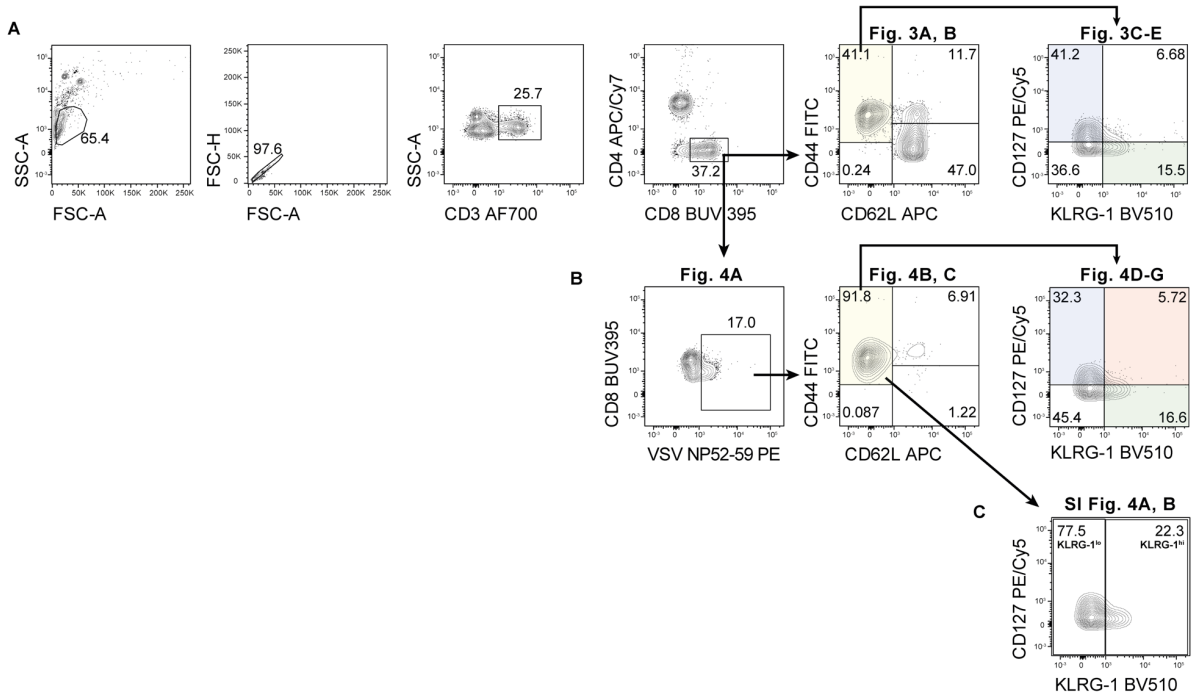

Supplementary Figure 8. Representative gating strategies for flow cytometric analyses of CTLs in VSV-infected FRC$^{\Delta IFNAR}$ and FRC^{wt} mice. (A-C) Shown are representative gating strategies for **(A)** Figure 3A-E, **(B)** Figure 4A-G and **(C)** SI Figure 3A, B. Numbers indicate percentages.

6 Discussion

To improve therapeutic approaches aiming at the induction of long-lasting T_M responses, a better understanding of the factors regulating $T_{(V)M}$ differentiation is required[1,192]. T cells receive a multitude of signals from their microenvironment, which control T cell homeostasis, activation and differentiation[7,62,193]. For example, IFN-I and IFN-γ regulate T cell responses in a direct manner. In particular, IFN-I acts as a third signal during T cell activation[65] and IFN-γR signaling in $CD4^+$ and $CD8^+$ T cells promotes T_{EFF} expansion and memory differentiation during LCMV infection[95–97]. Likewise, under lymphopenic conditions, IFN-γR signaling in $CD8^+$ T cells modulates T_{VM} differentiation[100]. So far, research has focused on T cell-intrinsic factors regulating $T_{(V)M}$ formation[7,193]. However, T cells are part of a multicellular environment, including other immune cells and stromal cells. For example, LSCs in the LNs release the T cell survival factor IL-7[10]. The LN-LSC compartment comprises different cell types contributing to the three-dimensional organ structure and closely interacting with many immune cells[60]. Similar to immune cells, IL-7-producing LSCs respond to inflammatory mediators such as IFN-I and IFN-γ[12], enabling them to interpret the inflammatory context. Whether and how this affects $T_{(V)M}$ fate decision was studied in the three papers presented in this thesis.

Trophic factors such as IL-7[170–172] and self-peptide-MHC-complexes[173–175] are crucial for T cell survival. However, only limited amounts of both factors are available in the body. Since T cells continuously utilize both factors, the peripheral T cell pool reaches its final size once the production and consumption of both factors reach an equilibrium[166]. Consequently, the availability of both factors correlates inversely with the size of the peripheral T cell pool. As a result, IL-7 and self-peptide-MHC complexes become more available in lymphopenic hosts[4,5,176]. This is sufficient to activate adoptively transferred T_N, which undergo LIP and differentiate into IFN-γ-producing T_{VM}[5,167]. Of note, not all T cell clones are equally sensitive to lymphopenia[184]. When the experiments for Knop et al. 2019[15] were designed, it was assumed that T cell-intrinsic factors determine lymphopenia sensitivity. However, the contribution of the microenvironment to the regulation of LIP was largely unclear. To study this, we utilized $CD4^+$ OT-II T cells, which hardly undergo LIP[184]. The major aim of this study was to define whether OT-II T cell-derived IFN-γ induces IFN-γR signaling in non-T cells, thus contributing to the suppression of OT-II LIP.

In Knop et al. 2019, we describe that OT-II T cells undergo LIP in IFN-γR-deficient lymphopenic mice, which is accompanied by DC expansion and IL-6 accumulation in the presence of an intact microflora[15]. We suggest that OT-II LIP in IFN-γR-deficient lymphopenic mice is driven by the OT-II-dependent activation of immature DCs[194], which up-regulate IL-6 in response to commensals[195] finally promoting the IL-6-associated $CD4^+$ T cell response[195–197].

However, we could not exclude that other IL-6-producing cell types contribute to the enhanced IL-6 levels. LIP is induced in SLOs[190] and FRCs are present in the T cell zone[60]. Interestingly, activated T cells induce IL-6 production in FRCs[198]. In turn, FRC-released IL-6 leads to epigenetic remodeling in activated T cells, induces the expression of pro-survival factors and affects T_M formation[198]. Whether FRCs release IL-6 during LIP of OT-II T cells and whether FRC-derived IL-6 regulates OT-II T_{VM} formation remain essential questions for the future.

OT-II T cells undergoing LIP in $Rag^{\gamma Rko}$ mice showed an up-regulation of CD127 (IL-7Rα), which suggests that IL-7 contributes to the survival of OT-II and their accumulation. We detected proliferating OT-II T cells in the LNs of $Rag^{\gamma Rko}$ mice, where FRCs and LECs produce IL-7[10,16]. Hence, FRC/LEC-released IL-7 might support LIP of OT-II T cells. However, various stromal cells in different organs produce IL-7[14,108–110,129]. In the intestine, lymphocytes produce IFN-γ in response to the microbiota, which leads to IFN-γ-induced up-regulation of IL-7 in intestinal epithelial cells[14]. We observed that the microbiota was essential for OT-II LIP. Hence, microbiota-induced IL-7 secretion in the intestine might be essential for OT-II LIP. Which IL-7-producing stromal cells/organs support LIP of OT-II T cells in $Rag^{\gamma Rko}$ mice remains to be determined.

In summary, in Knop et al., 2019, we provide evidence that the inability of OT-II cells to undergo LIP results from a complex interplay between IL-7-secreting stromal cells, the commensal microflora, OT-II-derived IFN-γ and IFN-γR signaling in DCs[15]. Hence, the degree of LIP is not only determined by the intrinsic properties of a particular $CD4^+$ T cell clone but also by its microenvironment.

Stromal cells are a part of the multicellular T cell microenvironment and secrete IL-7[14,108–110,129], which is crucial for T_N survival *in vivo*[127,191]. Importantly, T_N survival *in vivo* also requires LN accessibility[189,190]. Since IL-7 derived from LN-FRCs supports T_N survival *in vitro*[10], it was postulated that LN-FRCs-released IL-7 is also critical for maintaining T_N homeostasis *in vivo*. Although this model had dominated the literature for many years, *in vivo* proof was still missing. Therefore, in **Knop et al., 2020**, we used cell type-specific IL-7 knockout mice to elucidate the relative importance of LN-FRC-derived IL-7 for the maintenance of T_N homeostasis *in vivo*[16].

As opposed to the literature[10], we observed that FRC-released IL-7 was not critical for the survival of LN T_N *in vivo*. Likewise, LN-LEC-derived IL-7 was dispensable for T_N maintenance. In contrast, LN-FRC-secreted IL-7 was crucial for the survival of T_{CM}. In healthy mice, the memory T cell pool is generated via two processes: (1) activation of T_N in response to foreign Ag (T_M formation) and (2) LIP of T_N in neonatal mice (T_{VM} formation)[1,185,186]. All mice used in Knop et al., 2020 were maintained under specific pathogen-free (SPF) conditions. In SPF mice, $CD49d^-$ T_{VM} represent the vast majority (~90%) of the memory T cell pool, while ~10% are $CD49d^+$ foreign-Ag-induced T_M[199]. Hence, FRC-derived IL-7 may be essential for the

generation and/or maintenance of foreign-Ag-independent T_{VM}. Additionally, we showed that the formation of foreign-Ag-induced $CD8^+$ OT-I T_{CM} also relies on LN-FRC-secreted IL-7, which is known to improve cell metabolism[107,160,200]. For example, IL-7R signaling induces STAT5 phosphorylation and subsequent up-regulation of GLUT1, which enhances glucose up-take[200]. In T_M, IL-7R signaling fuels fatty acid oxidation for ATP production, thereby enhancing T_M longelivity[107]. Whether IL-7 induces similar metabolic changes in Ag-experienced and -unexperienced T_M remains unclear.

$IL\text{-}7R^+$ T_N and T_M continuously consume IL-7, thereby removing it from the system and limiting its availability. The prolonged absence of IL-7R signals leads to T cell death[201], suggesting that the competition for IL-7 serves as a major mechanism regulating T homeostasis[166,201,202]. In LNs of $FRC^{\Delta IL\text{-}7}$ mice, *Il7* mRNA levels were reduced by ~83%. The residual IL-7 levels in LNs of $FRC^{\Delta IL\text{-}7}$ mice might be sufficient to maintain T_N but not T_{CM}. This indicates that T_N and T_M utilize IL-7 differently. Indeed, T_N showed a superior utilization of IL-7, demonstrated by higher phosphorylation of STAT5 upon IL-7 stimulation *in vitro*.

Overall, we describe in Knop et al., 2020 that LN-FRC-derived IL-7 is crucial for the survival of T_{CM} but dispensable for the maintenance of T_N[16]. We suggest that T_N and T_{CM} colonize different ecological niches *in vivo* to circumvent competition for the FRC-derived survival factor IL-7. Hence, IL-7 produced by LN-FRCs represents a T cell-extrinsic factor mediating the survival of T_{CM}.

The expression of IL-7 in stromal cells is up-regulated by IFN-I[13]. This suggested that the IL-7-dependent maintenance of T_M is supported by IFNAR signaling in $IL\text{-}7^+$ in stromal cells. Furthermore, T_M fate decision is programmed early during immune responses, and FRCs expressing the IFNAR[12,203] are part of the T cell microenvironment in the LN. Therefore, we asked in **Knop et al., 2022** whether IFNAR signaling in FRCs affects T_M differentiation[17].

In activated LNs, the chemokines CXCL9/CXCL10 guide $CXCR3^+$ T_{EFF} to specialized niches modulating T_M fate decision. In particular, CXCR3 is expressed by T_{SLEC} that reside in the LN periphery[204]. T_{MP} likewise express CXCR3, but are preferentially located in the inner region of the LN due to higher expression of CCR7[204] that binds CCL19 produced by FRCs in the inner paracortex[12]. Importantly, the retention of T cells in the T cell zone preferentially induces the differentiation of T_{MP}[204]. We observed that the up-regulation of CXCL9/CXCL10 24 h after OT-I transfer and vaccination was impaired in LNs of $FRC^{\Delta IFNAR}$ mice. Therefore, IFN-I-induced CXCL9/CXCL10 up-regulation in FRCs might modulate spatial positioning of OT-I, impacting on early OT-I activation and subsequent T_M fate decision.

IFN-I is a pro-inflammatory cytokine that is released upon infection[24,25]. However, it is becoming increasingly clear that the constitutive production of IFN-I in the steady state leads to tonic IFNAR signaling, thereby elevating the activation state of immune responses.

For example, microbiota-induced tonic IFNAR signaling in lung epithelial cells enhances their resistance to subsequent influenza A infection[205]. In healthy $FRC^{\Delta IFNAR}$ mice, we did not detect changes in (1) FRC frequencies, (2) chemokine/IL-7 mRNA levels in the LNs, (3) expression of H-$2k^b$ (MHC-I), CD44, intercellular adhesion molecule 1 (ICAM-1), VCAM-1 and PD-L1 on LSCs, (4) T cell homeostasis and (5) the TCR repertoire. This suggests that these parameters are regulated independently of tonic IFNAR signaling in FRCs. However, we cannot exclude that tonic IFNAR signaling in FRCs alters so far unidentified factors that impinge on T_M fate decision. For example, constitutive levels of IFN-I support the association of a complex formed by IFNAR1 and IFN-γR2 in mouse embryonic fibroblasts[206]. This complex is required for the IFN-γ-induced activation of STAT1[206]. Hence, IFNAR signaling in FRCs could maintain their IFN-γ-responsiveness, thereby facilitating the IFN-γ-induced suppression of T cell responses, such as the induction of iNOS expression and NO release[146,147].

We also analyzed whether IFNAR signaling in FRCs modulated polyclonal T_M differentiation. In vesicular stomatitis virus (VSV)-infected $FRC^{\Delta IFNAR}$ mice, polyclonal $CD8^+$ $CD44^{hi}CD62L^{lo}$ T_{EM} accumulated 30 dpi. Additionally, we observed that in the nucleoprotein (NP)-specific $CD8^+$ $CD44^{hi}CD62L^{lo}$ T_{EM} population, the $CD127^{hi}KLRG\text{-}1^{lo}$ subset was decreased in $FRC^{\Delta IFNAR}$ mice, whereas the $CD127^{lo}KLRG\text{-}1^{hi}$ population was strongly increased. Interestingly, NP-specific $CD8^+$ $CD127^{hi}KLRG\text{-}1^{hi}$ T_{EM} appeared specifically in $FRC^{\Delta IFNAR}$ mice. This suggests that the phenotype of NP-specific $CD8^+$ T_{EM} is regulated by IFNAR signaling in FRCs. Although $KLRG\text{-}1^{lo}$ are well known to differentiate into T_M[73], $KLRG\text{-}1^{hi}$ cells give rise to protective T_M populations as well[207]. Whether $KLRG\text{-}1^{lo}$ or $KLRG\text{-}1^{hi}$ T_M are protective during secondary challenges in $FRC^{\Delta IFNAR}$ mice needs to be addressed.

A recent publication demonstrated that IFN-I-induced expression of PD-L1 on FRCs prevents the exhaustive activation of T_{EFF} during LCMV infection[203]. However, whether IFNAR signaling in FRCs modulates T_M differentiation remained an open question. We showed in Knop et al., 2022, that IFN-I-responsive FRCs modulate foreign-Ag-dependent $CD8^+$ T_M differentiation in a context-dependent fashion[17]. This suggests that FRCs interpret the inflammatory environment to adapt $CD8^+$ T_M differentiation to the kind of infecting pathogen.

As summarized in Figure 6.1, the three publications presented in this thesis highlight the importance of stromal cells in the regulation of T cell responses.

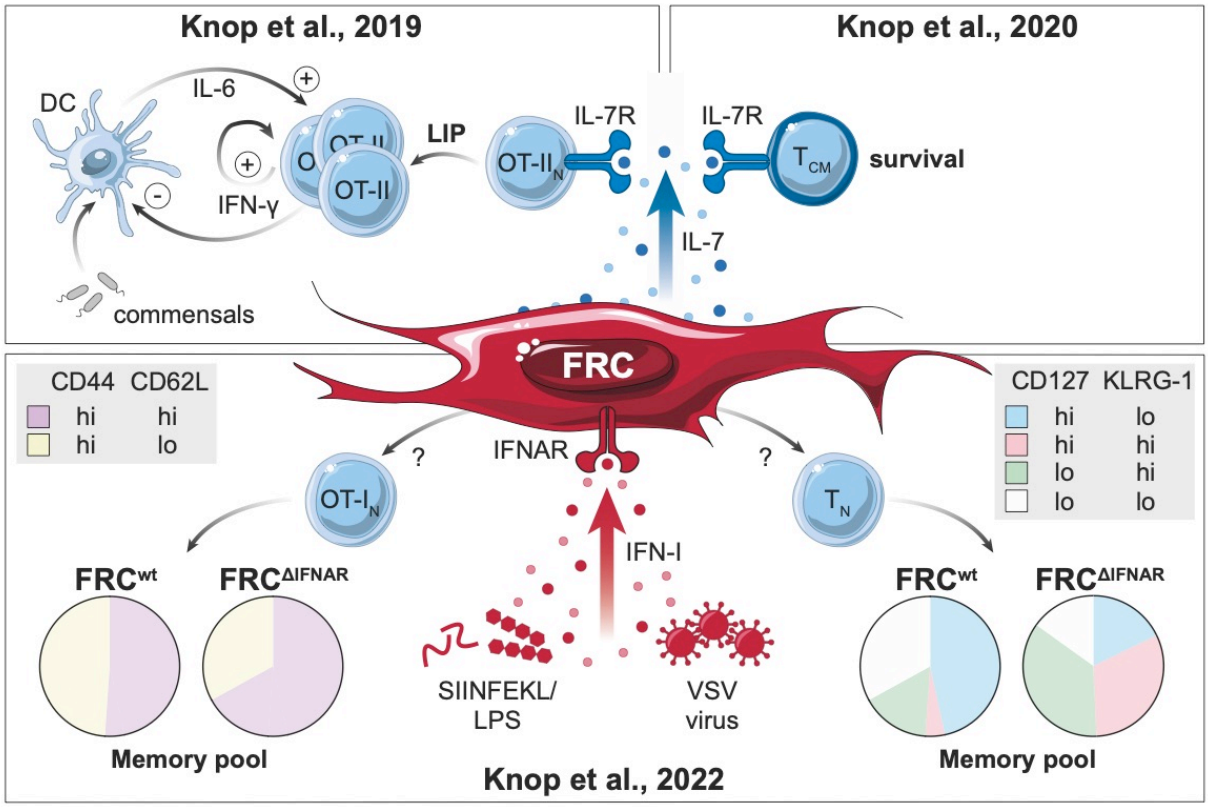

Figure 6-1. Graphical representation and interrelation of the three research articles presented in this thesis. FRCs express the IFNAR and regulate IL-7-dependent T cell responses. In **Knop et al., 2019** we studied CD4$^+$ OT-II T cells, which hardly undergo LIP under normal circumstances[15]. However, if lymphopenic mice are devoid of the IFN-γR, CD4$^+$ OT-II T cells expand massively due to autocrine IFN-γ action and DC-dependent overabundance of growth-promoting IL-6. Importantly, this type of OT-II LIP relies on an intact commensal microflora. In **Knop et al., 2020**, we confirm FRCs as a vital source of IL-7 in the LN[16], which had been proposed to be essential for the survival of T_N and T_M *in vivo*[10]. However, in FRC-specific IL-7 knockout mice, numbers of CD8$^+$ T_N were normal, but those of CD8$^+$ T_{CM} were reduced. Hence, we provide evidence for a selective contribution of FRC-derived IL-7 to CD8$^+$ T_{CM} survival. In **Knop et al., 2022**, we show that IFNAR signaling in FRCs modulates CD8$^+$ T_M fate decision in a context-dependent fashion[17]. After reconstitution with naive CD8$^+$ TCR-transgenic OT-I T cells (OT-I$_N$) and vaccination with their cognate peptide SIINFEKL in combination with lipopolysaccharide (LPS), we observed altered T_M differentiation in FRC$^{\Delta IFNAR}$ mice (bottom left). However, the phenotype of OT-I T_M cells differed from VSV-specific CD8$^+$ T_M cells, which were generated from the naive polyclonal CD8$^+$ T cell pool of FRC$^{\Delta IFNAR}$ mice (bottom right). This figure was created using illustrations from www.bioicons.com[21].

6.1 Implications

Our understanding of the factors that drive T_M differentiation is of major interest for therapeutic treatments, such as adoptive T cell therapies (ATTs) and vaccinations.

During ATTs, patient-derived, tumor-specific T cells are expanded *ex vivo* and are reinfused[208]. Lymphodepletion is a standard pre-treatment to increase the efficacy of ATTs and self-Ags often represent the targets of tumor-reactive T cells[209]. Consequently, *ex vivo* expanded tumor-reactive T cells undergo LIP in lymphopenic patients. Knop et al., 2019 underlines the role of T cell-extrinsic, host-derived factors during LIP and T_{VM} formation[15]. Hence, the modulation of IFN-γ-associated T cell responses by host cells should be considered in ATT approaches.

T_M present in the host synergize with transferred tumor-specific T cells during ATTs[210]. In particular, pre-existing T_M prevent the development of Ag-loss tumor variants after ATT and support long-term survival[211]. In Knop et al., 2020, we describe that the survival of T_{CM} depends on LN-FRC-derived IL-7[16]. It remains to be shown in the future whether T_{CM} responding to LN-FRC-released IL-7 contribute to the success of ATTs.

Upon vaccination, pro-inflammatory cytokines, such as IFN-I, are released, Ag is transported into the draining LNs and T cell responses are initiated. Suboptimal IFNAR signaling in particular cell types may affect the entire network of IFNAR-dependent cellular interactions controlling $CD8^+$ T_M differentiation and/or maintenance. For example, IFNAR signaling in LN-FRCs promotes effective primary anti-viral $CD8^+$ T cell responses[203]. Furthermore, pulmonary fibroblasts promote the accumulation of vaccination-induced $CD8^+$ T_M in the lung[212]. Hence, the targeted manipulation of IFNAR signaling in FRCs may be a novel therapeutic option to further optimize vaccination strategies aiming at the efficient generation of $CD8^+$ T_M.

7 References

1. Lugli E, Galletti G, Boi SK, Youngblood BA. Stem, Effector, and Hybrid States of Memory CD8+ T Cells. *Trends Immunol*. 2020;41(1):17-28. doi:10.1016/j.it.2019.11.004
2. Martin MD, Badovinac VP. Defining Memory CD8 T Cell. *Front Immunol*. 2018;9(NOV):2692. doi:10.3389/fimmu.2018.02692
3. Barata JT, Durum SK, Seddon B. Flip the coin: IL-7 and IL-7R in health and disease. *Nat Immunol*. 2019;20(12):1584-1593. doi:10.1038/s41590-019-0479-x
4. Guimond M, Veenstra RG, Grindler DJ, et al. Interleukin 7 signaling in dendritic cells regulates the homeostatic proliferation and niche size of CD4+ T cells. *Nat Immunol*. 2009;10(2):149-157. doi:10.1038/ni.1695
5. Sheu TT, Chiang BL. Lymphopenia, Lymphopenia-Induced Proliferation, and Autoimmunity. *Int J Mol Sci*. 2021;22(8). doi:10.3390/ijms22084152
6. Joshi NS, Kaech SM. Effector CD8 T cell development: a balancing act between memory cell potential and terminal differentiation. *J Immunol*. 2008;180(3):1309-1315. doi:10.4049/jimmunol.180.3.1309
7. Chang JT, Wherry EJ, Goldrath AW. Molecular regulation of effector and memory T cell differentiation. *Nat Immunol*. 2014;15(12):1104-1115. doi:10.1038/ni.3031
8. Harlé G, Kowalski C, Garnier L, Hugues S. Lymph Node Stromal Cells: Mapmakers of T Cell Immunity. *Int J Mol Sci*. 2020;21(20):7785. doi:10.3390/ijms21207785
9. Duckworth BC, Qin RZ, Groom JR. Spatial determinates of effector and memory CD8+ T cell fates. *Immunol Rev*. 2022;306(1):76-92. doi:10.1111/imr.13044
10. Link A, Vogt TK, Favre S, et al. Fibroblastic reticular cells in lymph nodes regulate the homeostasis of naive T cells. *Nat Immunol*. 2007;8(11):1255-1265. doi:10.1038/ni1513
11. Bajénoff M, Glaichenhaus N, Germain RN. Fibroblastic Reticular Cells Guide T Lymphocyte Entry into and Migration within the Splenic T Cell Zone. *The Journal of Immunology*. 2008;181(6):3947-3954. doi:10.4049/jimmunol.181.6.3947
12. Malhotra D, Fletcher AL, Astarita J, et al. Transcriptional profiling of stroma from inflamed and resting lymph nodes defines immunological hallmarks. *Nat Immunol*. 2012;13(5):499-510. doi:10.1038/ni.2262
13. Sawa Y, Arima Y, Ogura H, et al. Hepatic interleukin-7 expression regulates T cell responses. *Immunity*. 2009;30(3):447-457. doi:10.1016/j.immuni.2009.01.007
14. Shalapour S, Deiser K, Sercan Ö, et al. Commensal microflora and interferon-γ promote steady-state interleukin-7 production in vivo. *Eur J Immunol*. 2010;40(9):2391-2400. doi:10.1002/eji.201040441
15. Knop L, Frommer C, Stoycheva D, et al. Interferon-γ Receptor Signaling in Dendritic Cells Restrains Spontaneous Proliferation of CD4+ T Cells in Chronic Lymphopenic Mice. *Front Immunol*. 2019;10(FEB):1-10. doi:10.3389/fimmu.2019.00140
16. Knop L, Deiser K, Bank U, et al. IL-7 derived from lymph node fibroblastic reticular cells is dispensable for naive T cell homeostasis but crucial for central memory T cell survival. *Eur J Immunol*. Published online February 11, 2020:eji.201948368. doi:10.1002/eji.201948368
17. Knop L, Spanier J, Larsen P, et al. IFNAR signaling in fibroblastic reticular cells can modulate CD8 $^{+}$ memory fate decision. *Eur J Immunol*. 2022;52(6):895-906. doi:10.1002/eji.202149760
18. Murphy K, Weaver C. *Janeway Immunologie*. 9. Auflage. Springer-Verlag GmbH; 2018. doi:https://doi.org/10.1007/978-3-662-56004-4
19. Paul WE. *Fundamental Immunology*. 6th ed. Lippincott Williams & Wilkins; 2008.
20. Sego TJ, Aponte-Serrano JO, Ferrari Gianlupi J, et al. A modular framework for multiscale, multicellular, spatiotemporal modeling of acute primary viral infection and immune response in epithelial tissues and its application to drug

therapy timing and effectiveness. Peirce SM, ed. *PLoS Comput Biol*. 2020;16(12):e1008451. doi:10.1371/journal.pcbi.1008451

21. Simon Duerr. Bioicons. https://bioicons.com/.
22. Li D, Wu M. Pattern recognition receptors in health and diseases. *Signal Transduct Target Ther*. 2021;6(1):291. doi:10.1038/s41392-021-00687-0
23. Takeuchi O, Akira S. Pattern Recognition Receptors and Inflammation. *Cell*. 2010;140(6):805-820. doi:10.1016/j.cell.2010.01.022
24. Sadler AJ, Williams BRG. Interferon-inducible antiviral effectors. *Nat Rev Immunol*. 2008;8(7):559-568. doi:10.1038/nri2314
25. Trinchieri G. Type I interferon: friend or foe? *J Exp Med*. 2010;207(10):2053-2063. doi:10.1084/jem.20101664
26. Lee AJ, Ashkar AA. The Dual Nature of Type I and Type II Interferons. *Front Immunol*. 2018;9(SEP):1-10. doi:10.3389/fimmu.2018.02061
27. Isaacs A, Lindenmann J. Virus interference. I. The interferon. *Proc R Soc Lond B Biol Sci*. 1957;147(927):258-267. doi:10.1098/rspb.1957.0048
28. Weerd NA, Nguyen T. The interferons and their receptors—distribution and regulation. *Immunol Cell Biol*. 2012;90(5):483-491. doi:10.1038/icb.2012.9
29. Lazear HM, Schoggins JW, Diamond MS. Shared and Distinct Functions of Type I and Type III Interferons. *Immunity*. 2019;50(4):907-923. doi:10.1016/j.immuni.2019.03.025
30. Crouse J, Kalinke U, Oxenius A. Regulation of antiviral T cell responses by type I interferons. *Nat Rev Immunol*. 2015;15(4):231-242. doi:10.1038/nri3806
31. Ivashkiv LB, Donlin LT. Regulation of type I interferon responses. *Nat Rev Immunol*. 2014;14(1):36-49. doi:10.1038/nri3581
32. Muller U, Steinhoff U, Reis L, et al. Functional role of type I and type II interferons in antiviral defense. *Science (1979)*. 1994;264(5167):1918-1921. doi:10.1126/science.8009221
33. Hernandez N, Bucciol G, Moens L, et al. Inherited IFNAR1 deficiency in otherwise healthy patients with adverse reaction to measles and yellow fever live vaccines. *Journal of Experimental Medicine*. 2019;216(9):2057-2070. doi:10.1084/jem.20182295
34. Uribe-Querol E, Rosales C. Phagocytosis: Our Current Understanding of a Universal Biological Process. *Front Immunol*. 2020;11. doi:10.3389/fimmu.2020.01066
35. Rosales C. Neutrophils at the crossroads of innate and adaptive immunity. *J Leukoc Biol*. 2020;108(1):377-396. doi:10.1002/JLB.4MIR0220-574RR
36. Kambayashi T, Laufer TM. Atypical MHC class II-expressing antigen-presenting cells: can anything replace a dendritic cell? *Nat Rev Immunol*. 2014;14(11):719-730. doi:10.1038/nri3754
37. Eisenbarth SC. Dendritic cell subsets in T cell programming: location dictates function. *Nat Rev Immunol*. 2019;19(2):89-103. doi:10.1038/s41577-018-0088-1
38. Guermonprez P, Valladeau J, Zitvogel L, Théry C, Amigorena S. Antigen presentation and T cell stimulation by dendritic cells. *Annu Rev Immunol*. 2002;20:621-667. doi:10.1146/annurev.immunol.20.100301.064828
39. Delamarre L, Holcombe H, Mellman I. Presentation of Exogenous Antigens on Major Histocompatibility Complex (MHC) Class I and MHC Class II Molecules Is Differentially Regulated during Dendritic Cell Maturation. *Journal of Experimental Medicine*. 2003;198(1):111-122. doi:10.1084/jem.20021542
40. Larsen CP, Ritchie SC, Pearson TC, Linsley PS, Lowry RP. Functional expression of the costimulatory molecule, B7/BB1, on murine dendritic cell populations. *Journal of Experimental Medicine*. 1992;176(4):1215-1220. doi:10.1084/jem.176.4.1215
41. Lenschow DJ, Su GH, Zuckerman LA, et al. Expression and functional significance of an additional ligand for CTLA-4. *Proceedings of the National Academy of Sciences*. 1993;90(23):11054-11058. doi:10.1073/pnas.90.23.11054
42. Vivier E, Artis D, Colonna M, et al. Innate Lymphoid Cells: 10 Years On. *Cell*. 2018;174(5):1054-1066. doi:10.1016/j.cell.2018.07.017
43. Spits H, Cupedo T. Innate Lymphoid Cells: Emerging Insights in Development, Lineage Relationships, and Function. *Annu Rev Immunol*.

2012;30(1):647-675. doi:10.1146/annurev-immunol-020711-075053

44. Kanevskiy LM, Telford WG, Sapozhnikov AM, Kovalenko EI. Lipopolysaccharide induces IFN-γ production in human NK cells. *Front Immunol*. 2013;4(JAN). doi:10.3389/fimmu.2013.00011
45. Schroder K, Hertzog PJ, Ravasi T, Hume DA. Interferon-gamma: an overview of signals, mechanisms and functions. *J Leukoc Biol*. 2004;75(2):163-189. doi:10.1189/jlb.0603252
46. Bach EA, Aguet M, Schreiber RD. The IFN[gamma] receptor: a paradigm for cytokine receptor signaling. *Annu Rev Immunol*. 1997;15:563-591. doi:THE IFNγ RECEPTOR: A Paradigm for Cytokine Receptor Signaling
47. Valente G, Ozmen L, Novelli F, et al. Distribution of interferon-γ receptor in human tissues. *Eur J Immunol*. 1992;22(9):2403-2412. doi:10.1002/eji.1830220933
48. Gough DJ, Levy DE, Johnstone RW, Clarke CJ. IFNγ signaling—Does it mean JAK–STAT? *Cytokine Growth Factor Rev*. 2008;19(5-6):383-394. doi:10.1016/j.cytogfr.2008.08.004
49. Huang S, Hendriks W, Althage A, et al. Immune response in mice that lack the interferon-gamma receptor. *Science (1979)*. 1993;259(5102):1742-1745. doi:10.1126/science.8456301
50. Suzuki Y, Orellana M, Schreiber R, Remington J. Interferon-gamma: the major mediator of resistance against Toxoplasma gondii. *Science (1979)*. 1988;240(4851):516-518. doi:10.1126/science.3128869
51. Kile BT, Schulman BA, Alexander WS, Nicola NA, Martin HME, Hilton DJ. The SOCS box: a tale of destruction and degradation. *Trends Biochem Sci*. 2002;27(5):235-241. doi:10.1016/S0968-0004(02)02085-6
52. Boehm U, Klamp T, Groot M, Howard JC. Cellular Responses to Interferon-γ. *Annu Rev Immunol*. 1997;15(1):749-795. doi:10.1146/annurev.immunol.15.1.749
53. Ivashkiv LB. IFNγ: signalling, epigenetics and roles in immunity, metabolism, disease and cancer immunotherapy. *Nat Rev Immunol*. 2018;18(9):545-558. doi:10.1038/s41577-018-0029-z
54. Zhu J. T Helper Cell Differentiation, Heterogeneity, and Plasticity. *Cold Spring Harb Perspect Biol*. 2018;10(10):a030338. doi:10.1101/cshperspect.a030338
55. Cui W, Kaech SM. Generation of effector CD8+ T cells and their conversion to memory T cells. *Immunol Rev*. 2010;236(1):151-166. doi:10.1111/j.1600-065X.2010.00926.x
56. von Andrian UH, Mackay CR. T-Cell Function and Migration — Two Sides of the Same Coin. Mackay IR, Rosen FS, eds. *New England Journal of Medicine*. 2000;343(14):1020-1034. doi:10.1056/NEJM200010053431407
57. Cose S, Brammer C, Khanna KM, Masopust D, Lefrançois L. Evidence that a significant number of naive T cells enter non-lymphoid organs as part of a normal migratory pathway. *Eur J Immunol*. 2006;36(6):1423-1433. doi:10.1002/eji.200535539
58. Krishnamurty AT, Turley SJ. Lymph node stromal cells: cartographers of the immune system. *Nat Immunol*. 2020;21(4):369-380. doi:10.1038/s41590-020-0635-3
59. Chang JE, Turley SJ. Stromal infrastructure of the lymph node and coordination of immunity. *Trends Immunol*. 2015;36(1):30-39. doi:10.1016/j.it.2014.11.003
60. Malhotra D, Fletcher AL, Turley SJ. Stromal and hematopoietic cells in secondary lymphoid organs: partners in immunity. *Immunol Rev*. 2013;251(1):160-176. doi:10.1111/imr.12023
61. Arbonés ML, Ord DC, Ley K, et al. Lymphocyte homing and leukocyte rolling and migration are impaired in L-selectin-deficient mice. *Immunity*. 1994;1(4):247-260. doi:10.1016/1074-7613(94)90076-0
62. Muroyama Y, Wherry EJ. Memory T-Cell Heterogeneity and Terminology. *Cold Spring Harb Perspect Biol*. 2021;13(10):a037929. doi:10.1101/cshperspect.a037929
63. Liu Q, Sun Z, Chen L. Memory T cells: strategies for optimizing tumor immunotherapy. *Protein Cell*. 2020;11(8):549-564. doi:10.1007/s13238-020-00707-9
64. Chakraborty AK, Weiss A. Insights into the initiation of TCR signaling. *Nat Immunol*. 2014;15(9):798-807. doi:10.1038/ni.2940
65. Curtsinger JM, Valenzuela JO, Agarwal P, Lins D, Mescher MF. Cutting Edge: Type I IFNs Provide a Third Signal to CD8 T Cells to Stimulate Clonal Expansion and Differentiation. *The Journal of*

Immunology. 2005;174(8):4465-4469. doi:10.4049/jimmunol.174.8.4465

66. Mueller SN, Gebhardt T, Carbone FR, Heath WR. Memory T Cell Subsets, Migration Patterns, and Tissue Residence. *Annu Rev Immunol*. 2013;31(1):137-161. doi:10.1146/annurev-immunol-032712-095954
67. Kaech SM, Cui W. Transcriptional control of effector and memory CD8+ T cell differentiation. *Nat Rev Immunol*. 2012;12(11):749-761. doi:10.1038/nri3307
68. Astarita JL, Cremasco V, Fu J, et al. The CLEC-2-podoplanin axis controls the contractility of fibroblastic reticular cells and lymph node microarchitecture. *Nat Immunol*. 2015;16(1):75-84. doi:10.1038/ni.3035
69. Acton SE, Farrugia AJ, Astarita JL, et al. Dendritic cells control fibroblastic reticular network tension and lymph node expansion. *Nature*. 2014;514(7523):498-502. doi:10.1038/nature13814
70. Fellous M, Nir U, Wallach D, Merlin G, Rubinstein M, Revel M. Interferon-dependent induction of mRNA for the major histocompatibility antigens in human fibroblasts and lymphoblastoid cells. *Proceedings of the National Academy of Sciences*. 1982;79(10):3082-3086. doi:10.1073/pnas.79.10.3082
71. Shirayoshi Y, Burke PA, Appella E, Ozato K. Interferon-induced transcription of a major histocompatibility class I gene accompanies binding of inducible nuclear factors to the interferon consensus sequence. *Proceedings of the National Academy of Sciences*. 1988;85(16):5884-5888. doi:10.1073/pnas.85.16.5884
72. Figueiredo F, Koerner TJ, Adams DO. Molecular mechanisms regulating the expression of class II histocompatibility molecules on macrophages. Effects of inductive and suppressive signals on gene transcription. *J Immunol*. 1989;143(11):3781-3786. http://www.ncbi.nlm.nih.gov/pubmed/2511248
73. Kaech SM, Tan JT, Wherry EJ, Konieczny BT, Surh CD, Ahmed R. Selective expression of the interleukin 7 receptor identifies effector CD8 T cells that give rise to long-lived memory cells. *Nat Immunol*. 2003;4(12):1191-1198. doi:10.1038/ni1009
74. Veiga-Fernandes H, Freitas AA. The S(c)ensory Immune System Theory. *Trends Immunol*. 2017;38(10):777-788. doi:10.1016/j.it.2017.02.007
75. Brunner T. Fas (CD95/Apo-1) ligand regulation in T cell homeostasis, cell-mediated cytotoxicity and immune pathology. *Semin Immunol*. 2003;15(3):167-176. doi:10.1016/S1044-5323(03)00035-6
76. Henson SM, Akbar AN. KLRG1--more than a marker for T cell senescence. *Age (Dordr)*. 2009;31(4):285-291. doi:10.1007/s11357-009-9100-9
77. Sallusto F, Lenig D, Förster R, Lipp M, Lanzavecchia A. Two subsets of memory T lymphocytes with distinct homing potentials and effector functions. *Nature*. 1999;401(6754):708-712. doi:10.1038/44385
78. Pais Ferreira D, Silva JG, Wyss T, et al. Central memory CD8+ T cells derive from stem-like Tcf7hi effector cells in the absence of cytotoxic differentiation. *Immunity*. 2020;53(5):985-1000.e11. doi:10.1016/j.immuni.2020.09.005
79. Sallusto F, Geginat J, Lanzavecchia A. Central Memory and Effector Memory T Cell Subsets: Function, Generation, and Maintenance. *Annu Rev Immunol*. 2004;22(1):745-763. doi:10.1146/annurev.immunol.22.012703.104702
80. Masopust D, Vezys V, Marzo AL, Lefrançois L. Preferential localization of effector memory cells in nonlymphoid tissue. *Science*. 2001;291(5512):2413-2417. doi:10.1126/science.1058867
81. Jameson SC, Masopust D. Understanding Subset Diversity in T Cell Memory. *Immunity*. 2018;48(2):214-226. doi:10.1016/j.immuni.2018.02.010
82. Gerritsen B, Pandit A. The memory of a killer T cell: models of CD8(+) T cell differentiation. *Immunol Cell Biol*. 2016;94(3):236-241. doi:10.1038/icb.2015.118
83. van Stipdonk MJ, Lemmens EE, Schoenberger SP. Naïve CTLs require a single brief period of antigenic stimulation for clonal expansion and differentiation. *Nat Immunol*. 2001;2(5):423-429. doi:10.1038/87730
84. van Stipdonk MJB, Hardenberg G, Bijker MS, et al. Dynamic programming of CD8+ T lymphocyte

responses. *Nat Immunol*. 2003;4(4):361-365. doi:10.1038/ni912

85. Chang JT, Palanivel VR, Kinjyo I, et al. Asymmetric T lymphocyte division in the initiation of adaptive immune responses. *Science*. 2007;315(5819):1687-1691. doi:10.1126/science.1139393
86. Badovinac VP, Haring JS, Harty JT. Initial T Cell Receptor Transgenic Cell Precursor Frequency Dictates Critical Aspects of the CD8+ T Cell Response to Infection. *Immunity*. 2007;26(6):827-841. doi:10.1016/j.immuni.2007.04.013
87. Marzo AL, Klonowski KD, le Bon A, Borrow P, Tough DF, Lefrançois L. Initial T cell frequency dictates memory CD8+ T cell lineage commitment. *Nat Immunol*. 2005;6(8):793-799. doi:10.1038/ni1227
88. van der Gracht ETI, Beyrend G, Abdelaal T, et al. Memory CD8+ T cell heterogeneity is primarily driven by pathogen-specific cues and additionally shaped by the tissue environment. *iScience*. 2021;24(1):101954. doi:10.1016/j.isci.2020.101954
89. Simmons DP, Wearsch PA, Canaday DH, et al. Type I IFN drives a distinctive dendritic cell maturation phenotype that allows continued class II MHC synthesis and antigen processing. *J Immunol*. 2012;188(7):3116-3126. doi:10.4049/jimmunol.1101313
90. Montoya M, Schiavoni G, Mattei F, et al. Type I interferons produced by dendritic cells promote their phenotypic and functional activation. *Blood*. 2002;99(9):3263-3271. doi:10.1182/blood.V99.9.3263
91. Schaupp L, Muth S, Rogell L, et al. Microbiota-Induced Type I Interferons Instruct a Poised Basal State of Dendritic Cells. *Cell*. 2020;181(5):1080-1096.e19. doi:10.1016/j.cell.2020.04.022
92. Kolumam G a, Thomas S, Thompson LJ, Sprent J, Murali-Krishna K. Type I interferons act directly on CD8 T cells to allow clonal expansion and memory formation in response to viral infection. *J Exp Med*. 2005;202(5):637-650. doi:10.1084/jem.20050821
93. Havenar-Daughton C, Kolumam GA, Murali-Krishna K. Cutting Edge: The Direct Action of Type I IFN on CD4 T Cells Is Critical for Sustaining Clonal Expansion in Response to a Viral but Not a Bacterial Infection. *The Journal of Immunology*. 2006;176(6):3315-3319. doi:10.4049/jimmunol.176.6.3315
94. Crouse J, Bedenikovic G, Wiesel M, et al. Type I Interferons Protect T Cells against NK Cell Attack Mediated by the Activating Receptor NCR1. *Immunity*. 2014;40(6):961-973. doi:10.1016/j.immuni.2014.05.003
95. Whitmire JK, Tan JT, Whitton JL. Interferon-gamma acts directly on CD8+ T cells to increase their abundance during virus infection. *J Exp Med*. 2005;201(7):1053-1059. doi:10.1084/jem.20041463
96. Whitmire JK, Benning N, Whitton JL. Cutting edge: early IFN-gamma signaling directly enhances primary antiviral CD4+ T cell responses. *J Immunol*. 2005;175(9):5624-5628. doi:10.4049/jimmunol.175.9.5624
97. Whitmire JK, Eam B, Benning N, Whitton JL. Direct interferon-gamma signaling dramatically enhances CD4+ and CD8+ T cell memory. *J Immunol*. 2007;179(2):1190-1197. doi:10.1007/s13398-014-0173-7.2
98. Haring JS, Badovinac VP, Harty JT. Inflaming the CD8+ T Cell Response. *Immunity*. 2006;25(1):19-29. doi:10.1016/j.immuni.2006.07.001
99. Stoycheva D, Deiser K, Stärck L, et al. IFN-γ Regulates CD8 + Memory T Cell Differentiation and Survival in Response to Weak, but Not Strong, TCR Signals. *The Journal of Immunology*. 2015;194(2):553-559. doi:10.4049/jimmunol.1402058
100. Sercan Ö, Stoycheva D, Hämmerling GJ, Arnold B, Schüler T. IFN-γ Receptor Signaling Regulates Memory CD8 + T Cell Differentiation. *The Journal of Immunology*. 2010;184(6):2855-2862. doi:10.4049/jimmunol.0902708
101. Kastenmüller W, Brandes M, Wang Z, Herz J, Egen JG, Germain RN. Peripheral Prepositioning and Local CXCL9 Chemokine-Mediated Guidance Orchestrate Rapid Memory CD8+ T Cell Responses in the Lymph Node. *Immunity*. 2013;38(3):502-513. doi:10.1016/j.immuni.2012.11.012
102. Sung JH, Zhang H, Moseman EA, et al. Chemokine Guidance of Central Memory T Cells Is Critical for Antiviral Recall Responses in Lymph Nodes. *Cell*. 2012;150(6):1249-1263. doi:10.1016/j.cell.2012.08.015

103. Zhang L, Romero P. Metabolic Control of CD8+ T Cell Fate Decisions and Antitumor Immunity. *Trends Mol Med*. 2018;24(1):30-48. doi:10.1016/j.molmed.2017.11.005
104. Bishop EL, Gudgeon N, Dimeloe S. Control of T Cell Metabolism by Cytokines and Hormones. *Front Immunol*. 2021;12:653605. doi:10.3389/fimmu.2021.653605
105. Dimeloe S, Burgener AV, Grählert J, Hess C. T-cell metabolism governing activation, proliferation and differentiation; a modular view. *Immunology*. 2017;150(1):35-44. doi:10.1111/imm.12655
106. van der Windt GJW, Everts B, Chang CH, et al. Mitochondrial respiratory capacity is a critical regulator of CD8+ T cell memory development. *Immunity*. 2012;36(1):68-78. doi:10.1016/j.immuni.2011.12.007
107. Cui G, Staron MM, Gray SM, et al. IL-7-Induced Glycerol Transport and TAG Synthesis Promotes Memory CD8+ T Cell Longevity. *Cell*. 2015;161(4):750-761. doi:10.1016/j.cell.2015.03.021
108. Heufler C, Topar G, Grasseger A, et al. Interleukin 7 is produced by murine and human keratinocytes. *J Exp Med*. 1993;178(3):1109-1114. doi:10.1084/jem.178.3.1109
109. Watanabe M, Ueno Y, Yajima T, et al. Interleukin 7 is produced by human intestinal epithelial cells and regulates the proliferation of intestinal mucosal lymphocytes. *J Clin Invest*. 1995;95(6):2945-2953. doi:10.1172/JCI118002
110. Tokoyoda K, Egawa T, Sugiyama T, Choi BI, Nagasawa T. Cellular Niches Controlling B Lymphocyte Behavior within Bone Marrow during Development. *Immunity*. 2004;20(6):707-718. doi:10.1016/j.immuni.2004.05.001
111. Turley SJ, Fletcher AL, Elpek KG. The stromal and haematopoietic antigen-presenting cells that reside in secondary lymphoid organs. *Nat Rev Immunol*. 2010;10(12):813-825. doi:10.1038/nri2886
112. Rodda LB, Lu E, Bennett ML, et al. Single-Cell RNA Sequencing of Lymph Node Stromal Cells Reveals Niche-Associated Heterogeneity. *Immunity*. 2018;48(5):1014-1028.e6. doi:10.1016/j.immuni.2018.04.006
113. Blanchard L, Girard JP. High endothelial venules (HEVs) in immunity, inflammation and cancer. *Angiogenesis*. 2021;24(4):719-753. doi:10.1007/s10456-021-09792-8
114. Girard JP, Moussion C, Förster R. HEVs, lymphatics and homeostatic immune cell trafficking in lymph nodes. *Nat Rev Immunol*. 2012;12(11):762-773. doi:10.1038/nri3298
115. Johnson LA, Jackson DG. Inflammation-induced secretion of CCL21 in lymphatic endothelium is a key regulator of integrin-mediated dendritic cell transmigration. *Int Immunol*. 2010;22(10):839-849. doi:10.1093/intimm/dxq435
116. Acton SE, Astarita JL, Malhotra D, et al. Podoplanin-Rich Stromal Networks Induce Dendritic Cell Motility via Activation of the C-type Lectin Receptor CLEC-2. *Immunity*. 2012;37(2):276-289. doi:10.1016/j.immuni.2012.05.022
117. Denton AE, Carr EJ, Magiera LP, Watts AJB, Fearon DT. Embryonic FAP+ lymphoid tissue organizer cells generate the reticular network of adult lymph nodes. *J Exp Med*. 2019;216(10):2242-2252. doi:10.1084/jem.20181705
118. Chai Q, Onder L, Scandella E, et al. Maturation of Lymph Node Fibroblastic Reticular Cells from Myofibroblastic Precursors Is Critical for Antiviral Immunity. *Immunity*. 2013;38(5):1013-1024. doi:10.1016/j.immuni.2013.03.012
119. Luther SA, Tang HL, Hyman PL, Farr AG, Cyster JG. Coexpression of the chemokines ELC and SLC by T zone stromal cells and deletion of the ELC gene in the plt/plt mouse. *Proceedings of the National Academy of Sciences*. 2000;97(23):12694-12699. doi:10.1073/pnas.97.23.12694
120. Luther SA, Bidgol A, Hargreaves DC, et al. Differing Activities of Homeostatic Chemokines CCL19, CCL21, and CXCL12 in Lymphocyte and Dendritic Cell Recruitment and Lymphoid Neogenesis. *The Journal of Immunology*. 2002;169(1):424-433. doi:10.4049/jimmunol.169.1.424
121. Bajénoff M, Egen JG, Koo LY, et al. Stromal Cell Networks Regulate Lymphocyte Entry, Migration, and Territoriality in Lymph Nodes. *Immunity*. 2006;25(6):989-1001. doi:10.1016/j.immuni.2006.10.011
122. Acton SE, Onder L, Novkovic M, Martinez VG, Ludewig B. Communication, construction, and

fluid control: lymphoid organ fibroblastic reticular cell and conduit networks. *Trends Immunol*. 2021;42(9):782-794. doi:10.1016/j.it.2021.07.003

123. Sixt M, Kanazawa N, Selg M, et al. The Conduit System Transports Soluble Antigens from the Afferent Lymph to Resident Dendritic Cells in the T Cell Area of the Lymph Node. *Immunity*. 2005;22(1):19-29. doi:10.1016/j.immuni.2004.11.013
124. Gretz JE, Norbury CC, Anderson AO, Proudfoot AEI, Shaw S. Lymph-Borne Chemokines and Other Low Molecular Weight Molecules Reach High Endothelial Venules via Specialized Conduits While a Functional Barrier Limits Access to the Lymphocyte Microenvironments in Lymph Node Cortex. *Journal of Experimental Medicine*. 2000;192(10):1425-1440. doi:10.1084/jem.192.10.1425
125. Hirosue S, Dubrot J. Modes of Antigen Presentation by Lymph Node Stromal Cells and Their Immunological Implications. *Front Immunol*. 2015;6(SEP). doi:10.3389/fimmu.2015.00446
126. Alexandre YO, Mueller SN. Stromal cell networks coordinate immune response generation and maintenance. *Immunol Rev*. 2018;283(1):77-85. doi:10.1111/imr.12641
127. Schluns KS, Kieper WC, Jameson SC, Lefrançois L. Interleukin-7 mediates the homeostasis of naïve and memory CD8 T cells in vivo. *Nat Immunol*. 2000;1(5):426-432. doi:10.1038/80868
128. Sercan Alp Ö, Durlanik S, Schulz D, et al. Memory CD8 + T cells colocalize with IL-7 + stromal cells in bone marrow and rest in terms of proliferation and transcription. *Eur J Immunol*. 2015;45(4):975-987. doi:10.1002/eji.201445295
129. Shalapour S, Deiser K, Kühl AA, et al. Interleukin-7 links T lymphocyte and intestinal epithelial cell homeostasis. *PLoS One*. 2012;7(2):e31939. doi:10.1371/journal.pone.0031939
130. Okada T, Cyster JG. CC Chemokine Receptor 7 Contributes to Gi-Dependent T Cell Motility in the Lymph Node. *The Journal of Immunology*. 2007;178(5):2973-2978. doi:10.4049/jimmunol.178.5.2973
131. Worbs T, Mempel TR, Bölter J, von Andrian UH, Förster R. CCR7 ligands stimulate the intranodal motility of T lymphocytes in vivo. *J Exp Med*. 2007;204(3):489-495. doi:10.1084/jem.20061706
132. Iannacone M, Moseman EA, Tonti E, et al. Subcapsular sinus macrophages prevent CNS invasion on peripheral infection with a neurotropic virus. *Nature*. 2010;465(7301):1079-1083. doi:10.1038/nature09118
133. Lucas ED, Finlon JM, Burchill MA, et al. Type 1 IFN and PD-L1 Coordinate Lymphatic Endothelial Cell Expansion and Contraction during an Inflammatory Immune Response. *The Journal of Immunology*. 2018;201(6):1735-1747. doi:10.4049/jimmunol.1800271
134. Assen FP, Abe J, Hons M, et al. Multitier mechanics control stromal adaptations in the swelling lymph node. *Nat Immunol*. 2022;23(8):1246-1255. doi:10.1038/s41590-022-01257-4
135. Alapan Y, Thomas SN. Mechanics drive lymph node expansion. *Nat Immunol*. 2022;23(8):1139-1141. doi:10.1038/s41590-022-01277-0
136. Horsnell HL, Tetley RJ, de Belly H, et al. Lymph node homeostasis and adaptation to immune challenge resolved by fibroblast network mechanics. *Nat Immunol*. Published online July 26, 2022. doi:10.1038/s41590-022-01272-5
137. Gregory JL, Walter A, Alexandre YO, et al. Infection Programs Sustained Lymphoid Stromal Cell Responses and Shapes Lymph Node Remodeling upon Secondary Challenge. *Cell Rep*. 2017;18(2):406-418. doi:10.1016/j.celrep.2016.12.038
138. Samji T, Khanna KM. Understanding memory CD8 + T cells. *Immunol Lett*. 2017;185:32-39. doi:10.1016/j.imlet.2017.02.012
139. Ng CT, Nayak BP, Schmedt C, Oldstone MB a. Immortalized clones of fibroblastic reticular cells activate virus-specific T cells during virus infection. *Proceedings of the National Academy of Sciences*. 2012;109(20):7823-7828. doi:10.1073/pnas.1205850109
140. Wang X, Michie SA, Xu B, Suzuki Y. Importance of IFN-gamma-mediated expression of endothelial VCAM-1 on recruitment of CD8+ T cells into the brain during chronic infection with Toxoplasma gondii. *J Interferon Cytokine Res*. 2007;27(4):329-338. doi:10.1089/jir.2006.0154
141. Nakanishi Y, Lu B, Gerard C, Iwasaki A. CD8(+) T lymphocyte mobilization to virus-infected tissue requires CD4(+) T-cell help. *Nature*. 2009;462(7272):2-6. doi:10.1038/nature08511

142. Mueller SN, Hosiawa-Meagher KA, Konieczny BT, et al. Regulation of Homeostatic Chemokine Expression and Cell Trafficking During Immune Responses. *Science (1979)*. 2007;317(5838):670-674. doi:10.1126/science.1144830
143. Marine JC, Topham DJ, McKay C, et al. SOCS1 deficiency causes a lymphocyte-dependent perinatal lethality. *Cell*. 1999;98(5):609-616. doi:10.1016/S0092-8674(00)80048-3
144. Alexander WS, Starr R, Fenner JE, et al. SOCS1 Is a Critical Inhibitor of Interferon γ Signaling and Prevents the Potentially Fatal Neonatal Actions of this Cytokine. *Cell*. 1999;98(5):597-608. doi:10.1016/S0092-8674(00)80047-1
145. Kataru RP, Kim H, Jang C, et al. T lymphocytes negatively regulate lymph node lymphatic vessel formation. *Immunity*. 2011;34(1):96-107. doi:10.1016/j.immuni.2010.12.016
146. Lukacs-Kornek V, Malhotra D, Fletcher AL, et al. Regulated release of nitric oxide by nonhematopoietic stroma controls expansion of the activated T cell pool in lymph nodes. *Nat Immunol*. 2011;12(11):1096-1104. doi:10.1038/ni.2112
147. Siegert S, Huang HY, Yang CY, et al. Fibroblastic Reticular Cells From Lymph Nodes Attenuate T Cell Expansion by Producing Nitric Oxide. Fritz JH, ed. *PLoS One*. 2011;6(11):e27618. doi:10.1371/journal.pone.0027618
148. Khan O, Headley M, Gerard A, Wei W, Liu L, Krummel MF. Regulation of T Cell Priming by Lymphoid Stroma. Albert ML, ed. *PLoS One*. 2011;6(11):e26138. doi:10.1371/journal.pone.0026138
149. Krampera M, Cosmi L, Angeli R, et al. Role for interferon-gamma in the immunomodulatory activity of human bone marrow mesenchymal stem cells. *Stem Cells*. 2006;24(2):386-398. doi:10.1634/stemcells.2005-0008
150. Brown FD, Turley SJ. Fibroblastic Reticular Cells: Organization and Regulation of the T Lymphocyte Life Cycle. *The Journal of Immunology*. 2015;194(4):1389-1394. doi:10.4049/jimmunol.1402520
151. Satoh-Takayama N, Lesjean-Pottier S, Vieira P, et al. IL-7 and IL-15 independently program the differentiation of intestinal CD3-NKp46+ cell subsets from Id2-dependent precursors. *J Exp Med*. 2010;207(2):273-280. doi:10.1084/jem.20092029
152. Namen AE, Schmierer AE, March CJ, et al. B cell precursor growth-promoting activity. Purification and characterization of a growth factor active on lymphocyte precursors. *Journal of Experimental Medicine*. 1988;167(3):988-1002. doi:10.1084/jem.167.3.988
153. Chen D, Tang TX, Deng H, Yang XP, Tang ZH. Interleukin-7 Biology and Its Effects on Immune Cells: Mediator of Generation, Differentiation, Survival, and Homeostasis. *Front Immunol*. 2021;12:747324. doi:10.3389/fimmu.2021.747324
154. Lin J, Zhu Z, Xiao H, et al. The role of IL-7 in Immunity and Cancer. *Anticancer Res*. 2017;37(3):963-967. doi:10.21873/anticanres.11405
155. von Freeden-Jeffry U. Lymphopenia in interleukin (IL)-7 gene-deleted mice identifies IL-7 as a nonredundant cytokine. *Journal of Experimental Medicine*. 1995;181(4):1519-1526. doi:10.1084/jem.181.4.1519
156. Peschon JJ. Early lymphocyte expansion is severely impaired in interleukin 7 receptor-deficient mice. *Journal of Experimental Medicine*. 1994;180(5):1955-1960. doi:10.1084/jem.180.5.1955
157. Puel A, Ziegler SF, Buckley RH, Leonard. WJ. Defective IL7R expression in T-B+NK+ severe combined immunodeficiency. *Nat Genet*. 1998;20(4):394-397. doi:10.1038/3877
158. Kerdiles YM, Beisner DR, Tinoco R, et al. Foxo1 links homing and survival of naive T cells by regulating L-selectin, CCR7 and interleukin 7 receptor. *Nat Immunol*. 2009;10(2):176-184. doi:10.1038/ni.1689
159. Carrette F, Surh CD. IL-7 signaling and CD127 receptor regulation in the control of T cell homeostasis. *Semin Immunol*. 2012;24(3):209-217. doi:10.1016/j.smim.2012.04.010
160. Winer H, Rodrigues GOL, Hixon JA, et al. IL-7: Comprehensive review. *Cytokine*. 2022;160:156049. doi:10.1016/j.cyto.2022.156049
161. Kimura MY, Pobezinsky L a, Guinter TI, et al. IL-7 signaling must be intermittent, not continuous, during CD8+ T cell homeostasis to promote cell

survival instead of cell death. *Nat Immunol*. 2013;14(2):143-151. doi:10.1038/ni.2494

162. Martin CE, Spasova DS, Frimpong-Boateng K, et al. Interleukin-7 Availability Is Maintained by a Hematopoietic Cytokine Sink Comprising Innate Lymphoid Cells and T Cells. *Immunity*. 2017;47(1):171-182.e4. doi:10.1016/j.immuni.2017.07.005
163. Xue HH, Kovanen PE, Pise-Masison CA, et al. IL-2 negatively regulates IL-7 receptor alpha chain expression in activated T lymphocytes. *Proc Natl Acad Sci U S A*. 2002;99(21):13759-13764. doi:10.1073/pnas.212214999
164. Seddon B, Tomlinson P, Zamoyska R. Interleukin 7 and T cell receptor signals regulate homeostasis of CD4 memory cells. *Nat Immunol*. 2003;4(7):680-686. doi:10.1038/ni946
165. Mackall CL, Fry TJ, Gress RE. Harnessing the biology of IL-7 for therapeutic application. *Nat Rev Immunol*. 2011;11(5):330-342. doi:10.1038/nri2970
166. Takada K, Jameson SC. Naive T cell homeostasis: from awareness of space to a sense of place. *Nat Rev Immunol*. 2009;9(12):823-832. doi:10.1038/nri2657
167. Merayo-Chalico J, Rajme-López S, Barrera-Vargas A, Alcocer-Varela J, Díaz-Zamudio M, Gómez-Martín D. Lymphopenia and autoimmunity: A double-edged sword. *Hum Immunol*. 2016;77(10):921-929. doi:10.1016/j.humimm.2016.06.016
168. Mombaerts P, Iacomini J, Johnson RS, Herrup K, Tonegawa S, Papaioannou VE. RAG-1-deficient mice have no mature B and T lymphocytes. *Cell*. 1992;68(5):869-877. doi:10.1016/0092-8674(92)90030-g
169. Notarangelo LD, Kim MS, Walter JE, Lee YN. Human RAG mutations: Biochemistry and clinical implications. *Nat Rev Immunol*. 2016;16(4):234-246. doi:10.1038/nri.2016.28
170. Peschon JJ, Morrissey PJ, Grabstein KH, et al. Early lymphocyte expansion is severely impaired in interleukin 7 receptor-deficient mice. *Journal of Experimental Medicine*. 1994;180(5):1955-1960. doi:10.1084/jem.180.5.1955
171. Maraskovsky E, Teepe M, Morrissey PJ, et al. Impaired survival and proliferation in IL-7 receptor-deficient peripheral T cells. *J Immunol*. 1996;157(12):5315-5323. http://www.ncbi.nlm.nih.gov/pubmed/8955178
172. Rathmell JC, Farkash EA, Gao W, Thompson CB. IL-7 Enhances the Survival and Maintains the Size of Naive T Cells. *The Journal of Immunology*. 2001;167(12):6869-6876. doi:10.4049/jimmunol.167.12.6869
173. Tanchot C, Lemonnier F a, Perarnau B, Freitas a a, Rocha B. Differential requirements for survival and proliferation of CD8 naive or memory T cells. *Science (1979)*. 1997;276(June):2057-2062. doi:10.1126/science.276.5321.2057
174. Brocker T. Survival of Mature CD4 T Lymphocytes Is Dependent on Major Histocompatibility Complex Class II–expressing Dendritic Cells. *Journal of Experimental Medicine*. 1997;186(8):1223-1232. doi:10.1084/jem.186.8.1223
175. Kirberg J, Berns A, Boehmer H von. Peripheral T Cell Survival Requires Continual Ligation of the T Cell Receptor to Major Histocompatibility Complex–Encoded Molecules. *Journal of Experimental Medicine*. 1997;186(8):1269-1275. doi:10.1084/jem.186.8.1269
176. Goldrath AW, Bevan MJ. Low-affinity ligands for the TCR drive proliferation of mature CD8+ T cells in lymphopenic hosts. *Immunity*. 1999;11(2):183-190. doi:10.1016/S1074-7613(00)80093-X
177. Goldrath AW, Bogatzki LY, Bevan MJ. Naive T cells transiently acquire a memory-like phenotype during homeostasis-driven proliferation. *J Exp Med*. 2000;192(4):557-564. doi:10.1084/jem.192.4.557
178. Cho BK, Rao VP, Ge Q, Eisen HN, Chen J. Homeostasis-stimulated proliferation drives naive T cells to differentiate directly into memory T cells. *J Exp Med*. 2000;192(4):549-556. doi:10.1084/jem.192.4.549
179. Hamilton SE, Wolkers MC, Schoenberger SP, Jameson SC. The generation of protective memory-like CD8+ T cells during homeostatic proliferation requires CD4+ T cells. *Nat Immunol*. 2006;7(5):475-481. doi:10.1038/ni1326
180. Totsuka T, Kanai T, Nemoto Y, et al. IL-7 Is Essential for the Development and the Persistence of Chronic Colitis. *The Journal of Immunology*. 2007;178(8):4737-4748. doi:10.4049/jimmunol.178.8.4737

181. Calzascia T, Pellegrini M, Lin A, et al. CD4 T cells, lymphopenia, and IL-7 in a multistep pathway to autoimmunity. *Proceedings of the National Academy of Sciences*. 2008;105(8):2999-3004. doi:10.1073/pnas.0712135105
182. Kieper WC, Burghardt JT, Surh CD. A Role for TCR Affinity in Regulating Naive T Cell Homeostasis. *The Journal of Immunology*. 2004;172(1):40-44. doi:10.4049/jimmunol.172.1.40
183. Kassiotis G, Zamoyska R, Stockinger B. Involvement of Avidity for Major Histocompatibility Complex in Homeostasis of Naive and Memory T Cells. *J Exp Med*. 2003;197(8):1007-1016. doi:10.1084/jem.20021812
184. Ernst B, Lee DS, Chang JM, Sprent J, Surh CD. The Peptide Ligands Mediating Positive Selection in the Thymus Control T Cell Survival and Homeostatic Proliferation in the Periphery. *Immunity*. 1999;11(2):173-181. doi:10.1016/S1074-7613(00)80092-8
185. Min B, McHugh R, Sempowski GD, Mackall C, Foucras G, Paul WE. Neonates Support Lymphopenia-Induced Proliferation. *Immunity*. 2003;18(1):131-140. doi:10.1016/S1074-7613(02)00508-3
186. Schüler T, Hämmerling GJ, Arnold B. Cutting Edge: IL-7-Dependent Homeostatic Proliferation of CD8+ T Cells in Neonatal Mice Allows the Generation of Long-Lived Natural Memory T Cells. *The Journal of Immunology*. 2004;172(1):15-19. doi:10.4049/jimmunol.172.1.15
187. Bank U, Deiser K, Finke D, Hammerling GJ, Arnold B, Schüler T. Cutting Edge: Innate Lymphoid Cells Suppress Homeostatic T Cell Expansion in Neonatal Mice. *The Journal of Immunology*. 2016;196(9):3532-3536. doi:10.4049/jimmunol.1501643
188. Creative Commons. https://creativecommons.org/about/cclicenses/.
189. Dai Z, Lakkis FG. Cutting edge: Secondary lymphoid organs are essential for maintaining the CD4, but not CD8, naive T cell pool. *J Immunol*. 2001;167(12):6711-6715. doi:10.4049/jimmunol.167.12.6711
190. Dummer W, Ernst B, LeRoy E, Lee D, Surh C. Autologous regulation of naive T cell homeostasis within the T cell compartment. *J Immunol*. 2001;166(4):2460-2468. doi:10.4049/jimmunol.166.4.2460
191. Tan JT, Dudl E, LeRoy E, et al. IL-7 is critical for homeostatic proliferation and survival of naive T cells. *Proceedings of the National Academy of Sciences*. 2001;98(15):8732-8737. doi:10.1073/pnas.161126098
192. Saxena M, van der Burg SH, Melief CJM, Bhardwaj N. Therapeutic cancer vaccines. *Nat Rev Cancer*. 2021;21(6):360-378. doi:10.1038/s41568-021-00346-0
193. Cui W, Kaech SM. Generation of effector CD8+ T cells and their conversion to memory T cells. *Immunol Rev*. 2010;236(1):151-166. doi:10.1111/j.1600-065X.2010.00926.x
194. Schüler T, Blankenstein T. Naive CD8+ but not CD4+ T cells induce maturation of dendritic cells. *J Mol Med*. 2002;80(8):533-541. doi:10.1007/s00109-002-0360-4
195. Feng T, Wang L, Schoeb TR, Elson CO, Cong Y. Microbiota innate stimulation is a prerequisite for T cell spontaneous proliferation and induction of experimental colitis. *J Exp Med*. 2010;207(6):1321-1332. doi:10.1084/jem.20092253
196. Liu J, Han C, Xie B, et al. Rhbdd3 controls autoimmunity by suppressing the production of IL-6 by dendritic cells via K27-linked ubiquitination of the regulator NEMO. *Nat Immunol*. 2014;15(7):612-622. doi:10.1038/ni.2898
197. Heink S, Yogev N, Garbers C, et al. Trans-presentation of IL-6 by dendritic cells is required for the priming of pathogenic TH17 cells. *Nat Immunol*. 2017;18(1):74-85. doi:10.1038/ni.3632
198. Brown FD, Sen DR, LaFleur MW, et al. Fibroblastic reticular cells enhance T cell metabolism and survival via epigenetic remodeling. *Nat Immunol*. 2019;20(12):1668-1680. doi:10.1038/s41590-019-0515-x
199. Jergović M, Coplen CP, Uhrlaub JL, et al. Infection-induced type I interferons critically modulate the homeostasis and function of CD8+ naïve T cells. *Nat Commun*. 2021;12(1):5303. doi:10.1038/s41467-021-25645-w
200. Wofford JA, Wieman HL, Jacobs SR, Zhao Y, Rathmell JC. IL-7 promotes Glut1 trafficking and glucose uptake via STAT5-mediated activation of Akt to support T-cell survival. *Blood*.

2008;111(4):2101-2111. doi:10.1182/blood-2007-06-096297

201. Mazzucchelli R, Durum SK. Interleukin-7 receptor expression: intelligent design. *Nat Rev Immunol*. 2007;7(2):144-154. doi:10.1038/nri2023
202. Jameson SC. Maintaining the norm: T-cell homeostasis. *Nat Rev Immunol*. 2002;2(8):547-556. doi:10.1038/nri853
203. Perez-Shibayama C, Islander U, Lütge M, et al. Type I interferon signaling in fibroblastic reticular cells prevents exhaustive activation of antiviral CD8+ T cells. *Sci Immunol*. 2020;5(51):1-13. doi:10.1126/sciimmunol.abb7066
204. Duckworth BC, Lafouresse F, Wimmer VC, et al. Effector and stem-like memory cell fates are imprinted in distinct lymph node niches directed by CXCR3 ligands. *Nat Immunol*. Published online March 1, 2021. doi:10.1038/s41590-021-00878-5
205. Bradley KC, Finsterbusch K, Schnepf D, et al. Microbiota-Driven Tonic Interferon Signals in Lung Stromal Cells Protect from Influenza Virus Infection. *Cell Rep*. 2019;28(1):245-256.e4. doi:10.1016/j.celrep.2019.05.105
206. Takaoka A. Cross Talk Between Interferon-gamma and -alpha /beta Signaling Components in Caveolar Membrane Domains. *Science (1979)*. 2000;288(5475):2357-2360. doi:10.1126/science.288.5475.2357
207. Herndler-Brandstetter D, Ishigame H, Shinnakasu R, et al. KLRG1 + Effector CD8 + T Cells Lose KLRG1, Differentiate into All Memory T Cell Lineages, and Convey Enhanced Protective Immunity. *Immunity*. 2018;48(4):716-729.e8. doi:10.1016/j.immuni.2018.03.015
208. Klebanoff CA, Gattinoni L, Restifo NP. Sorting Through Subsets. *Journal of Immunotherapy*. 2012;35(9):651-660. doi:10.1097/CJI.0b013e31827806e6
209. Gattinoni L, Powell DJ, Rosenberg SA, Restifo NP. Adoptive immunotherapy for cancer: building on success. *Nat Rev Immunol*. 2006;6(5):383-393. doi:10.1038/nri1842
210. Mondino A, Manzo T. To Remember or to Forget: The Role of Good and Bad Memories in Adoptive T Cell Therapy for Tumors. *Front Immunol*. 2020;11:1915. doi:10.3389/fimmu.2020.01915
211. Walsh SR, Simovic B, Chen L, et al. Endogenous T cells prevent tumor immune escape following adoptive T cell therapy. *J Clin Invest*. 2019;129(12):5400-5410. doi:10.1172/JCI126199
212. Cupovic J, Ring SS, Onder L, et al. Adenovirus vector vaccination reprograms pulmonary fibroblastic niches to support protective inflating memory CD8+ T cells. *Nat Immunol*. 2021;22(8):1042-1051. doi:10.1038/s41590-021-00969-3

8 Appendix

8.1 List of abbreviations

Ag	antigen
APC	professional Ag-presenting cell
ATP	adenosine 5′-triphosphate
ATT	adoptive T cell therapy
AQP9	aquaporin 9
Bax	Bcl 2-like protein 4
Bcl-2	B-cell lymphoma 2
BCR	B cell receptor
BEC	blood endothelial cell
Bim	Bcl-2-like protein 11
BM	bone marrow
CCL	chemokine C-C motif ligand
CCR	C-C chemokine receptor type
CD	cluster of differentiation
CLEC-2	C-type lectin-like receptor 2
CTL	cytotoxic $CD8^+$ T cell
CXCL	chemokine C-X-C motif ligand
CXCR	C-X-C chemokine receptor
DC	dendritic cell
DN	double negative $gp38^-$ $CD31^-$
Foxo1	forkhead box O1
FRC	fibroblastic reticular cell
$FRC^{\Delta IFNAR}$	mice with a FRC-specific deletion of the IFNAR
$FRC^{\Delta IL\text{-}7}$	mice with a FRC-specific deletion of IL-7 production
GLUT-1	glucose transporter 1
gp38	podoplanin
HEV	high endothelial venule
HIV	human immunodeficiency virus
ICAM-1	intercellular adhesion molecule 1
IDO-1	indoleamine 2,3 dioxygenase 1
IFN	interferon
IFN-I	interferon type I
IFNAR	interferon α/β receptor

$IFNAR^{fl/fl}$	conditional IFNAR knockout mice
IFN-γR	interferon γ receptor
Ig	Immunoglobulin
IL	interleukin
$IL\text{-}7^{fl/fl}$	conditional IL-7 knockout mice
IL-7Rα	interleukin 7 receptor α chain; CD127
ILC	innate lymphoid cell
IRF	interferon regulatory factor
ISG	interferon-stimulated gene
ISGF	interferon-stimulated gene factor
iNOS	inducible nitric oxide synthase 2
JAK	Janus kinase
KLRG-1	killer-cell lectin-like receptor G1
LCMV	lymphocytic choriomeningitis virus
LEC	lymphatic endothelial cell
$LEC^{\Delta IL\text{-}7}$	mice with a LEC-specific deletion of IL-7 production
$LEC/FRC^{\Delta IL\text{-}7}$	mice with a FRC/LEC-specific deletion of IL-7 production
LIP	lymphopenia-induced proliferation
LN	lymph node
LPS	lipopolysaccharide
LSC	lymphoid stromal cell
MAPK/Erk	mitogen-activated protein kinase/ extracellular signal-regulated kinase
Mcl-1	myeloid cell leukemia-1
MHC-I	major histocompatibility complex class I
MHC-II	major histocompatibility complex class II
mTOR	kinase mammalian target of rapamycin
NFκB	nuclear factor kappa-light-chain-enhancer of activated B cells
NK	natural killer
NO	nitric oxide
NP	nucleoprotein of VSV
OT-I	$CD8^+$ T cell recognizing $ovalbumin_{257\text{-}264}$-peptide presented on $H\text{-}2^b$
OT-II	$CD4^+$ T cell recognizing $ovalbumin_{323\text{-}339}$-peptide presented on $I\text{-}A^2$
ova	ovalbumin
PAMP	pathogen-associated molecular pattern
PD-L1	programmed cell death protein 1 ligand
PECAM-1	platelet endothelial cell adhesion molecule; CD31
PI3K	phosphoinositide 3−kinase

PRR	pattern recognition receptor
Rag	recombination-activating gene
$Rag^{\gamma Rko}$	IFN-$\gamma R^{-/-}$ x $Rag1^{-/-}$ mice
RORγt	retinoid orphan receptor gamma t
SARS-CoV2	severe acute respiratory syndrome coronavirus type 2
SCID	severe combined immunodeficiency
SCS	subcapsular sinus
SLO	secondary lymphoid organ
SOCS-1	suppressor of cytokine signaling protein 1
SPF	specific pathogen-free
STAT	signal transducer and activator of transcription
TAG	triacylglyceride
T_{CM}	central memory T cell
T_{EFF}	effector T cell
T_{EM}	effector memory T cell
T_H	$CD4^+$ helper T cells
T_M	memory T cell
T_{MP}	memory precursor T cell
T_N	naive T cell
T_{SCM}	stem cell memory T cell
T_{SLEC}	short-lived/terminal effector T cell
T_{VM}	virtual memory T cell
$T_{(V)M}$	(virtual) memory T cell
T_{reg}	regulatory T cell
T_{RM}	tissue-resident memory T cell
TCR	T cell receptor
TNF-α	tumor necrosis factor α
TYK2	tyrosine kinase 2
VCAM-1	vascular cell adhesion molecule 1
VSV	vesicular stomatitis virus

8.2 List of figures

8.3 List of tables

8.4 List of publications

Knop L.*, J. Spanier*, P.-K. Larsen, A. Witte, U. Bank, I.R. Dunay, U. Kalinke, and T. Schüler. 2022. “IFNAR Signaling in Fibroblastic Reticular Cells Can Modulate CD8 + Memory Fate Decision.” *European Journal of Immunology*, April, 895-906, 52(6). https://doi.org/10.1002/eji.202149760.

Steffen, J., S. Ehrentraut, U. Bank, A. Biswas, C. Andreeta Figueiredo, O. Hölsken, H.P. Düsedau, V. Dovhan, **L. Knop**, J. Thode, S. Romero-Suáerz, C. Infante Duarte, J. Gigley, C. Romagnani, A. Diefenbach, C.S.N. Klose, T. Schüler and I.R. Dunay. 2022. “Type 1 Innate Lymphoid Cells Regulate the Onset of Toxoplasma Gondii-Induced Neuroinflammation.” *Cell Reports* 38 (13). https://doi.org/10.1016/j.celrep.2022.110564.

Rodrigo M.B., N. Kessler, **L. Knop**, N. Garbi, T. Schüler et al. 2021. “Guidelines for the Use of Flow Cytometry and Cell Sorting in Immunological Studies (Third Edition).” *European Journal of Immunology* 51 (12): 2708–3145. https://doi.org/10.1002/eji.202170126.
This publication is a compilation of protocols. The authors mentioned above wrote the chapter IV.6 Cytotoxicity. The author list of the whole compilation is not included due to length and can be found online.

Volckmar, J., **L. Knop**, T. Hirsch, S. Frentzel, C. Erck, M. van Ham, S. Stegemann-Koniszewski, and D. Bruder. 2021. “Chemical Conjugation of a Purified DEC-205-Directed Antibody with Full-Length Protein for Targeting Mouse Dendritic Cells In Vitro and In Vivo.” *Journal of Visualized Experiments : JoVE*, no. 168 (February). https://doi.org/10.3791/62018.

Bank, U., K. Deiser, C. Plaza-Sirvent, L. Osbelt, A. Witte, **L. Knop**, R. Labrenz, R. Jänsch, F. Richter, A. Biswas, A.C. Zenclussen, E. Vivier, C. Romagnani, A.A. Kühl, I.R. Dunay, T. Strowig, I. Schmitz and T. Schüler. 2020. “C-FLIP Is Crucial for IL-7/IL-15-Dependent NKp46+ ILC Development and Protection from Intestinal Inflammation in Mice.” *Nature Communications* 11 (1): 1056. https://doi.org/10.1038/s41467-020-14782-3.

Knop, L.*, K. Deiser*, U. Bank, A. Witte, J. Mohr, L. Philipsen, H.J. Fehling, A.J. Müller, U. Kalinke, and T. Schüler. 2020. “IL-7 Derived from Lymph Node Fibroblastic Reticular Cells Is Dispensable for Naive T Cell Homeostasis but Crucial for Central Memory T Cell Survival.” *European Journal of Immunology*, February, 846-857, 50(6), eji.201948368. https://doi.org/10.1002/eji.201948368.

Volckmar, J.*, **L. Knop***, S. Stegemann-Koniszewski, K. Schulze, T. Ebensen, C.A. Guzmán, and D. Bruder. 2019. “The STING Activator C-Di-AMP Exerts Superior Adjuvant Properties than the Formulation Poly(I:C)/CpG after Subcutaneous Vaccination with Soluble Protein Antigen or DEC-205-Mediated Antigen Targeting to Dendritic Cells.” *Vaccine* 37 (35): 4963–74. https://doi.org/10.1016/j.vaccine.2019.07.019.

Knop, L.*, C. Frommer*, D. Stoycheva, K. Deiser, U. Kalinke, T. Blankenstein, T. Kammertoens, I.R. Dunay, and T. Schüler. 2019. “Interferon-γ Receptor Signaling in Dendritic Cells Restrains Spontaneous Proliferation of CD4+ T Cells in Chronic Lymphopenic Mice.” *Frontiers in Immunology* 10 (FEB): 1–10. https://doi.org/10.3389/fimmu.2019.00140.

* These authors equally contributed to the work

8.5 Ehrenerklärung

Ich versichere hiermit, dass ich die vorliegende Arbeit ohne unzulässige Hilfe Dritter und ohne Benutzung anderer als der angegebenen Hilfsmittel angefertigt habe; verwendete fremde und eigene Quellen sind als solche kenntlich gemacht.

Ich habe insbesondere nicht wissentlich:
- Ergebnisse erfunden oder widersprüchlich Ergebnisse verschwiegen,
- statistische Verfahren absichtlich missbraucht, um Daten in ungerechtfertigter Weise zu interpretieren,
- fremde Ergebnisse oder Veröffentlichungen plagiiert,
- fremde Forschungsergebnisse verzerrt wiedergegeben.

Mir ist bekannt, dass Verstöße gegen das Urheberrecht Unterlassungs- und Schadensersatzansprüche des Urhebers sowie eine strafrechtliche Ahndung durch die Strafverfolgungsbehörden begründen kann.

Ich erkläre mich damit einverstanden, dass die Arbeit ggf. mit Mitteln der elektronischen Datenverarbeitung auf Plagiate überprüft werden kann.

Die Arbeit wurde bisher weder im Inland noch im Ausland in gleicher oder ähnlicher Form als Dissertation eingereicht und ist als Ganzes auch noch nicht veröffentlicht.

Magdeburg, 12.04.2023

Laura Knop